N°d'ordre NNT : xxx

THESE de DOCTORAT DE L'UNIVERSITE DE LYON
opérée au sein de
l'INSA Lyon

Ecole Doctorale 341
Ecosystèmes Evolution Modélisation Microbiologie

Spécialité/ discipline de doctorat : Micro-organismes, interactions, infections

Soutenue publiquement le 02/12/2019, par :
Marta Salvador Castell

Apolar lipids, the membrane adaptation toolbox of extremophiles

---

Devant le jury composé de :

BROOKS, Nicholas, Professeur des Universités, Imperial College London, Rapporteur
GIUDICINI-ORTICONI, Marie-Thèrese, Directrice de Recherche, Université d'Aix Marseille, Rapporteuse
PACIARONI, Alessandro, Directeur de recherche, Università degli Studi di Perugia, Rapporteur
POPOWYCZ, Florence, Professeur des Universités, INSA Lyon, Examinatrice
ROUMESTAND, Christian, Professeur des Universités, Université de Montpellier, Examinateur

OGER, Philippe, Directeur de Recherche, INSA Lyon, CNRS, Directeur de thèse
PETERS, Judith, Professeur des Universités, Université Grenoble Alpes, Co-directrice de thèse

Département FEDORA – INSA Lyon - Ecoles Doctorales – Quinquennal 2016-2020

SIGLE	ECOLE DOCTORALE	NOM ET COORDONNEES DU RESPONSABLE
CHIMIE	**CHIMIE DE LYON** **http://www.edchimie-lyon.fr** Sec. : Renée EL MELHEM Bât. Blaise PASCAL, 3e étage **secretariat@edchimie-lyon.fr** INSA : R. GOURDON	**M. Stéphane DANIELE** Institut de recherches sur la catalyse et l'environnement de Lyon IRCELYON-UMR 5256 Équipe CDFA 2 Avenue Albert EINSTEIN 69 626 Villeurbanne CEDEX **directeur@edchimie-lyon.fr**
E.E.A.	**ÉLECTRONIQUE, ÉLECTROTECHNIQUE, AUTOMATIQUE** **http://edeea.ec-lyon.fr** Sec. : M.C. HAVGOUDOUKIAN **ecole-doctorale.eea@ec-lyon.fr**	**M. Gérard SCORLETTI** École Centrale de Lyon 36 Avenue Guy DE COLLONGUE 69 134 Écully Tél : 04.72.18.60.97 Fax 04.78.43.37.17 **gerard.scorletti@ec-lyon.fr**
E2M2	**ÉVOLUTION, ÉCOSYSTÈME, MICROBIOLOGIE, MODÉLISATION** **http://e2m2.universite-lyon.fr** Sec. : Sylvie ROBERJOT Bât. Atrium, UCB Lyon 1 Tél : 04.72.44.83.62 INSA : H. CHARLES **secretariat.e2m2@univ-lyon1.fr**	**M. Philippe NORMAND** UMR 5557 Lab. d'Ecologie Microbienne Université Claude Bernard Lyon 1 Bâtiment Mendel 43, boulevard du 11 Novembre 1918 69 622 Villeurbanne CEDEX **philippe.normand@univ-lyon1.fr**
EDISS	**INTERDISCIPLINAIRE SCIENCES-SANTÉ** **http://www.ediss-lyon.fr** Sec. : Sylvie ROBERJOT Bât. Atrium, UCB Lyon 1 Tél : 04.72.44.83.62 INSA : M. LAGARDE **secretariat.ediss@univ-lyon1.fr**	**Mme Sylvie RICARD-BLUM** Institut de Chimie et Biochimie Moléculaires et Supramoléculaires (ICBMS) - UMR 5246 CNRS - Université Lyon 1 Bâtiment Curien - 3ème étage Nord 43 Boulevard du 11 novembre 1918 69622 Villeurbanne Cedex Tel : +33(0)4 72 44 82 32 **sylvie.ricard-blum@univ-lyon1.fr**
INFOMATHS	**INFORMATIQUE ET MATHÉMATIQUES** **http://edinfomaths.universite-lyon.fr** Sec. : Renée EL MELHEM Bât. Blaise PASCAL, 3e étage Tél : 04.72.43.80.46 **infomaths@univ-lyon1.fr**	**M. Hamamache KHEDDOUCI** Bât. Nautibus 43, Boulevard du 11 novembre 1918 69 622 Villeurbanne Cedex France Tel : 04.72.44.83.69 **hamamache.kheddouci@univ-lyon1.fr**
Matériaux	**MATÉRIAUX DE LYON** **http://ed34.universite-lyon.fr** Sec. : Stéphanie CAUVIN Tél : 04.72.43.71.70 Bât. Direction **ed.materiaux@insa-lyon.fr**	**M. Jean-Yves BUFFIÈRE** INSA de Lyon MATEIS - Bât. Saint-Exupéry 7 Avenue Jean CAPELLE 69 621 Villeurbanne CEDEX Tél : 04.72.43.71.70 Fax : 04.72.43.85.28 **jean-yves.buffiere@insa-lyon.fr**
MEGA	**MÉCANIQUE, ÉNERGÉTIQUE, GÉNIE CIVIL, ACOUSTIQUE** **http://edmega.universite-lyon.fr** Sec. : Stéphanie CAUVIN Tél : 04.72.43.71.70 Bât. Direction **mega@insa-lyon.fr**	**M. Jocelyn BONJOUR** INSA de Lyon Laboratoire CETHIL Bâtiment Sadi-Carnot 9, rue de la Physique 69 621 Villeurbanne CEDEX **jocelyn.bonjour@insa-lyon.fr**
ScSo	**ScSo*** **http://ed483.univ-lyon2.fr** Sec. : Véronique GUICHARD INSA : J.Y. TOUSSAINT Tél : 04.78.69.72.76 **veronique.cervantes@univ-lyon2.fr**	**M. Christian MONTES** Université Lyon 2 86 Rue Pasteur 69 365 Lyon CEDEX 07 **christian.montes@univ-lyon2.fr**

*ScSo : Histoire, Géographie, Aménagement, Urbanisme, Archéologie, Science politique, Sociologie, Anthropologie

Contents

Abstract

Most of Earth's biotopes are hold under extreme environmental conditions, namely distant from the optimal life conditions of humans. Nevertheless, a large biological diversity of organisms inhabit such environments, i.e. extremophiles. For instance, many living organisms reside at hydrothermal sources of deep oceans: temperatures above 100°C, high concentrations of reduced metals, absence of oxygen and high hydrostatic pressures, without an understanding of the molecular mechanisms enabling them to sustain such extreme conditions. The cell membrane is particularly sensitive to external conditions, but at the same time, it must maintain specific physical properties, such as fluidity and permeability, to preserve cell's integrity and functionality. This thesis work seeks to understand how the lipid bilayer can remain functional at high temperatures and high pressures and thus, allows life under extreme conditions.

This work determines novel membrane components, apolar lipids from the polyisoprenoid's family, that play the role of membrane regulators and confer stability to the lipid bilayer, along with dynamism and heterogeneity, essential properties for an optimal functional membrane. Apolar lipids are placed in the midplane of the lipid bilayer and adjust membrane curvature and permeability. Because such specific localization, apolar lipids reduce proton membrane permeability at high hydrostatic pressures. They establish functional blocks with differentiate functions that may facilitate the insertion of certain membrane's proteins and enable essential cell functions that require high curved membrane domains, such as fusion and fission. All the results demonstrate experimentally a new cell membrane architecture of extremophiles in which the presence and the quantity of apolar polyisoprenoids play a key role and constitute a new adaptation pathway to extreme conditions applicable to life origin.

List of abbreviations

a	Lattice parameter
ATP	Adenosine triphosphate
CF	5-(6)-Carboxyfluorescein
D, d	Periodicity of lipid bilayers
D_B, d_B	Lipid bilayer thickness
$2D_C$, $2d_c$	Thickness of the hydrophobic core of a lipid bilayer
D_w, d_w	Thickness of the water layer between two lipid layers
DLS	Diamond light source
DoPhPC	1,2-di-O-phytanyl-*sn*-glycero-3-phosphocholine
DoPhPE	1,2-di-O-phytanyl-*sn*-glycero-3-phosphoethanolamine
DPhPC	1,2-di-phytanyl-*sn*-glycero-3-phosphocholine
DPhPE	1,2-di-phytanyl-*sn*-glycero-3-phosphoethanolamine
DPPC	1,2-dipalmitoyl-*sn*-glycero-3-phosphocholine
FCS	Fluorescence correlation spectroscopy
FRAP	Fluorescence recovery after photobleaching
FRET	Fluorescence resonance energy transfer
GP	Generalized polarization
GUVs	Giant unilamellar lipid vesicles
H_{II}	Lipid hexagonal inversed phase
HHP	High hydrostatic pressure
HSP	Heat shock proteins
ILL	Institut Laue Langevin
L_α	Lipid lamellar liquid crystalline phase
L_β	Lipid lamellar gel phase
L_o	Lipid lamellar liquid ordered phase
HT	High temperature
Laurdan	6-Dodecanoyl-N,N-dimethyl-2-naphthylamine
LUVs	Large unilamellar lipid vesicles

MLVs	Multilamellar lipid vesicles
MO	Monoolein
NSE	Neutron spin echo
NSLD	Neutron scattering length density
P_p	Lipid packing parameter
PC	Phosphatidylcholine
PE	Phosphatidylethanolamine
Pyranine	8-Hydroxypyrene-1,3,6-trisulfonic acid
Q, q	Scattering vector
Q_{II}	Lipid cubic phase
RH	Relative humidity
SAXS	Small angle X-ray scattering
SLD	Scattering length density
Squalane	2,6,10,15,19,23-Hexamethyltetracosane
SUVs	Small unilamellar lipid vesicles
T_m	Temperature of lipid gel-to-fluid phase transition

Foreword

The aim of this thesis is to validate experimentally a novel membrane ultrastructure proposed to explain the adaptation to extreme conditions of Archaea that harbour membrane bilayers. The currently accepted dogma proposes that adaptation to extreme pHs and temperature is achieved in Archaea via the synthesis of membrane spanning, monolayer forming bipolar lipids. The novel membrane architecture attempts to explain how cell membranes from extremophiles incapable of synthesizing bipolar lipids remain functional under extreme conditions. According to this model, apolar polyisoprenoid lipids are inserted between the two leaflets of the membrane and modify the physicochemical properties of the membrane extending its stability and functional domains. Therefore, during this PhD work, I characterized the localization and the physicochemical impact of apolar polyisoprenoids on a membrane model composed of archaeal monopolar phospholipids under high temperature (HT) and high hydrostatic pressure (HHP).

This report is presented as a compendium of scientific reviews and articles corresponding to work already published in scientific journal, work under review and manuscript in preparation for submission. The first chapter is an introduction to the context of the study and the scientific questions relevant to my PhD. Through two reviews of the scientific literature, it presents key questions and state of the art of our understanding of life under extreme conditions, covering the effect of high pressure on cell components, particularly on the cell membrane, and the known adaptative mechanisms (Salvador-Castell (1) et al., 2020). The current PhD work addresses questions regarding with membrane physicochemical adaptation. In Bacteria and Archaea, membrane parameters are adjusted by regulating the lipid composition and by the so-called membrane regulators. At the beginning of this PhD, archaeal membrane regulators were yet to be identify. The second review is an extensive study presenting what molecules could act as putative membrane regulators in

Archaea. In our opinion, four families of molecules could play this role in Archaea: apolar polyisoprenoids, quinones, polyprenols and carotenoids. This survey and the present work support the hypothesis that non-polar polyisoprenoids are the most likely molecule present in archaeal cells that can act as membrane regulators (Salvador-Castell et al., 2019b). Chapter 2 is a concise description of the techniques employed for the characterization of the membrane, such as neutron scattering, small Angle X-ray Scattering (SAXS) and fluorescent approaches, and it contains the protocols used.

Chapter 3 presents the initial validation of the novel membrane architecture. Noticeably, there is a great lack of description of bilayers in this domain, as most work has been performed to characterize the behaviour of the monolayer or some very specific monopolar lipids such as the macrocyclic monopolar lipids in which the two isoprenoid chains are covalently linked. Thus, the first study presents the description of the archaeal bilayer membrane developed during his PhD, with a yet uncharacterized lipid mixture containing choline and ethanolamine based archaeal monopolar phospholipids. The second study presents the characterization of the position of the polyisoprenoid squalane, used as the putative polyisoprenoid membrane regulator, and the influence that it exerts on the properties of the membrane. This study reproduces the ratio of polar lipid/apolar lipid observed in the archaeon *Thermococcus barophilus*, for which this novel membrane architecture has been proposed (Cario et al., 2015). Since the quantity of apolar polyisoprenoids varies depending on microorganisms (Salvador-Castell et al., 2019b) and also during homeoviscous adaptation (Cario et al., 2015), it was also crucial to characterize the concentration-dependent effects of apolar isoprenoids on membrane parameters. This study is reported in Chapter 4. This chapter concatenates three manuscripts. The first article explores lipid self-assembly by SAXS, while the second one focusses on the characterization of lipid phases by neutron diffraction and the third one exposes the effect of non-polar polyisoprenoids on membrane permeability and fluidity by fluorescent techniques.

This document ends on a discussion of the relevance of the main conclusions of this work for our understanding of the adaptation to extreme conditions and the origins of life and the numerous perspectives opened up.

Chapter 1. Introduction

Earth presents many environments that, from a human being point of view, are considered harsh and too extreme to inhabit. Extreme habitats comprise environments with severe conditions of temperatures, high pressures, salinity, pH, etc., that would easily kill non-adapted organisms. For instance, the acidic hot springs in Yellowstone Park can reach 90 °C and pH 2; the cold and hypersaline Don Juan pond, placed in Antarctica, presents a salinity of 33.8 % (salt/water, w:w) and temperatures of -50 °C and the Beebe Hydrothermal Vent Field, located in the Cayman Trench at the Atlantic Ocean, has temperatures reaching 400 °C and hydrostatic pressures of 50 MPa (1 MPa = 10 bar).

One of the most studied extreme condition is HT (Blicher et al., 2009; Hope and Aschberger, 1970; Quinn, 1988; Somero, 1995). It is well established, for example, that HT, usually above 80 °C (Matsuura et al., 2015), causes the irreversible denaturation of proteins from non-adapted organisms. Consequently, cells synthesize the so-called “heat shock” proteins (HSP) to protect themselves against variations of HT. HSP and other stress response proteins are produced by cells to protect their proteome against all kind of stresses, such as anoxia and heavy metals exposure (Lindquist and Craig, 1988; Neumann et al., 1994). HSPs prevent denaturation of proteins, may help to refold denaturated proteins or to degradate irreversibly damaged proteins (Santoro, 2000). Another mechanism to protect the cellular

content from harsh conditions is the production of osmolytes (Yancey et al., 1982). Osmolytes, such as trimethylamine oxide or mannosylglycerate, are amino acids and derivatives accumulated by the cell to stabilize proteins' structures and therefore counteract the effects of stressful conditions (Gao et al., 2017). Osmolytes increase cell crowding and limit the structural arrangement of proteins (Salvador-Castell et al., 2019a).

As the first barrier between the cell and its surrounding environment, cell membranes are also highly influenced by variations of environmental conditions. A cell membrane is a two dimensional matrix composed of proteins and lipids, such as glycolipids and phospholipids (Figure 1.1) (Engelman, 2005; Goñi, 2014; Singer and Nicolson, 1972). It is not a mere barrier which retains cell content, cell membranes are the energetic factory of the cell. They regulate the inward and outward traffic of substrates and molecules, control cell growth by exo- and endocytosis, help the cell to maintain its shape and play a crucial role in cell signalling. Hence, cell membranes, and thus phospholipids, require specific physicochemical characteristics to be functional (Dowhan, 1997).

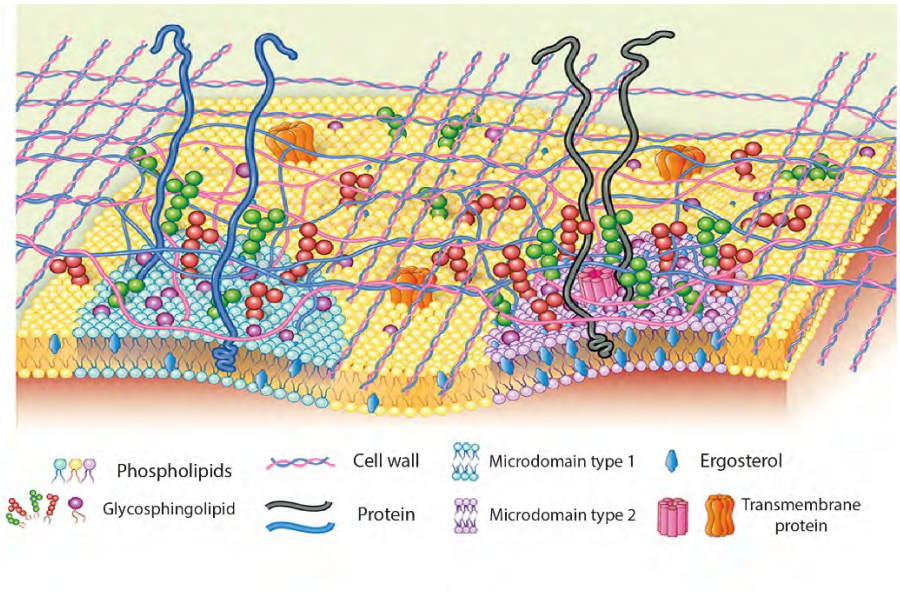

Figure 1.1. Model proposed for fungal membranes with two populations of membrane microdomains. From (Guimarães et al., 2014).

Phospholipids are amphiphilic molecules consisting of a hydrophilic head group and two hydrocarbon chains that are highly hydrophobic. Therefore, in solution, phospholipids self-assembly together in such a way that polar head groups are in contact with water and hydrocarbon chains are in contact with each other. Usually, phospholipids self-assembly as bilayers, which can form spherical objects enclosing aqueous solution. This is known as the

lamellar phase. Physicochemical properties of lipid bilayers rely heavily upon external conditions. At low temperatures and high pressures, the lipid bilayer is thicker, highly rigid and presents low permeability, such phase is known as gel phase (L_β). An increase in temperature or decrease in pressure increases the dynamics of the lipid bilayer, its fluidity and permeability. Here the lipid bilayer is in the fluid liquid-crystalline phase (L_α). The temperature in which the gel-to-fluid phase transition occurs is called melting temperature (T_m). A further increase of temperature, or decrease of pressure, leads to a too fluid phase. It is important to note that the functional state of the cell membrane is the L_α. The permeability and rigidity of both the L_β (low permeability, high rigidity) and fluid (high permeability, low rigidity) phases are not compatible with a biological function (Figure 1.2).

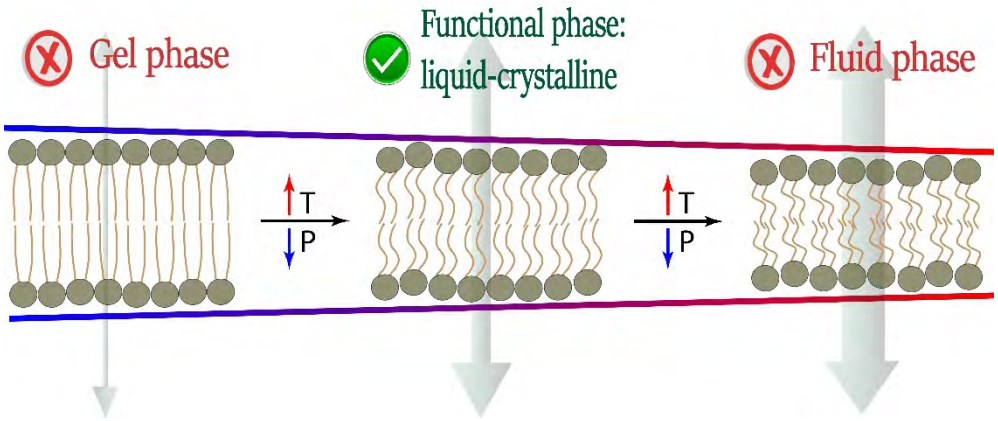

Figure 1.2. Phase transition in lipid bilayer. In functional cell membranes, lipid bilayer is found in the liquid-crystalline phase, however, variations of temperature (T) or pressure (P) may shift the membrane to non-functional phases. Grey arrows represent membrane permeability.

Cell membranes are thus highly affected by environmental conditions, such as temperature, pressure or pH. External harsh pH induces a change of internal cell pH which can modify enzymatic activities or protein folding, for example (Lund et al., 2014; Taylor, 1962). Moreover, extreme pH influences the integrity, softness (Angelova et al., 2018) and dynamics of cell membranes (M. Guiral et al., 2018).

High pressure is an environmental property found in several extreme habitats. This environmental parameter causes local changes on protein conformations, straightens the hydrocarbon chains of phospholipids and affects cell functions, such as genetic expressions, enzymatic reactions and motility. More detailed information about high pressure effects on

cells is found in the review entitled “High-pressure Adaptation of Extremophiles and Biotechnological Applications” (Salvador-Castell (1) et al., 2020), placed in this chapter.

In contrast to what was assumed for decades, extreme habitats are inhabited by organisms perfectly adapted to such conditions. They are called extremophiles. For example, organisms may have their optimal growth parameters at HT (hyperthermophiles), HHP (piezophiles) or low or high pH values (acidophiles, alkaliphiles). As an illustration, the microorganism *Methanopyrus kandleri* has its optimal temperature at 105 °C (Takai et al., 2008) and *Colwellia marinimaniae* presents its optimal growth conditions at 120 MPa (Kusube et al., 2017).

Because marine environments covers more than 70 % of the Earth surface with an average depth of 3800 m, corresponding approximately to a pressure of 38 MPa, piezophiles habit the largest habitat of Earth (Bartlett, 1999). They own distinctive characteristics allowing them to live under high hydrostatic pressures (HHP). For instance, piezophilic proteins have higher flexibility at ambient pressure in comparison to proteins from piezosensitive organisms (Martinez et al., 2016; Ohmae et al., 2012). The adaptation of their proteome is due both to specific molecular dynamics of the proteins themselves, but also to the different dynamics of their hydration shell (Golub et al., 2018; Martinez et al., 2016; Peters et al., 2014; Salvador-Castell et al., 2019a). For details on the impact of HHP on cells and on the adaptation strategies of piezophiles please refer to the review I of this chapter entitled “High-pressure Adaptation of Extremophiles and Biotechnological Applications” (Salvador-Castell (1) et al., 2020).

Hydrothermal vents are specific habitats in the deep-sea. Their ecosystem is rich and contents unique specifically adapted microorganisms (Howe, 2008; Jebbar et al., 2015). As an illustration, we can find giant tube worms like *Riftia pachyptila* (Arp and Childress, 1983), fishes from the family Zoarcidae (Biscoito et al., 2002) and sulfur-reducing bacteria, such as *Marinitoga piezophila* (Alain et al., 2002). Archaeal microorganisms (defined in the next paragraph) are also part of this ecosystem. For example, this is the habitat of *Thermococcus barophilus*, a hyperthermophile and piezophilic archaeon for which optimal growth conditions are 85 °C and 40 MPa (Marteinsson et al., 1999).

Since the classification established by C. Woese (Woese et al., 1990; Woese and Fox, 1977), Archaea are one of the three domains of life. They are unicellular prokaryotic

microorganisms and thus they are often confused with Bacteria. However, such domains differ in their ribosomal RNA, cell wall and by the presence of histones, i.e. proteins that "order" the DNA. Moreover, Archaea possess phospholipids with particular structures: isoprenoid hydrocarbon chains linked by ether bonds to *sn*-glycerol-1-phosphate (Figure 1.3) (De Rosa et al., 1986; Gambacorta et al., 1993). Archaeal cell membranes contain the usual monopolar phospholipids (diethers), which self-assembly in a bilayer, but also exceptional bipolar phospholipids (tetraethers) that can conform a lipid monolayer (De Rosa et al., 1983), much more rigid, less permeable and resistant to extreme conditions (Figure 1.3) (Chang, 1994; Jacquemet et al., 2009; Komatsu and Chong, 1998).

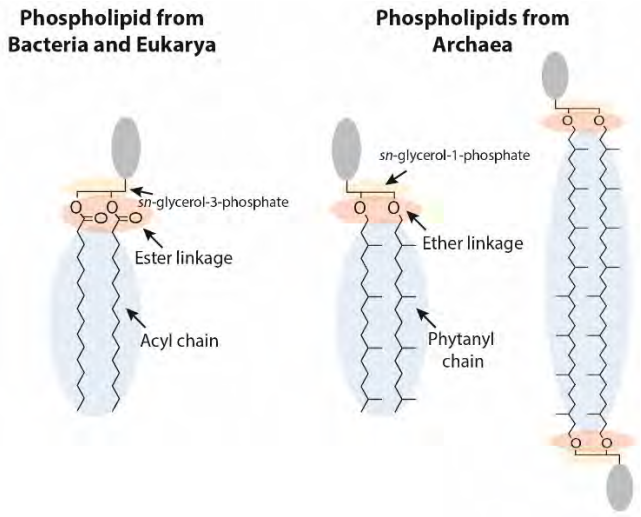

Figure 1.3. Comparison of usual bacterial and eukaryal phospholipids vs archaeal phospholipids. Grey spheres represent polar headgroups.

The presence of bipolar lipids has been specifically associated with the adaptation to HT environments. But this view has been challenged since bipolar lipids have been also extracted from mesophiles living close to ambient temperatures. For example, *Methanobacterium ruminantium*, which has its optimal growth temperature between 33°C and 40°C (Smith and Hungate, 1958), possesses 55 % of tetraethers (Tornabene, 1979). Moreover, there are hyperthermophilic archaea which membranes contain exclusively or a majority of monopolar lipids in their cell membranes. For instance, the Archaea growing at the record temperature of 122°C, *M. kandleri*, possesses only monopolar lipids (Hafenbradl et al., 1996). Similarly, archaea of the Thermococcales order, such as *T. barophilus* produce a majority of monopolar lipids while growing optimally at temperatures ranging from 85°C to 100°C (Cario et al., 2015). All these facts lead to the question how can the lipid bilayer of these

hyperthermophiles be stable at such temperatures and how can they thrive in extreme conditions? The model presented by Cario *et al.* may be the answer (Cario et al., 2015) (Figure 1.4).

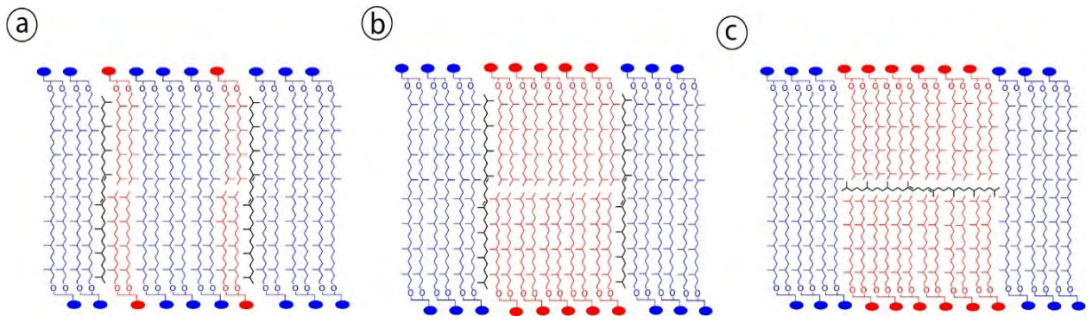

Figure 1.4. Schematic representation of possible archaeal membrane models presented by (Cario et al., 2015). *Red and blue molecules represent monopolar and bipolar phospholipids, respectively. The skeletal representation of the polyisoprenoid lycopene is in black.*

Cario et al. have studied the homeoviscous adaptation of the archaeon *T. barophilus* (Cario et al., 2015), corresponding to the cell capability to adapt its membrane lipid composition to keep it in a functional state (Sinensky, 1974). Properties of membranes are under constant surveillance by specialized transmembrane proteins, which might report on the hydrophobic region of the membrane, or soluble proteins, which interact reversibly with the membrane and may be, for example, sensitive to its charge density (Ernst et al., 2016). The rate by which lipids are synthesized depend on enzyme abundance and activity. For instance, a transcription factor may regulate a group of genes giving a coordinate effect. This allows cell membranes to be functional under a larger range of environmental conditions than just their optimal growth parameters. Hence, *T. barophilus* modifies its monopolar:bipolar phospholipid ratio according to external parameters, such as temperature and hydrostatic pressure. But this is not all, unexpectedly, this microorganism also adjusts the level of unsaturations of apolar polyisoprenoids as a function of HT and HHP (Cario et al., 2015). Polyisoprenoids are methyl branched lipids composed of terpene subunits. For instance, most of the polyisoprenoid lycopene has four unsaturations at 70 °C, but the majority present only two at 90 °C. There are few reasons which could explain the cellular functions of non-polar polyisoprenoids: 1) They are building blocks or degradation units of phospholipids. It is unlikely as the condensation type between lycopene and the hydrophobic chains of phospholipids is

different. 2) They are used as energy storage; such option is not supported as the percentage of lycopene found, ca. 1-2%, is very low. 3) They may be structural lipids of the archaeal cell membrane and they participate in the homeviscous adaptation (Figure 1.4). This kind of apolar lipids may play a role as a dynamic membrane regulator, just as cholesterol for mammal cells or hopanoids for bacteria do (Ourisson et al., 1987; Veatch and Keller, 2002). Membrane regulators are essential molecules to achieve the functional physicochemical properties of cell membranes. Both Eukarya and Bacteria cells contain them. Nevertheless, until now, this role has not been attributed to any molecule in the Archaea domain. In a recent study (review II of this chapter) (Salvador-Castell et al., 2019b), we have proposed that among four putative candidates, apolar polyisoprenoids, could be the archaeal membrane regulator. Therefore, the work presented in this thesis aims at demonstrating that non-polar polyisoprenoids can be inserted in the archaeal membrane and modulate membrane properties.

Review I. High-pressure adaptation of extremophiles and biotechonological applications

M. Salvador Castell [1], P. Oger [1], J. Peters [2,3]

[1] Université de Lyon, CNRS, UMR 5240, F-696211 Villeurbanne, France.
[2] Université Grenoble Alpes, LiPhy, F-38044 Grenoble, France.
[3] Institut Laue Langevin, F-38000 Grenoble, France.

Accepted to be published in "Physiological and Biotechnological Aspects of Extremophiles", Salwan R, Elsevier.

Abstract

During the last decades, high pressure has gained in importance as physical parameter, not only to study biomolecules, but also for its biotechnological applications. High pressure affects organism's ability to survive by altering most of cell's macromolecules. These effects can be used, for example, to inactivate microorganisms, enhance enzymatic reactions or to modulate cell activities. Moreover, some organisms are capable to grow under high pressures thanks to their adaptation at all cellular levels. Such adaptation confers a wide range of potentially interesting macromolecules still to be discovered. We firstly present the different effects of high pressure on cells and the diverse strategies used by them to cope with this harsh environment. Secondly, we give an overview over biotechnological applications of pressure-sensitive and pressure-adapted organisms.

Keywords: high Pressure, deep biosphere, stress, piezophile, adaptation

Introduction

High pressure (HP) characterizes many habitats on Earth, such as deep-sea, subsea floor and continental subsurface. Deep-sea is part of the oceans that encompasses the entire biosphere below 1000 m from the water surface and present pressures higher than 10 MPa. This hydrostatic pressure originates from the weight of the water column and corresponds to 10 MPa/km (Bartlett, 1999). The highest hydrostatic pressure detected in the ocean is approximately 110 MPa at 11,000 m depth at the Challenger Deep of Mariana Trench in the Pacific Ocean. Moreover, below the subsea floor, the pressure further increases due to the weight of the sedimentary material by roughly 15 MPa/ km and *ca*. 28 MPa/km in oceanic rock. Such biosphere contains a substantial part of the Earth biomass, which can potentially influence global biochemistry (Daniel et al., 2006; Hazael et al., 2016; Schrenk et al., 2010).

All high-pressure habitats are occupied by microorganisms and other complex organisms that highly contribute to the Earth's biomass (Kallmeyer et al., 2012; Orcutt et al., 2011). Pressure impact on organisms' growth allows to divide them in different categories. Organisms that cannot tolerate ambient pressure are designated as strict or obligate piezophiles. Inversely, facultative piezophiles are organisms that tolerate ambient pressure, but their optimal growth pressures are higher than 10 MPa (Figure 9.1). Other organisms withstand a range of optimal pressures from ambient pressure to low hydrostatic pressures, these organisms are called piezotolerants. Last, organisms which growth is inhibited by pressure are designed as piezosensitive (Oger and Cario, 2014).

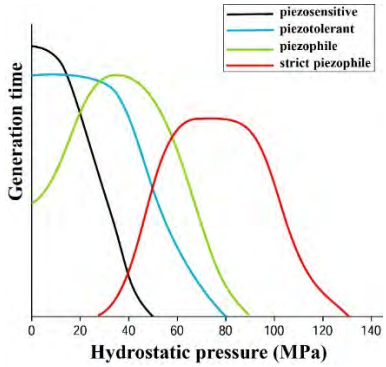

Figure 1. Schematic growth curves of microorganisms according to pressure (MPa).

Bacteria and Archaea domains contain facultative and obligate piezophiles. Examples of obligate piezophiles are the bacteria *Shewanella benthica* and *Colwellia marinimaniae*, which optimal growth pressures are 70 MPa and 120 MPa, respectively (Kusube et al., 2017; Nogi and Kato, 1999), and the archaeon *Pyrococcus yayanossi*, withstanding an optimal pressure of 50 MPa (Birrien et al., 2011). Obviously, piezophiles excel in sustaining pressure conditions beyond the usual limits for humans; however, the reasons for that adaptation are still

debated. The technical constraints to isolate obligate piezophiles are certainly responsible for the limited attention they get.

The curiosity in piezophiles has begun more than a century ago (Demazeau and Rivalain, 2011; Simonato et al., 2006), but the technological difficulties and the need of specialized equipment have caused that high-pressure studies are not, currently, developed in most laboratories. Nevertheless, the interest on pressure and its biotechnological applications have been growing during last decades.

1. Effects of pressure on macromolecules and cells

Pressure alters biomolecules by changing their volume. Thermodynamically, the variation in Gibbs free energy (G) is defined by equation 1

$$d(\Delta G) = -\Delta S dT + \Delta V dP, \quad (1)$$

where ΔS is the change in entropy, ΔV the difference in volume and T and P represent temperature and pressure, respectively. At constant temperature, dT = 0 and thus

$$(\frac{\partial G}{\partial P})_T = \Delta V. \quad (2)$$

This equation, conforming to Le Châtelier's principle (Le Chatelier, 1884), states that an increase in pressure will cause a shift to the state that occupies the smallest volume, meaning, for example, to the unfolded state for most globular proteins, where ΔG < 0. As a result, pressure modifies the volume of the system, but not its internal energy (as temperature does). Water with its low compressibility is a crucial partner for pressure action. Notably hydration water (water bound at the surface of macromolecules) is very sensitive to pressure and it can reorganize its network under pressure implying an effect on the macromolecule (Mentré and Hoa, 2001). Moreover, macromolecules present an extraordinary stability against pressure under low hydration conditions (Oliveira et al., 1994; Rayan and Macgregor, 2009).

Molecular interactions result from an equilibrium of electrostatic forces, such as Van der Waals and hydrogen bonding, along with hydrophobic interactions. Relatively low pressures affect these molecular bindings, which outcome to changes on the geometry and structure of biomolecules and therefore, on their physical properties (solubility, melting point, density) and reaction rates. In contrast, high pressures above 2 GPa are needed to impact non-covalent interactions (Balasubramaniam et al., 2015; Balny et al., 2002; Silva et al., 2014).

1.1. Nucleic acids

Although the unfolding volume of DNA duplexes is small, pressures up to 1 GPa have, in general, a stabilizing effect on canonical DNA (*e.g.* with common pair bases). This stabilizing effect may be related to the decrease of hydrogen bonds' distance. Consequently, pressure increases the duplex-single-strand transition temperature (Mentré and Hoa, 2001). Only in specific cases of synthetic polymers (*e.g.* adenine – thiamine copolymers) and salt

concentrations, pressure can lead to double-stranded melting (Rayan and Macgregor, 2005). Regardless, the mechanism is not the same as the heat-induced DNA melting, as under pressure, water molecules penetrate DNA base pairs destabilizing their interactions (Rayan and Macgregor, 2009; Takahashi and Sugimoto, 2013).

There is a lack of information about the effect of pressure on RNA but, generally, it has been observed that RNA is more pressure sensitive than DNA. For example, pressure induces a structure reorganization of tRNA (Giel-Pietraszuk and Barciszewski, 2005; Schuabb et al., 2015) and it destabilizes small RNA oligomers (Garcia and Paschek, 2008). Non-canonical pair structures (different from the usual Watson-Crick pair bases), such as G-quadruplexes or stem-loops, are less stable under pressure than canonical structures by a factor of 10 (Takahashi and Sugimoto, 2015, 2013).

Although canonical DNA duplexes are stabilized by pressure, DNA—protein interactions may be perturbed due to changes in the electrostatic and hydrophobic interactions. Accordingly, pressure affects negatively all molecular reactions where DNA is involved, such as replication, transcription and recombination (Abe, 2007; Heremans, 2004).

1.2. Proteins

Most of the knowledge about pressure effects on proteins is based on studies on globular proteins (Al-Ayoubi et al., 2017; Marion et al., 2015; Panick et al., 1998). Some of these studies reveal that structural transitions of globular proteins due to pressure are based on a hydration mechanism that accompanies protein conformational changes. At higher pressure, the hydration degree is increased by the entrance of water into the protein cavities generating an increase of the surface in contact with the solvents, thus contributing to the volume change (Roche et al., 2012). Pressure mainly alters tertiary and quaternary structures of proteins, but secondary structures (α-helices, β-sheets, and turns) are much less sensitive to water penetration and to destabilization by pressure. For this reason, the state unfolded by pressure may be a hydrated globular structure with large amounts of folded structure (Meersman et al., 2013; Silva et al., 2014). It should be recalled that water plays a key role on pressure denaturation, since this volume change can only be attended to proteins in solution. Dry proteins are highly stable against pressure (Balny et al., 2002; Eisenmenger and Reyes-De-Corcuera, 2009; Smeller, 2002).

The unfolding of many monomeric proteins begins above 200 MPa (Daniel et al., 2006), however, enzymatic activities are usually modified at lower pressures. In fact, the application of pressures < 200 MPa confers higher thermostability to most proteins (Smeller, 2002; Winter and Dzwolak, 2005). Consequently, superposing pressure and temperature application usually accelerates most of enzymatic reactions, such as hydrolases and transferase reactions (Eisenmenger and Reyes-De-Corcuera, 2009). As an illustration, the efficiency of coconut husk

hydrolysis by cellulases from *Penicillium variable* is increased at 300 MPa and 50ºC (Dutra Albuquerque et al., 2016). Moreover, reactions can already be enhanced by pressure at low temperatures (Eisenmenger and Reyes-De-Corcuera, 2009). For example, the activity of the enzyme polyphenoloxidase from onion is increased up to 140% at 450 MPa and 25ºC (Butz et al., 1994).

Pressure generally changes the equilibrium between subunits from oligomers or between two different proteins, even at relatively low pressures (*ca.* 50 MPa) (Huang et al., 2014). At this pressure, for example, ribosomes' subunits are dissociated (Abe, 2007) and larger protein assemblies such as cytoskeletal proteins are disturbed resulting in reversible morphological changes (Gao et al., 2018). However, other oligomers are more resistant to pressure such as the tetrameric urate oxidase, which dissociates at *ca.* 150-175 MPa (Girard et al., 2010).

In fact, a protein in its native state possesses distinct, nearly isoenergetic conformational substates, which may have similar or dissimilar functions or the same function with different rates (statistical substates). As pressure can decrease the folding rate and increase the unfolding one, it can shift the population of protein substates on the basis of their volumetric differences (Librizzi et al., 2018; Luong et al., 2015; Silva et al., 2002). This capability allows the characterization of various intermediate substates by pressure, which may occur in the folding process (Collins et al., 2011). Moreover, pressure can change the reaction rates, providing new information about the dynamics and reactions of proteins (Meersman et al., 2013). This was confirmed, for example, by a dynamic study of myoglobin, where it has been shown that pressure reduces protein motions and increases the structural similarities between the different conformational substates (Librizzi et al., 2018).

Few studies have been performed on pressure effects on non-globular proteins, such as fibrous, disordered and membrane proteins. Examples are the studies on collagen structure (Potekhin et al., 2009), the intrinsically disordered protein alpha synuclein (Roche et al., 2013), the Lmr transmembrane protein (Vogel et al., 2008) or the ion channel MscS (Macdonald and Martinac, 2005). An important point is that the behaviour of transmembrane proteins against environmental stresses is affected by the protein structure but also by its lipid surrounding (Ulmer et al., 2002).

Membrane proteins and membrane lipids form an ensemble; they influence mutually as a product of biochemical or environmental changes which can compromise membrane processes such as energy production or ion fluxes. The influence of the lipid matrix on the protein response to pressure has been studied for few proteins (Kapoor et al., 2012; Periasamy et al., 2009; Powalksa et al., 2007). For example, the transporter efficiency of the tryptophan permease Tat2 from yeast cells is affected due to a modification of membrane fluidity under

HP (Campanaro et al., 2005). Therefore, membrane integrative studies are necessary to better describe membrane protein behaviour.

1.3. Phospholipids

Lipids, and specially their hydrocarbon chains possess a high compressibility (Brooks et al., 2011). When pressure is applied on a phospholipid bilayer, the acyl chains are straightened resulting in a thicker and more ordered bilayer. Namely, pressure induces the lipid phase transition from a liquid-crystalline (phase essential for the biological function of the membrane) to a more rigid phase called the gel phase. Additionally, pressure can also promote the apparition of new phases, such as interdigitated phases or non-lamellar phases (*i.e.*, cubic or hexagonal) (Brooks et al., 2011; Ding et al., 2017; Matsuki et al., 2007; Trapp et al., 2013; Winter and Jeworrek, 2009). Nevertheless, all lipids do not have the same sensitivity to pressure. For example, lipids with longer hydrophobic chains are higher responsive to pressure. This may result in a phase separation in domains on membranes formed by a mixture of lipids (McCarthy et al., 2015).

Pressure may also have an impact on more complex macromolecules, such as lipoproteins. Recent studies on human plasma lipoproteins under HHP revealed a reduced flexibility and higher compressibility of its triglyceride rich form, the form associated to pathological health conditions (Golub et al., 2017; Lehofer et al., 2018) compared to the native one.

1.4. Cells

Surprisingly, pressure is the unique physical parameter capable of inducing heat- and cold-shock proteins' as a cell response to the same stress. *Escherichia coli* exposed to 53 MPa induces 55 proteins, 11 heat-shock and 4 cold-shock proteins among them. *E. coli* may try to neutralize the damage produced by pressure at different cell levels, such as stability of macromolecules and membrane functionality (Welch et al., 1993).

As mentioned above, pressures up to 100 MPa affect most of the cellular functions such as enzymatic reactions, gene expression, cell motility and morphology, and the cell membrane itself (Figure 9.2). Since pressure is transmitted through a fluid, it is uniformly transmitted (Pascal's law) over the whole cell and therefore, it makes it difficult to identify the main cause of cell death. Moreover, pressure-induced cell inactivation relies upon the nature of microorganism and its physiological conditions, such as water content and salt presence.

Overall, eukaryotes are more pressure-sensitive than prokaryotes and piezosensitive bacilli and spiral-shaped bacteria are inactivated at lower pressures than cocci (Huang et al., 2014; Ludwig, 2003). For instance, pressures above 150 MPa usually reduce the viability of mammalian cells and may induce cell death by apoptosis from 200 MPa on or through a

necrotic-like pathway at 300 MPa (Frey et al., 2004). On the other hand, bacteria cocci may resist to much higher pressure variations, for example, *Staphylococcus aureus* cell inactivation begins at 350 MPa (Ludwig, 2003).

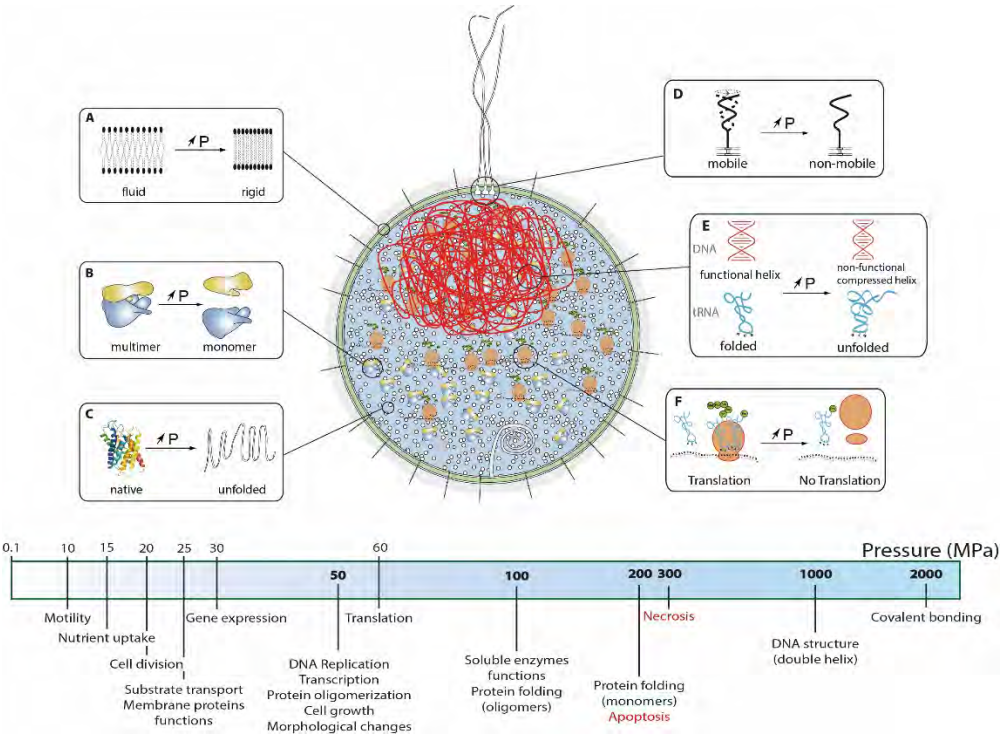

Figure 2. Above, illustration of effects on different cell macromolecules: A: lipids, B: multimer proteins, C: proteins, D: flagella, E: DNA (red) and tRNA, F: RNA translation. Adapted from (Oger and Jebbar, 2010)*. Below, cellular macromolecules (black) and cells (red) common affected at high pressure.*

In addition, most gram-negative bacteria seem to be less resistant to pressure than gram-positive (Wuytack et al., 2002). Gram-negative bacteria possess a much more complex membrane which makes it a target for pressure damage (Ritz et al., 2000). Last, microorganisms in the exponential growth phase present lower pressure-tolerance than in their stationary growth phase (Pagán and Mackey, 2000; Patterson, 2005). For example, exponential-phase cells may present a filamentous shape under pressure which can disrupt the membrane functions (Abe, 2007; Mañas and Mackey, 2004). Moreover, stationary-cells have the capability to synthesize stress-response proteins to adapt and, therefore, better resist to different harsh conditions (Hill et al., 2002).

Spores present formidably high resistance to harsh environments, likely due to their structure with numerous protective layers and their low water content (Black et al., 2007). Interestingly, relatively moderate pressures (50 to 300 MPa) cause the germination of a dormant spore. Though, higher pressures are often less effective to induce germination (Michiels et al., 2008). Pressure alone is not very effective to inactivate bacterial spores and a treatment together with temperature is necessary (Wang et al., 2016).

2. Pressure adaptation in piezophiles

The biodiversity of piezophiles is huge (Howe, 2008; Jorgensen and D'Hondt, 2006; Orcutt et al., 2013, 2011). Organisms adapted to pressure include unicellular bacteria, archaea, eukaryotes as invertebrates, fishes and even deep diving marine mammals (Dover et al., 2002; Grassle, 1985; Kelly and Yancey, 1999). For example, large invertebrates like mussels, crabs and shrimps inhabit hydrothermal vents and some marine mammals can be exposed to almost 20 MPa without presenting any negative symptom (Bliznyuk et al., 2018; Castellini et al., 2001). There are differences in the microorganisms adapted to HP, as some are also adapted to low temperatures (psychrophiles) and others to high temperatures (hyperthermophiles), which increases the piezophilic diversity. Hyperthermophilic and piezophilic organisms are found near vent sites, where temperatures range from 350 °C to 2°C in only few cm distance. Altogether, this represents a reserve of microorganisms with great potential for technological and pharmaceutical applications, such as new enzymes, antibiotics or cancer cell line active derivatives.

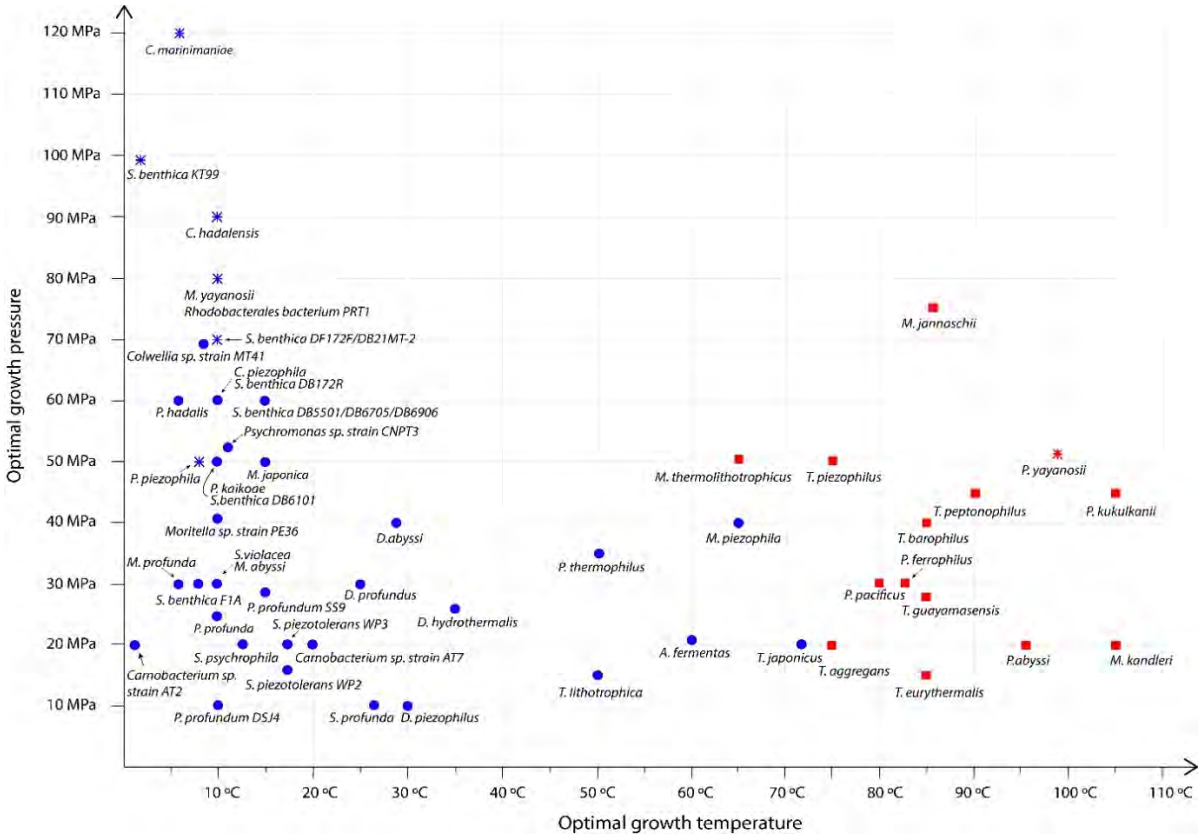

Figure 3. Optimal growth temperature and pressure for all idenfied piezotolerant and piezophile bacteria (blue) and archaea (red). A. represents Anoxybater; C. represents Colwellia; D. represents Desulfovibrio except for Dermacoccus abyssi; M. represents Moritella except for Marinitoga piezophila, Methanocaldococcus jannaschii, Methanococcus thermolithotrophicus and Methanopyrus kandleri; P. represents Psychromonas except for Piezobacter thermophilus, Profundionmas piezophila, Photobacterium profundum, Paleococcus ferrophilus, Paleococcus pacificus, Pyrococcus abyssi , Pyrococcus yayanosii and Pyrococcus kukulkanii; S. represents Shewanella; T. represents Thermococcus except for Thioprofundum lithotrophica and Thermosipho japonicus. Adapted from (Jebbar et al., 2015). *References for C. marinimaniae* (Kusube et al., 2017)*, T.piezophilus* (Dalmasso et al., 2016) *and P. kukulkanii* (Callac et al., 2016).

Most piezophiles identified in the deep sea are bacteria, they are psychrophiles and piezophiles. However, some archaea reside in hydrothermal vents, being hyperthermophiles and piezophiles (Fang et al., 2010) (Figure 9.3). Psychrophiles and hyperthermophiles piezophiles had follow different pathways to adapt to temperature and therefore, their pressure adaptation process may also be distinct. Beside temperature adaptation, piezophiles are acclimated to salt presence, *i.e.* they are slight halophiles, and finally, some piezophiles are also adapted to nutrient limitation, *i.e.* designated as oligotrophs (Daniel et al., 2006). Consequently, piezophiles may adopt a common strategy to cope with various stresses simultaneously and therefore it's tricky to identify and separate specific pressure-adaptation pathways from other stress adaptation (Zhang et al., 2015). Additionally, not all pressure-adaptation mechanisms are deleted at ambient pressure, and therefore the homologue piezosensitive organism may use the same mechanism (Oger and Jebbar, 2010), which hinders a possible comparison between mechanisms from piezophile and a similar pressure-sensitive organism.

Extremophiles have developed great capabilities to adapt to harsh and even fluctuating conditions (*e.g.* temperature, pressure, composition of the host rocks) thanks to synthesis of unique macromolecules, such as extracellular polysaccharides (Nicolaus et al., 2010), lipids (Oger and Cario, 2013), proteins (Reed et al., 2013) and even specialized organs (Bright and Lallier, 2010). These macromolecules adapted to extreme environments, such as high pressure, present a high potential to develop new biotechnological applications.

2.1. Genomes

To date, it has not been possible to detect any piezospecific gene. Consequently, it is not possible to determine if an organism is piezophile by molecular techniques, it is necessary to do cultivation approaches and to determine the growth rates at different pressures. However, it has been found that the pressure regulated operons ORFs 1–3 are distributed among different piezophilic *Shewanella* species (Li et al., 1998).

The high genetic manageability and hyper-responsiveness to pressure of the piezophile *Photobacterium profundum* strain SS9 has made it a reference for researchs on pressure adaptation. Studies on its RecD gene, responsible for a DNA-binding protein, indicates that this gene may have an important role for piezo adaptation together with its role of DNA metabolism and cell division (Abe et al., 1999; Bidle and Bartlett, 1999). This conclusion is sustained by the discovery of a pressure-sensitive mutant of SS9 that lacks the RecD gene and, besides, by the capability of *E. coli* to divide normally under HP after the transfer of this gene. Recently, it has been described that the gene Ypr153w is possibly responsible for the tryptophan permease's Tat2 stability in *Saccharomyces cerevisiae* under pressure. It is a gene

which has also been identified in other related species as *Debaryomyces* and *Candida* strains which have been isolated from sediment samples of deep sea floors (Kurosaka and Abe, 2018). Another possible HP adaptation could be the 16s rRNA longer stems found in strains from *Photobacterium*, *Colwellia* and *Shewanella* (Lauro et al., 2007).

2.2. Proteins

Relatively few enzymes from piezophiles have been studied under pressure. Although there are no apparent differences between the crystal structures of an enzyme from a piezophile and its piezosensitive homologue, there is a variation in the stability between both enzymes caused by a difference in flexibility and hydration of the proteins (Kitahara et al., 2000). Most molecular motion studies about pressure adaptation have been done *in vitro*, or investigating, for example, molecular dynamics (Q. Huang et al., 2017). Nevertheless, nowadays *in vivo* studies have gained in importance thanks to, for example, neutron scattering and NMR experiments that can examine timescales from few nanoseconds to hundreds of milliseconds (Boehr et al., 2010; Martinez et al., 2016; Peters et al., 2014).

It has been shown that some proteins are involved in HP adaptation as well as in adaptation to other stresses (Hsp60, Hsp70, OmpH, RecA, F1F0 ATPases, Cct and Tat2) (Bartlett et al., 1995). A system highly studied under pressure is the Omp/Tox system. The proteins ToxS and ToxR from *P. profundum* SS9 are responsible for regulating the genes that encode the membrane proteins OmpH, OmpL and OmpI. Pressure reduces the abundance and the activity of ToxR, which therefore upregulates the protein OmpH among others, the system acts as a piezometer. Regardless, the systems ToxS and ToxR do not confer HP adaptation and their role under pressure is not clear (Bartlett, 2002; Simonato et al., 2006).

The protein adaptation to extreme conditions is a balance between the imperative stability (higher number of bounds) to be functional and the flexibility (lower number of bounds) to be capable to adapt to different conditions (Feller, 2013). One of the most studied enzymes is dihydrofolate reductase (DHFR). Studies comparing DHFR from the piezosensitive *E. coli* and from the facultative psychro-piezophile bacteria *Moritella profunda* reveals that applying pressure decreases EcDHFR's activity and increases MpDHFR's activity up to 50 MPa before diminishing its activity at higher HP. MpDHFR seems to have higher sensitivity to pressure due to its higher flexibility (Ohmae et al., 2012). Such flexibility may explain the higher absolute activity of piezophile proteins (Ichiye, 2018).

However, most of the studies are done in protein-isolated solutions, which differs from their native state. An innovative quasi-elastic neutron scattering study examined the dynamics from whole cells of the piezophile *Thermococcus barophilus* and the piezosensitive *Thermococcus kodakarensis* microorganism under atmospheric pressure and 40 MPa. This study revealed that the HP adaptation on whole cells is based on an overall higher proteins'

flexibility within the cells and, in addition, on the modification of their hydration water layers (Martinez et al., 2016).

Proteins from piezophiles may have a larger total volume of small internal cavities, which makes the protein more compressible and less sensitive to distortion caused by pressure (Ichiye, 2018). Moreover, the presence of more cavities of small size allows water penetration at HP and consequently increases the hydration but, as seen in MpDHFR, cavities are not big enough to cause the protein denaturation but allow the protein to be more flexible. The presence of more small cavities could decrease the amount of water molecules contained in each cavity (a volume of $15A^3$ is necessary for a single water molecule and an increase of approximately $45A^3$ is required for each extra molecule (Sonavane and Chakrabarti, 2008)). It is important to consider that cavities are not mere "packing defects" but that they play a role in conformational changes and in controlling binding and catalysis of the proteins [106,107].

Generally, monomeric proteins are more resistant to pressure than oligomeric proteins. However, it has been shown that multimeric proteins may be adapted to resist pressure. For example, studies on the hyperthermophile and piezophile TET3 peptidase from *Pyrococcus horikoshii* indicate that the protein multimerizes into a dodecamer structure instead of conserving its classical barrel-shape multimer conformation. Dodecamer multimerization protects the hydrogen bonding between the different subunits and increases its stability against temperature and pressure up to 300 MPa (Rosenbaum et al., 2012).

A general extrinsic cell response to pressure-stress is the presence of piezolytes and other low weight organic compounds called osmolytes (e.g., sugars and amino acids) to protect cell macromolecules, such as proteins, from pressure modification (Jebbar et al., 2015) and therefore adapt their dynamics. Some piezophiles accumulate these low-weight molecules in response to an increase in pressure and others to a decrease, indicating in the latter case that the growth at lower pressure than optimal is perceived as a stress for these piezophiles (Oger and Cario, 2013). For example, trimethylamine oxide (TMAO) is a pressure co-solute that helps proteins to remain active under HP in certain fishes and crustaceans, while the hyperthermophilic and piezophilic *Thermococcus barophilus* accumulates mannosyl-glycerate when grown in sub-optimal conditions (ambient pressure) (Cario et al., 2016).

Few studies have been done on pressure adaptation of higher complex pluricellular organisms. For example, it is thought that the regulation of N-methyl-D-aspartate receptor (NMDR), a cell membrane protein found in nerve cells, is responsible for the absence of the high-pressure nervous syndrome (HPNS) on deep dive mammalians (Bliznyuk et al., 2018; Brown and Thatje, 2018). The regulation of this protein may be done by modulating its interaction with lipids, for example by the presence of cholesterol, and thanks to the protein's particular tertiary structure in piezo-tolerant organisms.

2.3. Membrane lipids

Cells have the capability to customize their cell membrane lipid composition metabolically to maintain it in a functional liquid crystalline phase with specific functional physicochemical properties, such as fluidity, permeability and membrane curvature, in spite of environmental stresses. This process is known as homeoviscous adaptation (Sinensky, 1974).

Eukarya and bacteria possess different lipids from those in archaea but their homeoviscous adaptations have similarities (Figure 9.4). Eukaryal and bacterial lipids are composed by straight hydrocarbon chains linked by ester bonds on 1,2 –*sn*- glycerol and a phosphodiester-linked polar group or sugar. On the other hand, archaeal lipids have isoprenoid hydrocarbon chains bound by ether bonds on 2,3-*sn*-glycerol. Partly, the adaptation of archaea to extreme conditions may thus rise from their particular lipid structure (Van de Vossenberg et al., 1998).

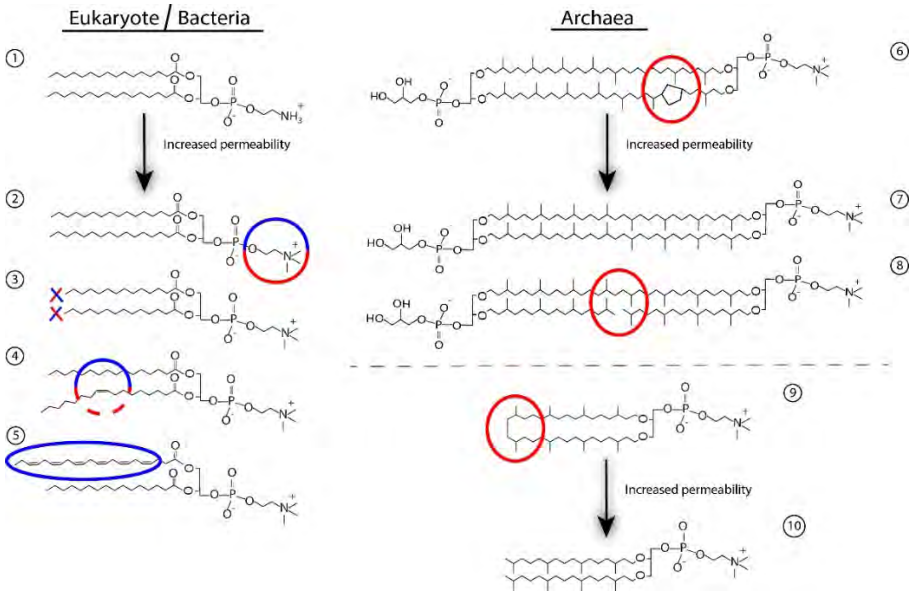

Figure 4. Different kind of homeoviscous adaptation to change membrane permeability according to environmental conditions. Blue: mechanisms present in eukaryote and bacteria; red: mechanisms present in archaea; blue and red: adaptation mechanism found in all domains. At left, bacteria-type phospholipids, for example, one lipid present in cell membranes is 1,2-dipalmitoyl-sn-glycero-3-phosphoethanolamine, DPPE (1), if organism change its lipid head group (phosphoethanolamine) to a bigger one (for example phosphatidylcholine, DPPC (2)) it will increase the membrane permeability. Another homeoviscous adaptation is to change the chain length, bacteria and eukarya can do it by adding or deleting two carbons, for example deleting two carbons from (2) would give to 1,2-dimyristoyl-sn-glycero-3-phosphocholine DMPC (3). Archaea may also change acyl chain length but with groups of 5 carbons (its subunit is the isoprene). Last, membrane permeability also increases by adding unsaturations in the hydrophobic regions of lipids, it will lead to, for example, 1,2-dioleoyl-sn-glycero-3-phosphocholine DOPC (4) and to all-cis-docosa-4,7,10,13,16,19-hexa-enoic acid (5). Monounsaturated lipids may also be present in archaea, but it is still controversial. Hydrophobic region of lipids from archaea are based on isoprenoid structures (5 carbons) and they possess a variety of head groups. Archaea has the capability to create glycerol dialkyl glycerol tetraethers GDGT (dipolar lipids) with cyclopentane rings, which will decrease membrane permeability, as in (6). Dipolar lipids in absence of cyclopentane rings are represented in (7) and glycerol tribiphytanyl glycerol tetraethers GTGT (dipolar lipids crosslinked) in (8). Archaea also presents monopolar lipids (10) designed as dialkyl glycerol diether DGD and it exists monopolar lipids crosslinked (9) which will be less permeable. For further details, see (Oger and Cario, 2013).

The common routes of lipid adaptation of deep-sea microorganisms' membranes are the change of the acyl chain length, the addition or removal of mono-unsaturated lipids and the change in the polar head groups (Oger and Cario, 2013; Siliakus et al., 2017). Longer acyl chains translate into more rigid membranes, in contrary adding just one unsaturation to lipid chains makes the membrane more permeable and larger head groups increase the membrane fluidity by disrupting the membrane packing. In addition, psychrophilic bacteria present polyunsaturated fatty acids (PUFAs), such as docosahexaenoic acid and eicosapentaenoic acid , which, just as lipids with one unsaturation, increase the permeability of the membrane under low temperatures (Usui et al., 2012). The function of PUFAs is not clear, one of the hypotheses is that they may play a role in cell division under HP, as demonstrated for *Shewanella violacea* (Kawamoto et al., 2011). Another hypothesis is that PUFAs, which also are highly specialized lipids from animals' cell membranes, are produced by bacteria as an interaction with deep-sea animals (Michiels et al., 2008). Last, another possibility is that, in addition to increase membrane permeability as mono-unsaturated lipids do, they may have an effect on energy production and conservation (Valentine and Valentine, 2004).

Besides that, archaea possess tetraether lipids, which may form a less permeable monolayer instead of the common bilayer. In addition, some archaeal species comprise lipids with cyclopentane rings and isoprenoid chains that are crosslinked, which decreases membrane permeability. The change in the different ratios from di- and tetra-ether lipids and the presence of cyclopentanes and crosslinked chains modifies as well the properties of the cell membrane.

Only two studies have been done to examine the lipid composition under pressure: one on *Methanocaldococcus jannaschii* and another on *T. barophilus* (Cario et al., 2015; Kaneshiro and Clark, 1995). Both present an increment in the diether: tetraether lipid ratio to counteract the increase in rigidity provoked by pressure on the cell membrane.

3. Pressure biotechnological applications

HP application is mostly used in food processing since it does not affect non-covalent interactions (at least up to 2 GPa) and it can inactivate bacteria and viruses without changing markedly nutrients and flavours of food. Furthermore, pressure can change the reaction rates, which may favour the extraction of the required product (Balasubramaniam et al., 2015).
Besides, pressure may be used for diverse biotechnological and biopharmaceutical applications, for example to explore new therapies (Adkins et al., 2018; Hradilova et al., 2017), conserve vaccines [123], improve cryopreservation (Gu et al., 2017) or for orthopaedics' surgery (Brouillet et al., 2009).

3.1. Food Industry

3.1.1. Food preservation

HP (400 — 600 MPa) inactivates microorganisms, like yeast, moulds and viruses. It affects the cell at different levels, such as nutrient transport and cell reproduction, lead to cell death (H. W. Huang et al., 2017; Wang et al., 2016). Moreover, HP hardly affects low-molecular weight compounds (*e.g.* amino acids, vitamins and flavour molecules), so organoleptic and nutritional properties are only slightly modified (Farkas and Hoover, 2000). Nevertheless, HP alone cannot inactivate bacterial spores and thus an association with other parameters, such as pH, chemicals or thermal processes may be needed. Nevertheless, pressure reduces considerably the working temperature, as 70 °C instead of 180 °C is enough to inactivate spores if it is combined with 600 MPa (Wang et al., 2016). Such decrease in temperature can help preserve quality and minimise off-flavour generations. Therefore, HP techniques are useful as a complement on thermal processes but also to inactivate microorganisms on products where temperature cannot be applied. As an illustration, high pressure pasteurization of cold-pressed juices eliminates pathogens without impairment of its fresh-like qualities increasing the shelf life of the product (Bull et al., 2004; Polydera et al., 2003).

HP extends the shelf life of a high variety of food products. For example, fresh shrimps treated at 435 MPa have a shelf life of 15 days, three times longer than the shelf life of the untreated shrimps (Kaur et al., 2015). Similarly, fresh cheese treated at 300–400 MPa has a shelf life at 4 °C of 14–21 days, which is greatly higher than the 7 days for the untreated cheese (Evert-Arriagada et al., 2012).

Food is a complex matrix and inactivation efficiency depends on different factors as treatment conditions, microorganisms to inactivate and its food matrix characteristics. For example, meat treated at 300 MPa has a cooked like appearance but if it is processed at 100–200 MPa and 60 °C, it is more tender than the untreated meat (Sazonova et al., 2017). Consequently, inactivation conditions must be defined for every food product. HP is not efficient for low water content food (such as flour) or food with high content of air bubbles and if the food needs to be wrapped before treatment only plastic packaging is acceptable, as packaging material needs a compressibility of at least 15% (H. W. Huang et al., 2017).

3.1.2. Pre-treatment

HP may also be applied as a pre-treatment. On the one hand, it has been demonstrated that the application of sublethal HP on cells gives them cross-resistance to other stresses. This opens the possibility to improve the survival of microorganisms of health interest during food processing and preservation. For example, the most studied probiotic, *Lactobacillus rhamnosus,* is more resistant to heat after an application of 100 MPa for 10 min (Ananta and Knorr, 2004), this cross resistance may be important to maintain it after milk processing.

On the other hand, pre-treatment can be useful to facilitate the extraction of internal nutritional components. HP increases cell permeability, thus facilitating the mass transfer rate, and finally, increasing the release of extracts. It has been shown that the time extraction of caffeine from green tea leaves is reduced from 20h to 1 min if a pressure of 500 MPa is applied; extraction of anthocyanin from red grape skin is increased by 23% by applying 600 MPa of pressure and the extraction yield of gingenosides from *Panax quinquefolium* root increases linearly between 100 MPa and 500 MPa (Zhao et al., 2014).

3.1.3. Allergenicity and digestibility

Several proteins can provoke allergic reactions caused by an immune disorder on the IgE binding. Because HP tends to denature proteins, it has been shown to induce a modification of their allergenicity (Vanga et al., 2017), both on protein solutions and on food systems. For example, pressures of 300–700 MPa reduce the allergenicity of a ginkgo seed protein and of soybean allergens (Zhou et al., 2016). Another interesting example is the use of HP together with proteases to obtain hypoallergenic rice (Kim et al., 2015; Peñas et al., 2011). However, the effect of HP on allergenicity is not universal. There is no allergenicity change caused by pressure on almonds, or on the protein Mald1 from apples (Houska et al., 2009; Li et al., 2013). Mald1 native state possess a high internal cavity occupied by water (Ahammer et al., 2017) and therefore, pressure may not be able to conform significant hydration changes since the protein is already highly hydrated.

HP may not only influence the allergenicity of the food products but can also help to increase its digestibility by exposing inaccessible sites of proteins and, thereby, enhancing the efficiency of protein hydrolysis. For example, the time required for proteolysis of β-lactoglobulin, the major allergen in cow's milk, is reduced from 48h to 20 min at 200 MPa (Chicón et al., 2008).

3.2. Medical applications

3.2.1. Antiviral vaccines

Several viruses are inactivated or dissociated by pressure. Under pressure, the atomic contacts among subunits are superseded by interactions with the solvent and therefore once pressure is released, viruses cannot come back to their native form. For example, pressure inactivates picornaviruses by causing the lack of VP4 from the intern capsid (Oliveira et al., 1999). Both viruses with polyhedral and helicoidal symmetry are sensitive to pressure. Even so, not all viruses are equally reactive to pressure. For example, the foot-and-mouth-disease picanovirus is highly sensitive, but poliovirus is much more resistant to HP (Oliveira et al., 1999).

Interestingly, viruses re-associate under their fusogenic state under pressure, a less infectious and highly immunogenic form (Dumard et al., 2017; Oliveira et al., 1999; Silva et al.,

1996). This is why high pressure has been suggested for antiviral vaccine development. It has been demonstrated that immunization against HP-inactivated virus is equally effective as against intact virus and has a higher immunity response than isolated viral subunits (Silva et al., 2002, 1992).

3.2.2. Bacterial ghosts

Bacterial ghosts are empty cell envelopes, they are usually obtained by the expression of a lysis gene that lead to the cell material leakage. As their cell surface is not affected, they retain immunogenic properties and they are usually used as delivery systems for subunit or DNA based vaccines (Hajam et al., 2017; Tabrizi et al., 2004). Antigen-presenting cells, like dendritic cells and macrophages, interacts very effectively with these bacterial ghosts. HP allows a new method to produce them, but in contrary to bacterial ghosts produced by lysis gene, HP-produced bacterial ghosts retains their cell material. This may be an advantage as it will not be necessary to insert the macromolecules to deliver after cell lysis. For example, HP bacterial ghosts have been obtained by applying a pressure of 100 MPa for 15 min to *E.coli* (Vanlint et al., 2008).

3.2.3. Vaccine preservation

Most vaccines are heat labile, which confers problems of access to them as they need to be kept under refrigeration during their transport and preservation. HP may be a solution to this problem since it could confer heat resistance to attenuated virus. For example, it has been demonstrated that pressures of 310 MPa stabilizes attenuated poliovirus, one of the most heat labile vaccine, at temperatures of 37ºC (Ferreira et al., 2009).

3.2.4. Cryopreservation

Oocyte cryopreservation by vitrification is one technique used to maintain women's fertility but blastocyst formation rate after this process is still low due to the production of ROS components, therefore techniques to improve it are being studied. As remarked above, sublethal HP stress makes the cells more resistant to thermal treatments and oocytes are not an exception. For example, pig oocytes, bovine and mouse blastocysts show a higher resilience against cryopreservation after receiving a non-lethal HP treatment (Pribenszky et al., 2008, 2005; Saragusty and Arav, 2011). Moreover, it has been demonstrated that HP treatment (20-40 MPa for 90-120 min) of bull and boar spermatozoa before cryopreservation preserve their viability, motility and fertility (Gu et al., 2017).

3.3. Biotechnological applications

3.3.1. Bio-purification

An antigen may be purified from its medium by affinity chromatography due to a steric recognition with an antibody linked to a matrix. The recognition causes an increase in molecular volume and, as pressure causes a volume decrease, it could be useful to apply pressure to dissociate the product of interest without using drastic elution processes which reduce the lifetime of matrices (Lemay, 2002). This has been demonstrated for the recovery of β-galactosidase: four 15 min cycles of 150 MPa at 4°C recovers 32% of *E. coli* β-galactosidase compared with the 46% recovered by adding a solution of pH=11 (Estevez-Burugorri et al., 2000). Although the product yield is lower when using HP, the method is simpler and has a lower impact on matrices than the current elution process.

HP ability to disrupt immune complexes has been proven on anti-prostate specific antibody from its antigen (Cheung et al., 1998; Estevez-Burugorri et al., 2000), its dissociation was increased by 22-37% when pressures from 140 to 550 MPa were applied. Pressure may also optimize the dissociation of amphiphilic biomolecules from a fixed adsorbent: 80% of Triton-X can be recovered form a bed absorption if a pressure of 250 MPa is applied on the system (Niemeyer and Jansen, 2007).

Last, as pressure can dissociate aggregates, it may be used for the retrieval of proteins from inclusion bodies, *i.e.* aggregates of incompletely folded proteins. Traditionally, to separate proteins from inclusion bodies it is necessary to use high concentrations of agents that destroy the spatial structure of proteins with a necessary subsequent difficult refolding. However, a pressure of 240 MPa is effective to dissociate the inclusion bodies of endostatins and a subsequent application of 40 MPa induces the refolding of 78% of the protein (Chura-Chambi et al., 2013).

3.3.2. Modulation of cell activity

Already relative low applied pressures can enhance the cell activity to our profit, as for example observed at 10 MPa for ethanol production by *Saccharomyces cerevisiae* (Picard et al., 2007) which occurs three times faster than at atmospheric pressure. Another example is on the fermentation by *Clostridium thermocellum* (Bothun et al., 2004). This *Clostridium* transforms cellobiose to biofuels but also synthesizes additional non-desired products (*e.g.* acetate, H_2, CO_2). When the fermentation happens under pressure of 7 or 17 MPa, the microorganism modifies the metabolic pathways and shifts the production to desired metabolites, reaching an increase of 60-fold.

However, as HP is considered a stress for most cells, it will translate into the expense of additional energy for cell maintenance and growth, reducing the product yield. For example, HP reduces the fermentation rate of lactic acid fermentation due to the inhibitory

effect on the growth of *Streptococcus thermophilus*, *Lactobacillus bulgaricus* and *Bifidobacterium lactis* (Mota et al., 2015). To avoid the loss of efficiency rates under HP, efforts are made to enhance the resistance of mesophilic microorganisms to HP, leading to organisms with higher performance under HP (Mota et al., 2013).

4. Biotechnological applications of piezophiles

There are more than 3000 enzymes identified to date and most of them are used for biotechnological applications. Nevertheless, these enzymes are not enough to respond to the new technological challenges that appear each day (Dumorné et al., 2017). One of the problems is the stability of the enzymes under industrial conditions, so it is necessary to find enzymes which are highly resistant to harsh conditions and here deep-sea enzymes may play a major role. Pressure-stable enzymes are able to conduct biocatalysis under HP, modifying therefore specific enzymatic reactions, and have even higher thermostability. For example, Biolabs® has already commercialized a DNA polymerase from a hyperthermophile and piezophile *Pyrococcus*, which presents a half-life of 23 hours at 95 C (Deep Vent DNA Polymerase, Catalog #M0258L, New England BioLabs, Inc) (Hikida et al., 2017). Moreover, piezophile enzymes may possess different properties than their surface homologues, which may open new possibilities for industry (Schroeder et al., 2018). The market for industrial enzymes is growing every year and the exploitation of extremozymes is a huge and mostly unexplored resource (Dalmaso et al., 2015).

As we have seen, lipids from extremophiles are unique. Archaea in particular contain lipids which confer to the cell a highly stable and impermeable membrane. The unique stability may be used in biotechnological or pharmaceutical applications, for example to protect therapeutic peptides from the harsh environment of the gastrointestinal tract (Benvegnu et al., 2009; Jacobsen et al., 2017). Additionally, lipids from many piezophile bacteria comprise omega 3-PUFAs within their cell membrane, which are precursors of hormones in many animals. Consequently, it could be used for treatment of hypertriglyceridemia diseases and clinical studies for this purpose have already been approved (Schroeder et al., 2018).

The high marine biodiversity has woken up the interest to search new compounds with biopharmaceutical potential (Tortorella et al., 2018). Marine derived molecules may present beneficial functions as, for example, antitumor potential, pain reliever, or antimicrobial activities (Jacobsen et al., 2017; Schroeder et al., 2018; Tortorella et al., 2018). For instance, studies have identified some bioactive compounds from marine echinoderms (such as the piezotolerant *Cucumaria frondosa*) with antiproliferative, antimetastatic and immunomodulatory activities (Janakiram et al., 2015).

5. Conclusion and future perspectives

All pressure-specific impacts allow to modify macromolecules and cells in unique ways. For example, HP is capable to alter reaction rates since it induces a shift towards the state with the smallest volume. Moreover, such volume modification may be also useful for purification of chromatography systems and, since HP is able to change protein structures, to decrease food allergenicity and produce antiviral vaccines. Pressure affects most of cell functions and among them, increases cell permeability, which can be advantageous to facilitate food extraction. Furthermore, application of non-lethal pressures provides the cell with resistance to other stress, such as temperature. This characteristic has been largely studied as a pre-treatment for probiotics, vaccines' preservation and oocytes' cryopreservation. Last, employment of lethal pressures inactivates undesired microorganisms without affecting covalent bonds of nutrients, such technique is already used by food industry to increase products' shelf life.

Food industry was pioneer in using pressure to inactivate microorganisms or as a pre-treatment and, although HP processing still constitutes a minority, the development of HP equipment and the increase in manufacturers have boost the number of HP industrial machines to more than 300 and this global market to $9.8 billion in 2015 (H. W. Huang et al., 2017). Nevertheless, pressure capability does not stop here. Promising applications, such as antiviral vaccines, the use of pressure for bio-purification or to modify cell activities has led to a greater interest on this physical parameter. In addition, piezophile organisms open a range of possibilities to use pressure-adapted molecules, and for example, give access to highly thermostable enzymes, which may even possess favourable enzymatic rates. Moreover, they provide a major opportunity to find new bioactive molecules for medicine and biotechnological applications, such as antitumor or pain reliever molecules found in marine biosphere.

Review II. In search for the membrane regulators for Archaea

Marta Salvador-Castell [1,2] , Maxime Tourte [1,2] and Philippe M. Oger [1,2,*]

[1] Université de Lyon, CNRS, UMR 5240, F-69621 Villeurbanne, France
[2] Université de Lyon, INSA de Lyon, UMR 5240, F-69621 Villeurbanne, France
***** Correspondence: philippe.oger@insa-lyon.fr

Published in International Journal of Molecular Sciences:

Salvador-Castell, M., Tourte, M., Oger, P.M., 2019. In search for the membrane regulators of Archaea. *International Journal of Molecular Sciences* **20**, 4434. https://doi.org/10.3390/ijms20184434

International Journal of
Molecular Sciences

MDPI

Review

In Search for the Membrane Regulators of Archaea

Marta Salvador-Castell [1,2], Maxime Tourte [1,2] and Philippe M. Oger [1,2,*]

[1] Université de Lyon, CNRS, UMR 5240, F-69621 Villeurbanne, France
[2] Université de Lyon, INSA de Lyon, UMR 5240, F-69621 Villeurbanne, France
* Correspondence: philippe.oger@insa-lyon.fr

Received: 7 August 2019; Accepted: 6 September 2019; Published: 9 September 2019

Abstract: Membrane regulators such as sterols and hopanoids play a major role in the physiological and physicochemical adaptation of the different plasmic membranes in Eukarya and Bacteria. They are key to the functionalization and the spatialization of the membrane, and therefore indispensable for the cell cycle. No archaeon has been found to be able to synthesize sterols or hopanoids to date. They also lack homologs of the genes responsible for the synthesis of these membrane regulators. Due to their divergent membrane lipid composition, the question whether archaea require membrane regulators, and if so, what is their nature, remains open. In this review, we review evidence for the existence of membrane regulators in Archaea, and propose tentative location and biological functions. It is likely that no membrane regulator is shared by all archaea, but that they may use different polyterpenes, such as carotenoids, polyprenols, quinones and apolar polyisoprenoids, in response to specific stressors or physiological needs.

Keywords: archaea; membrane organization; membrane modulators; polyterpenes; carotenoids; polyprenols; quinones; polyisoprenoids; adaptation

1. Introduction

In 1972, Singer and Nicolson reconciled the numerous observations about cell membranes to construct the now well-established fluid mosaic model [1]. Since then, the ultrastructure of cell membranes has further evolved to accommodate the lipid phases, i.e., gel or liquid crystalline, lipid phase partition, membrane curvature and the presence of lipid membrane regulators, which are currently gaining much attention in membrane structuration, function and regulation [2–4]. Lipid membrane regulators allow to expand the functional state of the lipid membrane to broader environmental conditions. The best studied membrane regulator is cholesterol, a sterol derivative present in animal cell membranes [3,5–10]. Although Bacteria do not synthesize sterols, their hopanoids have been accepted as "sterol surrogates" [11,12]. Sterols or hopanoids are absent in Archaea, and whether Archaea have membrane regulators remains a hotly debated question. The current review sums up the data available on putative archaeal membrane regulators and poses the groundwork for their identification in Archaea.

2. Structure of Bacterial and Eukaryal Membrane Regulators

Sterols are the most well-known lipid membrane regulators. The term sterols covers a variety of compounds synthesized from 2,3-epoxide-squalene and consisting of an aliphatic chain with 7–10 carbons and four flat fused rings, the outermost one exhibiting an sn-3 hydroxyl group [6]. The three major kingdoms of the Eukarya, e.g., mammals, fungi and plants, synthesize different types of sterols, cholesterol, ergosterol and sitosterols and stigmasterols respectively. Hopanoids are pentacyclic triterpenoids synthesized from squalene. Such term regroups C30 derivatives such as diploptene, a hydrophobic molecule, and C35 molecules such as bacteriohopane, and their

derivatives [13]. In hydrophilic hopanoids, hydroxyl groups are bound to the branched aliphatic chain, which therefore results in an "inverted" polarity in comparison to sterols. Sterols and hopanoids belong to a much larger group of natural compounds called polyterpenes, i.e., hydrocarbon oligomers resulting from successive condensations of isoprene precursors, namely, isopentenyl pyrophosphate (IPP) and dimethyallyl diphosphate (DMAP) (Figure 1). Polyterpenes represent one of the largest class of naturally occurring compounds and are widely distributed in Eukaryotes, Bacteria as well as Archaea. Although all polyterpenes of the three domains of life originate from IPP and DMAP, these precursors are synthesized via two independent, non-homologous pathways: the methylerythritol 4-phosphate pathway in Bacteria and the mevalonate pathway in Eukaryotes and Archaea [14,15].

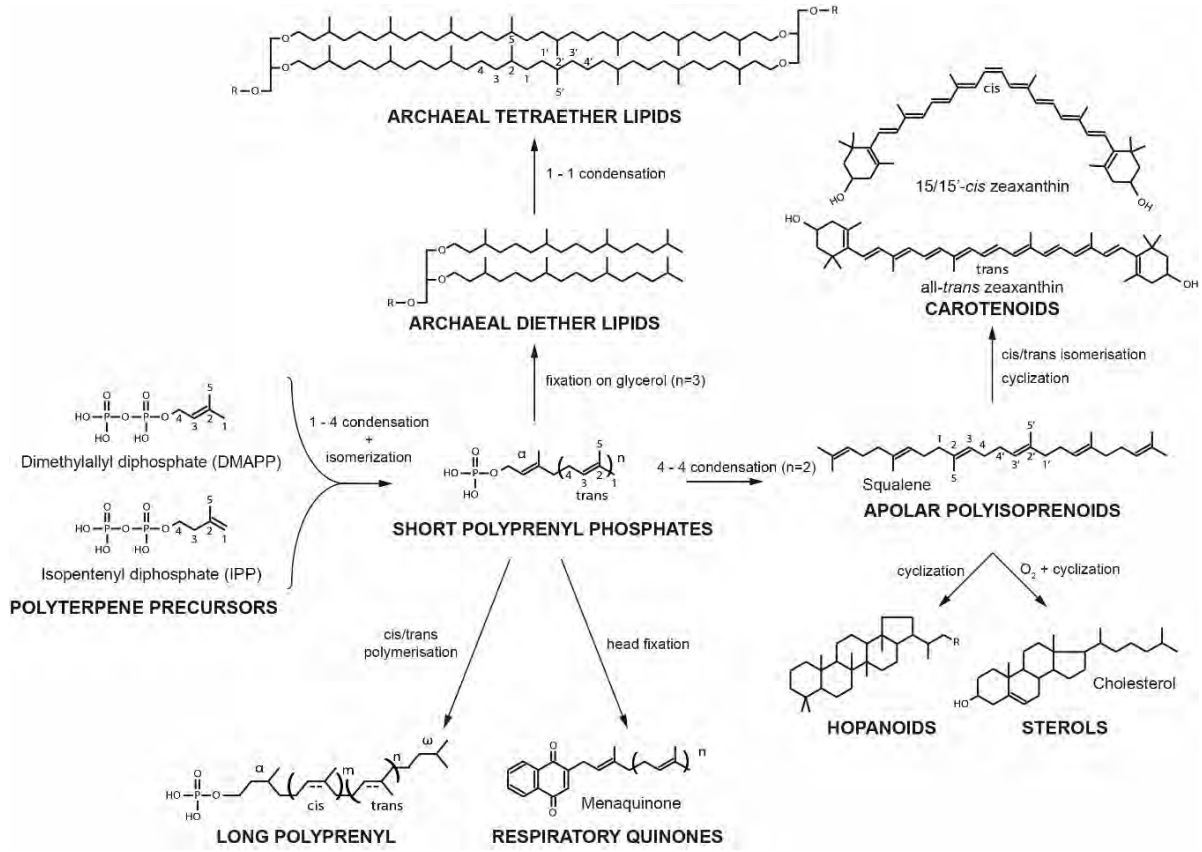

Figure 1. Most representative polyterpenes and their biosynthetic link. Carbon nomenclature and isoprene conformations are indicated as mentioned hereafter.

3. Mechanisms of Membrane Regulation in Eukarya and Bacteria

The impact of sterols, and particularly of cholesterol, on lipid membranes has been largely studied. Sterols are oriented perpendicular to the membrane surface with the hydroxyl facing the phospholipid ester carbonyl and stabilize the functional phospholipid liquid-crystalline phase, i.e., decrease gel-to-liquid lipid phase transition temperature (T_m). Sterols modulate membrane parameters by tightening and reducing the average tilt of phospholipid acyl chains [16], therefore decreasing acyl chains' motion [17] while increasing the viscosity and the order of lipid membranes [18]. They also limit lipid membrane passive permeability to ions and small molecules [17]. Last, cholesterol is the essential component of the thicker liquid-ordered phase present in eukaryotic cell membranes, previously called "lipid raft", which is essential for membrane functional differentiation. This cholesterol-induced lipid phase leads to a discontinuity of the membrane boundary and, therefore, to a line-tension between both phases [19]. This tension may facilitate cell membrane bending and, consequently, cell processes as fusion and fission, which are essential for numerous physiological mechanisms including cell division, cell compartmentalization or vesicle formation.

The hydrophobic hopanoid, diploptene, is placed in the midplane of the lipid bilayer with an average tilt angle of about 51° to the membrane plane, whereas bacteriohopanetetrol presents an orientation similar to that of cholesterol with an average tilt angle of 14° [20]. Hopanoids, although with different efficiencies, can induce order and decrease fluidity and permeability of model membranes, even though they do not show a significant effect on bilayer elasticity [12,13,20,21]. Similarly to cholesterol, hopanoids can induce the formation of more ordered phases at physiological concentrations [20]. Whether they are involved in membrane domain formation in Bacteria remains to be demonstrated.

4. Candidate Surrogates for Sterol and Hopanoid Membrane Regulators in Archaea

As Archaea apparently lack both sterols and hopanoids and considering the physiological importance of membrane regulators in bacterial and eukaryal membranes, we can suppose the existence of membranes regulators in Archaea as well. However, one has to keep in mind that archaeal and bacterial/eukaryal lipids strongly differ in their structure. The former ones being based on ether-linked isoprenoid chains, while the later are ester-linked fatty acids. Regardless, the numerous functions of sterols/hopanoids in the membranes, and especially their importance in maintaining membrane functionality under stress conditions, are coherent with the way of life of Archaea, which generally thrive in the most extreme environments. Since Archaea are supposed to be one of the most ancient phylum on Earth and that isoprenoid lipid synthesis can be traced back to the last universal common ancestor [22], we hypothesize that lipid regulators in Archaea should also originate from the isoprenoid synthesis pathway, be widely distributed in Archaea and impact cell membrane properties. The next sections present an exhaustive collation of the data on the four types of polyterpenes that have been found in Archaea, i.e., carotenoids, polyprenols, quinones and apolar polyisoprenoids.

5. Carotenoids

Carotenoids comprise a large group of natural polyterpene pigments synthesized in the three domains of life [23]. They present a characteristic end-group on each side of a polyprenyl chain that usually contains eight or ten isoprene units. To date, about 1200 natural carotenoids have been identified [24] and are classified in two subclasses as a function of the polarity of their end-groups: apolar and polar end-groups for Carotenes and Xantophylls, respectively. Carotenoids may be further divided into two subcategories according to the conformation of their polyprenyl chain. Trans-carotenoids, have only trans-unsaturations, a linear structure and present their functional groups on different sides of the carbon chain. Cis-carotenoids harbor a cis-unsaturation, which induces a kink in the chain and exposes their functional groups on the same side of the carbon chain (Figure 1).

5.1. Distribution in Archaea

Very little is known about the distribution of carotenoids in Archaea, as only the Natrialbales, Halobacteriales and Haloferacales orders, as well as few species of the Sulfolobales order were investigated so far (Figure 2A). A diversity of xanthophylls, e.g., zeaxanthin, astaxanthin, canthaxanthin, 3-hydroxyechinenone and bacterioruberin, together with their precursor, isopentenyldehydrorhodopin, were identified in these archaeal orders (Figure 2A) [25–30]. In contrast to plants or bacteria which synthesize a large diversity of carotenes, β-carotene is the only carotene identified in Archaea [26,31,32]. Carotenoids may represent a significant fraction of lipids, such as 0.2% (*w/w*) in *Haloferax alexandrinus*, an extreme halophile, most of them being bacterioruberin and canthaxanthin with small quantities of 3-hydroxyechinenone and β-carotene [26]. Similarly, significant quantities of bacterioruberin were found in *Haloferax japonica,* another extremely halophilic archaea [33]. In contrast, only zeaxanthin was identified in the thermoacidophilic archaeon *Sulfolobus shibatae* [25].

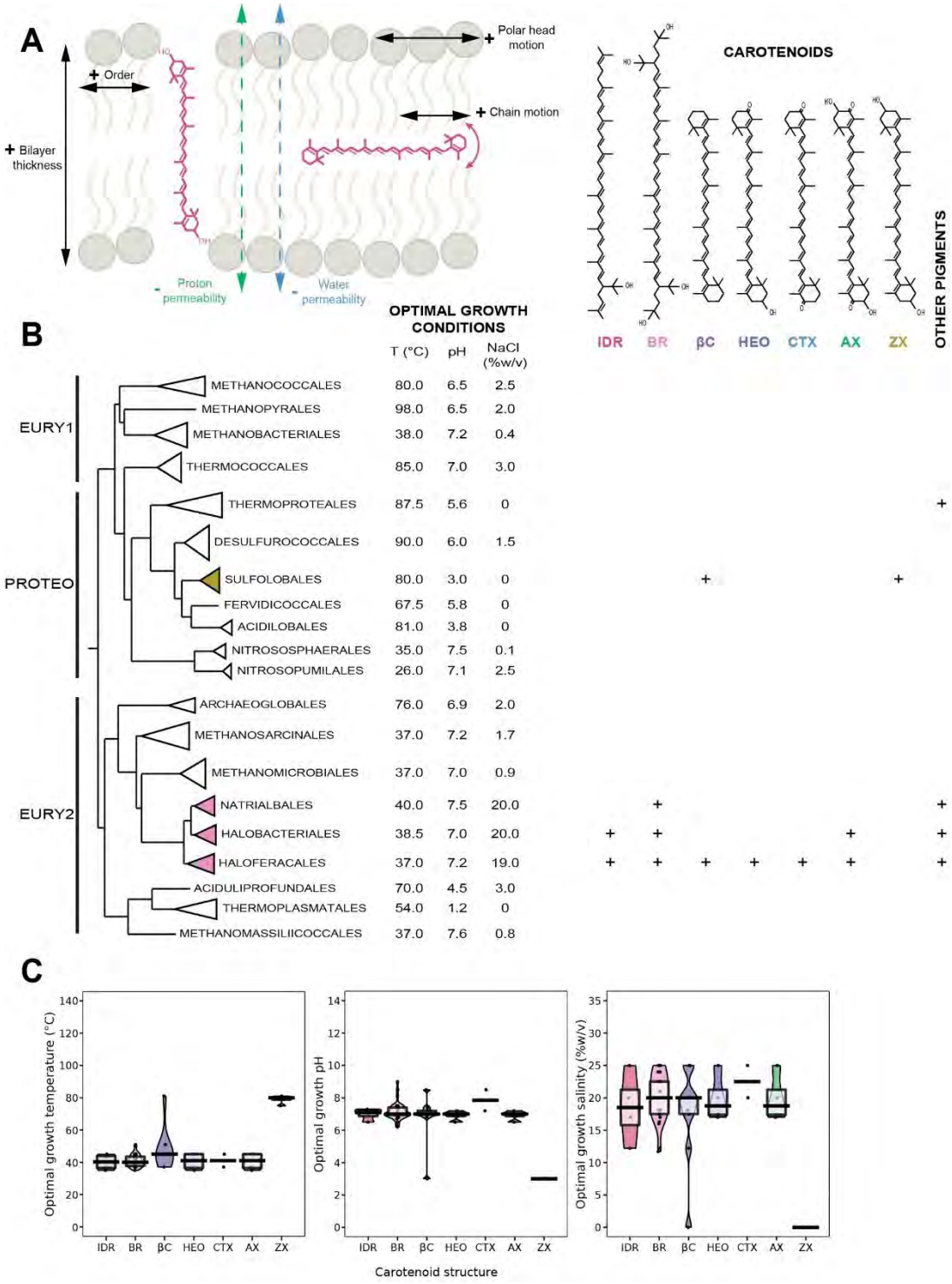

Figure 2. Physicochemistry, distribution and adaptive response of carotenoids in Archaea. (**A**), Position and impacts of carotenoids on membrane physicochemical properties. (**B**), Structures and distribution of carotenoids within the Archaea domain. The tree topology has been adapted from [34]. (**C**), Pirateplot of the optimal growth conditions of the organisms in which the different types of carotenoids were detected. Colors indicate the chain lengths as in B. Abbreviations: IDR, isopentenyldehydrorhodopin; BR, bacterioruberin; BC, β-carotene; HEO, 3-hydroechinenone; CTX, canthaxanthin; AX, astaxanthin; ZX, zeaxanthin. EURY1, Euryarchaeota cluster I; PROTEO, Proteoarchaeota; EURY2, Euryarchaeota cluster II.

5.2. Biological Function of Carotenoids

There is only scarce specific data on the biological function of carotenoids in Archaea. However, it is well-established that carotenoids act as antioxidants and protect cell membrane against the oxidative effect of free radicals via direct quenching in Bacteria and Eukarya [35]. The antioxidant effect of carotenoids has been established in vitro [35–37] and in vivo [38]. Early studies have shown that the scavenging of radical cations is higher for apolar carotenoids [39], and that the number of unsaturations, the type of end-groups or the membrane lipid composition define their antioxidant properties [40,41]. Carotenoids also play a role in the modulation of the physicochemical properties of membranes [42]. For example, bacterioruberin is an essential part of specific transmembrane proteins [43,44] and controls membrane organization through its high impact on membrane physics and dynamics [45]. Therefore, it is reasonable to assume similar antioxidant or membrane regulator functions in Archaea, especially in the view that many archaea are extremophiles. However, one should not forget that the function of carotenoids is affected by its lipid environment, and thus may significantly differ between Archaea and Bacteria/Eukarya.

5.3. Insertion of Carotenoids in the Membrane

The insertion of carotenoids in the membrane depends on their polarity. Apolar carotenoids insert within the hydrophobic part of the lipid membrane. β-carotene, which is the only one found in Archaea, is placed in a bacterial bilayer at 55° from the axis normal to the plane of the membrane [42], although it retains a considerable mobility [46]. In contrast, polar carotenoids, which possess two polar regions placed at each side of the isoprenoid chain, are oriented parallel to the fatty acid chains with their polar end groups anchored in the headgroup regions on both sides of the membrane, therefore physically bridging the two lipid leaflets of the bacterial bilayer. Due to the similar backbone of carotenoids and archaeal lipids, it is probable that both polar and apolar carotenoids may be inserted alongside the isoprenoid chains of the lipids and that their mobility may differ largely from that found in Bacteria. The polar and apolar carotenoids found in Archaea are all based on a β-carotene structure, which length has been estimated at 32 Å and 38 Å for astaxanthin and bacterioruberin, respectively [4,5,21]. Molecular dynamics simulations have found a thickness of 39 Å for the archaeal tetraether monolayer [47]. A similar thickness, 38 Å, is measured for the archaeal bilayer (Salvador Castell/Oger, unpublished results), which means that bacterioruberin may correctly connect both leaflets of the phospholipid bilayer in specific regions of the cell membrane and easily interact with transmembrane proteins. It is still unclear how the known short archaeal polar carotenoids, i.e., hydroechinenone, canthaxanthin, astaxanthin, zeaxanthin, (Figure 2B) would insert in the monolayer of the Sulfolobales or in the bilayer membrane of halophiles.

5.4. Carotenoids as Putative Membrane Regulators in Archaea

In Bacteria, carotenoids exhibit numerous similarities with membrane regulators. Furthermore, 10 mol% of polar carotenoids has a similar impact on the structure and dynamic properties of membranes as 15–20 mol% of cholesterol: an increase in order which impacts the rigidity of lipid membranes [48], and decreases membrane fluidity [49] and a decrease in alkyl chain motion (liquid-ordered phase) [36,48,50]. Moreover, carotenoids decrease water [46], small molecules [51] and proton permeability [52] and penetration of oxygen [53], decrease T_m by about 1.5–2.5 °C [41] and reduce lipid cooperativity [41] (Figure 2A). Similarly to cholesterol, unsaturations on the lipid hydrocarbon chains decrease the physical impact of xanthophylls [54]. Xanthophylls disturb the membrane polar region [55] and promote the adhesion [56], aggregation and fusion of liposomes [57], which may indicate a change on the intrinsic membrane curvature [58]. Carotenoids display the physicochemical impact on membranes as true membrane regulators, and thus could play this role as well in archaeal membranes, which would constitute a fast and efficient adaptation mechanism to changing external conditions. Although, due to the limited data available, no clear adaptive correlation can be drawn today (Figure 2C), several observations

support this view. For example, carotenoids are powerful scavengers of free radicals in halophilic archaea. Indeed, the absence of bacterioruberin in *Halobacterium salinarum* increases the effect of DNA-damaging agents such as UV and ionizing radiations, hydrogen peroxide and mitomycin-C [28,59]. The production of carotenoids is also dependent on growth conditions [60], such as sub-optimal [61,62] or supra-optimal salinity [63,64], illumination and oxygenation [65]. Thus, carotenoids may help prevent cell lysis under non-optimal growth conditions by increasing the stability of cell membranes. Unfortunately, due to the limited data available, no adaptive correlation can be drawn (Figure 2C).

6. Polyprenols

Polyprenols are a family of diverse membrane-bound linear polyisoprenoids found in the three domains of life. They have various biological functions, such as biosynthesis of higher terpenes, protein prenylation and glycosylation as well as protection of lipids against peroxidation [66]. Polyprenols have polyisoprenoid chain lengths ranging from 2 up to 100 isoprene units, the eukaryotic polyprenyl alcohols being generally longer (C90–100) than their bacterial and archaeal homologs (C55). Polyprenols have a restricted type of polar headgroups, e.g., alcohol, phosphate or diphosphate. The polyisoprenoid chains are either all-*trans*, such as in the ones involved in terpene synthesis, or of the *cis* type, as is the case for the majority of membrane-bound polyprenols [67]. In polyprenols, the isoprene closest to the polar head is referred as the alpha-unit and the omega-unit is the farthest. Despite their large structural diversity, polyprenols are sorted in only two classes: (1) polyprenols, in which the alpha-unit is unsaturated and (2) dolichols, where the alpha-unit is saturated [68]. Such alpha saturation only has minor impacts on molecular properties as polyprenol and dolichol derivatives behave and locate similarly within membrane bilayers [69]. However, polyprenols are assumed to belong to the dolichol type in Eukarya and Archaea and of the polyprenol type in Bacteria [68].

6.1. Distribution in Archaea

As critical lipid carriers for membrane protein glycosylation, polyprenols were looked for in the three domains of life and are somewhat well documented in Archaea. As mentioned above, Bacteria mostly produce polyprenols with 11 isoprene units, even though molecules with eight to 12 units have been reported [70,71]. Gram-negative bacteria synthesize only polyprenyl-alcohols, whereas phosphate derivatives dominate in gram-positive bacteria [68]. In contrast to Bacteria, Eukaryotes produce dolichols of a wider range of chain lengths. For instance, dolichols possess 18 to 21 isoprene units in mammals and dolichols with up to 40 units were detected in plants [72,73]. Although the proportions might vary according to cell types, phosphate derivatives remain the dominant form of polyprenols in Eukaryotes [68]. Nevertheless, dolichyl-alcohol may represent up to 90% of the dolichol derivatives' pool, even though their function still remains unclear [74]. In contrast to Bacteria, in which the alpha-isoprene unit is unsaturated, and to Eukarya, in which the alpha-isoprene unit is the only saturated isoprene, dolichols with both saturated alpha- and omega-isoprene units were detected in every Archaea [75] (Figure 3B). Dolichyl-phosphates have been identified as the most physiologically relevant form of polyprenol derivatives in Archaea, and are present in all groups studied to date. Similarly to Bacteria, the most common polyprenols in Archaea consist of 11 isoprene units, but polyprenols with six to 14 units were detected in *Sulfolobus acidocaldarius* [76] and *Pyrococcus furiosus* [77] (Figure 3B). Apart from the alpha- and omega-isoprene units, the degree of unsaturation is highly variable, ranging from fully saturated to fully unsaturated molecules, even in a single archaeal species, such as *Sulfolobus acidocaldarius* [76]. Thus, although only polyprenyl-phosphates might be present in archaeal membranes, which may partake in protein glycosylation, a large variety of polyprenol side chain structures of yet-unidentified function has been revealed in Archaea (Figure 3B). Interestingly, dolichyl-alcohols were also detected in Archaea, but only in the methanogenic archaea Methanobacteriales and Methanomassillicoccales [78,79] while the rest of the methanogens, such as Methanococcales and Methanosarcinales, produce dolichyl-phosphates [80,81]. However, it should be considered that dolichyl-alcohols were only observed when using an acidification step during lipid extraction [78,79], which may have led to the hydrolysis of the polar head group

and introduce an analytical bias [78,82]. Dolichyl-diphosphates were identified only in Crenarchaeota [83], whereas dolichyl-monophosphates were found in every other Archaea (Figure 3B) [84]. In addition, we show here that the euryarchaeal cluster I/proteoarchaea species tend to produce shorter polyprenols, i.e., around 10 isoprene units, than their counterparts of the euryarchaeal cluster II, i.e., around 12 units (Figure 3B). Similarly to Crenarchaeota, Eukaryotes also use long, dolichyl-diphosphates, which further supports the putative proteoarchaeotal ancestry of Eukaryotes [85]. Further studies of archaeal polyprenols, and especially within Crenarchaeota, would thus shed light on one of the currently most debated topics in evolutionary biology.

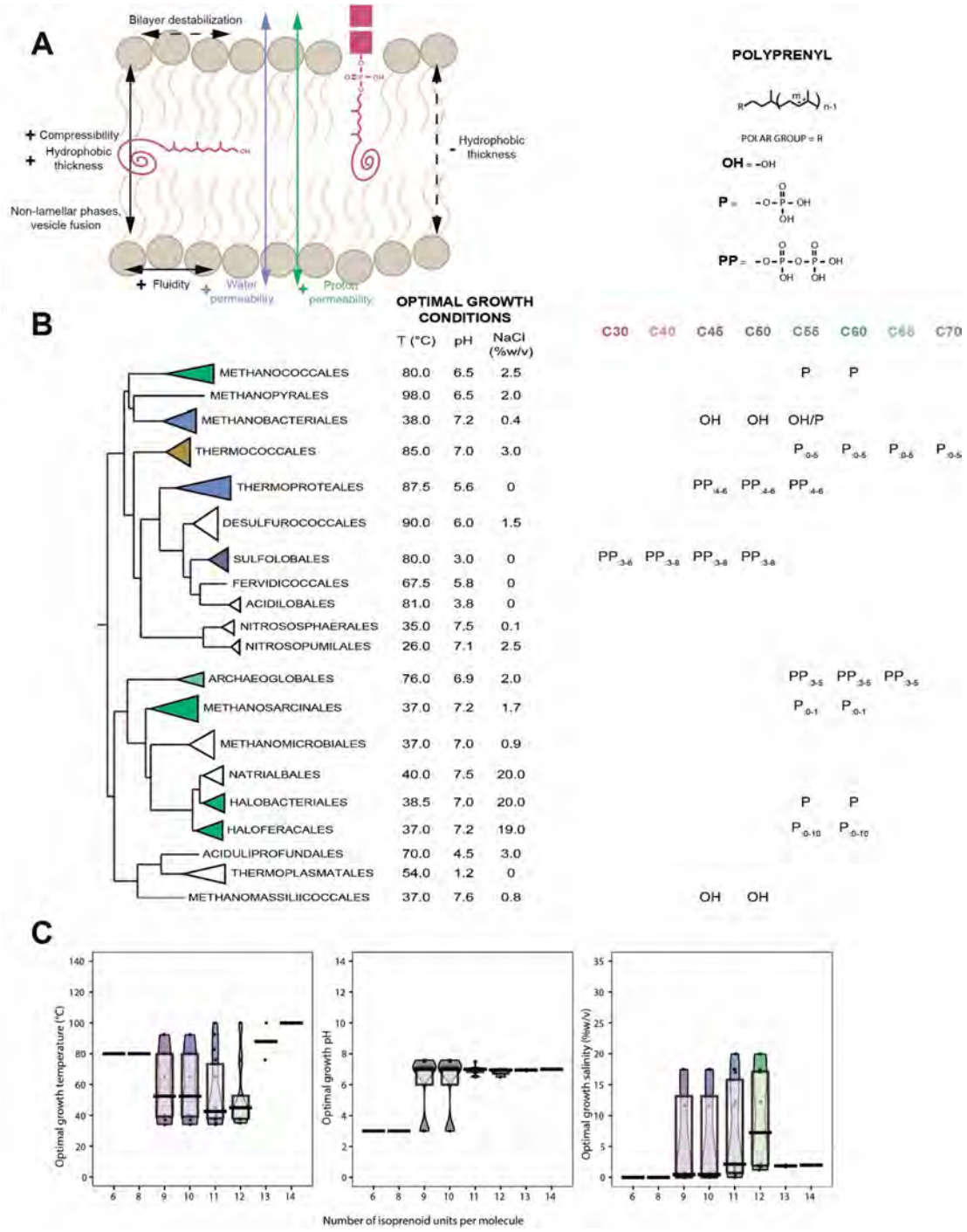

Figure 3. Physicochemistry, distribution and adaptive response of polyprenols in Archaea. (**A**), Position and impacts of polyprenols on membrane physicochemical properties. (**B**), Structures and distribution

of polyprenols within the Archaea domain. The tree topology has been adapted from [34]. In polyprenol structure, *m* refers to the number of cis isoprene units whereas *n* correspond to the trans units. The sum of m, n and alpha and omega units correspond to the total number of carbons, indicated in colors. Unsaturation degrees are indicated below the polar head group. (**C**), Pirateplot of the optimal growth conditions of the organisms in which the different lengths of polyprenols were detected. Colors indicate the chain lengths as in B. Abbreviations: EURY1, Euryarchaeota cluster I; PROTEO, Proteoarchaeota; EURY2, Euryarchaeota cluster II.

6.2. Biological Function of Polyprenols

Polyprenols are key components of the membrane protein glycosylation pathway and are thus required for the proper biosynthesis of critical cell structures, such as cell wall of various Bacteria [86] and eukaryotic spores [87]. In addition, polyprenols have been suggested to stabilize protein domains and complexes [88,89] and act as antioxidants that scavenge free radical oxygen species to protect surrounding lipids from peroxidation [90]. Altogether, these results indicate that polyprenol derivatives may have direct and indirect roles in tolerance to environmental conditions.

6.3. Insertion of Polyprenols in the Membrane

The less polar residues, i.e., polyprenyl-alcohols, tend to form aggregates that are horizontally buried in the membrane, whereas the more polar residues, i.e., polyprenyl-phosphates, are dispersed and vertically anchored with their polar head placed in the polar region of the membrane [91–94] (Figure 3A). Despite variable length, all studies demonstrate that the structural characteristics of polyprenols are strikingly analogous. For example, C55 and C95 polyprenols both compress their long hydrophobic tail into a similar chair-like conformation, such that they both only penetrate a single membrane leaflet [69,89,94,95]. Consequently, even though polyprenyl-phosphates harbor various side chain length, they may similarly impact membrane properties in the three domains of life.

6.4. Polyprenols as Putative Membrane Regulators in Archaea

Insertion of polyprenols into model membranes demonstrated that they might form aggregates, or domains, that could exert critical structural, functional and metabolic consequences on lipid bilayers [96]. In contrast to cholesterol, polar polyprenols were suggested to decrease the temperature of the lamellar-to-hexagonal phase transition, probably by specifically associating with phosphatidylethanolamine lipids [97]. For instance, polyprenols promote non-bilayer phase formation [92,97,98], and thus the formation and the fusion of membrane vesicles [99,100]. However, the effects of polyprenols on lipid membrane parameters appear to be dependent on the length of their polyisoprenoid chains [97]. Polyprenols with longer chain, such as C120 and C160 homologs, increase the thickness of the membrane hydrophobic core and lipid motional freedom [91], enhance membrane fluidity [98,101,102], and drastically increase ion [103,104] and water permeabilities [97,98,105]. In contrast, shorter chain polyprenols, such as C55 and C95, promote hydrophobic interactions with the lipid acyl chains [95], and thus reduce water permeability, especially in polyprenyl-phosphate based membranes [99]. In plants, these medium-chain polyprenols reduce lipid acyl chain motion, and thus membrane fluidity, in the protein-dense thylakoid membranes [106,107]. Although polar headgroups appear to greatly impact the membrane location of polyprenols, no study has been performed to estimate their impact on membrane parameters. Last, it is important to point out that all studies were performed in conditions (1% to 20% of polyprenols) far from those found in natural biological systems (less than 0.1%) [68], which implies that all effects of polyprenols on membrane regulation may not have been identified yet. To date, there is little evidence of a link between polyprenols and a response to environmental stressors. However, plants accumulate polyprenols in response to hypersaline stress [108] and a polyprenol kinase mutant of *Streptococcus mutans* exhibited a higher sensitivity to acidic conditions [109], suggesting that polyprenyl-phosphates may be involved in stress

response. In Archaea, different polyprenol side chain structures were correlated with optimal growth conditions (Figure 3C). Archaea thriving at higher temperatures tend to produce polyprenols with shorter side chains, which sounds consistent with the tightening impact of short chain polyprenols on membranes. Halophilic environments are extremely unfavorable to bioenergetics [110]. However, halophilic archaea produce long polyprenols, with up to 12 isoprene units [111], which reinforce membrane impermeability to ions and thus allow to create gradients [110]. Polyprenol chain length did not seem to correlate with the optimal pH. However, hyperthermophilic archaea, such as *Pyrococcus furiosus* ($T_{opt} \approx 100$ °C) and *Sulfolobus acidocaldarius* ($T_{opt} \approx 80$ °C), produce highly saturated dolichyl-phosphates [76,77] (Figure 3B), which suggests that the number of unsaturations in polyprenyl-alcohols is also part of the adaptive response to extreme conditions, as demonstrated for membrane lipids [112].

7. Quinones

7.1. Distribution in Archaea

Quinones are a diverse group of membrane-bound amphiphilic isoprenoid derivatives ensuring electron and proton transfers in the respiratory chains of organisms throughout the entire tree of life. Due to their key position in the central metabolism of the cell, quinones are prevalent in all three domains of life, although their polar headgroups and side chain lengths vary. The cycles of the polar headgroups are used to classify quinones into benzoquinones, such as ubiquinones (Ub) and plastoquinones [113,114], naphtoquinones, such as phylloquinones and menaquinones (MK) [113,115] and sulfolobusquinones (SQ) [115]. Methanophenazines (MP) [116], which are analogous to quinones both in structure and function, are also included in this classification. Animals and plants synthesize long-chain ubiquinones, mainly Ub_{10}, whereas fungi synthesize Ub_6 to Ub_{10} [114]. Some Eukarya also synthesize phylloquinones or plastoquinones found in chloroplastic membranes [117]. Bacteria synthesize Ub and MK with side chains ranging from six to 10 prenyl units [118]. In contrast, most archaea produce short-chain MK with four to eight prenyl units, although two groups of archaea synthesize specific quinones: SQ with side chain of three to six units in Sulfolobales [119] and MP with five prenyl units in Methanosarcinales [120] (Figure 4B). Some archaea may synthesize long menaquinones such as MK_9 and MK_{10} [121]. The nomenclature of quinones used in the current review ($Q_{m:n}$) describes the polar headgroup (Q), the size of the isoprenoid side chain (m) and its number of unsaturations (n).

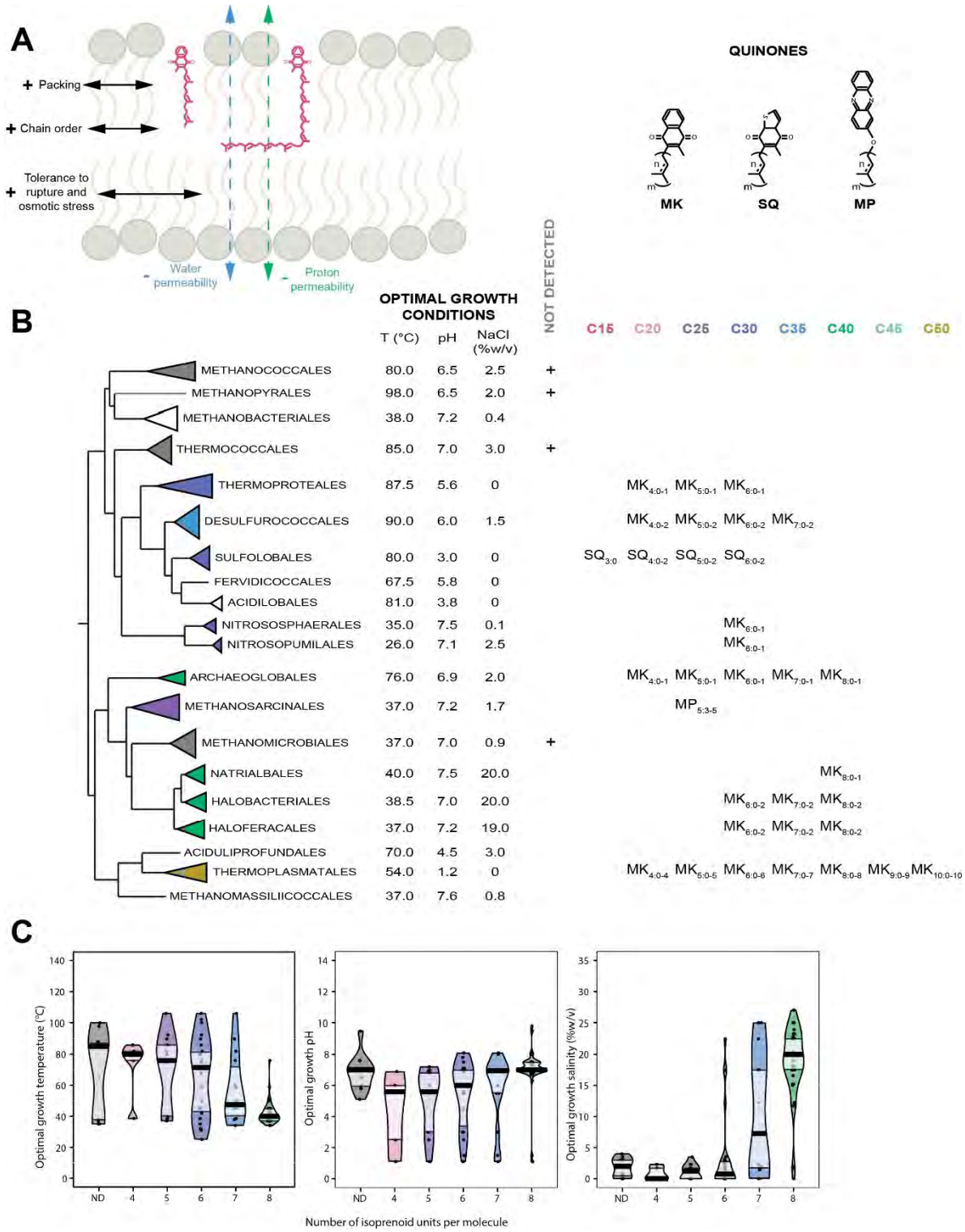

Figure 4. Physicochemistry, distribution and adaptive response of quinones in Archaea. (**A**), Position and impacts of quinones on membrane physicochemical properties. (**B**), Structures and distribution of quinones within the Archaea domain. The tree topology has been adapted from [34]. The different chain lengths are represented and the polar heads and insaturation degrees are indicated. (**C**), Pirateplot of the optimal growth conditions of the organisms in which the different side chain lengths of quinones were detected. Colors indicate the quinone apolar chain lengths as in B. Abbreviations: MK, menaquinone; SQ, sulfolobusquinone; MP, methanophenazine. EURY1, Euryarchaeota cluster I; PROTEO, Proteoarchaeota; EURY2, Euryarchaeota cluster II.

7.2. Biological Function of Quinones

The main function of quinones is to ensure the transfer of electrons and protons in the respiratory chains in the plasma membrane. The quinone polar headgroups composed of cyclic groups with distinct redox potentials constitute their critical biological moiety. On the other hand, the quinone apolar region is composed of polyisoprenoid side chains varying in size and saturation degree and is supposed to serve as an anchor in the membrane much like for polyprenols.

7.3. Insertion of Quinones in the Membrane

Despite a great deal of effort, the exact location of the quinone in the membrane remains uncertain. It seems clear that it is independent of the nature of the polar headgroup but is strongly impacted by the quinone side chain length [122–125]. Short-chain quinones, e.g., with an isoprenyl side chain no longer than the lipid acyl chain, lie parallel to the lipids while the quinones with longer chains, and especially Ub_{10}, are progressively translocated within the midplane of the bilayer [126], regardless of the polar headgroup [125]. Most studies locate the polar headgroups of quinones like Ub_1, Ub_2, Ub_6 or Ub_{10} into the bilayers with the quinone ring in the lipid polar head region, close to the glycerol moiety, thus quite distant from the lipid water interface [127–129]. Such position would explain quinone stability and lateral motility within a bilayer, but would require an energetically less favorable shift of the polar head from the inner to the outer membrane side ("flip-flop") to allow the transfer of protons and electrons. In contrast, other studies locate Ub_{10} within the midplane of the bilayer [130], which would help enhance lateral diffusion but would be highly unstable, due to the insertion of a polar headgroup in the extremely hydrophobic core, and non-functional, as protons and electrons are supposed to transit from one membrane side to the other. Different simulations established that the location of the quinone may depend on its initial position, in the bilayer or in the midplane, and on the bilayer phospholipid composition. However, none could reproduce the fast shifts detected in mitochondrial bilayers [131,132]. Altogether, these results suggest that the location near the polar head region might actually be the most physiologically relevant quinone position, with their isoprenoid chains parallel to the lipids chains. The quinones whose polyprenyl chain lengths exceed that of the lipid acyl chains may lie in part in the midplane of the bilayer, similarly to long chain polyprenols [123].

7.4. Quinones as Putative Membrane Regulators in Archaea

Apart from their main biological function, quinones have been suggested to act as membrane stabilizers and modulate membrane mechanical strength and permeability [133]. Long-chain ubiquinones increase packing and lipid order, thus limiting proton and sodium leakages and the release of hydrophobic components [126,134], and enhance the resistance to rupture and detergents [134,135] (Figure 4A). In contrast, quinones with short chain length, i.e., that do not exceed the lipid acyl chain, such as Ub_2 and Ub_4, drastically decrease melting temperatures [124]. Some archaea adapt their quinone content to correspond to the redox potential of their environment. For instance, *Thermoplasma acidophilum* produces a 1/1/1 ratio of Methionaquinones, Monomethylmenaquinones (MMK) and MK but almost exclusively MMK under aerobic and anaerobic conditions, respectively [136]. Similarly, the quinone composition is correlated to oxygen content and carbon source in *Sulfolobus solfataricus* [137] and *Acidianus ambivalens* [138]. However, despite growing under very different environmental conditions, most archaea possess identical quinone polar headgroups, suggesting that the polar moiety of archaeal quinone reflect the organism metabolic type rather than partake in membrane adaptation. Several line of evidence data demonstrate that quinone tails may participate in archaeal membrane adaptation, as demonstrated in Bacteria such as *Escherichia coli* [139] and *Listeria monocytogenes* [140] for the tolerance to osmotic shock or growth at low temperature. Indeed, various chain lengths, e.g., from 15 to 50 carbons, and saturation degrees, e.g., from fully saturated to one unsaturation per prenyl unit, were described in archaeal quinones, suggesting that the polyprenyl tails may support adaptive functions. If no specific study has tried to correlate the polyprenyl chain length and growth conditions in Archaea, we show here a clear

correlation between polyprenyl chain length and optimal growth conditions in Archaea (Figure 4C). Interestingly, all environmental parameters, i.e., temperature, pH and salinity, seem to affect the size of quinone tails in Archaea, whereas no clear trend could be drawn for their polar heads (Figure 5). Under high temperature, Archaea tend to produce quinones with shorter side chains, which would be consistent with the proposition that the long isoprenoid chains, which are partially inserted in the midplane, tend to destabilize the bilayer, while the short chains, which only reside within the hydrophobic core of the leaflet, tend to improve membrane packing and lipid chain order. Similarly, the higher the salinity the longer the side chains, consistent with the suggested reduction of water, ion and proton permeabilities, all required in the deleterious bioenergetic landscape imposed by high salt conditions, associated with the long side chains which populate the midplane of the membrane bilayer [110].

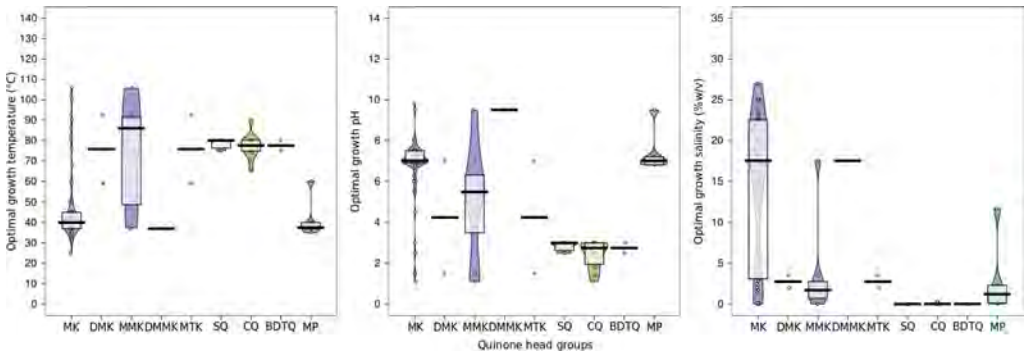

Figure 5. Correlation between optimal growth conditions and quinone head group. Menaquinone based quinones are depicted in purple (MK, DMK, MMK, DMMK, MTK), Sulfolobusquinone based quinones in yellow (SQ, CQ, BDTQ) and Methanophenazine (MP) in green. See the phylogenetic tree for head group structure. Abbreviations: MK, Menaquinones; DMK, Demethylmenaquinones; MMK, Monomethylmenaquinones; DMMK, Dimethylmenaquinones; MTK, Methionaquinones; SQ, Sulfolobusquinones; CQ, Caldariellaquinones; BDTQ, Benzodithiophenoquinones.

8. Apolar Polyisoprenoids

Apolar polyisoprenoids, composed of four to eight isoprene subunits, are a vast and essential group of naturally occurring hydrocarbon compounds. As precursors of most terpenoids, apolar polyisoprenoids are present in all three domains of life. Squalene, formed by six terpenes subunits, is the precursor of steroland hopanoid derivatives [141–143], while lycopene, composed of eight terpenes subunits, is the precursor of carotenoids [144]. Although Archaea may lack some or all of these final products, apolar polyisoprenoids are broadly distributed in this domain [145], among which squalene is the most frequently found compound.

8.1. Distribution in Archaea

As terpenoids precursors, apolar polyisoprenoids are broadly present in Eukarya, from shark (squalene) to tomatoes (lycopene) [146,147]. They are highly prevalent in acidophilic and alkaliphilic bacteria, which contain up to 40 mol% of polyisoprenoids, within which 10–12 mol% are of the squalene series [148,149]. Apolar polyisoprenoids with 4 to 8 units were identified in almost all the archaeal species tested, resulting in a broad distribution in the Archaea domain (Figure 6B). Archaea can be divided into two classes according to the length of their polyisoprenoids: (1) species that synthesizes short polyisoprenoids, with four to six isoprene units, such as Methanococcales and Sulfolobales, and (2) those that synthesize long polyisoprenoids, with six to eight isoprene units, e.g., Haloferacales and Thermococcales (Figure 6B). Although the proportions of apolar polyisoprenoids in archaeal membranes remain mostly unknown, it has been demonstrated that the linear isoprenoids of the lycopene series represent 1–2% of total lipids in *Thermococcus barophilus* [150] and 0.4% in *Thermococcus hydrothermalis* [151], two hyperthermophilic

and piezophilic archaea. In addition, the degree of unsaturation of polyisoprenoids in Archaea remains poorly characterized.

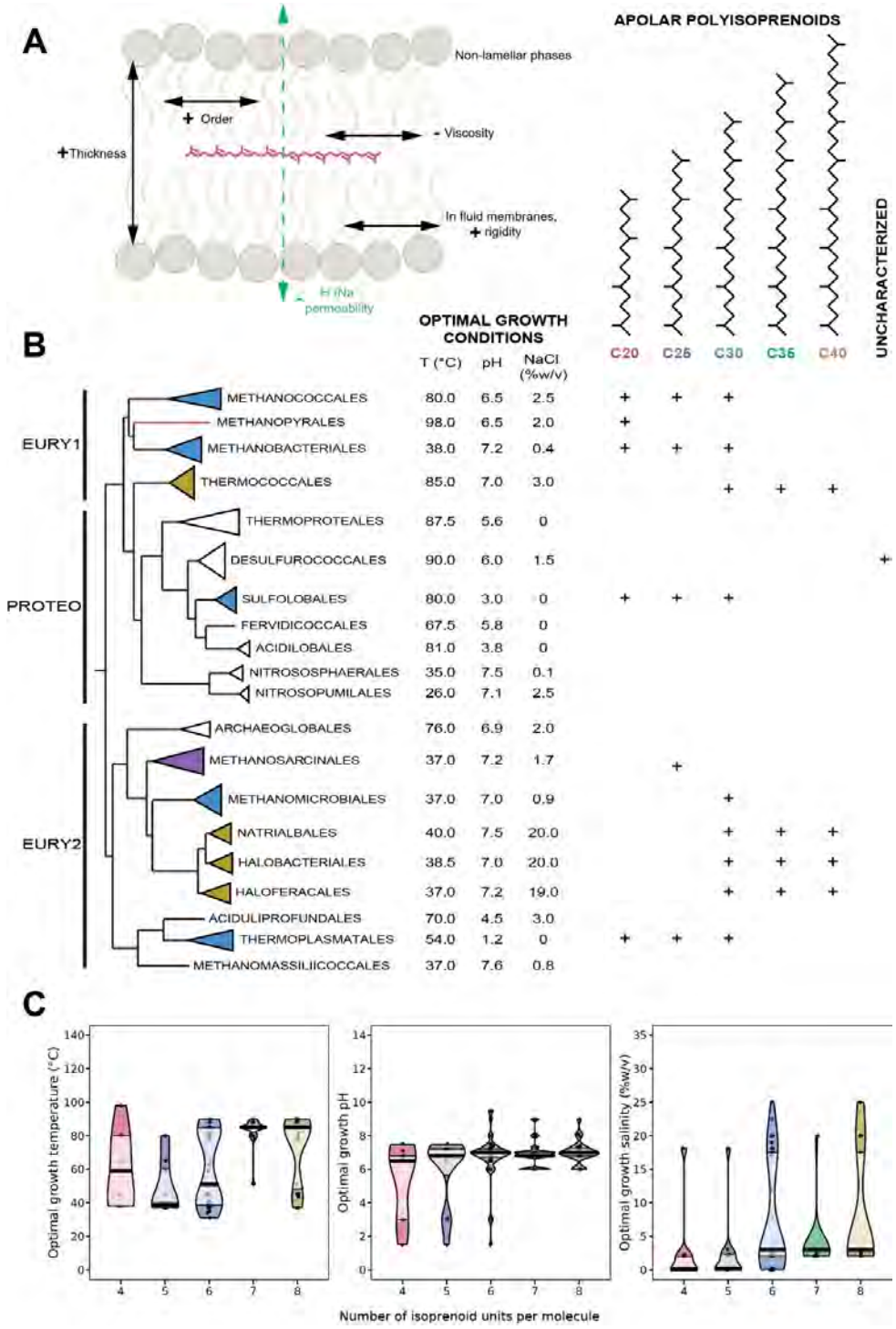

Figure 6. Physicochemistry, distribution and adaptive response of apolar polyisoprenoids in Archaea. (**A**), Position and impacts of apolar polyisoprenoids on membrane physicochemical properties. (**B**), Structures and distribution of apolar polyisoprenoids within the Archaea domain. The tree topology has been adapted from [34]. (**C**), Pirateplot of the optimal growth conditions of the organisms in which the different lengths of apolar polyisoprenoids were detected. Colors indicate the chain lengths as in B. Abbreviations: EURY1, Euryarchaeota cluster I; PROTEO, Proteoarchaeota; EURY2, Euryarchaeota cluster II.

8.2. Biological Function of Apolar Polyisoprenoids

Besides being synthetic intermediates for essential biomolecules, squalene has been studied as a possible antioxidant. Early studies have shown that squalene is an efficient singlet oxygen scavenging agent [152] and effectively protects lipid from peroxidation [153], but this antioxidant ability was recently challenged [154]. The structural similarity between apolar polyisoprenoids and the phytanyl chain constitutive of archaeal lipids [155,156] could lead to the belief that apolar polyisoprenoids are only intermediates in bipolar lipid biosynthesis or the products of polar lipid metabolism. However, both types of molecules derive from two different synthesis pathways: whereas the two phytanyl (C20) chains of bipolar archaeal lipids are linked through a 1-1 condensation, the central isoprene units of apolar polyisoprenoids and their derivatives result from the condensation of two polyprenyl-diphosphates through a 4-4 bound (Figure 1). Nonetheless, several studies suggest that apolar polyisoprenoids might be membrane regulators [150,157,158].

8.3. Insertion of Apolar Polyisoprenoids in the Membrane

Only a single study reports the localization of apolar polyisoprenoids in archaeal membranes. In membranes reconstructed from lipids of the archaeon *Halobacterium salinarum*, squalene was shown to prevent pyrelene, a fluorescent probe, to populate the midplane of the membrane bilayer, while reducing the local viscosity around the probe [159], which suggested that squalene was inserted in the hydrophobic core of the lipid bilayer perpendicularly to the membrane plane. However, neutron diffraction using squalane, the saturated form of squalene, and the eukaryal/bacterial phospholipid1,2-dioleoyl-sn-glycero-3-phosphocholine, demonstrated that squalane lies in the center of the lipid bilayer, parallel to the plane and partially extending into the lipid fatty acyl chains [158]. Our unpublished data confirm these later results in membranes reconstructed from different archaeal lipids, which allows us to generalize this localization for all bilayer-forming archaeal lipids (Salvador Castell/Oger unpublished results). In contrast to squalane, which is a flat molecule, squalene is more physically constrained due to the presence of unsaturations [160] and has several kinks, which indicates that it should remain more easily in the bilayer midplane and not insert within the hydrophobic core of the bilayer leaflets. The impact of the insertion of apolar polyisoprenoids on membrane parameters is yet to be reported for archaeal lipids, but several trends can be extrapolated from results with bacterial-like membranes (Figure 6A). First, the effects have been shown to vary with the lipid composition of the host membrane. Squalene increases rigidity of moderately fluid membranes, but has a rather softening effect on already rigid membranes [161]. In this context, in which squalene is in competition with other membrane regulators, such as cholesterol, membrane rigidity is driven by the squalene to sterol ratio [161]. In addition, apolar polyisoprenoids, such as squalane, squalene or lycopene, facilitate the formation of non-lamellar phases. For example, they induce the reduction of the lamellar-to-hexagonal phase transition temperature in bacterial-like [162,163], or archaeal-like membranes, indicating a stabilization of the non-lamellar phase. This signifies that apolar polyisoprenoids induce a higher negative curvature in the lipid bilayer, which could explain the higher aggregation and fusion of liposomes observed in the presence of lycopene [57]. In addition, chemical models predict that apolar polyisoprenoids populating the membrane midplane would decrease water, proton and sodium permeability. Thus, apolar polyisoprenoids could be essential to generate gradients to gain energy in more extreme environments, where these gradients may be harder to achieve [157]. This was partially confirmed with squalene in soybean membranes, demonstrating an altered proton pump [164], and with lycopene in bacterial-like liposomes showing increase water impermeability [139].

8.4. Apolar Polyisoprenoids as Putative Membrane Regulators in Archaea

There is a large body of evidence supporting a possible role of apolar polyisoprenoids as membrane regulators. To begin with, studies about lycopene contents of *Haloferax volcanii*

and *Zymomonas mobilis* show that apolar polyisoprenoid levels are growth phase dependent, with increased synthesis in stationary phase [165,166]. The high energy-cost of lycopene synthesis, i.e., 24 ATP and 12 NADH per molecule, suggests that the presence of squalene-type isoprenoids must be essential for cell viability in the stationary phase. In addition, archaea adapt the degree of unsaturation of their apolar polyisoprenoids in response to environmental conditions. For instance, the level of unsaturation varies as a function of H_2 availibity in cells grown in serum bottles vs. In fermenters [167]. In the polyextremophile *Thermococcus barophilus*, the degree of unsaturation of the pool of polyisoprenoids, from C_{30} to C_{40}, is regulated in response to variations of temperature and hydrostatic pressure, which is part of the homeoviscous response of the membrane in this species along with variations in membrane polar lipids [150]. The novel membrane architecture proposed for *T. barophilus* suggests that apolar polyisoprenoids may be inserted in parallel to the membrane plane in the midplane of the archaeal bilayer. Thus, if validated, this architecture implies the existence of membrane domains of different compositions and properties, opening the possibility that the archaeal membrane can be spatially organized and functionalized (Figure 6C). In addition, the presence of the polyisoprenoids is supposed to compensate for the lack of monolayer-forming lipids in these species. Supporting this model, the length of apolar polyisoprenoids is positively correlated with (1) temperature, mesophilic archaea producing four to five isoprene long-hydrocarbons whereas hyperthermophilic microorganisms harbor six to eight isoprene units (Figure 6C); (2) pH, acidophiles synthesize shorter isoprenoid chains, i.e., C_{20} to C_{30}, than alkaliphiles, i.e., C_{30} to C_{40} isoprenoids, and (3) salinity, halophiles present up to 40% of C_{30} to C_{40} apolar polyisoprenoids, longer than those of species thriving in low salinities [168]. Apolar polyisoprenoids may act by reducing the diffusion of ions and water across membranes, similarly to ring-based sterols [3,17,169]. As the proportion of tetraether, monolayer forming archaeal lipid is also correlated with temperature and pH, the long-chain polyisoprenoids are correlated with archaea harboring bilayers, in which the presence of polyisoprenoids would reinforce membrane resistance to stress. Altogether, our results suggest that apolar polyisoprenoids are essential membrane lipids of Archaea, allowing them to withstand a large range of stressful conditions, and behave as true membrane regulators.

9. Conclusions

Polyterpenes are a vast group of hydrocarbon compounds found in every known organism. Although they were initially described as having only physiological roles, such as pigments, hormones, protein regulators or energy transduction molecules (Figure 7), some of the most well-known polyterpenes, such as sterols and hopanoids, have been demonstrated to act as regulators of membrane properties.

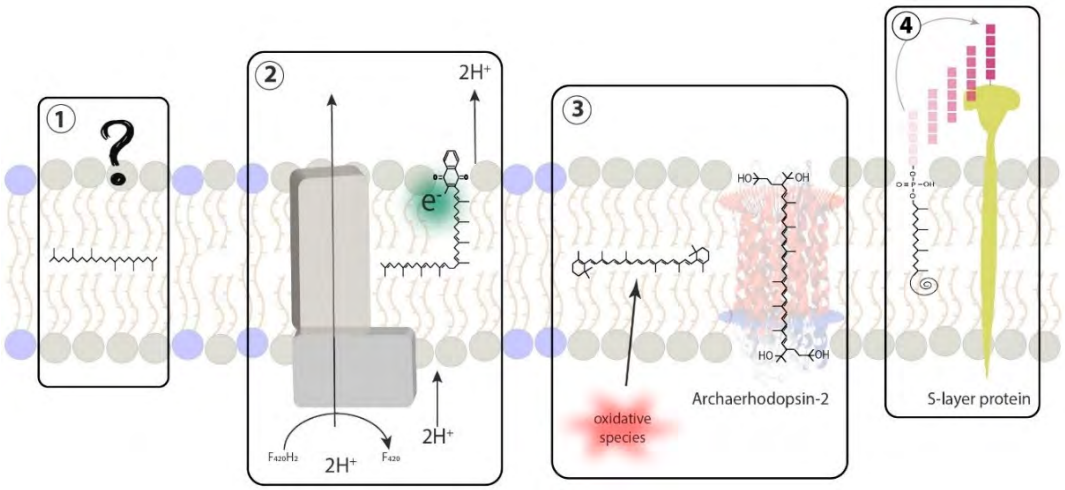

Figure 7. Schematic representation of major terpenoids found in Archaea and their respective biological functions. Blue and grey phospholipids represent archaeal tetraether and diether lipids, respectively. (1) squalane-type polyisoprenoids are widespread polyterpenes with yet-uncharacterized membrane function, (2) quinones are critical membrane-bound electron and proton carriers in energy transduction of various organisms, (3) carotenoids are well-characterized lipid-soluble antioxidants that may associate with transmembrane proteins and, (4) polyprenols are membrane-bound sugar carriers that are essential for transmembrane protein glycosylation.

Since Archaea are able to synthesize neither sterols nor hopanoids, the known membrane regulators, we looked for other polyterpenes that might support such membrane adaptive functions in Archaea. All four families of polyterpenes are synthesized by at least some species of Archaea. Although the data is quite scarce, it shows that all four type of molecules have the potential to act as membrane regulators in Archaea, and that they may be involved in the response to different stresses or in different branches of the Archaea. Of the four families, only quinones are not produced by all Archaea, and thus might not be the best surrogate of sterols or hopanoids. However, there is convincing evidence that the length of their polyisoprenoid tail influences membrane properties and that they are produced in specific compositions as a function of growth conditions. The carotenoids are very similar to quinones in their phylogenetic repartition, which seem restricted to certain branches of the Archaea, and their capability to impact on membrane properties. However, carotenoids have not been searched to the same extent as quinones, and it is thus possible that they might be more common than anticipated today. Their demonstrated properties in bacterial membranes are very similar to classical membrane regulators, such as reducing proton and water permeabilities. Thus, we anticipate a similar function in Archaea which synthesizes them, with a possible connection with the response to salinity and high pH stresses. Polyprenols, which constitute the third family, are also expected to lie vertically in the membrane with their long polyisoprenoid chains condensed into a chair-like conformation within the hydrophobic core of the membrane. Such conformation would affect the properties of the lipid bilayer, while being adapted as a function of different stressors, such as temperature or salinity. Apolar polyisoprenoids may be the best surrogates of sterols and hopanoids in Archaea, since they have already been demonstrated to enhance membrane properties to maintain membrane functionality in response to stress. However, further evidence will be required to demonstrate their presence and impact on membrane in all Archaea. Regardless of the family, the putative regulation effects of polyterpenes on membrane properties seem correlated with the length of their polyisoprenoid chains. As a general rule, archaea synthesizing monolayer-forming lipids tend to accumulate polyterpenes with shorter side chains, when the species forming bilayer membranes tend to accumulate polyterpenes with longer side chains. This is consistent with the model of Cario and colleagues who suggested that the polyisoprenoid chains may play a role equivalent to that of the monolayer-forming lipids, e.g., increased rigidity and impermeability to ions and water, shift in resistance to stress, in species incapable of synthesizing bipolar lipids [150].

In Archaea, it is highly probable that more than one type of membrane regulator exists, much like in Eukarya or Bacteria, since the trend of accumulation of the different polyterpenes may be negatively correlated. For example, hyperthermophiles accumulate longer polyisoprenoids but shorter polyprenols and quinones than mesophiles, and acidophiles and alkaliphiles accommodate higher amounts of medium-length quinones, with alkaliphilic archaea possessing particularly large quantities of polyisoprenoids (Figure 8). More importantly, the presence of such lipid membrane regulators implies the existence of membrane domains, opening the possibility to the existence of functionalized regions in archaeal membranes.

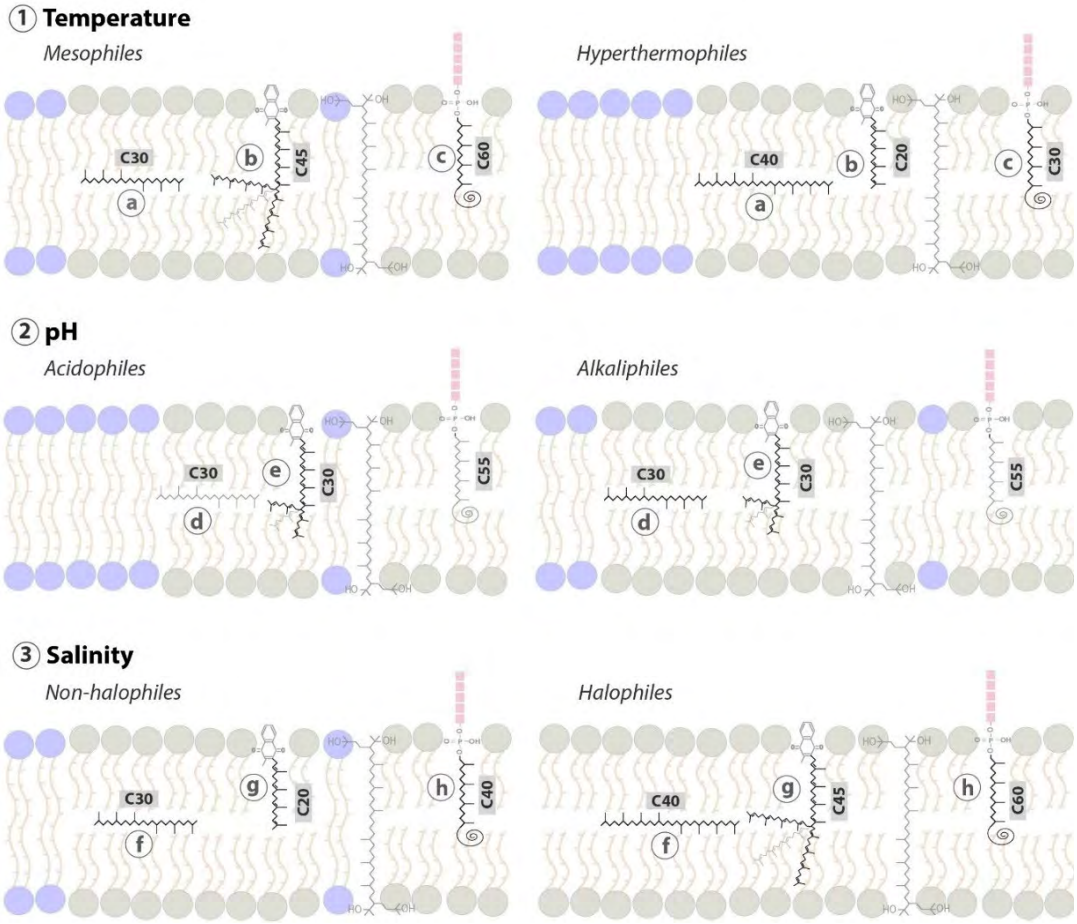

Figure 8. Schematic representation of putative membrane properties modulation by polyterpenes in response to different environmental conditions in Archaea. (**1**) Adaptations to temperature: (**a**) longer apolar polyisoprenoids are present in hyperthermophiles. (**b**) and (**c**) mesophiles present menaquinones and polyprenols with higher acyl chains than hyperthermophiles. (**2**) Adaptations to pH: (**d**) alkaliphiles possess higher quantities of apolar polyisoprenoids molecules. (**e**) Both, acidophiles and alkaliphiles own menaquinones with medium-length acyl chains. (**3**) Adaptations to salinity: (**f**) extreme halophiles present longer apolar polyisoprenoids lipids. (**g**) and (**h**) menaquinones and polyprenols with long acyl chain length are present in extremely halophilic archaea. Grey and blue molecules represent archaeal diether and tetraether lipids, respectively.

Author Contributions: Conceptualization, M.S.-C., M.T. and P.M.O.; Formal analysis, M.T.; Funding acquisition, P.M.O.; Investigation, M.S.-C. and M.T.; Project administration, M.S.-C., M.T. and P.M.O.; Supervision, P.M.O.; Visualization, M.S.-C. and M.T.; Writing—Original draft, M.S.-C. and M.T.; Writing—Review and editing, M.S.-C., M.T. and P.M.O.

Funding: M.S.-C. and M.T. are supported by Ph.D. grants from the French Ministry of Research and Technology. The authors would like to thank the French National Research Agency for funding the ArchaeoMembranes project (ANR-17-CE11-0012-01) and the CNRS Interdisciplinary program 'Origines' for funding the ReseArch project.

Conflicts of Interest: The authors declare no conflict of interest.

Abbreviations

IPP	Isopentenyl pyrophosphate
DMAP	Dimethylallyl diphosphate
T_m	Lipid phase transition temperature
IDR	Isopentenyldehydrorhodopsin
BR	Bacterioruberin
BC	β-carotene
HEO	3-hydroechinenone
CTX	Canthaxanthin
AX	Astaxanthin
ZX	Zeaxanthin
EURY1	Euryarchaeota cluster I
PROTEO	Proteoarchaeota
EURY2	Euryarchaeota cluster II
T_{opt}	Optimal growth temperature
Ub_x	Ubiquinones and its number of isoprenoid units (x)
MK	Menaquinones
MMK	Monomethylmenaquinones
MTK	Methionaquinones
DMK	Demethylmenaquinones
DMMK	Dimethylmenaquinones
SQ	Sulfolobusquinones
CQ	Caldariellaquinones
BDTQ	Benzodithiophenoquinones
MP	Methanophenazines
$Q_{m:n}$	Polar head group from quinone (Q), size of the isoprenoid side chain (m) and its number of unsaturations (n)
ATP	Adenosine triphosphate
NADH	Nicotinamide adenine dinucleotide

References

1. Singer, S.J.J.; Nicolson, G.L.L. The fluid mosaic model of the structure of cell membranes. *Science* **1972**, *175*, 720–731. [CrossRef] [PubMed]
2. Nicolson, G.L. The fluid-mosaic model of membrane structure: Still relevant to understanding the structure, function and dynamics of biological membranes after more than 40 years. *Biochim. Biophys. Acta-Biomembr.* **2014**, *1838*, 1451–1466. [CrossRef] [PubMed]
3. Subczynski, W.K.; Pasenkiewicz-Gierula, M.; Widomska, J.; Mainali, L.; Raguz, M. High cholesterol/low cholesterol: Effects in biological membranes: A review. *Cell Biochem. Biophys.* **2017**, *75*, 369–385. [CrossRef] [PubMed]
4. Harayama, T.; Riezman, H. Understanding the diversity of membrane lipid composition. *Nat. Rev. Mol. Cell Biol.* **2018**, *19*, 281–296. [CrossRef] [PubMed]
5. Oldfield, E.; Chapman, D. Dynamics of lipids in membranes: Heterogeneity and the role of cholesterol. *FEBS Lett.* **1972**, *23*, 285–297. [CrossRef]
6. Demel, R.A.; De Kruyff, B. The function of sterols in membranes. *Biochim. Biophys. Acta* **1976**, *457*, 109–132. [CrossRef]
7. Yeagle, P.L. Cholesterol and the cell membrane. *Bba-Rev. Biomembr.* **1985**, *822*, 267–287. [CrossRef]
8. García-Arribas, A.B.; Alonso, A.; Goñi, F.M. Cholesterol interactions with ceramide and sphingomyelin. *Chem. Phys. Lipids* **2016**, *199*, 26–34. [CrossRef]
9. Grouleff, J.; Irudayam, S.J.; Skeby, K.K.; Schiøtt, B. The influence of cholesterol on membrane protein structure, function, and dynamics studied by molecular dynamics simulations. *Biochim. Biophys. Acta-Biomembr.* **2015**, *1848*, 1783–1795. [CrossRef]

10. Marquardt, D.; Kučerka, N.; Wassall, S.R.; Harroun, T.A.; Katsaras, J. Cholesterol's location in lipid bilayers. *Chem. Phys. Lipids* **2016**, *199*, 17–25. [CrossRef]
11. Ourisson, G.; Rohmer, M.; Poralla, K. Prokaryotic hopanoids and other polyterpenoid sterol surrogates. *Ann. Rev. Microbiol.* **1987**, *41*, 301–333. [CrossRef] [PubMed]
12. Sáenz, J.P.; Broda, M.; Lagny, T.J.; Grosser, D.; Lavrynenko, O.; Bradley, A.S.; Simons, K. Hopanoids as functional analogues of cholesterol in bacterial membranes. *Proc. Natl. Acad. Sci. USA* **2015**, *112*, 11971–11976. [CrossRef] [PubMed]
13. Belin, B.J.; Busset, N.; Giraud, E.; Molinaro, A.; Silipo, A.; Newman, D.K. Hopanoid lipids: From membranes to plant-bacteria interactions. *Nat. Rev. Microbiol.* **2018**, *16*, 304–315. [CrossRef] [PubMed]
14. Lombard, J.; Moreira, D. Origins and early evolution of the mevalonate pathway of isoprenoid biosynthesis in the three domains of life. *Mol. Biol. Evol.* **2011**, *28*, 87–99. [CrossRef] [PubMed]
15. Paniagua-Michel, J.; Olmos-Soto, J.; Ruiz, M.A. Pathways of Carotenoid Biosynthesis in Bacteria and Microalgae. In *Microbial Carotenoids from Bacteria and Microalgae: Methods and Protocols, Methods in Molecular Biology*, 1st ed.; Barredo, J.-L., Ed.; Springer Science & Business Media: Heidelberg, Germany, 2012; Volume 892, pp. 1–12.
16. Róg, T.; Pasenkiewicz-Gierula, M. Cholesterol Effects on the Phosphatidylcholine Bilayer Nonpolar Region: A Molecular Simulation Study. *Biophys. J.* **2001**, *84*, 1818–1826. [CrossRef]
17. Bloch, K.E. Sterol, Structure and Membrane Function. *Crit. Rev. Biochem.* **1983**, *14*, 47–92. [CrossRef]
18. Chen, Z.; Rand, R.P. The influence of cholesterol on phospholipid membrane curvature and bending elasticity. *Biophys. J.* **1997**, *73*, 267–276. [CrossRef]
19. Baumgart, T.; Hess, S.; Webb, W. Imaging coexisting fluid domains in biomembrane models coupling curvature and line tension. *Nature* **2003**, *425*, 821–824. [CrossRef] [PubMed]
20. Poger, D.; Mark, A.E. The relative effect of sterols and hopanoids on lipid bilayers: When comparable is not identical. *J. Phys. Chem. B* **2013**, *117*, 16129–16140. [CrossRef] [PubMed]
21. Krajewski-Bertrand, M.A.; Hayer, M.; Wolff, G.; Milon, A.; Albrecht, A.-M.; Heissler, D.; Nakatanif, Y.; Ourisson, G. Tricyclohexaprenol and an octaprenediol, two of the "primitive" amphiphilic lipids do improve phospholipidic membranes. *Tetrahedron* **1989**, *46*, 3143–3154. [CrossRef]
22. Coleman, G.A.; Pancost, R.D.; Williams, T.A. Investigating the origins of membrane phospholipid biosynthesis genes using outgroup-free rooting. *Genome Biol. Evol.* **2019**, *11*, 883–898. [CrossRef] [PubMed]
23. Landrum, J.T. *Carotenoids Biological Functions and Properties*, 1st ed.; CRC Press: Boca Raton, FL, USA, 2010.
24. Yabuzaki, J. Carotenoids Database: Structures, chemical fingerprints and distribution among organisms. *Database* **2017**, *2017*, 1–11. [CrossRef]
25. Kull, D.R.; Pfander, H. Isolation and structure elucidation of carotenoid glycosides from the thermoacidophilic Archaea *Sulfolobus shibatae*. *J. Nat. Prod.* **1997**, *60*, 371–374. [CrossRef]
26. Asker, D.; Awad, T.; Ohta, Y. Lipids of *Haloferax alexandrinus* strain TMT: An extremely halophilic canthaxanthin-producing archaeon. *J. Biosci. Bioeng.* **2002**, *93*, 37–43. [CrossRef]
27. Leuko, S.; Coyle, C.M.; Neilan, B.A.; Walter, M.R.; Marshall, C.P.; Burns, B.P. Carotenoid analysis of halophilic archaea by resonance Raman spectroscopy. *Astrobiology* **2007**, *7*, 631–643.
28. Mandelli, F.; Miranda, V.S.; Rodrigues, E.; Mercadante, A.Z. Identification of carotenoids with high antioxidant capacity produced by extremophile microorganisms. *World J. Microbiol. Biotechnol.* **2012**, *28*, 1781–1790. [CrossRef]
29. Jehlička, J.; Edwards, H.G.M.; Oren, A. Bacterioruberin and salinixanthin carotenoids of extremely halophilic Archaea and Bacteria: A Raman spectroscopic study. *Spectrochim. Acta Part. A Mol. Biomol. Spectrosc.* **2013**, *106*, 99–103. [CrossRef] [PubMed]
30. Squillaci, G.; Parrella, R.; Carbone, V.; Minasi, P.; La Cara, F.; Morana, A. Carotenoids from the extreme halophilic archaeon *Haloterrigena turkmenica*: Identification and antioxidant activity. *Extremophiles* **2017**, *21*, 933–945. [CrossRef] [PubMed]
31. Kushwaha, S.C.; Pugh, E.L.; Kramer, J.K.G.; Kates, M. Isolation and identification of dehydrosqualene and C40-carotenoid pigments in *Halobacterium cutirubrum*. *Biochim. Biophys. Acta (Bba)/Lipids Lipid Metab.* **1972**, *260*, 492–506. [CrossRef]
32. Lobasso, S.; Lopalco, P.; Mascolo, G.; Corcelli, A. Lipids of the ultra-thin square halophilic archaeon *Haloquadratum walsbyi*. *Archaea* **2008**, *2*, 177–183. [CrossRef]

33. Yatsunami, R.; Ando, A.; Yang, Y.; Takaichi, S.; Kohno, M.; Matsumura, Y.; Ikeda, H.; Fukui, T.; Nakasone, K.; Fujita, N.; et al. Identification of carotenoids from the extremely halophilic archaeon *Haloarcula japonica*. *Front. Microbiol.* **2014**, *5*, 1–5. [CrossRef] [PubMed]
34. Adam, P.S.; Borrel, G.; Brochier-Armanet, C.; Gribaldo, S. The growing tree of Archaea: New perspectives on their diversity, evolution and ecology. *ISME J.* **2017**, *11*, 2407–2425. [CrossRef] [PubMed]
35. Krinsky, N.I. Carotenoid protection against oxidation. *Pure Appl. Chem.* **1979**, *51*, 649–660. [CrossRef]
36. McNulty, H.P.; Byun, J.; Lockwood, S.F.; Jacob, R.F.; Mason, R.P. Differential effects of carotenoids on lipid peroxidation due to membrane interactions: X-ray diffraction analysis. *Biochim. Biophys. Acta-Biomembr.* **2007**, *1768*, 167–174. [CrossRef] [PubMed]
37. Johnson, Q.R.; Mostofian, B.; Fuente Gomez, G.; Smith, J.C.; Cheng, X. Effects of carotenoids on lipid bilayers. *Phys. Chem. Chem. Phys.* **2018**, *20*, 3795–3804. [CrossRef] [PubMed]
38. Merhan, O. The biochemistry and antioxidant properties of carotenoids. In *Carotenoids*, 1st ed.; Cvetkovic, D., Nikolic, G., Eds.; InTech: Rijeka, Croatia, 2017; pp.51–66.
39. Miller, N.J.; Sampson, J.; Candeias, L.P.; Bramley, P.M.; Rice-Evans, C.A. Antioxidant properties of carotenes and xanthophylls. *FEBS Lett.* **1996**, *384*, 240–242. [CrossRef]
40. Albrecht, M.; Takaichi, S.; Steiger, S.; Wang, Z.-Y.; Sandmann, G. Novel hydroxycarotenoids with improved antioxidative properties produced by gene combination in *Escherichia coli*. *Nat. Biotechnol.* **2000**, *18*, 843–846. [CrossRef]
41. Gruszecki, W.I.; Widomska, J.; Strzałka, K.; Kostecka-Gugała, A.; Latowski, D. Calorimetric studies of the effect of cis-carotenoids on the thermotropic phase behavior of phosphatidylcholine bilayers. *Biophys. Chem.* **2008**, *140*, 108–114.
42. Gruszecki, W.I.; Strzałka, K. Carotenoids as modulators of lipid membrane physical properties. *Biochim. Biophys. Acta-Mol. Basis. Dis.* **2005**, *1740*, 108–115. [CrossRef]
43. Yoshimura, K.; Kouyama, T. Structural role of bacterioruberin in the trimeric structure of Archaerhodopsin-2. *J. Mol. Biol.* **2008**, *375*, 1267–1281. [CrossRef]
44. Kouyama, T.; Kanada, S.; Takeguchi, Y.; Narusawa, A.; Murakami, M.; Ihara, K. Crystal structure of the light-driven chloride pump halorhodopsin from *Natronomonas pharaonis*. *J. Mol. Biol.* **2010**, *396*, 564–579. [CrossRef] [PubMed]
45. Lazrak, T.; Wolff, G.; Albrecht, A.M.; Nakatani, Y.; Ourisson, G.; Kates, M. Bacterioruberins reinforce reconstituted *Halobacterium* lipid membranes. *Biochim. Biophys. Acta-Biomembr.* **1988**, *939*, 160–162. [CrossRef]
46. Socaciu, C.; Bojarski, P.; Aberle, L.; Diehl, H.A. Different ways to insert carotenoids into liposomes affect structure and dynamics of the bilayer differently. *Biophys. Chem.* **2002**, *99*, 1–15. [CrossRef]
47. Shinoda, W.; Shinoda, K.; Baba, T.; Mikami, M. Molecular dynamics study of bipolar tetraether lipid membranes. *Biophys. J.* **2005**, *89*, 3195–3202. [CrossRef] [PubMed]
48. Gabrielska, J.; Gruszecki, W.I. Zeaxanthin (dihydroxy-β-carotene) but not β-carotene rigidities lipid membranes: A 1H-NMR study of carotenoid-egg phosphatidylcholine liposomes. *Biochim. Biophys. Acta-Biomembr.* **1996**, *1285*, 167–174. [CrossRef]
49. Subczynski, W.K.; Markowska, E.; Gruszecki, W.I.; Sielewiesiuk, J. Effects of polar carotenoids on dimyristoylphosphatidylcholine membranes: A spin-label study. *Biochim. Biophys. Acta-Biomembr.* **1992**, *1105*, 97–108. [CrossRef]
50. Subczynski, W.K.; Wisniewska, A.; Widomska, J. Can macular xanthophylls replace cholesterol in formation of the liquid-ordered phase in lipid-bilayer membranes? *Acta Biochim. Pol.* **2012**, *59*, 109–114. [CrossRef] [PubMed]
51. Strzałka, K.; Gruszecki, W.I. Effect of β-carotene on structural and dynamic properties of model phosphatidylcholine membranes. I. An EPR spin label study. *Biochim. Biophys. Acta-Biomembr.* **1994**, *1194*, 138–142. [CrossRef]
52. Berglund, A.H.; Nilsson, R.; Liljenberg, C. Permeability of large unilamellar digalactosyldiacylglycerol vesicles for protons and glucose - Influence of α-tocopherol, β-carotene, zeaxanthin and cholesterol. *Plant Physiol. Biochem.* **1999**, *37*, 179–186. [CrossRef]
53. Subczynski, W.K.; Markowska, E.; Sielewiesiuk, J. Effect of polar carotenoids on the oxygen diffusion-concentration product in lipid bilayers. An EPR spin label study. *Biochim. Biophys. Acta-Biomembr.* **1991**, *1068*, 68–72. [CrossRef]

54. Subczynski, W.K.; Markowska, E.; Sielewiesiuk, J. Spin-label studies on phosphatidylcholine-polar carotenoid membranes: Effects of alkyl-chain length and unsaturation. *Biochim. Biophys. Acta-Biomembr.* **1993**, *1150*, 173–181. [CrossRef]
55. Suwalsky, M.; Hidalgo, P.; Strzalka, K.; Kostecka-Gugala, A. Comparative X-ray studies on the interaction of carotenoids with a model phosphatidylcholine membrane. *Z. Fur. Nat-Sect. C. J. Biosci.* **2002**, *57*, 129–134.
56. Augustynska, D.; Jemioła-Rzemiå ska, M.; Burda, K.; Strzałka, K. Influence of polar and nonpolar carotenoids on structural and adhesive properties of model membranes. *Chem. Biol. Interact.* **2015**, *239*, 19–25. [CrossRef] [PubMed]
57. Xia, S.; Tan, C.; Zhang, Y.; Abbas, S.; Feng, B.; Zhang, X.; Qin, F. Modulating effect of lipid bilayer-carotenoid interactions on the property of liposome encapsulation. *Colloids Surf. B. Biointerfaces* **2015**, *128*, 172–180. [CrossRef] [PubMed]
58. Holthuis, J. Regulating membrane curvature. In *Regulatory Mechanisms of Intracellular Membrane Transport*, 1st ed.; Keränen, S., Jäntti, J., Eds.; Springer: Heidelberg, Germany, 2004; pp. 39–64.
59. Shahmohammadi, H.R.; Asgarani, E.; Terato, H.; Saito, T.; Ohyama, Y.; Gekko, K.; Yamamoto, O.; Ide, H. Protective roles of bacterioruberin and intracellular KCl in the resistance of *Halobacterium salinarium* against DNA-damaging agents. *J. Radiat. Res.* **1998**, *39*, 251–262. [CrossRef]
60. Calegari-Santos, R.; Diogo, R.A.; Fontana, J.D.; Bonfim, T.M.B. Carotenoid production by halophilic archaea under different culture conditions. *Curr. Microbiol.* **2016**, *72*, 641–651. [CrossRef]
61. D'Souza, S.E.; Altekar, W.; D'Souza, S.F. Adaptive response of *Haloferax mediterranei* to low concentrations. *Arch. Microbiol.* **1997**, *168*, 68–71. [CrossRef]
62. Bidle, K.A.; Hanson, T.E.; Howell, K.; Nannen, J. HMG-CoA reductase is regulated by salinity at the level of transcription in *Haloferax volcanii*. *Extremophiles* **2007**, *11*, 49–55. [CrossRef]
63. Asker, D.; Ohta, Y. Production of canthaxanthin by extremely halophilic bacteria. *J. Biosci. Bioeng.* **1999**, *88*, 617–621. [CrossRef]
64. Kushwaha, S.C.; Juez-Pérez, G.; Rodriguez-Valera, F.; Kates, M.; Kushner, D.J. Survey of lipids of a new group of extremely halophilic bacteria from salt ponds in Spain. *Can. J. Microbiol.* **1982**, *28*, 1365–1372. [CrossRef]
65. Gochnauer, M.B.; Kushwaha, S.C.; Kates, M.; Kushner, D.J. Nutritional control of pigment and isoprenoid compound formation in extremely halophilic bacteria. *Arch. Mikrobiol.* **1972**, *84*, 339–349. [CrossRef]
66. Swiezewska, E.; Danikiewicz, W. Polyisoprenoids: Structure, biosynthesis and function. *Prog. Lipid Res.* **2005**, *44*, 235–258. [CrossRef] [PubMed]
67. Skorupinska-Tudek, K.; Wojcik, J.; Swiezewska, E. Polyisoprenoid alcohols - Recent results of structural studies. *Chem. Rec.* **2008**, *8*, 33–45. [CrossRef] [PubMed]
68. Hartley, M.D.; Imperiali, B. At the membrane frontier: A prospectus on the remarkable evolutionary conservation of polyprenols and polyprenyl-phosphates. *Arch. Biochem. Biophys.* **2012**, *517*, 83–97. [CrossRef] [PubMed]
69. Knudsen, M.J.; Troy, F.A. Nuclear magnetic resonance studies of polyisoprenols in model membranes. *Chem. Phys. Lipids* **1989**, *51*, 205–212. [CrossRef]
70. Bauersachs, T.; Schouten, S.; Compaoré, J.; Stal, L.J.; Sinninghe Damsté, J.S. Occurrence of C35-C45 polyprenols in filamentous and unicellular cyanobacteria. *Org. Geochem.* **2010**, *41*, 867–870. [CrossRef]
71. Szabo, E.I.; Amdur, B.H.; Socransky, S.S. Lipid composition of *Streptococcus mutans*. *Caries Res.* **1978**, *12*, 21–27. [CrossRef]
72. Jones, M.B.; Rosenberg, J.N.; Betenbaugh, M.J.; Krag, S.S. Structure and synthesis of polyisoprenoids used in N-glycosylation across the three domains of life. *Biochim. Biophys. Acta-Gen. Subj.* **2009**, *1790*, 485–494. [CrossRef]
73. Swiezewska, E.; Sasak, W.; Mankowski, T.; Jankowski, W.; Vogtman, T.; Krajewska, I.; Hertel, J.; Skoczylas, E.; Chojnacki, T. The search for plant polyprenols. *Acta Biochim. Pol.* **1994**, *41*, 221–260.
74. Manat, G.; Roure, S.; Auger, R.; Bouhss, A.; Barreteau, H.; Mengin-Lecreulx, D.; Touzé, T. Deciphering the metabolism of undecaprenyl-phosphate: the bacterial cell-wall unit carrier at the membrane frontier. *Microb. Drug Resist.* **2014**, *20*, 199–214. [CrossRef]
75. Guan, Z.; Eichler, J. Liquid chromatography/tandem mass spectrometry of dolichols and polyprenols, lipid sugar carriers accross evolution. *Biochim. Biophys. Acta* **2011**, *1811*, 800–806. [CrossRef] [PubMed]

76. Guan, Z.; Meyer, B.H.; Albers, S.V.; Eichler, J. The thermoacidophilic archaeon *Sulfolobus acidocaldarius* contains an unsually short, highly reduced dolichyl phosphate. *Biochim. Biophys. Acta-Mol. Cell Biol. Lipids* **2011**, *1811*, 607–616. [CrossRef][PubMed]
77. Chang, M.M.; Imperiali, B.; Eichler, J.; Guan, Z. N-linked glycans are assembled on highly reduced dolichol phosphate carriers in the hyperthermophilic archaea *Pyrococcus furiosus*. *PLoS ONE* **2015**, *10*, e0130482. [CrossRef] [PubMed]
78. Yoshinaga, M.Y.; Gagen, E.J.; Wörmer, L.; Broda, N.K.; Meador, T.B.; Wendt, J.; Thomm, M.; Hinrichs, K.-U. *Methanothermobacter thermautotrophicus* modulates its membrane lipids in response to hydrogen and nutrient availability. *Front. Microbiol.* **2015**, *6*, 5. [CrossRef] [PubMed]
79. Becker, K.W.; Elling, F.J.; Yoshinaga, M.Y.; Söllinger, A.; Urich, T.; Hinrichs, K.U. Unusual butane- and pentanetriol-based tetraether lipids in *Methanomassiliicoccus luminyensis*, a representative of the seventh order of methanogens. *Appl. Environ. Microbiol.* **2016**, *82*, 4505–4516. [CrossRef] [PubMed]
80. Larkin, A.; Chang, M.M.; Whitworth, G.E.; Imperiali, B. Biochemical evidence for and alternate patway in N-linked glycoprotein biosynthesis. *Nat. Chem. Biol.* **2013**, *9*, 367–373. [CrossRef]
81. Ogawa, T.; Emi, K.; Koga, K.; Yoshimura, T.; Hemmi, H. A cis -prenyltransferase from *Methanosarcina acetivorans* catalyzes both head-to-tail and nonhead-to-tail prenyl condensation. *FEBS J.* **2016**, *283*, 2369–2383. [CrossRef]
82. Hartmann, E.; König, H. Isolation of lipid activated pseudomurein precursors from *Methanobacterium thermoautotrophicum*. *Arch. Microbiol.* **1990**, *153*, 444–447. [CrossRef]
83. Hartmann, E.; König, H. Uridine and dolichyl diphosphate activated oligosaccharides are intermediates in the biosynthesis of the S-layer glycoprotein of *Methanothermus fervidus*. *Arch. Microbiol.* **1989**, *151*, 274–281. [CrossRef]
84. Taguchi, Y.; Fujinami, D.; Kohda, D. Comparative analysis of archaeal lipid-linked oligosaccharides that serve as oligosaccharide donors for Asn glycosylation. *J. Biol. Chem.* **2016**, *291*, 11042–11054. [CrossRef]
85. Guy, L.; Ettema, T.J.G. The archaeal "TACK" superphylum and the origin of eukaryotes. *Trends Microbiol.* **2011**, *19*, 580–587. [CrossRef] [PubMed]
86. de Kruijff, B.; van Dam, V.; Breukink, E. Lipid II: A central component in bacterial cell wall synthesis and a target for antibiotics. *Prostaglandins Leukot. Essent. Fat. Acids* **2008**, *79*, 117–121. [CrossRef] [PubMed]
87. Hoffman, R. A link between polyprenols and outer spore wall formation in *Saccharomyces cerevisiae*. For the Degree of Doctor of Philosophy, Stony Brook University, Stony Brook, NY, USA, 2017.
88. Troy, F.A. Polysialylation: From bacteria to brains. *Glycobiology* **1992**, *2*, 5–23. [CrossRef] [PubMed]
89. Zhou, G.P.; Troy, F.A. Characterization by NMR and molecular modeling of the binding of polyisoprenols and polyisoprenyl recognition sequence peptides: 3D structure of the complexes reveals sites of specific interactions. *Glycobiology* **2003**, *13*, 51–71. [CrossRef] [PubMed]
90. Huang, L.; Zhang, C.; Zhang, Y.; Zhang, Q.; Xie, P.; Xu, F.; Ding, S. Synthesis and biological activity of polyprenols. *Fitoterapia* **2015**, *106*, 184–193.
91. Vigo, C.; Grossman, S.H.; Drost-Hansen, W. Interaction of dolichol and dolichyl phosphate with phospholipid bilayers. *Biochim. Biophys. Acta* **1984**, *774*, 221–226. [CrossRef]
92. Valtersson, C.; van Duyn, G.; Verkleij, A.J.; Chojnacki, T.; de Kruijff, B.; Dallner, G. The influence of dolichol, dolichol esters, and dolichyl phosphate on phospholipid polymorphism and fluidity in model membranes. *J. Biol. Chem.* **1985**, *260*, 2742–2751.
93. De Ropp, J.S.; Troy, F.A. 2H NMR Investigation of the organization and dynamics of polyisoprenols in membranes. *J. Biol. Chem.* **1985**, *260*, 15669–15674.
94. Arantes, P.R.; Pedebos, C.; Pol-fachin, L.; Poleto, M.D.; Verli, H. Dynamics of membrane-embedded lipid-linked oligosaccharides for the three domains of life. *ChemRxiv* **2019**. Preprint.
95. Zhou, G.P.; Troy, F.A. NMR study of the preferred membrane orientation of polyisoprenols (dolichol) and the impact of their complex with polyisoprenyl recognition sequence peptides on membrane structure. *Glycobiology* **2005**, *15*, 347–359. [CrossRef]
96. McCloskey, M.A.; Troy, F.A. Paramagnetic isoprenoid carrier Lipids. 2. Dispersion and dynamics in lipid membranes. *Biochemistry* **1980**, *19*, 2061–2066. [CrossRef]
97. Chojnacki, T.; Dallner, G. The biological role of dolichol. *Biochem. J.* **1988**, *251*, 1–9. [CrossRef] [PubMed]

98. Lamson, M.J.; Herbette, L.G.; Peters, K.R.; Carson, J.H.; Morgan, F.; Chester, D.C.; Kramer, P.A. Effects of hexagonal phase induction by dolichol on phospholipid membrane permeability and morphology. *Int. J. Pharm.* **1994**, *105*, 259–272. [CrossRef]
99. Streiff, S.; Ribeiro, N.; Wu, Z.; Gumienna-Kontecka, E.; Elhabiri, M.; Albrecht-Gary, A.M.; Ourisson, G.; Nakatani, Y. "Primitive" Membrane from Polyprenyl Phosphates and Polyprenyl Alcohols. *Chem. Biol.* **2007**, *14*, 313–319. [CrossRef][PubMed]
100. Van Duijn, G.; Valtersson, C.; Chojnacki, T.; Verkleij, A.J.; Dallner, G.; de Kruijff, B. Dolichyl phosphate induces non-bilayer structures, vesicle fusion and transbilayer movement of lipids: A model membrane study. *Biochim. Biophys. Acta-Biomembr.* **1986**, *861*, 211–223. [CrossRef]
101. Walinska, K. Comparison of the influence of the polyprenol structure on model membranes. *Desalination* **2004**, *163*, 239–245. [CrossRef]
102. Monti, J.A.; Christian, S.T.; Schutzbach, J.S. Effects of dolichol on membrane permeability. *Biochim. Biophys. Acta-Biomembr.* **1987**, *905*, 133–142. [CrossRef]
103. Janas, T.; Walińska, K.; Chojnacki, T.; Świezewska, E.; Janas, T. Modulation of properties of phospholipid membranes by the long-chain polyprenol (C160). *Chem. Phys. Lipids* **2000**, *106*, 31–40. [CrossRef]
104. Janas, T.; Walińska, K.; Janas, T. Electroporation of polyprenol-phosphatidylcholine bilayer lipid membranes. *Bioelectrochem. Bioenerg.* **1998**, *45*, 215–220. [CrossRef]
105. Schutzbach, J.S.; Jensen, J.W. Bilayer membrane destabilization induced by dolichylphosphate. *Chem. Phys. Lipids* **1989**, *51*, 213–218. [CrossRef]
106. Van Gelder, K.; Rea, K.A.; Virta, L.K.A.; Whitnell, K.L.; Osborn, M.; Vatta, M.; Khozin, A.; Skorupinska-Tudek, K.; Surmacz, L.; Akhtar, T.A. Medium-chain polyprenols influence chloroplast membrane dynamics in *Solanum lycopersicum*. *Plant Cell Physiol.* **2018**, *59*, 2350–2365. [CrossRef] [PubMed]
107. Akhtar, T.A.; Surowiecki, P.; Siekierska, H.; Kania, M.; Van Gelder, K.; Rea, K.A.; Virta, L.K.A.; Vatta, M.; Gawarecka, K.; Wojcik, J.; et al. Polyprenols are synthesized by a plastidial cis-prenyltransferase and influence photosynthetic performance. *Plant Cell* **2017**, *29*, 1709–1725. [CrossRef] [PubMed]
108. Baczewska, A.H.; Dmuchowski, W.; Jozwiak, A.; Gozdowski, D.; Bra˛goszewska, P.; Da˛browski, P.; Swiezewska, E. Effect of salt stress on prenol lipids in the leaves of *Tilia* 'Euchlora'. *Dendrobiology* **2014**, *72*, 177–186. [CrossRef]
109. Lis, M.; Kuramitsu, H.K. Characterization of a suppressor mutation complementing an acid-sensitive mutation in *Streptococcus mutans*. *FEMS Microbiol. Lett.* **2003**, *229*, 179–182. [CrossRef]
110. Kellermann, M.Y.; Yoshinaga, M.Y.; Valentine, R.C.; Wörmer, L.; Valentine, D.L. Important roles for membrane lipids in haloarchaeal bioenergetics. *Biochim. Biophys. Acta-Biomembr.* **2016**, *1858*, 2940–2956. [CrossRef] [PubMed]
111. Calo, D.; Guan, Z.; Naparstek, S.; Eichler, J. Different routes to the same ending: Comparing the N-glycosylation processes of *Haloferax volcanii* and *Haloarcula marismortui*, two halophilic archaea from the Dead Sea. *Mol. Microbiol.* **2011**, *81*, 1166–1177. [CrossRef] [PubMed]
112. Oger, P.M.; Cario, A. Adaptation of the membrane in Archaea. *Biophys. Chem.* **2013**, *183*, 42–56. [CrossRef] [PubMed]
113. Thomson, R.H. *Naturally Occurring Quinones IV*, 4th ed.; Springer: Dordrecht, The Netherlands, 1997.
114. Nowicka, B.; Kruk, J. Occurrence, biosynthesis and function of isoprenoid quinones. *Biochim. Biophys. Acta-Bioenerg.* **2010**, *1797*, 1587–1605. [CrossRef]
115. Elling, F.J.; Becker, K.W.; Könneke, M.; Schröder, J.M.; Kellermann, M.Y.; Thomm, M.; Hinrichs, K.U. Respiratory quinones in Archaea: Phylogenetic distribution and application as biomarkers in the marine environment. *Env. Microbiol.* **2016**, *18*, 692–707. [CrossRef]
116. Abken, H.-J.; Tietze, M.; Brodersen, J.; Bäumer, S.; Beifuss, U.; Deppenmeier, U. Isolation and characterization of methanophenazine and function of phenazines in membrane-bound electron transport of *Methanosarcina mazei* Gö1. *J. Bacteriol.* **1998**, *180*, 2027–2032.
117. Goodwin, T.W. The prenyllipids of the membranes of higher plants. In *Lipids and Lipid Polymers in Higher Plants*, 1st ed.; Tevini, M., Lichtenthaler, H.K., Eds.; Springer; Berlin/Heidelberg, Germany: New York, NY, USA, 1977; pp. 29–42.
118. Collins, M.D.; Jones, D. Distribution of isoprenoid quinone structural types in bacteria and their taxonomic implication. *Microbiol. Rev.* **1981**, *45*, 316–354. [PubMed]

119. Thurl, S.; Witke, W.; Buhrow, I.; Schäfer, W. Quinones from Archaebacteria, II. Different types of quinones from sulphur-Dependent Archaebacteria. *Biol. Chem. Hoppe. Seyler.* **1986**, *367*, 191–198. [CrossRef] [PubMed]
120. Elling, F.J. Factors Controlling the Lipid Composition of Marine Planktonic Thaumarchaeota. For the Degree Doctor of Philosophy, Universität Bremen, Bremen, Germany, 2015.
121. Golyshina, O.V.; Lünsdorf, H.; Kublanov, I.V.; Goldenstein, N.I.; Hinrichs, K.U.; Golyshin, P.N. The novel extremely acidophilic, cell-wall-deficient archaeon *Cuniculiplasma divulgatum* gen. nov., sp. nov. represents a new family, *Cuniculiplasmataceae* fam. nov., of the order Thermoplasmatales. *Int. J. Syst. Evol. Microbiol.* **2016**, *66*, 332–340. [CrossRef][PubMed]
122. Ulrich, E.L.; Girvin, M.E.; Cramer, W.A.; Markley, J.L. Location and mobility of ubiquinones of different chain lengths in artificial membrane vesicles. *Biochemistry* **1985**, *24*, 2501–2508. [CrossRef] [PubMed]
123. Lenaz, G.; Samori, B.; Fato, R.; Battino, M.; Castelli, G.P.; Domini, I. Localization and preferred orientations of ubiquinone homologs in model bilayers. *Biochem. Cell Biol.* **1991**, *70*, 504–514. [CrossRef]
124. Roche, Y.; Peretti, P.; Bernard, S. DSC and Raman studies of the side chain length effect of ubiquinones on the thermotropic phase behavior of liposomes. *Thermochim. Acta* **2006**, *447*, 81–88. [CrossRef]
125. Teixeira, M.H.; Arantes, G.M. Effects of lipid composition on membrane distribution and permeability of natural quinones. *RSC Adv.* **2019**, *9*, 16892–16899. [CrossRef]
126. Jemiola-Rzeminska, M.; Kruk, J.; Skowronek, M.; Strzalka, K. Location of ubiquinone homologues in liposome membranes studied by fluorescence anisotropy of diphenyl-hexatriene and trimethylammonium-diphenyl-hexatriene. *Chem. Phys. Lipids* **1996**, *79*, 55–63. [CrossRef]
127. Stidham, M.A.; McIntosh, T.J.; Siedow, J.N. On the localization of ubiquinone in phosphatidylcholine bilayers. *Biochim. Biophys. Acta-Bioenerg.* **1984**, *767*, 423–431. [CrossRef]
128. Cornell, B.A.; Keniry, M.A.; Post, A.; Robertson, R.N.; Weir, L.E.; Westerman, P.W. Location and activity of ubiquinone 10 and ubiquinone analogs in model and biological membranes. *Biochemistry* **1987**, *26*, 7702–7707. [CrossRef]
129. Galassi, V.V.; Arantes, G.M. Partition, orientation and mobility of ubiquinones in a lipid bilayer. *Biochim. Biophys. Acta-Bioenerg.* **2015**, *1847*, 1560–1573. [CrossRef] [PubMed]
130. Hauß, T.; Dante, S.; Haines, T.H.; Dencher, N.A. Localization of coenzyme Q10 in the center of a deuterated lipid membrane by neutron diffraction. *Biochim. Biophys. Acta-Bioenerg.* **2005**, *1710*, 57–62. [CrossRef] [PubMed]
131. Söderhäll, J.A.; Laaksonen, A. Molecular dynamics simulations of ubiquinone inside a lipid bilayer. *J. Phys. Chem. B* **2001**, *105*, 9308–9315. [CrossRef]
132. Kaurola, P.; Sharma, V.; Vonk, A.; Vattulainen, I.; Róg, T. Distribution and dynamics of quinones in the lipid bilayer mimicking the inner membrane of mitochondria. *Biochim. Biophys. Acta-Biomembr.* **2016**, *1858*, 2116–2122. [CrossRef][PubMed]
133. Clarke, C.F.; Rowat, A.C.; Gober, J.W. Is CoQ a membrane stabilizer? *Nat. Chem. Biol.* **2014**, *10*, 242–243. [CrossRef] [PubMed]
134. Agmo Hernández, V.; Eriksson, E.K.; Edwards, K. Ubiquinone-10 alters mechanical properties and increases stability of phospholipid membranes. *Biochim. Biophys. Acta-Biomembr.* **2015**, *1848*, 2233–2243. [CrossRef] [PubMed]
135. Lucy, J.A.; Dingle, J.T. Fat-soluble vitamins and biological membranes. *Nature* **1964**, *204*, 156–160. [CrossRef]
136. Shimada, H.; Shida, Y.; Nemoto, N.; Oshima, T.; Yamagishi, A. Quinone profiles of *Thermoplasma acidophilum* HO-62. *J. Bacteriol.* **2001**, *183*, 1462–1465. [CrossRef]
137. Nicolaus, B.; Trincone, A.; Lama, L.; Palmieri, G.; Gambacorta, A. Quinone Composition in Sulfolobus solfataricus Grown under Different Conditions. *Syst. Appl. Microbiol.* **1992**, *15*, 18–20. [CrossRef]
138. Trincone, A.; Lanzotti, V.; Nicolaus, B.; Zillig, W.; De Rosa, M.; Gambacorta, A. Comparative lipid composition of aerobically and anaerobically grown *Desulfurolobus ambivalens*, an autotrophic thermophilic Archaeobacterium. *J. Gen. Microbiol.* **1989**, *135*, 2751–2757.
139. Sévin, D.C.; Sauer, U. Ubiquinone accumulation improves osmotic-stress tolerance in *Escherichia coli*. *Nat. Chem. Biol.* **2014**, *10*, 266–272. [CrossRef] [PubMed]
140. Seel, W.; Flegler, A.; Zunabovic-Pichler, M.; Lipski, A. Increased isoprenoid quinone concentration modulates membrane fluidity in *Listeria monocytogenes* at low growth temperatures. *J. Bacteriol.* **2018**, *200*, e00148-18. [CrossRef] [PubMed]

141. Ourisson, G.; Nakatani, Y. The terpenoid theory of the origin of cellular life: the evolution of terpenoids to cholesterol. *Chem. Biol.* **1994**, *1*, 11–23. [CrossRef]
142. Xu, R.; Fazio, G.C.; Matsuda, S.P.T. On the origins of triterpenoid skeletal diversity. *Phytochemistry* **2004**, *65*, 261–291. [CrossRef] [PubMed]
143. Matsumi, R.; Atomi, H.; Driessen, A.J.M.; van der Oost, J. Isoprenoid biosynthesis in Archaea-Biochemical and evolutionary implications. *Res. Microbiol.* **2011**, *162*, 39–52. [CrossRef] [PubMed]
144. Córdova, P.; Baeza, M.; Cifuentes, V.; Alcaíno, J. Microbiological Synthesis of Carotenoids: Pathways and Regulation. In *Progress in Carotenoid Research*, 1st ed.; Queiroz Zepka, L., Jacob-Lopes, E., Rosso, V.V., Eds.; InTech, 2018; pp. 63–83.
145. Langworthy, T.A.; Tornabene, T.G.; Holzer, G. Lipids of archaebacteria. *Zent. Fur Bakteriol. Angew. Und Okol. Microbiol. Abt. L. Orig. C. Hyg.* **1982**, *3*, 228–244. [CrossRef]
146. Heller, J.H.; Heller, M.S.; Springer, S.; Clark, E. Squalene content of various shark livers. *Nature* **1957**, *179*, 919–920. [CrossRef]
147. Agarwal, A.; Shen, H.; Agarwal, S.; Rao, A.V. Lycopene content of tomato products: Its stability, bioavailability and in vivo antioxidant properties. *J. Med. Food* **2003**, *4*, 9–15. [CrossRef]
148. Clejan, S.; Krulwich, T.A.; Mondrus, K.R.; Seto-Young, D. Membrane lipid composition of obligatively and facultatively alkalophilic strains of *Bacillus*. *J. Bacteriol.* **1986**, *168*, 334–340. [CrossRef]
149. Banciu, H.; Sorokin, D.Y.; Rijpstra, W.I.C.; Sinninghe Damsté, J.S.; Galinski, E.A.; Takaichi, S.; Muyzer, G.; Kuenen, J.G. Fatty acid, compatible solute and pigment composition of obligately chemolithoautotrophic alkaliphilic sulfur-oxidizing bacteria from soda lakes. *Fems. Microbiol. Lett.* **2005**, *243*, 181–187. [CrossRef]
150. Cario, A.; Grossi, V.; Schaeffer, P.; Oger, P.M. Membrane homeoviscous adaptation in the piezo-hyperthermophilic archaeon *Thermococcus barophilus*. *Front. Microbiol.* **2015**, *6*, 1–12. [CrossRef] [PubMed]
151. Lattuati, A.; Guezennec, J.; Metzger, P.; Largeau, C. Lipids of *Thermococcus hydrothermalis*, an archaea isolated from a deep- sea hydrothermal vent. *Lipids* **1998**, *33*, 319–326. [CrossRef] [PubMed]
152. Kohno, Y.; Egawa, Y.; Itoh, S.; Nagaoka, S.; Takahashi, M.; Mukai, K. Kinetic study of quenching reaction of singlet oxygen and scavenging reaction of free radical by squalene in n-butanol. *Biochim. Biophys. Acta-Lipids Lipid Metab.* **1995**, *1256*, 52–56. [CrossRef]
153. Conforti, F.; Statti, G.; Loizzo, M.R.; Sacchetti, G.; Poli, F.; Menichini, F. In vitro antioxidant effect and inhibition of α-amylase of two varieties of *Amaranthus caudatus* seeds. *Biol. Pharm. Bull.* **2005**, *28*, 1098–1102. [CrossRef] [PubMed]
154. Warleta, F.; Campos, M.; Allouche, Y.; Sánchez-Quesada, C.; Ruiz-Mora, J.; Beltrán, G.; Gaforio, J.J. Squalene protects against oxidative DNA damage in MCF10A human mammary epithelial cells but not in MCF7 and MDA-MB-231 human breast cancer cells. *Food Chem. Toxicol.* **2010**, *48*, 1092–1100. [CrossRef]
155. De Rosa, M.; Gambacorta, A.; Gliozzi, A. Structure, biosynthesis, and physicochemical properties of archaebacterial lipids. *Microbiol. Rev.* **1986**, *50*, 70–80. [PubMed]
156. Gambacorta, A.; Trincone, A.; Nicolaus, B.; Lama, L.; De Rosa, M. Unique features of lipids of Archaea. *Syst. Appl. Microbiol.* **1993**, *16*, 518–527. [CrossRef]
157. Haines, T.H. Do sterols reduce proton and sodium leaks through lipid bilayers? *Prog. Lipid Res.* **2001**, *40*, 299–324. [CrossRef]
158. Haußß, T.; Dante, S.; Dencher, N.A.; Haines, T.H. Squalane is in the midplane of the lipid bilayer: Implications for its function as a proton permeability barrier. *Biochim. Biophys. Acta* **2002**, *1556*, 149–154. [CrossRef]
159. Lanyi, J.K.; Plachy, W.Z.; Kates, M. Lipid interactions in membranes of extremely halophilic bacteria. II. Modification of the bilayer structure by squalene. *Biochemistry* **1974**, *13*, 4914–4920. [CrossRef]
160. Kowert, B.A.; Watson, M.B.; Dang, N.C. Diffusion of squalene in n-alkanes and squalane. *J. Phys. Chem. B* **2014**, *118*, 2157–2163. [CrossRef] [PubMed]
161. Spanova, M.; Zweytick, D.; Lohner, K.; Klug, L.; Leitner, E.; Hermetter, A.; Daum, G. Influence of squalene on lipid particle/droplet and membrane organization in the yeast *Saccharomyces cerevisiae*. *Biochim. Biophys. Acta - Mol. Cell Biol. Lipids* **2012**, *1821*, 647–653. [CrossRef] [PubMed]
162. Siegel, D.P.; Banschbach, J.; Yeagle, P.L. Stabilization of H II phases by low leves of diglycerides and alkanes: An NMR, calorimetric, and X-ray diffraction study. *Biochemistry* **1989**, *28*, 5010–5019. [CrossRef]
163. Lohner, K.; Degovics, G.; Laggner, P.; Gnamusch, E.; Paltauf, F. Squalene promotes the formation of nonbilayer stuctures in phospholipid model membranes. *Biochim. Biophys. Acta* **1993**, *1152*, 69–77. [CrossRef]

164. Palanco, M.E.; Skovgaard, N.; Hansen, J.S.; Berg-Sørensen, K.; Hélix-Nielsen, C. Tuning biomimetic membrane barrier properties by hydrocarbon, cholesterol and polymeric additives. *Bioinspir. Biomim.* **2017**, *13*, 016005. [CrossRef] [PubMed]
165. Horbach, S.; Neuss, B.; Sahm, H. Effect of azasqualene on hopanoid biosynthesis and ethanol tolerance of *Zymomonas mobilis*. *FEMS Microbiol. Lett.* **1991**, *79*, 347–350. [CrossRef]
166. Russell, D.J. Lycopene Carotenogenesis and Function in the Haloarchaeon *Haloferax volcanii*. For the Degree Doctor of Philosophy, University of Nottingham, Nottingham, UK, 2013.
167. Manquin, B.P.; Morgan, J.A.; Ju, J.; Müller-Späth, T.; Clark, D.S. Production of C35 isoprenoids depends on H_2 availability during cultivation of the hyperthermophile *Methanococcus jannaschii*. *Extremophiles* **2004**, *8*, 13–21. [CrossRef] [PubMed]
168. Upasani, V.N.; Desai, S.G.; Moldoveanu, N.; Kates, M. Lipids of extremely halophilic archaeobacteria from saline environments in India: A novel glycolipid in *Natronobacterium* strains. *Microbiology* **1994**, *140*, 1959–1966. [CrossRef] [PubMed]
169. Papahadjopoulos, D.; Nir, S.; Ohki, S. Permeability properties of phospholipid membranes: Effect of cholesterol and temperature. *Biochim. Biophys. Acta-Biomembr.* **1971**, *266*, 561–583. [CrossRef]

Chapter 2. Methods

2.1. Basic theory

2.1.1. Scattering background

Since scattering theory has been presented in many textbooks (Bée, 1988; Harroun et al., 2006; Schnablegger and Singh, 2013), here I will only outline the theoretical principles of the techniques used during my thesis: neutron diffraction and SAXS.

Although the scattering laws for X-rays and neutrons are the same, there is a major difference: While X-rays are scattered by electrons, neutrons are scattered by atomic nuclei. Consequently, for X-ray scattering, the scattering intensity of one electron is always identical and therefore, atoms with a higher atomic number will scatter more. Whereas for neutrons the scattering ability of the atomic nuclei differs in a random way. Such atomic characteristic is known as the neutron scattering cross section and is tabulated (Sears, 1992).

Scattering depends on the interaction between matter and the incoming particles, e.g. neutrons or X-rays. Based on the wave-particle dualism, the particles are described as waves through their wavevector $\vec{k}$ (Eq. 2.1):

$$|\vec{k}| = \frac{2\pi}{\lambda} \qquad (Eq.\,2.1)$$

where λ is the wavelength of the radiation. Thus, considering the kinetic energy $E = \frac{1}{2}mv^2$, where *m* is the mass and *v* is the velocity, and the de Broglie wavelength $\lambda = \frac{2\pi\hbar}{mv}$, the energy of a particle can be defined in terms of its wavevector $\vec{k}$ (Eq. 2.2):

$$E = \frac{\hbar^2 k^2}{2m} \qquad (Eq.\,2.2)$$

In a scattering experiment, the incoming particle experiences a change of its momentum, i.e. changes its direction and/or velocity, after interacting with matter. This phenomenon is described by the momentum transfer vector, or the scattering vector, $\vec{Q}$ or $\vec{q}$, which is defined as the difference between the outgoing ($\overrightarrow{k_f}$) and the incoming ($\overrightarrow{k_i}$) wave vector (Eq. 2.3):

$$\vec{Q} = \overrightarrow{k_f} - \overrightarrow{k_i} \qquad (Eq.\,2.3)$$

Similarly, the energy transfer is defined as (Eq.2.4):

$$\Delta E = E_f - E_i \qquad (Eq.\,2.4)$$

Elastic scattering occurs when there is no energy transfer between the incident particle and the sample, i.e. the incoming wave can only change its direction. Conversely, inelastic scattering takes place when the incoming wave has transferred or absorbed energy from the matter (Figure 2.1).

For elastic scattering, the scattering vector $\vec{Q}$ can be defined by the trigonometric relation $\frac{Q}{2} = k_i sin\theta$, which is presented on figure 2.1. Combined with Eq. 2.1, it gives (Eq. 2.5):

$$Q = \frac{4\pi}{\lambda_i} sin\theta \qquad (Eq.\,2.5)$$

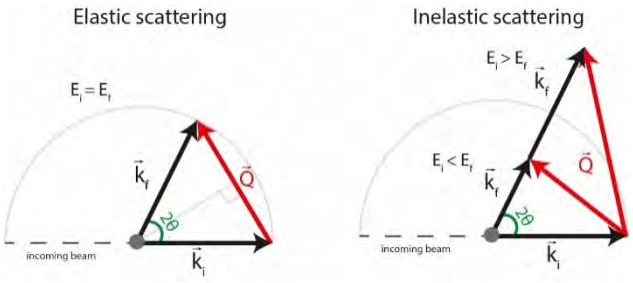

Figure 2.1. Schematic representation of scattering phenomenon. Left, no energy exchange between the incoming and the outgoing wave ($\overrightarrow{k_i} = \overrightarrow{k_f}$ and $\overrightarrow{E_i} = \overrightarrow{E_f}$). Consequently, the momentum $\vec{Q}$ can be solved by a trigonometric approach. It is called elastic scattering. Right, inelastic scattering, in which the outgoing wave has not the same energy than the incoming ($\overrightarrow{k_i} \neq \overrightarrow{k_f}$ and $\overrightarrow{E_i} \neq \overrightarrow{E_f}$). 2θ is the scattering angle.

If the sample is sufficiently well ordered, the scattered particles can interfere positively producing coherent waves. It is called coherent scattering and gives information on the relative positions of atomic nuclei, i.e. the matter's structure. Conversely, when there is no positive interference between waves scattered from different atomic nuclei, it is still possible to observe interferences between the waves scattered from one and the same nucleus, but at

different times. It is called incoherent scattering and it does not retain information about the structure, but the evolution in time of one nucleus.

For coherent scattering, when a constructive interference occurs due to some periodicity D in the sample structure, which can be related to the reciprocal spacing as $D = \frac{2\pi}{Q}$, equation 2.5 can be expressed as Bragg's law in terms of the real space (Eq. 2.6):

$$\lambda_i = 2Dsin\theta \qquad (Eq. 2.6)$$

Note that in X-ray scattering usually the $\vec{Q}$ vector is replaced by $\vec{S}$ where $\vec{S} = \frac{\vec{Q}}{2\pi}$ and consequently, $S = \frac{1}{D}$.

2.1.2. Neutron scattering

The Neutron is a subatomic neutral particle present in all atomic nuclei except ^{1}H. Because neutrons are uncharged particles, they have a low probability to interact with matter and therefore they are deeply penetrating and non-damaging. Moreover, their wavelength is similar to the interatomic spacings, so they are suited for structural studies. However, neutron sources are scarce. Neutron production for science is currently done by nuclear reactors, through the fission of uranium nuclei, or by spallation sources, where accelerated subatomic particles, e.g. protons, expel neutrons from nuclei of a heavy metal element, such as tungsten (Harroun et al., 2006).

The interaction between neutrons and atomic nuclei is complex since it involves nuclear spins and magnetics moments. Consequently, neutron scattering cross section does not follow any general trend and even differs between isotopes. The total scattering cross section of a nucleus is defined as the surface of a sphere with the scattering length, *b*, as its radius (Eq. 2.7):

$$\sigma_{tot} = 4\pi b^2 \qquad (Eq. 2.7)$$

The magnitude of *b* is about 10^{-12} cm; therefore, the scattering cross section is in the range of 10^{-24} cm^2, or in other words, in the range of 1 barn.

Since the neutron interacts with the spin of the nucleus, for nuclei with non-zero spin I, the system composed by the neutron and the nucleus will have a total spin state of $\left|I + \frac{1}{2}\right|$ or $\left|I - \frac{1}{2}\right|$, both having a different scattering length. In the case where the nucleus has a zero-spin value, i.e. ^{4}He,^{12}C,^{16}O and ^{32}S, the spin state of the nucleus-neutron-system will be the

spin of the neutron, i.e. $\frac{1}{2}$. Therefore, the neutron scattering cross section will have two contributions: the coherent and the incoherent (Eq. 2.8):

$$\sigma_{tot} = \sigma_{coh} + \sigma_{inc} \qquad (Eq. 2.8)$$

On the one hand, in the coherent contribution all nuclei have the same scattering length, which would be therefore equal to the average scattering length of the system (Eq. 2.9):

$$\sigma_{coh} = 4\pi < b >^2 \qquad (Eq. 2.9)$$

On the other hand, the incoherent contribution would be defined as (Eq. 2.10):

$$\sigma_{inc} = \sigma_{tot} - \sigma_{coh} = 4\pi < b^2 > - 4\pi < b >^2 = 4\pi(< b^2 > - < b >^2) \quad (Eq. 2.10)$$

Most of the nuclei from atoms found in biological samples, such as carbon, nitrogen and oxygen, are mainly coherent (σ_{coh} (^{12}C)= 5.56 barns, σ_{coh} (^{14}N)= 11.1 barns and σ_{coh} (^{16}O)= 4.23 barns). Nevertheless, there is an important exception: ^{1}H, which has a coherent cross section of 1.76 barns, and it is mainly incoherent (σ_{inc} (^{1}H)= 80.27 barns). Moreover, deuterium, an isotope of hydrogen, owns a higher coherent cross section (σ_{coh} (^{2}H) = 5.57 barns) and lower incoherent cross section (σ_{inc} (^{2}H)= 7.64 barns) than its protonated counterpart (Sears, 1992) (Figure 2.2). Despite the dual contribution on neutron scattering, some techniques allow to focus on the incoherent signal, to study atomic dynamics, or on the coherent one, to examine atomic structural organization.

All mentioned properties of neutrons, particularly the contrast variation between hydrogen isotopes, make them powerful to study biological samples. First, as H_2O and D_2O have very different scattering length densities, it is possible to contrast almost any biological sample in solution by using a correct mixture of H_2O/D_2O (Figure 2.2). Second, as a protonated molecule and its deuterated counterpart are almost identical in terms of functionality, but they own highly different neutron cross sections, it is possible to deuterate molecules or parts of them to highlight specific parts of the system under investigation.

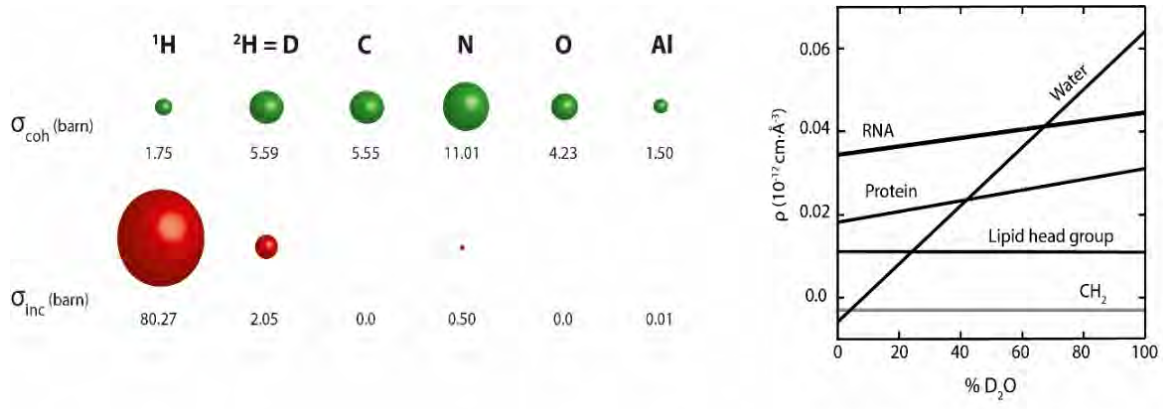

Figure 2.2. Left, neutron scattering cross sections σ for some elements (Sears, 1992)*. Right, average scattering length density of common biological macromolecules as a function of %D2O in the solvent. From* (Harroun et al., 2006)*.*

2.1.2.1. Neutrons to study molecular dynamics

Molecular dynamics are studied by the incoherent part of neutron scattering and give information about the averaged evolution in time of one atom. We can distinguish three types of scattering events depending on the exchange of energy between the atom nuclei and neutrons: elastic, quasi elastic and inelastic.

Elastic incoherent scattering gives information about the average atomic dynamics on a time scale that depends on the energy resolution of the instrument. From it, we can extract information about the mean square displacements (MSD).

Quasi elastic neutron scattering can distinguish different types of motions occurring in the sample (translational or rotational diffusion). As its name suggests, it is visible on the scattering signal by a broadening of the elastic peak.

Inelastic neutron scattering arises information on the vibrational motions of atoms. It can be used, for example, to study the rotational modes of molecules, molecular vibrations, magnetic excitations or electronic transitions.

2.1.2.2. Neutrons to examine the molecular structure: neutron diffraction

Neutron scattering techniques permit to study the coherent scattering part of atoms giving a spatial distribution of atoms from the sample. In the case of this thesis, the samples were a multistack of lipid bilayers ordered on a substrate. A widely used technique is neutron diffraction. The amplitude of the scattered wave is called structure factor (Eq. 2.11):

$$S(Q) = \sum_i b_i e^{iQr_i} \qquad (Eq.\ 2.11)$$

where *i* is each atom of the sample. It is a function of the spatial distribution of the atoms. The structure factor squared is proportional to the measured intensity *I (Q)* (Eq. 2.12):

$$I(Q) \propto |S(Q)|^2 \qquad (Eq.\ 2.12)$$

Because each nucleus has different scattering lengths, the scattering length density (SLD) is the average of the sum of the scattering lengths over a given volume δV (Eq. 2.13):

$$\rho(r)\delta V = \sum_i b_i \qquad (Eq.\ 2.13)$$

Moreover, SLD is the Fourier transform of the structure factor (Eq. 2.14):

$$\rho(r) = \int S(Q)e^{-iQr}dQ \qquad (Eq.\ 2.14)$$

When a sample owns large-positional order, the structure factor is represented as F_h. The 1D SLD from a multistack of lipid bilayers can be extracted by the magnitude of the structure factor $|F_h|$ (2.15):

$$\rho_r(z) = \frac{2}{D}\sum_{h=1}^{h_{max}} |F_h| \cos(\frac{2n\pi}{D}z) \qquad (Eq.\ 2.15)$$

where D is the periodicity of bilayers or lamellar repeat spacing of the ordered sample, i.e. the thickness of the bilayer including a water layer (Figure 2.3). The Fourier transform is related to the integrated intensities of Bragg peaks, after background subtraction, as $|F_h| = \pm\sqrt{I_h}$ (Katsaras, 1995). In the case of oriented samples, the intensity needs to be corrected by Q_z, i.e. the *Q*-value of the Bragg peak position, giving to $|F_h| = \pm\sqrt{I_h Q_z}$ (Lyatskaya et al., 2000). As $|F_h|$ is a complex function but the complex part is lost in the measured intensity, it is necessary to deal with the phase problem. Nevertheless, if the structure studied is centrosymmetric, as it is the case of a multistack of lipid bilayers, its Fourier transform is real and consequently, it can be only given by $+|F_h|$ or $-|F_h|$. To resolve the phase problem, it is possible to use the linear correlation of the structure factors. Because the cell is centrosymmetric, the scattering density will be constant or will change linearly with the percentage of D_2O in the solution. Since $z = \pm\frac{D}{2}$ (Figure 2.3), the linear slope should be positive or negative. Consequently, it is possible to solve the phase by plotting the structure factors *vs* D_2O content (Worcester and Franks, 1976), which must show a linear relation.

Several parameters of the lipid bilayer can be extracted from the SLD (Nagle and Tristram-Nagle, 2000) (Figure 2.3). Here, I will refer to the bilayer thickness (D_B); the hydrophobic core thickness corresponding to $D_c = \frac{V_c}{A}$, where V_c is the volume of the hydrophobic core and A is the average interfacial area/lipid. Furthermore, $D_B = 2\frac{V_l}{A}$, where V_l is the lipid molecular volume. The water layer thickness is defined as $D_w = D - D_B$.

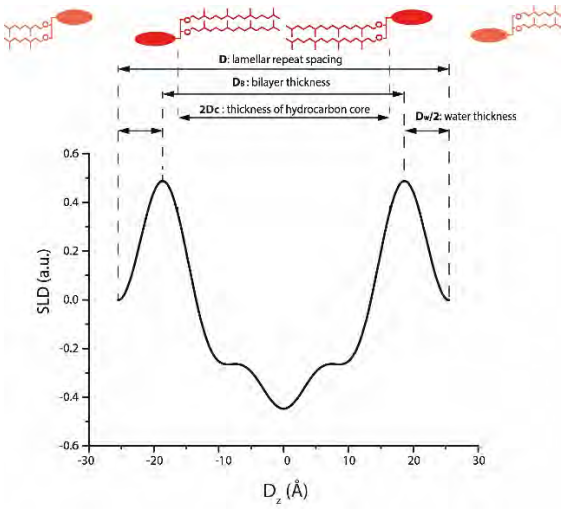

Figure 2.3. Typical neutron scattering length density profile (SLD) of a lipid bilayer as function of the bilayer depth, z-axis. D_z= 0 Å represents the bilayer midplane. The Two maxima correspond to the lipid headgroups.

2.1.3. X-rays to study the structure of soft matter: small angle X-ray scattering

X-rays interact primarily with electrons and each electron contributes the same amount on the average scattering ($\sigma = 7.93977 \cdot 10^{-26}$ cm^2). Therefore, X-ray scattering efficiency depends on the number of electrons per material volume, i.e. the X-ray atomic scattering factor increases with atomic number.

X-rays are produced by laboratory sources or by synchrotron facilities which have a higher photon flux. In a synchrotron, charged particles, such as electrons or positrons, move through a circular path at high speed providing a continuous wavelength spectrum. The impact of an X-ray photon to an electron produces free electrons and, after acceleration, multiplication and amplification processes, generates electric pulses that are counted and displayed as “count rate” or “intensity” (Schnablegger and Singh, 2013). It is recorded in the plane of detection giving a 2D scattering pattern. However, since most of the time the 1D scattering would give the same information, it is common to reduce the signal by averaging after background subtraction (Figure 2.4).

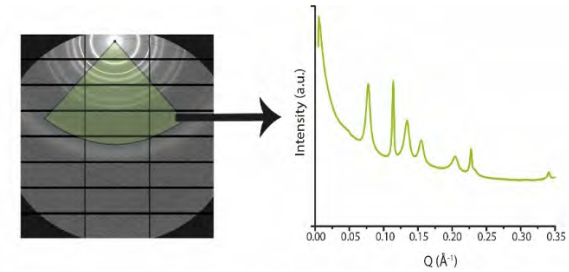

Figure 2.4. Circular average of a SAXS diffraction pattern.

SAXS is a widely used elastic scattering technique that reveals structural correlations in the sample. It is a central technique to study soft matter as it reveals information on the size and shape of particles. For instance, it has been largely used to study the self-assembly of amphiphiles, as the case here, but also to study the structure of proteins at low resolution. The advantage is that it does not require a crystalline sample.

Phospholipids in solution self-assembly constituting structures with long-range order, i.e. they crystallize. In crystalline substances the structure factor is usually called lattice factor and it is based on high intensity peaks at well-defined angles. Just as in all diffraction techniques, such positions on the Q-scale indicate the sample symmetry (Figure 2.5):

- Lamellar symmetry: 1 (100), 2 (200), 3 (300), 4 (400), 5 (500) ...
- Cubic symmetries:
    - Pn3m: $\sqrt{2}$ (110), $\sqrt{3}$ (111), 2 (200), $\sqrt{6}$ (211), $\sqrt{8}$ (220) ...
    - Im3m: $\sqrt{2}$ (110), 2 (200), $\sqrt{6}$ (211), $\sqrt{8}$ (220), $\sqrt{10}$ (310) ...
    - Fd3m: $\sqrt{3}$ (111), $\sqrt{8}$ (220), $\sqrt{11}$ (311), $\sqrt{12}$ (222), $\sqrt{16}$ (400) ...
- 2D hexagonal symmetry (p6mm): 1 (10), $\sqrt{3}$ (11), 2 (20), $\sqrt{7}$ (21), 3 (30) ...

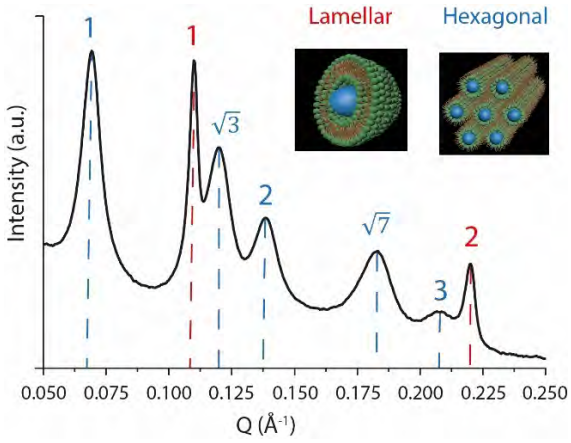

Figure 2.5. Example of a SAXS diffraction of a sample from lipids self-assembled under a lamellar phase (red) and hexagonal phase (blue). Numbers on the peaks indicate the ratio of each peak position. Drawings represent both lipid phases, lipid headgroups are in green, hydrocarbon chains in brown and water in blue.

The values in parentheses are the Miller indices *h,k,l*, which indicate the orientation of a plane for each symmetric position. The lattice parameter (a) is the distance between two

symmetric structures. For lamellar symmetries it corresponds to the periodicity D, $a_{lam} = D = \frac{2\pi}{Q_n}$ and for the hexagonal symmetries it is defined as $a = \frac{2}{3}D = \frac{4\pi}{3Q_n}$, where Q_n is the Q-position of the Bragg peak. Last, the lattice parameter of cubic symmetries can be found by plotting the positions of the Bragg's peaks on the S-scale *vs* $(h^2 + k^2 + l^2)^{1/2}$. The plot should intercept through the origin and will be linear with a slope of $\frac{1}{a_{cubic}}$.

2.1.4. Fluorescence spectroscopy

Fluorescence is a well-known phenomenon which has been largely described in textbooks (Lakowicz, 2006; Valeur and Berberan-Santos, 2012). Here, I will only introduce some basic concepts.

Fluorescence occurs when an electron is excited by the energy of a photon and after a brief interval, it relaxes to its ground state. Sometimes the electron loses part of the absorbed energy by going to lower excited states and therefore, it will have less energy when it is back to its ground state. Hence, since the wavelength is inversely proportional to the energy, the emission wavelength will be longer than the excitation wavelength. The difference in energy or wavelength is called Stokes shift. The fluorescence phenomenon is often illustrated by an electronic-state diagram, i.e. Jablonski diagram (Figure 2.6).

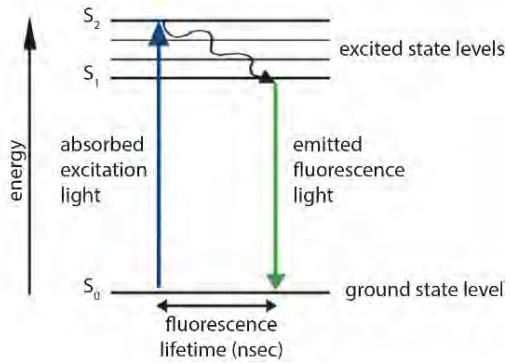

Figure 2.6. Fluorescence phenomenon represented in the Jablonski diagram (Llères et al., 2007)

Because electrons will have different excited state levels and they will find different ground state levels after the fluorescence phenomenon, the excitation and the emission wavelength present a range of values. However, each fluorophore would have a maximal excitation and emission wavelength. Consequently, it is important to use the maximal λ_{exc} to obtain the maximum intensity at the emission. Most of fluorescent dyes are polyaromatic hydrocarbons or heterocycles. During my thesis, I used Carboxyfluorescein, Pyranine and Laurdan.

2.1.4.1. Carboxyfluorescein

5-(6)-Carboxyfluorescein (CF) is a fluorescein derivative but with a carboxyl group added (Figure 2.7). It is a fluorophore with an excitation wavelength of 495 nm and emission wavelength of 518 nm. It is not incorporated into the lipid bilayer, but it can be encapsulated into liposomes (multilamellar or unilamellar lipid vesicles).

CF at high concentrations, i.e. > 10 mM, is mostly self-quenched, thus when encapsulated in liposomes at such concentrations, it is non-fluorescent (Chen and Knutson, 1988). Its leakage through the lipid bilayer will diminish its concentration and therefore, its fluorescent intensity will increase (Figure 2.7). It is a fluorescent dye widely used to study membrane permeability of lipid bilayers from liposomes. A total leakage of the probe from liposomes will provide the maximum fluorescent intensity of the sample. Hence, a percentage of the CF efflux, which will be proportional to the permeability of the lipid bilayer, can be determined (Eq. 2.16) (Weinstein et al., 1981):

$$\%\ CF\ efflux = \frac{F_t - F_0}{F_{max} - F_o} \qquad (Eq.\ 2.16)$$

where F_t, F_0 and F_{max} are the fluorescence intensities at time t, time zero, and after total solubilization by a detergent, such as Triton X-100.

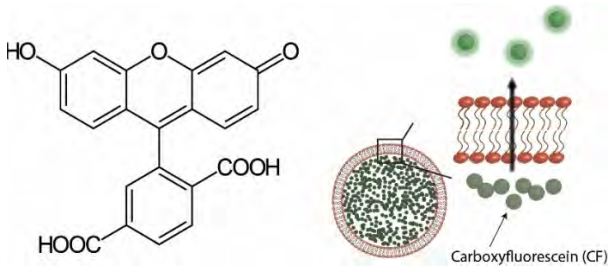

Figure 2.7. Left, skeletal formula of CF. Right, scheme of the CF efflux technique.

2.1.4.2. Pyranine

8-Hydroxypyrene-1,3,6-trisulfonic acid (HPTS) or Pyranine is a highly water soluble, thus membrane-impermeable, fluorescent dye from the group of arylsulfonates (Figure 2.8). At pH 7.5, its maximum excitation wavelength is 460 nm and its maximum emission wavelength is 510 nm. It is a pH sensitive dye; this means that a pH change causes a shift on its emission spectrum (Gan et al., 1998) (Figure 2.8). Such characteristic has been widely used to determine membranes proton permeability. Pyranine is encapsulated inside liposomes at neutral pH and as protons penetrate into liposomes, Pyranine emission intensity will decrease (Figure 2.8).

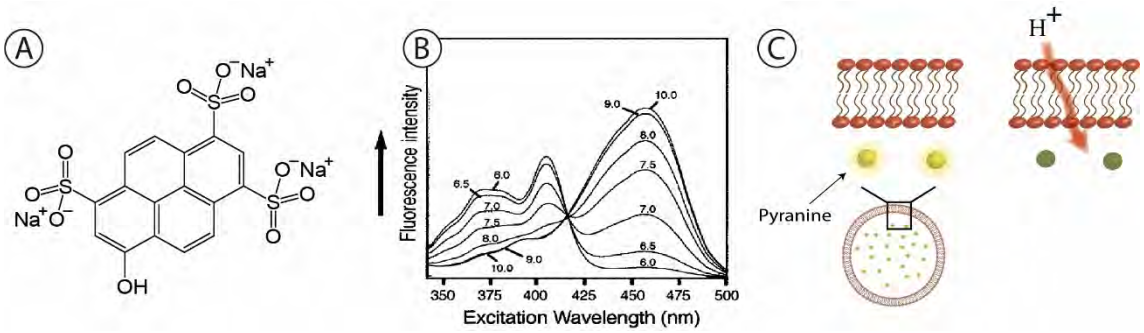

Figure 2.8. A) Left, skeletal formula of Pyranine. B) Pyranine excitation spectra at different pH, from (Gan et al., 1998)*. C) Scheme of the technique that uses Pyranine as a sensor of liposomes' internal pH.*

2.1.4.3. Laurdan

6-Dodecanoyl-N,N-dimethyl-2-naphthylamine (Figure 2.9), more commonly known as Laurdan, is a fluorophore that is anchored in lipid bilayers. It is largely used to investigate lipid phase transitions and fluidity of the membrane. The polycyclic aromatic compound naphthalene possesses a dipole moment that causes reorientation of water molecules which results in a red shift of the probe emission (Parasassi et al., 1998). After excitation at 350 nm, the emission spectrum of Laurdan in phospholipid membranes present two local maxima, one at about 440 nm for ordered lipid (L_β) phases and the other around 490 nm for the more disordered and fluid lipid phases (L_α) (Figure 2.9). Because the membrane is more disordered at liquid-crystalline phase compared to the fluid phase, naphthalene will be surrounded by more water molecules causing the red shift. To precisely quantify the polarity change, the general polarization (GP) term is defined as (Eq. 2.17):

$$Laurdan\ GP = \frac{I_{440} - I_{490}}{I_{440} + I_{490}} \qquad (Eq.\ 2.17)$$

where I_{440} and I_{490} are the emission intensities at 440 and 490 nm, respectively. Laurdan GP values can range from +1 to -1, *i.e.* -1 being the highest lipid membrane fluidity (Parasassi et al., 1991).

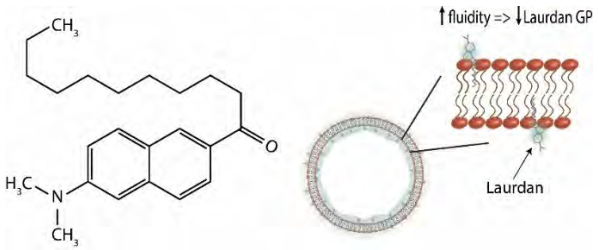

Figure 2 9. Left, skeletal structure of Laurdan. Right, schematic representation of Laurdan position in the lipid bilayer.

2.2. Sample preparation

2.2.1. Lipids used

1,2-di-O-phytanyl-*sn*-glycero-3-phosphocholine (DoPhPC) and 1,2-di-O-phytanyl-*sn*-glycero-3-phosphoethanolamine (DoPhPE) were bought from Avanti Polar Lipids (Alabaster, USA) (Figure 2.10). Purity guaranteed was > 99%. Such lipids own the same characteristics than archaeal monopolar lipids. They were systematically used as a mixture of DoPhPC: DoPhPE at 9:1 molar proportion. The model polyisoprenoid molecule was 2,6,10,15,19,23-hexamethyltetracosane, best known as squalane, and it was bought from Sigma-Aldrich (Montana, USA) (Figure 2.10).

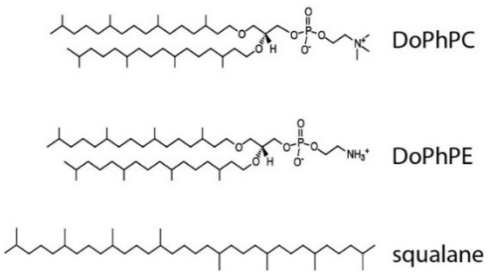

Figure 2.10. Skeletal representation of lipids used during this thesis.

2.2.2. Neutron diffraction on D16: multistack of oriented lipid bilayers

D16 is a small-Q diffractometer of the Institut Laue Langevin (ILL) located at Grenoble, France (Cristiglio et al., 2015) (Figure 2.11). Two wavelengths, i.e. 4.5 Å or 5.6 Å, can be selected and the diffracted neutrons are recorded in a 2D detector. The detector was placed 12° from the sample and its angle, i.e. omega, was rotated from -0.5° to 12°. Accessible Q-range was from 0.06 $Å^{-1}$ to 0.51 $Å^{-1}$.

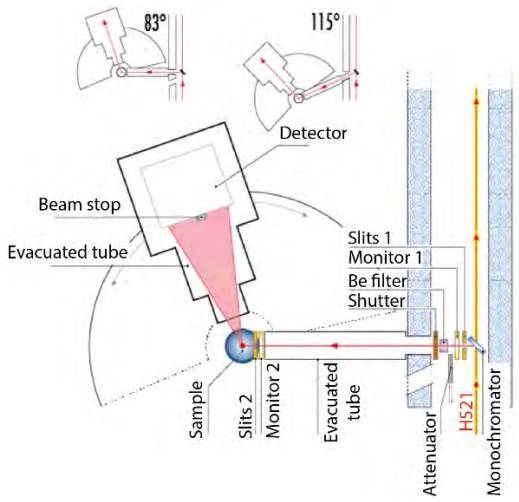

Figure 2.11. Sketch of the neutron diffractometer D16 from ILL. H521 correspond to the neutron guide. From ill.eu.

Lipid bilayers were studied as a multistack of hundreds of lipid bilayers on a substrate to enhance the intensity of the scattered neutrons. The substrates used were one-side polished ultraclean silicon wafers with a thickness of 275 ± 25 µm purchased from Si-Mat (Germany). All wafers were cut with a diamond pen to fit inside the different sample holders.

Right-size wafers were rinsed with ethanol and dried by a nitrogen flux. Then, 3 mg of the lipid mixture in a chloroform: methanol (2:1) solution was deposited on the polished side of the wafer (Figure 2.12a). The solution chloroform: methanol is widely used to allow the complete solubilization of lipids, but in this case also to avoid a too fast evaporation of the solvent when deposited on the wafer. The solution should be deposited onto the wafers with the lipids in a fluid state (temperature above T_m). Because archaeal lipids do not present any phase transition for a large range of temperatures (-120 °C to 120 °C), here the step can be done at room temperature. It is important to correctly spread the solution through all the wafer; the solution must be in contact with the edges of the wafer but avoiding the spill. For this, it is possible to place the wafer on a completely flat surface or to use the "rock and roll method" (Tristram-Nagle, 2007). In the second case, the wafer is moved gently through all directions to distribute the solution. Last, after evaporation of the solvent, the lipid film is formed (Figure 2.12b).

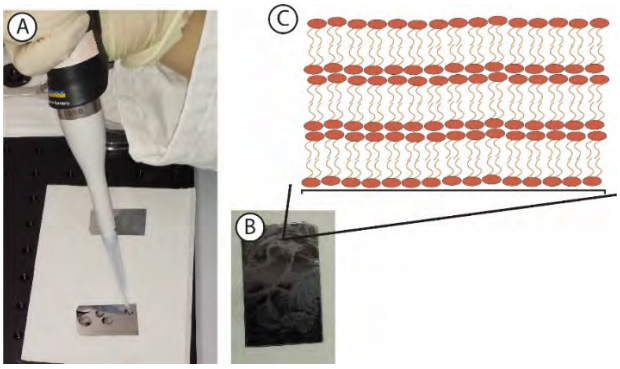

Figure 2.12. A) First steps of lipid deposition on a Si wafer. B) Dried lipid films on the wafer. C) Representation of the organization of lipids on the wafer, red circles represent lipid headgroups and hydrophobic chains are in brown.

After lipid deposition, the wafer with the lipid film is placed under vacuum overnight to remove all traces of solvent. Then, the sample anneals at temperatures above T_m for 48h (in this case, a temperature of 40 °C was chosen) in a desiccator with a desired $\%H_2O$ - $\%D_2O$ solution to allow complete pre-hydration of lipid films. Nevertheless, because sample hydration will drop almost instantly when placing it in the sample cell, another lipid hydration after closing the sample holder will be necessary. During my thesis, I used three types of sample holders depending on sample environmental conditions: BerILL chamber, HT sample holder and HT – HHP cell.

1) BerILL is an aluminium humidity chamber (Figure 2.13) (Gonthier et al., 2019). Aluminium is the component of choice for most neutrons' sample holders as it is almost transparent for neutrons (Figure 2.2). The wafer is placed vertically on the goniometer and correctly aligned using a laser. H_2O/D_2O is placed in a copper bath of the chamber bottom. The vacuum is done around the sample chamber and sustained for a low background scattering. To assure a constant temperature, BerILL has two thermostat fluid circulations: one near the sample, and another at the copper bath. The relative humidity is precisely controlled by choosing the up and bottom temperatures. There are temperature and humidity sensors near the sample.

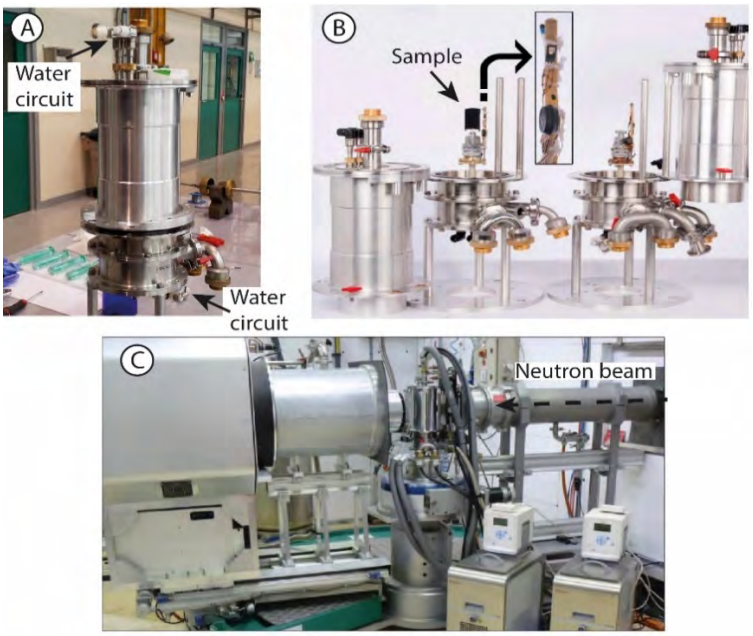

Figure 2.13. A) Picture of BerILL chamber, the two thermostat fluid circulations are highlighted. B) Two BerILL chambers opened with detail of the sensors near the sample. From (Gonthier et al., 2019). *C) D16 diffractometer with the BerILL chamber installed. From* (Cristiglio et al., 2015).

2) The HT sample holder is an aluminium flat cell with an upper and lower component (Figure 2.14). To put the Si wafer inside, first, four pieces of aluminium foil are placed in each edge of the cell. Then, a drop of 50 µl of water with the chosen H_2O/D_2O-contrast is deposited on its centre to allow the later hydration of the sample. Aluminium foils avoid the full contact of the wafer with the water drop. The wafer is placed in the sample holder and four more pieces of aluminium foil are added to fix it and to avoid the contact of the wafer with the upper part of the cell. For a correct measurement, the cell needs to be hermetically closed. Therefore, it is necessary to fill the joint with silicone. It can be easily done with the help of a syringe and a pipette tip. Last, the sample holder with the upper part of the cell and tightening with the screws.

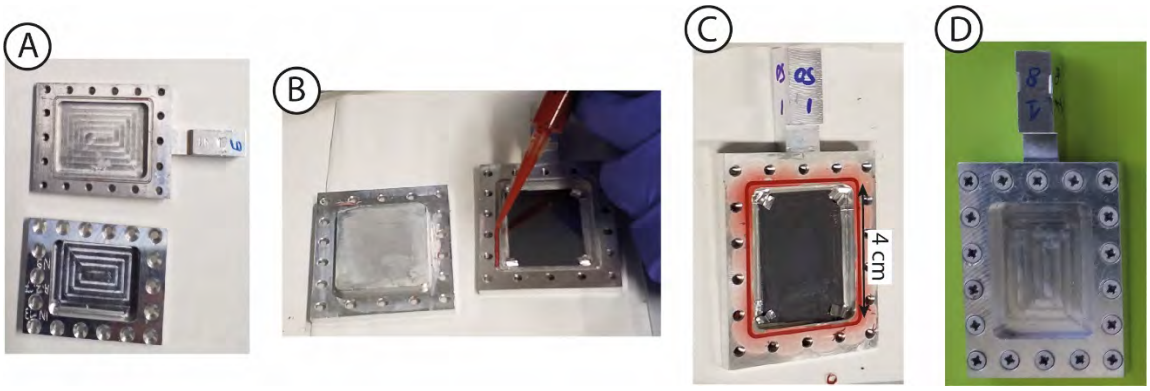

Figure 2.14. A) HT cell opened. B) Filling the joint with silicon. C) Picture of the HT cell with the wafer and four pieces of aluminium foil. D) Closed HT cell.

3) The HT-HHP cell is made of TiZr that confers strength enough to resist conditions up to 100 °C and 250 MPa (Peters et al., 2018) (Figure 2.15). Since in this case lipid bilayers need to be in contact with a liquid to transmit pressure, two wafers are placed face-to-face to increase the scattering signal and avoid the drop formation on the samples, which would destroy the desired multi-layer organization. In addition, a piece of aluminium foil of the same size than the wafers is introduced in the cell insert. This facilitates to put and remove the "sandwich" of wafers from the insert, but it also avoids the direct contact of water with the sample. 10 µl of water with the desired H_2O/D_2O contrast are added. After hydration of approximately two hours, the insert is placed into the cell and all its components are assembled. Fluorinert ® was used as pressure transmitter.

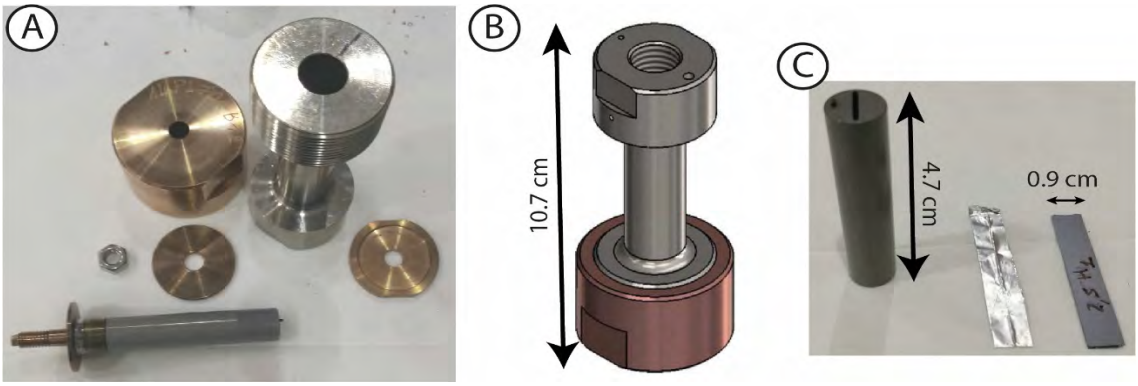

Figure 2.15. A) Components of the HT-HHP cell. B) Assembled HT-HHP cell. From (Peters et al., 2018)*. C) Detail of the insert and the piece of aluminium foil and the two wafers placed inside it.*

Both HT and HT - HHP sample holders are measured inside a cyostat (orange equipment in Figure 2.16a) to precisely control the temperature. In order to place the samples in the neutron beam, sample holders were assembled on their corresponding stick (Figure 2.16b and c), which is introduced from the top of the cryostat. Moreover, the stick for the HT-HHP was specially conceived to conduct the HHP transmitter, i.e. water or Fluorinert ®, to the

sample holder, thereby enabling the increase of pressure on the sample (Lelièvre-Berna et al., 2017).

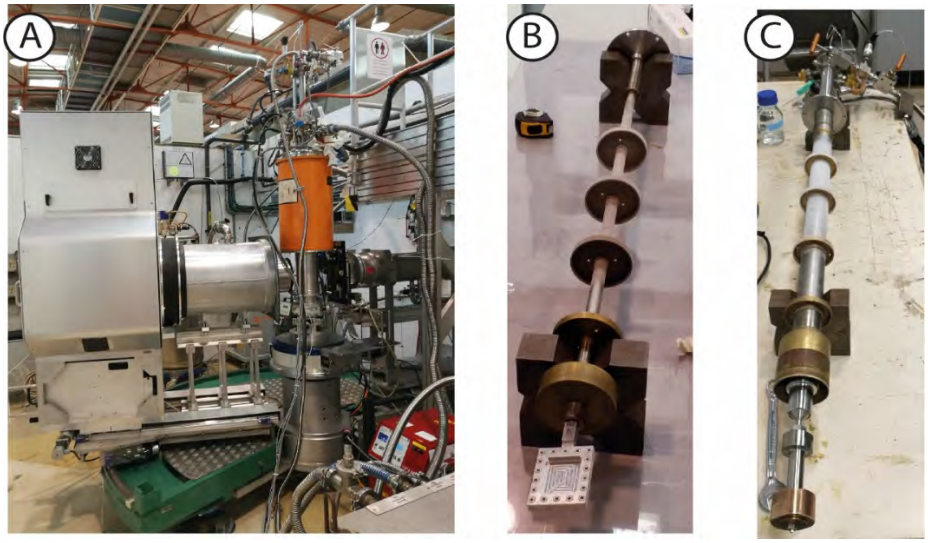

Figure 2.16. A) Picture of D16 diffractometer with the cryostat installed. B) HT cell and corresponding stick. C) HT-HHP and corresponding stick to transmit hydrostatic pressure.

2.2.3. SAXS on I22: non-oriented lipids in solution

I22 is a SAXS beamline at Diamond light source (DLS) located at Oxfordshire, England (Smith et al., 2019) (Figure 2.17). It can be operated in the range 3.7 keV to 22 keV and its beam is of approximately 300 µm by 250 µm. The energy used here was 17 keV, i.e. λ= 0.73 Å. The studied Q-range was from 0.01 $Å^{-1}$ to 0.45 $Å^{-1}$.

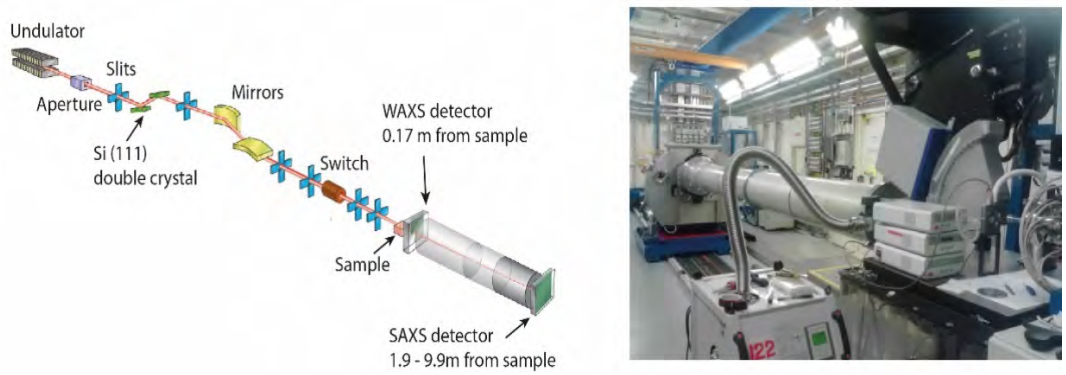

Figure 2.17. Sketch (left) and picture (right) of I22 beamline from DLS. From diamond.ac.uk

HHP cell is based on two perpendicular bores enclosed by a thick wall (Brooks et al., 2010) (Figure 2.18a). It is suitable for experiments up to 500 MPa and 120 °C. The sample holder consists of an 8 mm across and 1.5 mm thickness disk of a deformable polytetrafluoroethylene (PTFE) plastic with 3 mm diameter and 50 µm thickness Mylar plastic windows (Figure 2.18b). The 3 mm aperture has a volume of 11 mm^3. Such sample holder is

specially designated for high viscosity samples as is the case here. The Mylar windows are attached to the PTFE disk by two-face adhesive film.

In this SAXS experiment, lipids were not ordered on a substrate and they were self-assembled, for example as multilamellar vesicles (Figure 2.18c). 5 mg of lipids were mixed with 20 µl of water followed by vortexing and 5 cycles of freeze-thawing for a correct homogeneity. Prior to measuring, samples were subject to two cycles of pressure to 100 MPa to further homogenise the sample and check for leakage. After each pressure ramp, the pressure was decreased and the signal at 0.1 MPa was compared to the signal before the pressure ramp to check for radiation damage during the measurement. No significant differences were observed.

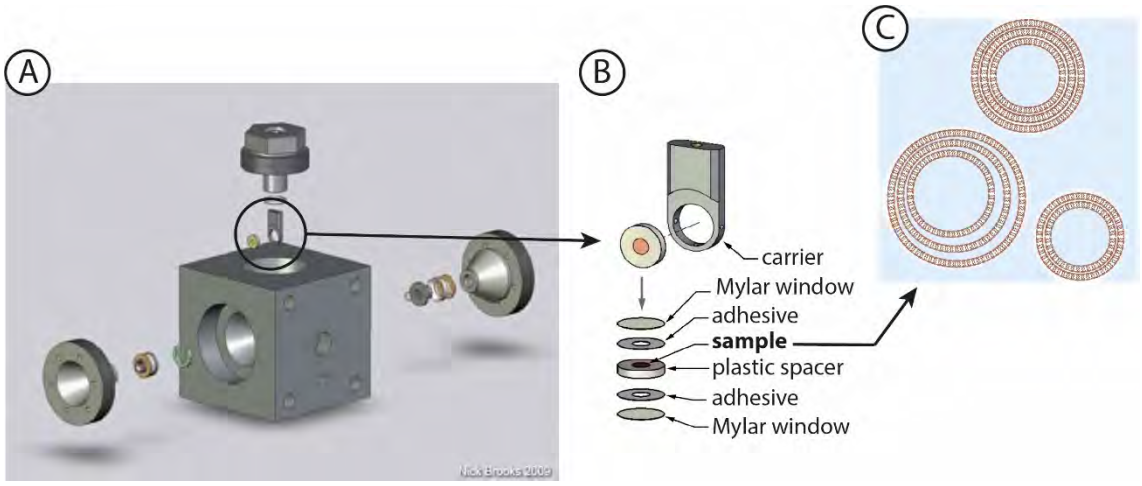

Figure 2.18. A) HT-HHP cell used. From imperial.ac.uk. B) Detail of the sample holder. From (Brooks et al., 2010)*. C) Schematic representation of a sample measured: non-oriented lipids in solution forming multilamellar vesicles.*

2.2.4. Fluorescent techniques

The right amount of DoPhPC: DoPhPE (9:1) in absence or in presence of squalane for a final concentration of 6 mM was weighted in a clean vial. Squalane was added from a chloroform solution. Then, 150 µl of chloroform: methanol (2:1) was added in the vial to homogenise. From here, it is necessary to distinguish the techniques in which the fluorescent dye was encapsulated, i.e. CF efflux and Pyranine fluorescence, from the one for which the probe was inserted in the lipid bilayer, i.e. Laurdan GP. In the first two cases, the fluorescent dye was added later, while for the Laurdan GP measurement, 2.5 µl of Laurdan 1 mM in dimethyl sulfoxide was added now. After vortexing, the solvent was evaporated by a nitrogen flux and it was left under vacuum overnight to ensure solvent complete evaporation. The lipid film (Figure 2.19) was hydrated with the right solution depending on the technique:

1) CF: CF 40 mM in HEPES 10mM, 100mM KCl, 1mM EDTA pH 7.8. CF presents some difficulties to be solubilized at this high concentration. It is necessary to first bring the solution at pH: 11 with NaOH 1M and once it is completely solubilized, bring it back to pH: 7.8 with HCl 1M.
2) Pyranine: 5 mM Pyranine in HEPES 5 mM at pH 7
3) Laurdan GP: Tris 50 mM at pH 7

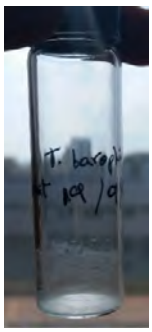

Figure 2.19. Picture of a typical lipid film obtained after solvent evaporation.

Due to hydration and the amphiphile character of lipids, they were self-assembled as multilamellar vesicles. The solution was vortexed followed by 5 cycles of freeze-thaw: the dispersion of liposomes was quickly frozen using liquid nitrogen (-195 °C) and heated at 60 °C. If liquid nitrogen was not available, it could be replaced by leaving the dispersion at 4 °C during 1h. Although here we already have a dispersion of liposomes, it is necessary to obtain a dispersion containing unilamellar vesicles with a homogenized size. For this purpose, the dispersion was extruded 11 times through a 100 nm polycarbonate filter using the Avanti Mini-extruder ® (Avanti Polar Lipids) to obtain large unilamellar vesicles (LUVs) (Figure 2.20) (Hope et al., 1985). It is necessary to consider several factors for lipids' extrusion: 1) The temperature of all the system (dispersion, block and syringes) needs to be above T_m, in this case I did the extrusion at 50 °C; 2) an extruded solution should be clearer by eye than before extrusion; 3) it is important to recover the dispersion after passing it through the filter an odd number of times, this avoids to recover impurities that were left on the filter.

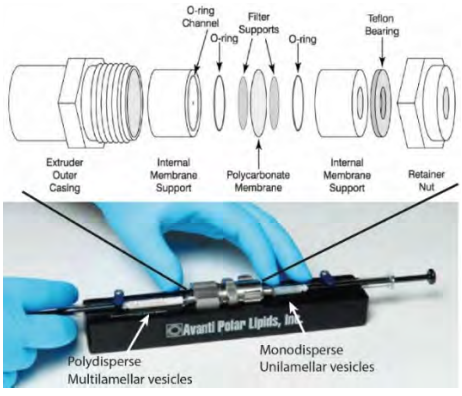

Figure 2.20. Mini extruder from Avanti Polar Lipids and detail of different components. From Avanti.com

Once obtained the monodispersed solution of liposomes, it is imperative to separate the non-encapsulated dyes from the liposomes, except from the Laurdan GP protocol since Laurdan was incorporated at low concentrations into the lipid bilayer. The non-encapsulated dyes and liposomes separation was done by size exclusion chromatography using a PD-10 column (GE Healthcare), which contains 8.3 ml of Sephadex G-25. After adding 500 µl of dispersion, liposomes leave the column after eluting with *ca.* 3 ml of buffer. To prevent leakages from liposomes, this step should be done at temperatures below lipids' T*m*, for DoPhPC:DoPhPE mixtures, room temperature was correct since no phase transition has been detected for these lipids. Fluorescence measurements up to 60 °C and 100 MPa were done immediately, excitation and emission wavelength were chosen according to the fluorescent dye:

1) CF: λ_{exc}= 492 nm and λ_{em}= 500-600 nm, with the maximum at 518 nm. At the end of the measurement, all trapped fluorescent dyes were released by adding 0.1 % of detergent, such as Triton X-100.
2) Pyranine: λ_{exc}= 470 nm and λ_{em}= 480-560 with the maximum at 510 nm. For this experiment, first, we measured the liposomes dispersion increasing temperature or pressure, this was called "blank". Second, the same protocol was followed than for the "blank" but adding 10 µl of HCl 0.1 mM. Finally, results from the "blank" measurement were subtracted to the second measurement. Hence, the effect of adding protons was exposed.
3) Laurdan: λ_{exc}= 390 nm and λ_{em}= 410-510 nm, with the maximum at 440 nm or 490 nm.

Fluorescent measurements were done as function of temperature and pressure. In the case of temperature, the Jasco 115 Spectrofluorometer FP – 8500 was connected to a water thermostat bath. HHP were applied by a home-made device build by the Membrane Biophysics group from Imperial College London (Figure 2.21) with a LED source of λ_{exc}= 470 nm. Hydrostatic pressure was applied using a hand pump pressure generator and sapphire windows were used to isolate the system.

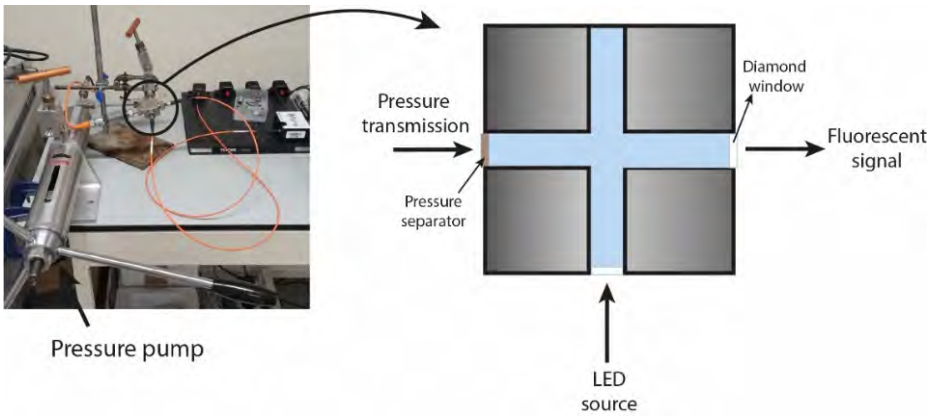

Figure 2.21. Left, picture of the pressure system for fluorescent measurements at HHP. Right, scheme of pressure cell which enclose the sample.

Chapter 3. Validity of a novel membrane architecture

Today, the model presented by Singer and Nicolson in 1972 (Singer and Nicolson, 1972) is still commonly used as description of the cell membrane. In this model, the cell membrane was presented as a multicomponent homogenous fluid, in which the components where dispersed and lipids where in the "liquid crystalline, L_α" phase. Hence, it describes the whole cell membrane with a unique structure and dynamic. Nevertheless, after decades of research, the vision of the model has evolved.

The current picture is more sophisticated due, for example, to the existence of membrane domains, corresponding each to a particular phase with specific physicochemical characteristics. For instance, certain lipids, such as sphingomyelins and saturated phospholipids, form together with cholesterol membrane domains in a "liquid ordered, L_o" phase (Brown and London, 1998). Although, it is still a fluid phase, such domains present a higher structural order and lower dynamics than the L_α, which confers them specific functions, such as the anchorage of specific membrane proteins. In addition, the cell membrane may present domains of lamellar gel phases (L_β), where the alkyl chains are ordered and do not diffuse. Last, although indeed the lamellar L_α bilayer constitutes the main structure of a biological cell membrane, the presence of non-lamellar phases and the existence of non-lamellar-former lipids increases the intricacy of natural cell membranes. For instance, cubic phases could act as subcellular space organizers in which proteins may be accommodated as demonstrated on the monoolein-water-lysozyme system (Larsson, 1989).

Non-lamellar phases are formed to release the curvature frustration of lipids (Helfrich, 1973) which are determined mainly by their shape (Figure 3.1). It has been rationalized using the critical geometric packing parameter (P_p) concept introduced by Israelachvili (Israelachvili et al., 1976), although an alternative quantitative method that calculates the splay, the area at the end chain, has been recently presented (Kulkarni, 2019). P_p is defined by $P_p = \frac{v}{a \cdot l}$ where v is the molecular volume, l is the molecular length and a is the molecular area at the lipid-water interface. For $P_p < 1$, molecules are inverted cones and tend to produce positive curvatures. For $P_p \sim 0$, lipids have a cylindrical shape and adopt zero curvature, giving rise to lamellar phases. For $P_p > 1$, lipids present conical shapes and adopt negative curvatures and self-assemble under inverted phases.

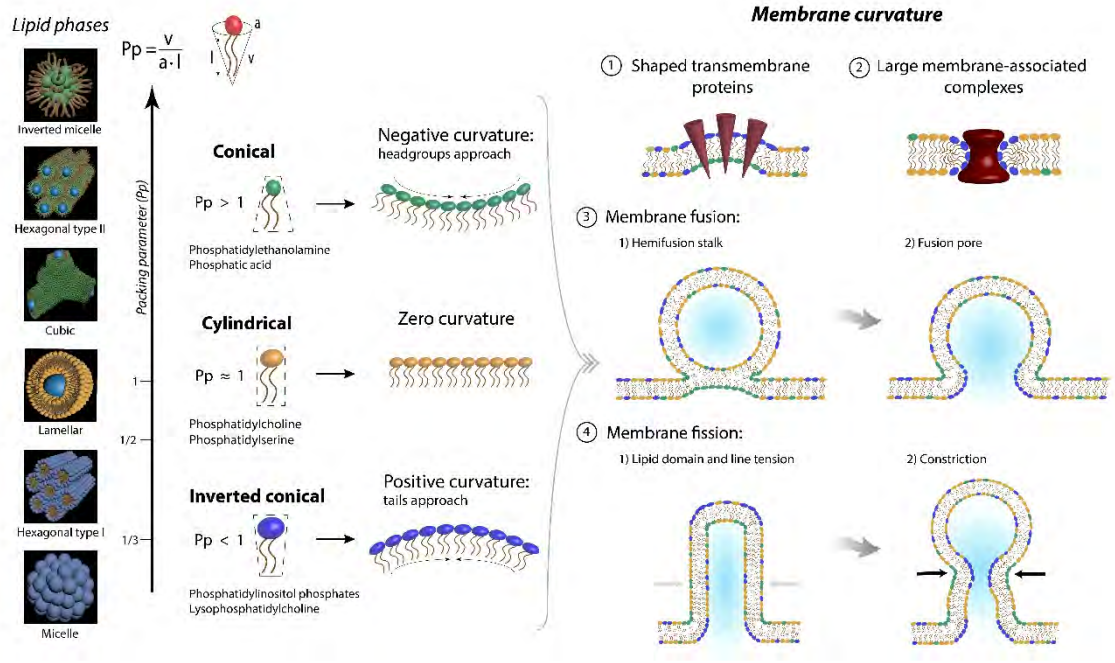

Figure 3.1. Sketch of different lipid phases and their significance for cell membranes

Phospholipid molecules containing small polar head groups are non-lamellar forming lipids. For example, lipids such as cardiolipin, lipids with phosphatidylethanolamine (PE) or phosphatic acid as headgroups, mono- and diacilglycerols such as monoolein (MO), monoelaidin, monolinolein and fatty acids have an inverted conical shape and induce various inverted types of nanostructures. Moreover, addition of cholesterol, a lipid with an extremely small head group, promotes the formation of non-lamellar phases in lipids that comprises PE, but also phosphatidylcholine (PC) with polyunsaturated chains (Marquardt et al., 2016). Composition alterations of the ratio between lamellar and non-lamellar former lipids tune the flexibility and the curvature of the membrane (Ninham et al., 2017), which allows the cell membrane to adapt itself and maintain essential function under different environmental conditions. Examples of such cell functions are protein anchorage, fusion, fission (Figure 3.1)

and intercellular communication by nanotubes and nanopods, i.e. extracellular vesicles associated to filamentous structures (Gill et al., 2019). This may explain why non-lamellar former lipids are present at high levels in biological membranes, usually at values up to 30 mol% of the total lipid content (Meersman et al., 2013). Protein anchorage, endo- and exocytosis processes and even nanotubes are present in all three domains of life. For instance, the Archaea *Thermococcus gammatolerans* and *Thermococcus kodakarensis* produce membrane vesicles and nanotubes (Marguet et al., 2013).

Thus, our current understanding of the cell membrane is that of a heterogeneous and dynamical structure influenced by the curvature conferred from its lipids and the lateral heterogeneity provided by the presence of domains, which could even be presented in the form of non-lamellar structures, in order to partition the cell membranes into functional units. Each unit can accommodate specific proteins/lipids which will help compartmentalize cellular functions in the cell.

Article I. Structural characterization of an archaeal-like lipid bilayer as function of hydration and temperature

Marta Salvador-Castell [1], Bruno Demé [2], Philippe Oger [1] & Judith Peters [2,3]

[1] Université de Lyon, INSA de Lyon, CNRS, UMR 5240, 69211 Villeurbanne, France

[2] Institut Laue Langevin, 38000 Grenoble, France

[3] Université Grenoble Alpes, LiPhy, CNRS, 38000 Grenoble, France

Manuscript in preparation for Chemistry and physics of lipids

Foreword

This article presents the characterisation of the physicochemical behaviour of the reconstructed model membrane used throughout this thesis. This model membrane is composed of the archaeal-like monopolar lipids DoPhPC and DoPhPE in a molar proportion 9 to 1. Although, membrane lipids have been largely studied using eukaryal-like lipids, information about archaeal-like lipids remains scarce. For example, although there is some information about the ester analogue of DoPhPC, i.e. DPhPC, few studies have been done with the ether lipids. In addition, most studies have focused on the bipolar, monolayer forming lipids which are a specificity of the archaeal hyperthermophiles. Moreover, since the cell membrane is a mixture of lipids, here we have chosen to use a portion of DoPhPE, an electrically neutral molecule with a particular small headgroup, leading to a lipid composition never studied. Therefore, it was necessary to characterize the lipid bilayer for a further comparison of the membrane in presence of apolar polyisoprenoids.

The lipid membrane was described as function of humidity and temperature by neutron diffraction. I have used the neutron diffractometer D16 from ILL (Cristiglio et al., 2015) and the BerILL humidity chamber (Gonthier et al., 2019) to control environmental conditions. I have determined the structural parameters of the membrane together with the neutron scattering length density (NSLD) to obtain a complete view of the membrane organization. On the one side, humidity is an essential parameter that highly affects lipid bilayer characteristics by modifying, for example, the lipid bilayer thickness or lipid self-assembly. Here, lipids under low relative humidity (RH) self-assembly under non-lamellar phases, while above 90 % RH, it

self-organized as a lamellar phase. On the other side, since we are interested in extreme conditions, the description of the membrane model at high temperatures is essential for this project. Accordingly, I have determined the structural properties of the archaeal membrane at temperatures up to 70°C. We have tried to measure it at higher temperatures, but the stability of the structural organization of the membrane became too low to obtain interpretable signal. The membrane shows good structuration, i.e. four Bragg peaks, just up to 40°C, but at 70°C only two orders of diffraction were present indicating a poorer organisation at high temperatures. This finding reveals that the bilayer lipid is not structured at high temperatures, even if it is composed of archaeal-like lipids.

Structural characterization of an archaeal-like lipid bilayer as function of hydration and temperature

Marta Salvador-Castell [1], Bruno Demé [2], Philippe Oger [1] & Judith Peters [2,3]

[1] Université de Lyon, INSA de Lyon, CNRS, UMR 5240, 69211 Villeurbanne, France

[2] Institut Laue Langevin, 38000 Grenoble, France

[3] Université Grenoble Alpes, LiPhy, CNRS, 38000 Grenoble, France

Manuscript in preparation for Chemistry and physics of lipids

Abstract

Today, a wide variety of phospholipids is well-known, and almost all characterized lipids are originating from Bacteria. Another example of a large lipid diversity is in archaeal cell membranes. Archaea, the most extremophile domain of life, contain ether and branched lipids which provide specific bilayer properties. We determined the structural characteristics of ordered archaeal-like phospholipids as function of hydration and temperature by neutron diffraction. Hydration and temperature are both crucial parameters for the self-assembly and physicochemical properties of lipid bilayers. In this study, we have detected non-lamellar phases of archaeal lipids at low hydration level and exclusively lamellar phases at levels of 90% relative humidity or more. Moreover, at 90% relative humidity, a phase transition between two lamellar phases is discernible. Conversely, at full hydration, lamellar phases are present up to 70°C and no phase transition was observed within the temperature range studied (from 25°C to 70°C). In addition, we have determined the neutron scattering length density and bilayer's structural parameters from different hydration and temperature conditions. At highest levels of hydration, the system exhibits rearrangements on its corresponding hydrophobic region. Furthermore, the water uptake of the lipids examined is remarkably high. We discuss the effect of ether linkage and branched lipids on the particular characteristics of archaeal phospholipids.

Keywords

Archaea, diphytanoyl phospholipids, ether lipids, phase transition, neutron diffraction

Introduction

The Archaea domain is constituted by unicellular microorganisms that have been adapted to withstand extreme conditions, such as high temperature, high hydrostatic pressures and outermost pH values. All these environments represent a stress for the non-adapted organisms. For example, high temperature would lead to an unstable, unreasonably permeable cell membrane and the loss of the physicochemical properties of the functional lipid phase. To sustain these extreme conditions, phospholipids assembling the archaeal membranes are unique and differ from usual bacterial lipids. Archaeal lipids consist of *sn*-glycerol – 1 – phosphate backbone, ether linkages, and phytanoyl hydrocarbon chains while most bacterial lipids include *sn*-glycerol – 3 – phosphate backbone, ester linkages, and straight acyl chains (De Rosa et al., 1986; Gambacorta et al., 1993).

Phytanoyls form methyl-branched chains that confer extraordinarily high stability to the archaeal cell membrane. The most studied diphytanoyl lipid, 1,2-diphytanoyl-sn-glycero-3-phosphocholine (DPhPC), has proven to have a low permeability to ions and water and is highly resistant to oxidation (Milianta et al., 2015; Redwood et al., 1971; Tristram-Nagle et al., 2010). For instance, its water permeability is about three times lower than for its straight chain homologue, 1,2-dipalmitoyl-*sn*-glycero-3-phosphocholine (DPPC) (Guler et al., 2009; Milianta et al., 2015). Moreover, probably because the methyl branches are equally spaced along the chains, DPhPC does not present a gel-to-liquid phase transition in a broad range of temperature (-120°C to 120°C) (Lindsey et al., 1979). The equidistant localization of the methyl chains causes trans-gauche conformers to be nearly energetically equivalent and hence, gel-to-liquid transitions should be low-enthalpy process. Moreover, the phytanoyl chains favour the lateral interdigitation of hydrocarbon chains, which diminish the motion of the chains and provide unique structural stability (Shinoda et al., 2004a, 2003).

Ether lipids are much less investigated so far than DPhPC and only scarce information is available, for example it is known that ether bonds are more stable than ester ones conferring higher strength on hydrolysis (Baba et al., 1999). Since ether oxygens are less polar than ester bonds, the solvation and hydrogen bonding of DPhPC and its ether analogue DoPhPC may be different, impacting on the mechanics and electrostatics of the interfacial layer (Yasmann and Sukharev, 2015).

Last, although phosphatidylcholine is the universal membrane component, in native membranes it is always accompanied by phospholipids with other headgroups as phosphatidylserine, phosphatidylinositol and phosphatidylethanolamine (PE). A change in the headgroup modifies electrostatic energies, water incorporation and the gel-to-liquid transition temperature (Nagle, 1976). For example, since the choline head group possesses

the methyl groups, it does not allow close oxygen and nitrogen contacts, contrary to the ammonium group that forms a strong electrostatic and hydrogen bonds between oxygen and nitrogen (Andersson et al., 2011). In consequence, PE lipids are stiffer than PC, as demonstrated for diphytanoil lipids (Yasmann and Sukharev, 2015). Furthermore, the distinct headgroups modulate the bending modulus of the lipid bilayer inducing particular curvatures (Israelachvili et al., 1976; Kulkarni, 2019). For example, while DPhPC is the only diphytanoil lipid that produces stable lipid multilayers in oriented samples, DPhPE's negative curvature is so important that the lipid alone self-assemblies under non-lamellar phases, such as cubic and hexagonal (Kara et al., 2017). Nevertheless, lipid mixtures containing DPhPC and up to 50% of DPhPE form unilamellar vesicles (Andersson et al., 2011).

Temperature and hydration are usual experimental parameters to determine the physical properties of the membrane and they are fundamental to determine lipid bilayer characteristics. The water content and temperature may cause lipid phase transitions and change the alignment of multilayers (Trapp et al., 2010b, 2010a; Yang and Huang, 2002). Phospholipids are highly sensitive to hydration, especially when approaching 100% relative humidity (RH) (Rand and Parsegian, 1989; White et al., 1987). Usually, the bilayer thickness is decreased and lipid phase transitions are shifted to higher temperatures with decreasing hydration (Kučerka et al., 2011; Trapp et al., 2010a). Interestingly, although water is almost completely excluded from the hydrophobic chain region of the lipid bilayer, the type of hydrocarbon chain impacts the lipid water-adsorption capability. Therefore, it has been shown that phytanoyl compounds adsorb twice more water than their linear analogues (Gauger et al., 2002).

In this study, we examined by neutron diffraction the effect of humidity and temperature on an archaeal like lipid bilayer composed by 1,2-di-O-phytanyl-*sn*-glycero-3-phosphocholine and 1,2-di-O-phytanyl-*sn*-glycero-3-phosphoethanolamine (DoPhPE) (9:1) oriented on a flat substrate. This technique gives indeed access to many structural parameters and permits to relate them to hydration and temperature.

Results and discussion

I. Hydration

From diffraction data, the q-values of Bragg peaks indicate the lattice parameter D, i.e. the distance between lipid bilayers including the water leaflet. As shown in figure 1, higher levels of relative humidity (RH) shift Bragg peaks to lower q-values indicating an increase of D.

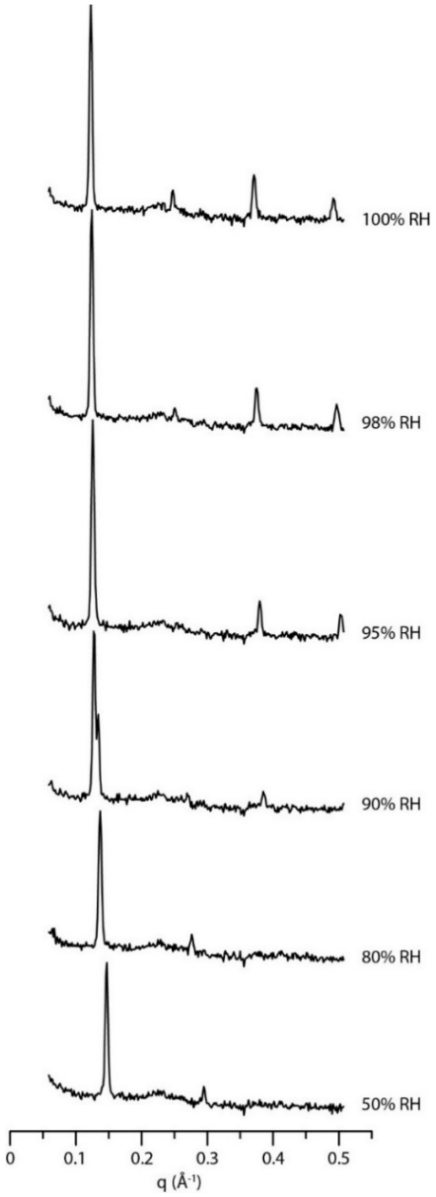

Figure 5. Neutron diffraction data DoPhPC:DoPHPE (9:1) obtained by neutron diffraction at 25ºC as function of relative humidity. The samples were hydrated with 8% D_2O.

The 2D diffractograms of the mixture DoPhPC:DoPhPE (9:1) at 50% RH and 80% RH reveal the presence of an isotropic phase (Figure S1). Previously, it has been shown that the addition of such apolar molecules, just like alkanes and other hydrocarbons (Lindblom and Rilfors, 1992), help to self-assembly phospholipids under non-lamellar phases by releasing

chain packing frustration (Salvador-Castell (4) et al., n.d.). The diffraction pattern of DoPhPC:DoPhPE (9:1) at 90% RH indicates an inhomogeneity of the sample due to the stable coexistence of two lamellar phases, which implies a phase transition. Previous studies have indicated similar phase transitions for DPhPC depending on hydration. For example, at 80% RH, Wu *et al.* have detected a lamellar-to-lamellar phase transition (Wu et al., 1995) which was lately attributed to a lipid headgroup rearrangement (Hung et al., 2000), and Hsieh *et al.* have found a marked polymorphism including non-lamellar phases, such as the hexagonal phase, under humidity levels lower than 80% RH (Hsieh et al., 1997).

Lipids hydrated above 90% RH arrange as a system self-organized under lamellar phases and up to four Bragg orders are easily detected. Nevertheless, such four orders, compared to the bacterial lipids that can reach up to 10 orders (Nagle and Tristram-Nagle, 2000), are indicative of a system with little order, probably due to their disordered hydrocarbon chains. Although phytanoyl chains are positioned perpendicular to the bilayer plane as the acyl chains lipids, their distribution is broader, providing a high disorder in the hydrophobic region (Shinoda et al., 2003; Stewart et al., 1990). A molecular dynamics simulation study from Husslein et al (1998) has even found that some of the chains are parallel to the bilayer plane.

To get insight about the lamellar phases observed at high humidity levels, we have measured the neutron density profiles for such conditions (Figure 2). Neutron scattering length densities (NSLD) profiles present the conventional shape for a lipid bilayer: a main peak from the phosphate group placed at the headgroup of phospholipids, a central region that corresponds to the hydrophobic chains of the bilayer and a minimum density from the terminal methyl. Furthermore, two secondary peaks near the main peaks could be indicative that phospholipids are in the gel phase. As expected, the lipid system studied here is not in a gel phase. Interestingly, it seems that hydration changes the hydrocarbon conformation of the region from 10 Å to the bilayer midplane, although this region is highly impermeable to water molecules (Shinoda et al., 2004b).

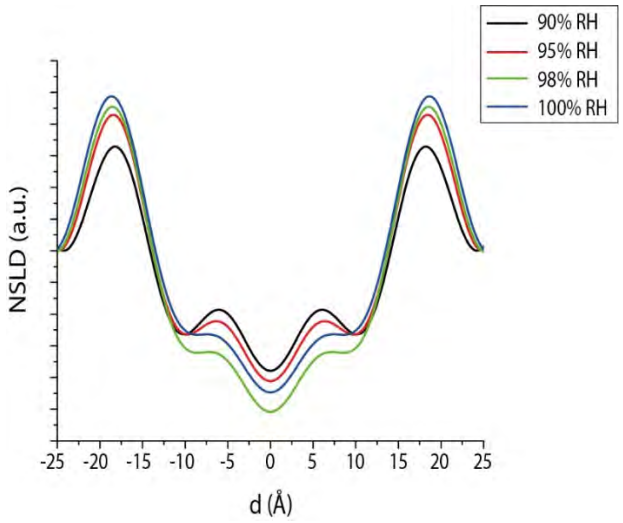

Figure 6. Neutron scattering length density obtained by neutron diffraction at 25°C as function of humidity: 90% RH (black), 95% RH (red), 98% RH (green), 100% RH (blue).

From the NSLD it is possible to extract the characteristic parameters of a lipid bilayer beside the lattice parameter (D) (Nagle and Tristram-Nagle, 2000) (Table 1). The peak-to-peak distance indicates the head-to-head length of the lipid bilayer (D_B), $2D_c$ corresponds to the thickness of the bilayer hydrophobic region, D_w the thickness of the water layer between lipid bilayer and n_w the number of water molecules. The DoPhPC:DoPhPE mixture at 100 %RH presented the following values: D= 50.4 ± 0.1 Å; D_b= 37.4 ± 0.2 Å; $2D_c$= 31.4 ± 0.6 Å and D_w= 13.0 ± 0.1 Å The values obtained are of the order of the values obtained for DPhPC, for which D_B was determined as 38 Å (Wu et al., 1995) and 35.4 Å (Tristram-Nagle et al., 2010) and $2D_c$ as 27.2 Å (Tristram-Nagle et al., 2010) and 27.8 Å (Kučerka et al., 2011). Once the lamellar phases are exclusively present, i.e. above 90% RH, the values are nearly unchanged and as expected, the fluctuations on the lattice parameters are mainly due to a slightly thicker water layer at higher humidity levels. Interestingly, the number of water molecules uptake (16.2 ± 0.2) is much higher than for usual bacterial straight lipids (6.5 for DPPC (Pohle et al., 1998)), but also slightly higher than for ester branched lipids (14.5 for DPhPC (Gauger et al., 2002)) which is probably due to the presence of the ether bound.

Table 1. Structural parameters from DoPhPC:DoPHPE (9:1) obtained by neutron diffraction as function of relative humidity. The samples were hydrated with 8% D_2O.

(Å)	**50% RH**	**80% RH**	**90% RH**	**95% RH**	**98% RH**	**100% RH**
D	42.3 ± 0.2	45.2 ± 0.2	48.6 ± 0.1	49.5 ± 0.1	50.2 ± 0.1	50.4 ± 0.1
D_B			36.5 ± 0.2	36.9 ± 0.2	37.4 ± 0.2	37.4 ± 0.2
$2D_C$			30.6 ± 0.6	30.8 ± 0.4	31.1 ± 0.6	31.4 ±0.6
D_w			12.1 ± 0.1	12.8 ± 0.1	13.0 ±0.1	13.0 ± 0.1
n_w			15.4 ± 0.3	16.1 ± 0.2	16.2 ± 0.2	16.2 ± 0.2

II. Temperature

The diffractogram patterns of fully hydrated and oriented DoPhPC:DoPhPE (9:1) lipid present lamellar phases at temperatures from 25°C up to 70°C (Figure 3). Moreover, the 2D diffractograms do not show any residual non-lamellar phase (Figure 2). Previously, it was found that its ester analogue lipid DPhPC self-assemblies under non-lamellar phases at temperatures above 35°C (Kara et al., 2017), nevertheless, it is likely that a dehydration of such samples occurred when temperature was increased. Here, since the BerILL chamber allowed us to increase temperature by carefully controlling humidity, the lamellar phase was present at least up to 70°C.

As temperature increases, the Bragg peaks' intensities decrease due to the higher molecular motility and disorder (Figure 3). Thus, at 25°C and 40°C, the usual four Bragg peaks for this system are easily detectable, however, at 55°C only three peaks are visible and at 70°C only the first two orders from a lamellar phase are discernible. A higher number of orders result in a more complex NSLD, in consequence, only the NSLD obtained at 25°C and 40°C are comparable (Figure 4). As observed by adjusting the level of hydration, the difference between the NSLDs from both temperatures are mainly from 10 Å to the bilayer midplane indicating a different organization of the hydrophobic region of the lipid bilayer.

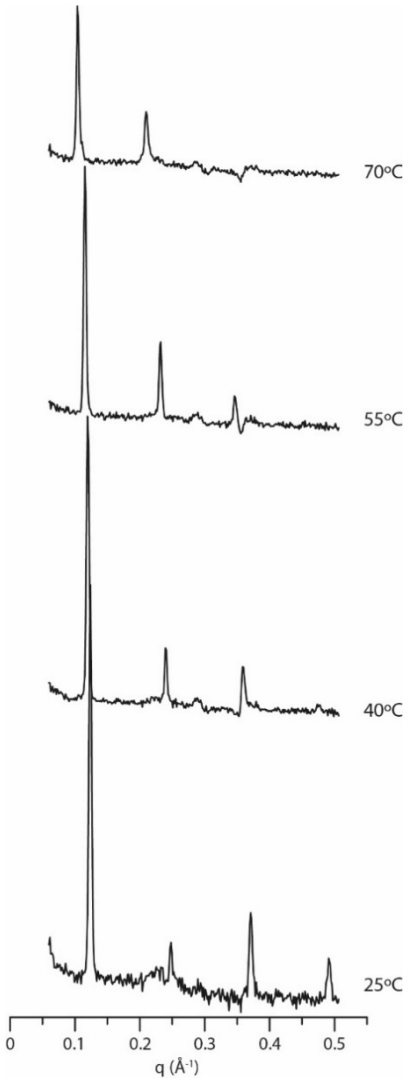

Figure 7. Neutron diffraction data DoPhPC:DoPhPE (9:1) obtained by neutron diffraction at 100% RH with 8% D_2O as function of temperature.

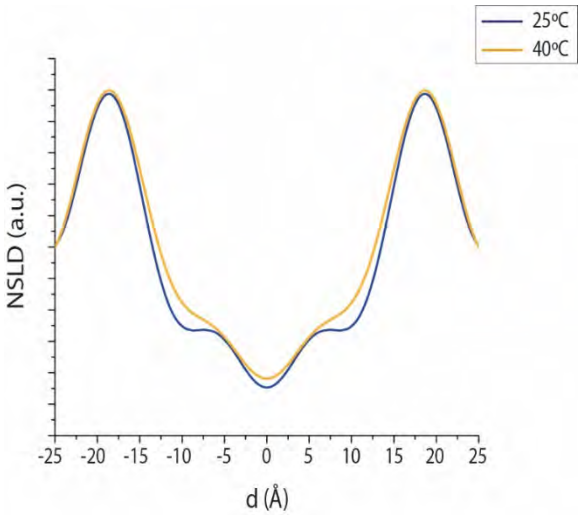

Figure 8. Neutron diffraction data DoPhPC:DoPhPE (9:1) obtained by neutron diffraction at 100% RH as function of temperature: 25ºC (blue) and 40ºC (ochre).

The lipid bilayer consisting of ether lipids and branched chains is insensitive to the change of temperature from 25°C to 40°C (Table 2). The bilayer thickness (D_B) is of 38.3 ± 0.2 Å at 25°C and its hydrophobic region ($2D_c$) is of 32.2 ± 0.6 Å, both values are the same within the error bars when the sample is at 40°C. Such low sensitivity to temperature can be attributed to the already existing disorder of the methyl branched chains at 25°C. Conversely, the $2D_c$ from lipids formed by linear acyl chains decreases at higher temperatures due to a higher thermal disorder (Kučerka et al., 2011).

Nevertheless, the lamellar lattice D increases at higher temperatures and, for example, goes from 50.7 ± 0.1 Å at 25 °C to 60.0 ± 0.1 Å at 70°C. Such change of the lamellar lattice parameter is due to an increase of the thickness of the water layer (D_w) between lipid bilayers. For instance, D_w increases by about 2 Å from 25°C to 40°C.

Table 2. Structural parameters from DoPhPC:DoPhPE (9:1) fully hydrated with 8% D_2O obtained by neutron diffraction as function of temperature.

(Å)	**25 °C**	**40 °C**	**55 °C**	**70 °C**
D	50.7 ± 0.1	52.5 ± 0.1	54.2 ± 0.2	60 ± 0.2
D_B	38.3 ± 0.2	38.2 ± 0.2		
$2D_C$	32.2 ± 0.6	31.8 ± 0.6		
D_w	12.6 ± 0.1	14.3 ± 0.1		
n_w	15.3 ± 0.2	17.5 ± 0.2		

Conclusions

Our aim was to study the effect of hydration and temperature on ordered multistack layers of the archaeal-like lipid system composed of DoPhPC:DoPhPE (9:1). We were able to determine the lipid structural data and phases at different levels of relative humidity and temperature by neutron diffraction using a precise humidity chamber.

On the one hand, hydration levels up to 80% RH display a system self-organized under lamellar and non-lamellar phases, while above 90% RH only the lamellar phases were present. At 90% RH, a phase transition between two lamellar phases was clearly detected. Moreover, as observed on the NSLD, the change of sample hydration causes a rearrangement of its hydrophobic region.

On the other hand, the studied lipid system at full hydration is self-assemblied under lamellar phases from 25°C to 70°C and no phase transition was discernible. The NSLD and

structural data from the sample at 25°C and 40°C does not change significantly. This absence of temperature effects is explained by the already high disorder conferred by the branched chains; thus, higher thermal disorder cannot impact more on the system. Nevertheless, we could detect a modest increase of water thickness due to a temperature increase.

Acknowledgements

This work was supported by the French National Research Agency programmes ANR 2010 BLAN 1725-04 and ANR 17-CE11-0012-01 to PO and JP. MSC was supported by a PhD grant from the French Ministry of Research.

Materials and methods

Chemicals

The synthetic archaeal lipids, 1,2-di-O-phytanyl-*sn*-glycero-3-phosphocholine and 1,2-di-O-phytanyl-*sn*-glycero-3-phosphoethanolamine were purchased from Avanti Polar Lipids Inc. (Albaster, USA). Bilayers were prepared by spreading 3 mg of DoPhPC:DoPhPE (9:1 molar) in chloroform: methanol (2:1) on a silicon wafer and dried under high vacuum.

Neutron diffraction

Neutron diffraction experiments were performed on multistacks of oriented membrane bilayers on the D16 small momentum transfer diffractometer (Cristiglio et al., 2015) at the Institut Laue Langevin (France) using the incident wavelength λ = 4.55 Å by a 2Θ scan, and an accessible q-range from 0.06 $Å^{-1}$ to 0.51 $Å^{-1}$. The wafer was placed on a goniometer head and rehydrated inside a humidity chamber, named BerILL, that allows a precise control of relative humidity and temperature of the samples (Gonthier et al., 2019). BerILL includes a hygrometer next to the sample to precisely measure its hydration level. For the first humidity setting, the sample was equilibrated for at least 6 hours and 2 hours of extra equilibration was used for 80%, 90%, 95%, 98% and 100% RH. . Each sample diffractogram was subtracted from the signal of the empty BerILL chamber. The ILL data is available at 10.5291/ILL-DATA.8-02-762 (Oger et al., 2016).

The lamellar d-spacing of the lipid bilayer was determined from the observed 2Θ of the Bragg peak positions according to $n\lambda=2D\sin\vartheta$, where D is the lamellar spacing of the bilayers in the z direction, perpendicular to the lipid bilayer, n is the diffraction order and λ is the selected neutron wavelength. The sum of neutron scattering lengths per unit volume is known as neutron scattering length density (NSLD) profile. The NSLD profile can be calculated as a discrete set of Fourier coefficients f_n according to the formula (Katsaras, 1995):

$$\rho_{bilayer}(z) = \frac{2}{D}\sum_{n=1}^{M} f_n v_n cos\left(\frac{2n\pi}{D}z\right) \qquad \text{(eq. 1)}$$

where coefficients f_n can be found due to the formula $I_n = \frac{|f_n|^2}{Q_z}$, Q_z is the Lorentz correction factor equal to q for oriented bilayers and I_n is the integrated intensity of the n^{th} Bragg peak; and v_n corresponds to the phase of the structure factor. The assigned phases were -, -, +, -.

Supplementary figures

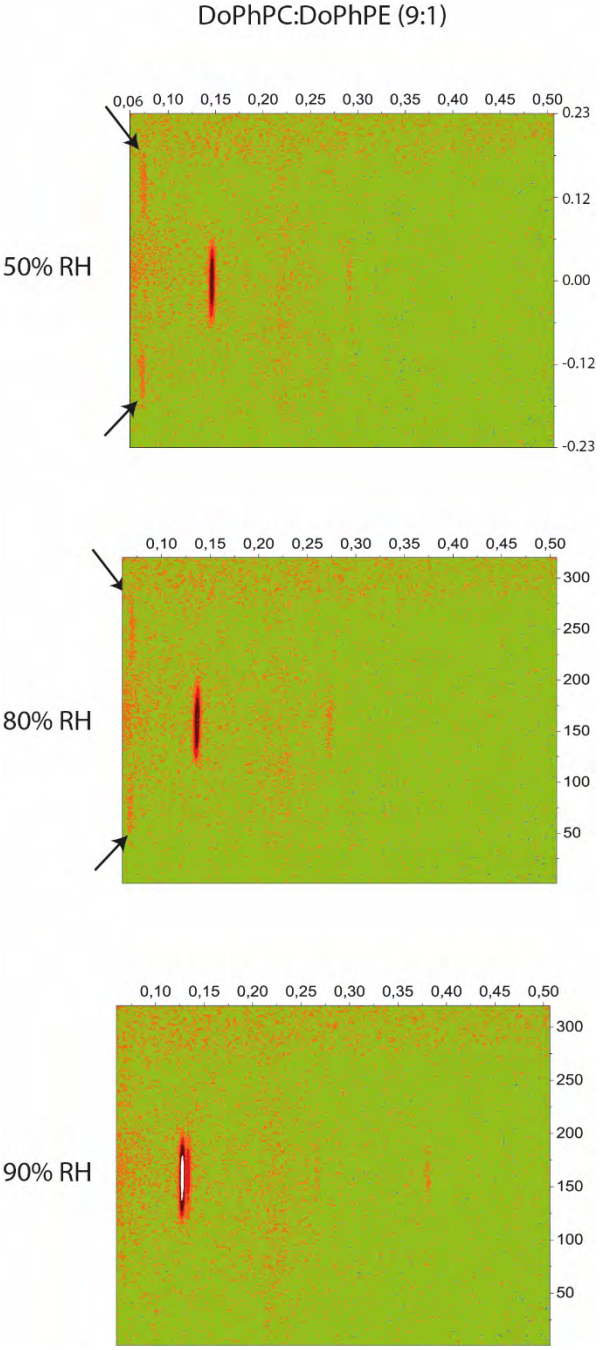

Figure S1. 2D neutron diffraction patterns of DoPhPC:DoPhPE (9:1) obtained by neutron diffraction at 25°C as function of relative humidity. Arrows indicate the diffraction signals corresponding to non-lamellar phases.

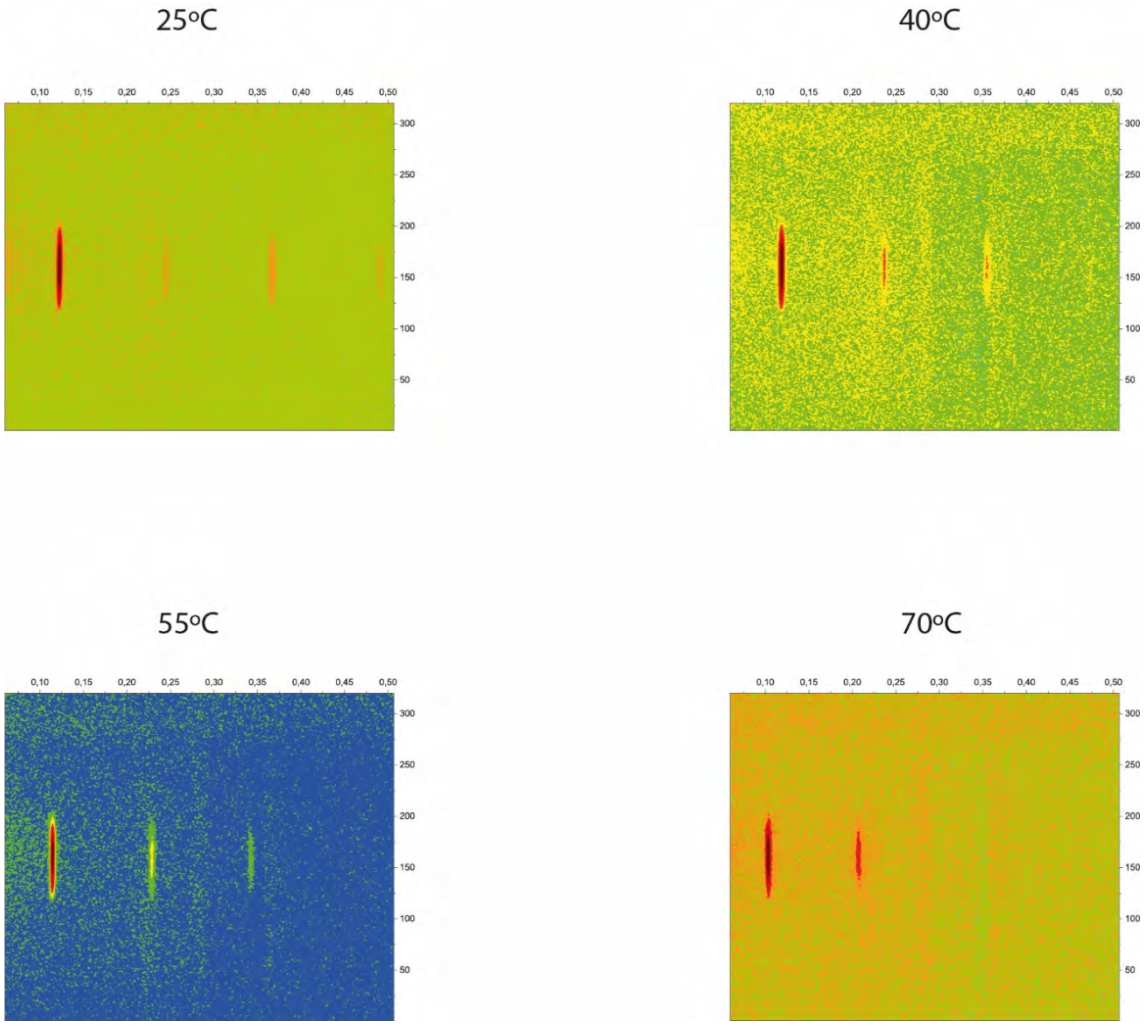

Figure S2. 2D neutron diffraction patterns of DoPhPC:DoPhPE (9:1) at 100% RH as function of temperature.

Article II. Apolar lipids, the archaeal toolbox to membrane adaptation to extreme conditions

Marta Salvador-Castell [1], Maksym Golub [2,3], Nelli Erwin [4], Bruno Demé [3], Nicholas J. Brooks [5], Roland Winter [4], Judith Peters [2,3*] & Philippe Oger[1*]

[1] Université de Lyon, CNRS, UMR 5240, F-69621 Villeurbanne, France

[2] Université Grenoble Alpes, LiPhy, F-38044 Grenoble, France

[3] Institut Laue Langevin, F-38000 Grenoble, France

[4] Technische Universität Dortmund, 44227 Dortmund, Germany

[5] Imperial College London, South Kensington Campus, London SW7 2AZ, England

Manuscript submitted to Proceedings of the National Academy of Sciences

Foreword

Apolar polyisoprenoids are apolar lipids suggested to act as structural lipids (Cario et al., 2015) and the most probable membrane regulators of archaeal cell membranes (Salvador-Castell et al., 2019b). This paper shows experimentally the effect of such molecules on an archaeal membrane model comprised of monopolar phospholipids. The lipid bilayer was composed of DoPhPC:DoPhPE (9:1), which characterization is presented in the previous article of this chapter (Salvador-Castell (2) et al., n.d.) whereas 1 mol% of squalane was used as apolar polyisoprenoid. The choice of such polyisoprenoid was based on: 1) its wide distribution through the Archaea domain (Salvador-Castell et al., 2019b) and 2) the availability of the hydrogenated and deuterated synthetic molecule, which were required for its localization. The percentage of polyisoprenoid was chosen to match the quantity found in the hyperthermophile and piezophile archaeon *T. barophilus* (Cario et al., 2015).

In order to validate the new archaeal membrane model in which apolar polyisoprenoids are present, I first needed to confirm that such molecules are, indeed, capable to insert in the archaeal lipid bilayer. Therefore, by comparing the NSLD of a sample including hydrogenated or deuterated squalane, I could show the increased electron density characteristic for the location of the deuterated squalane molecule, in the bilayer midplane regardless of the temperature and pressure conditions. To further validate the hypothesis of Cario and colleagues about this novel model membrane architecture (Cario et al., 2015), it was next essential to investigate the effects of apolar lipids on the membrane and evaluate

whether they matched the prediction of the theoretical chemical model, e.g. enhanced rigidity and impermeability to water and protons. Hence, I determined the effect of squalane on lipids' self-assembly by SAXS, on membrane structure by neutron diffraction, on lipid molecular vibrations by FT-IR and on membrane permeability by fluorescent approaches. All this was done at HT and HHP.

This article demonstrates beyond any doubt that apolar polyisoprenoids are able to stabilize the archaeal lipid bilayer to modify membrane curvature and induce the formation of non-lamellar phases to contribute to lateral organization as observed with the induction of phase separation and to alter lipid bilayer permeability under extreme conditions. Finally, squalane is able to change all such membrane properties without significantly affecting membrane fluidity. The results presented in this article demonstrate that non-polar polyisoprenoids are indeed part of the archaeal cell membrane providing essential functions for its optimal functionality. These results also support the proposal that apolar polyisoprenoids may play the role of membrane regulators in Archaeal.

Apolar lipids, the archaeal toolbox to membrane adaptation to extreme conditions

Marta Salvador-Castell [1], Maksym Golub [2,3], Nelli Erwin [4], Bruno Demé [3], Nicholas J. Brooks [5], Roland Winter [4], Judith Peters [2,3*] & Philippe Oger[1*]

[1] Université de Lyon, CNRS, UMR 5240, F-69621 Villeurbanne, France.

[2] Université Grenoble Alpes, LiPhy, F-38044 Grenoble, France.

[3] Institut Laue Langevin, F-38000 Grenoble, France.

[4] Technische Universität Dortmund, 44227 Dortmund, Germany.

[5] Imperial College London, South Kensington Campus, London SW7 2AZ, England.

Manuscript submitted to Proceedings of the National Academy of Sciences

Abstract

Life on Earth spans remarkably diverse habitats, including extreme environments in which cell membranes must maintain specific physical properties (*e.g.,* fluidity and permeability) to preserve their integrity and functionality. It is thought that life originated in extreme marine environments and subsequently adapted to terrestrial conditions; however, the mechanisms that allow biomembranes to adapt to external conditions are not yet established. We investigated a key modification observed in temperature- and pressure-adapted archaeal membranes: the modulation of apolar isoprenoid concentration. We constructed and validated membrane models formed from synthetic archaeal lipids and squalane. Using neutron diffraction, we localized the squalane in the membrane and demonstrated the physicochemical effects of the intercalant on membrane dynamics and stability under high-temperature and high-pressure conditions using small-angle X-ray scattering and fluorescence spectroscopy. We showed that apolar isoprenoids modulate the structure of archaeal membranes, playing a decisive role in their adaptation to extreme conditions.

Keywords

Extremophiles, adaptation, cell membrane, phospholipids, membrane regulators

Introduction

Biological membranes are not impermeable but form a selective barrier that is indispensable for numerous cellular processes. It is crucial for cells to maintain this barrier in a functional state, which is a fluid-like liquid-crystalline phase, regardless of environmental conditions. Many physicochemical parameters can disrupt the structure and function of membranes and consequently alter the cascade of cellular functions that depend on their integrity. High temperatures, for example, result in higher molecule agitation to the point that ordinary membrane lipids may pack too loosely to maintain the functional selectively permeable liquid-crystalline structure. It is widely accepted that prokaryotes adapted to extreme temperatures accumulate bipolar ether-linked isoprenoid lipids in their membranes (De Rosa et al., 1983; Woese et al., 1978). These membrane-spanning lipids self-assemble into monolayers that are highly stable due to restricted motility of the hydrocarbon chains and the presence of the isoprenoid methyl groups that block water penetration through the membrane (Koga, 2012). Thus, the lipid monolayer tightly compacts the cell membrane (Shinoda et al., 2005) and reduces its fluidity and permeability (Elferink et al., 1994). However, recent observations have challenged this dogma. First, a tetraether-containing membrane might not be a prerequisite for heat tolerance, as evidenced by the absence of tetraether lipids in the membranes of *Aeropyrum pernix* (T_{max}=100°C) (Sako et al., 1996) and *Methanopyrus kandleri* (T_{max}=122°C) (Hafenbradl et al., 1996). Second, numerous hyperthermophilic archaea produce a mixture of tetra- and diether lipids, amongst which tetraether lipids might represent less than 10% of membrane lipids (Sprott et al., 1997). This finding raises questions about the thermal stability of the archaeal lipid bilayer but also suggests that archaea may have developed adaptive routes to hyperthermophily that might not require tetraether lipids.

The key molecular and assembly interactions that allow hyperthermophiles with membrane bilayers to survive under high-stress conditions remain a hotly debated topic. A recent membrane architecture model (Figure 1a) (Cario et al., 2015) suggests that apolar isoprenoid molecules may act as structural membrane components, increasing the stability of the membrane at higher hydrostatic pressures and temperatures. This model predicts that apolar isoprenoids would populate the midplane of the bilayer, thereby altering its physicochemical properties while causing significant changes to lipid dynamics in the membrane (Haines, 2001). The presence of the intercalant would limit charge transfer between the two membrane leaflets, decreasing proton and water permeability and increasing membrane rigidity, extending the conditions for stability and functionality, and thereby providing a rationale for the ability of these hyperthermophiles to withstand temperatures above the boiling point of water. If confirmed, this hypothesis has numerous implications: Amongst them, it suggests the existence of membrane domains with different

compositions and physicochemical properties, which raises the possibility of membrane-lateral structural functionalization in archaea, along with all the known consequences of this possibility on membrane-assisted cellular processes (Sezgin et al., 2017).

Here, we present an extensive analysis of an archaeal membrane, demonstrating that apolar polyisoprenoids can insert in the midplane of the bilayer and that they strongly modify membrane properties, providing strong support for the possibility that apolar intercalants constitute one of the evolutionary routes to high-temperature and high-pressure adaptation in prokaryotes from early cells to today.

Results and discussion

I. Apolar isoprenoids intercalate in the midplane of an archaeal lipid bilayer

Cario and colleagues (Cario et al., 2015) have proposed that the location and molecular orientation of apolar intercalants with respect to the membrane plane is a key question in the novel cell membrane model proposed for poly-extremophilic archaea, since it controls the membrane's physicochemical properties and the extent of its stability. To locate the intercalant precisely, we have constructed synthetic membranes to allow precise control of their composition, and we have taken advantage of contrast variation neutron scattering, which can be used to selectively highlight different areas within the structure and provide a detailed map of the membrane's assembly structure and molecular interactions.

Synthetic archaeal membrane bilayers were produced from a 9:1 molar ratio of two synthetic archaeal lipids, 1,2-di-O-phytanyl-*sn*-glycero-3-phosphocholine (DoPhPC) and 1,2-di-O-phytanyl-*sn*-glycero-3-phosphoethanolamine (DoPhPE), which reproduces the bilayer structure of *Thermococcus barophilus* membrane (Figure 1b, red lipids). Protonated and perdeuterated pure squalane were introduced into the membrane at 1 mol% (Figure 1b, black molecule). Squalane is the closest synthetic isoprenoid homologue of lycopane, and the isoprenoid synthesized by *T. barophilus* and 1 mol% corresponds to the isoprenoid concentration found in *T. barophilus* (Cario et al., 2015) and many other extremophiles (Tornabene et al., 1979). The neutron scattering length density (NSLD) at different squalane H-D contrasts (Figure 1c) shows the expected membrane profile for H-squalane-containing membranes with a maximum scattering length density at the lipid phosphate groups and a minimum at the methyl groups. D-squalane-containing membranes show a marked increase in NSLD at the centre of the membrane, clearly locating the squalane in the midplane of the archaeal lipid bilayer. The width of the D-squalane peak in the NSLD is consistent with the

squalane molecules being oriented parallel to the membrane surface and perpendicular to the polar lipid isoprenoid chains.

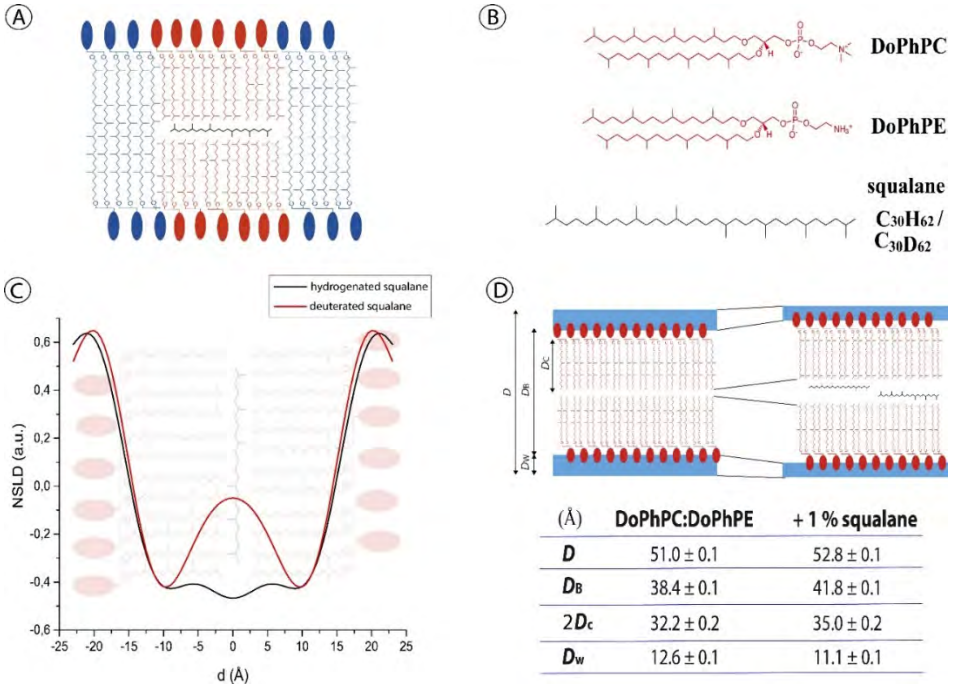

(Å)	DoPhPC:DoPhPE	+ 1 % squalane
D	51.0 ± 0.1	52.8 ± 0.1
D_B	38.4 ± 0.1	41.8 ± 0.1
$2D_c$	32.2 ± 0.2	35.0 ± 0.2
D_w	12.6 ± 0.1	11.1 ± 0.1

***Figure 1**. Apolar isoprenoid molecules as structural membrane components placed in the midplane bilayer. A) Apolar lipid's (black) proposed location in an archaeal lipid membrane, composed of diether (red) and tetraether (blue) lipids. B) Skeletal formula of the lipids used: 1,2-di-O-phytanyl-sn-glycero-3-phosphocholine (DoPhPC), 1,2-di-O-phytanyl-sn-glycero-3-phosphoethanolamine (DoPhPE) and 2,6,10,15,19,23-hexamethyltetracosane (squalane), hydrogenated and deuterated. C) Neutron scattering length density (NSLD) of DoPhPC:DoPhPE (9:1) + 1 mol% hydrogenated squalane (black) and deuterated squalane (red) measured on D166 (ILL, Grenoble, France). D) Structural parameters: lamellar repeat spacing (D), bilayer thickness (D_B), hydrocarbon region thickness ($2D_C$) and water layer thickness (D_w) for bilayers of DoPhPC:DoPhPE (9:1) in the absence and presence of 1 mol% squalane.*

The NSLD data offer a range of additional structural parameters for the archaeal phospholipid bilayer (Table in Figure 1d) (Nagle and Tristram-Nagle, 2000). The lamellar repeat distance (d-spacing, *D*) represents the distance between two bilayers, including the interlamellar water thickness. In the presence of 1 mol% squalane, the d-spacing increases from 51.0 Å to 52.8 Å. The Gibbs-Luzzati bilayer thickness (D_B), which corresponds to the distance between the centres of the polar heads in the two membrane leaflets, is equal to 38.4 Å in the absence of squalane, which is similar to that found previously by molecular dynamics simulations (Shinoda et al., 2005). In the presence of 1 mol% squalane, D_B increases to 41.8 Å. Similarly, the thickness of the hydrocarbon chain region ($2D_c$) increases from 32.2 Å in the absence to 35.0 Å in the presence of 1 mol% squalane. All these parameters are consistent with the apolar molecule being inserted into the bilayer midplane. At the same time, we observed a decrease in the water thickness between bilayers (D_w) from 12.6 Å to 11.1 Å in the presence of squalane.

II. Squalane induces the formation of non-lamellar phases in archaeal lipid membranes

Low concentrations of apolar molecules can substantially influence the assembly structure membranes, for example, inducing phase transitions between lamellar and non-lamellar cubic or hexagonal phases (Siegel et al., 1989). Such structural transitions can be driven by the apolar alkanes' ability to partition between the bilayer leaflets and relieve packing frustration that would otherwise energetically prohibit the formation of curved phases (Gruner et al., 1985). Changes in membrane curvature are critical to a wide range of cellular processes, including cell membrane fusion / fission and lipid sorting, which require substantial membrane rearrangements (Hyde et al., 1997; Jarsch et al., 2016; Lindblom and Rilfors, 1989).

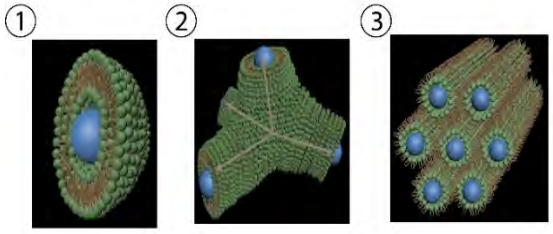

DoPhPC:DoPhPE **+ 1% squalane**

(°C)	Lipid phase d-spacing 1 bar	Lipid phase d-spacing 1000 bar	Lipid phase d-spacing 1 bar	Lipid phase d-spacing 1000 bar
10	Lamellar		Lamellar	
	62.7 Å ± 0.6	62.9 Å ± 0.6	67.6 Å ± 0.3	69.8 Å ± 0.3
			Cubic	
25	Lamellar		Lamellar	
	60.0 Å ± 0.6	60.2 Å ± 0.6	69.6 Å ± 0.7	72.2 Å ± 0.7
			Cubic	
40	Lamellar		Lamellar	
	64.6 Å ± 0.9	64.9 Å ± 0.9	69.6 Å ± 0.5	72.2 Å ± 0.5
			Cubic	
55	Lamellar		Hexagonal	
	63 Å ± 1	63 Å ± 1	88 Å ± 1	93 Å ± 1
			Cubic	
70	Lamellar		Hexagonal	
	N.D.	N.D.	82.0 Å ± 0.3	90.0 Å ± 0.3
			Cubic	
85	Lamellar		Hexagonal	
	N.D.	N.D.	80.1 Å ± 0.3	84.8 Å ± 0.3
			Cubic	

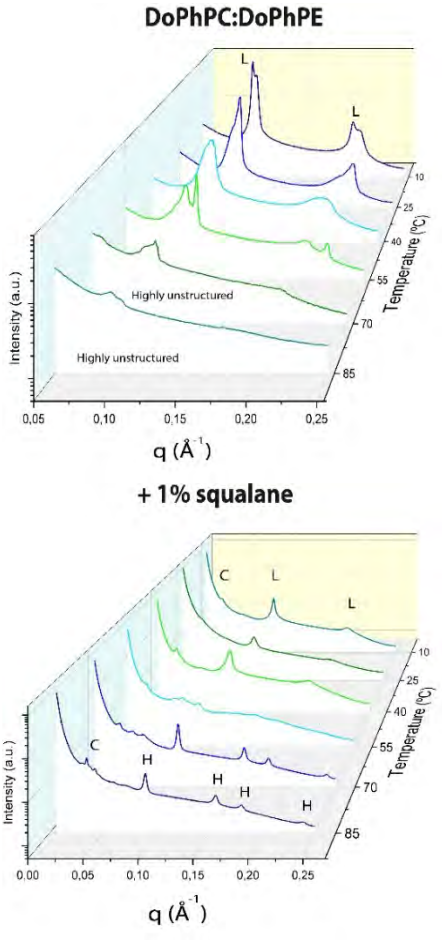

***Figure 2. Squalane induces lipid self-assembly in highly curved non-lamellar phases**. Left, top: 3D representations of different lipid phases: 1) lamellar, 2) Pn3m (cubic), 3) hexagonal. Table: Different lipid phases present in DoPhPC:DoPhPE (9:1) and in the presence of 1 mol% squalane at different temperatures. Left, bottom: lattice parameters (d-spacing) obtained at 1 bar and 1000 bar for the lamellar and hexagonal phases measured at I22 (DLS, Didcot, United Kingdom). Right: Radial SAXS intensities of DoPhPC:DoPhPE (9:1) in the absence (top) and presence of 1 mol% squalane (bottom) at different temperatures. Phases could be identified by the ratios of their Bragg peaks (lamellar (L) phase: 1:2:3; cubic (C) phase: √2:√3:2:√6; hexagonal (H) phase:1:√3:2:√7:3).*

We used small-angle X-ray scattering (SAXS) to explore the possibility of squalane-induced phase transitions by determining the structure of fully hydrated synthetic archaeal lipids (DoPhPC:DoPhPE (9:1)) and the impact of 1 mol% squalane on their self-assembled structure as a function of temperature (10 to 85°C, 15°C steps) and hydrostatic pressure (1 to 1000 bar, 50 bar steps). In the absence of the apolar intercalant, only lamellar phases were found regardless of the temperature (T) and pressure (P) (Table in Figure 2). There was no clear gel-to-liquid or liquid-to-gel phase transition; however, the coexistence of two lamellar phases was observed (Figure 2 right top) up to at least 70°C. At the highest temperatures tested, the scattering pattern became rather broad, indicating a loss of lamellar ordering, which is consistent with the known stability range for this type of lipid bilayer. Increasing hydrostatic pressure had a very limited impact on the bilayer structure (Table in Figure 2 bottom). With 1 mol% squalane, two types of non-lamellar phases were observed (Figure 2 right). Below 55°C, coexistence between a cubic and a lamellar phase was induced, whereas above 55°C, the lamellar phase transformed to an inverse hexagonal phase that coexisted with the cubic phase up to at least 85°C. Again, no phase transition was observed as a function of hydrostatic pressure, but the lattice parameters of all phases increased with increasing pressure, which is consistent with the ordering of the lipid hydrocarbon chains (Figure S1). A number of factors are known to promote the formation of non-lamellar phases in phospholipid bilayers: headgroup dehydration, interaction with multivalent ions, acyl chain unsaturation and increases in chain length (Ninham et al., 2017; Seddon, 1990). These factors are unlikely to be significant in our membrane system, since the polar headgroups are fully hydrated and the acyl chains are not varied. Thus, squalane must be the factor promoting phase transitions to the cubic and hexagonal phase, most likely by allowing structural flexibility at the bilayer midplane and negative curvature of the lipid interface. Interestingly, a similar squalane-induced lamellar-to-hexagonal phase transition has also been reported in a bacterial lipid system, although the precise location of squalane was not identified in that case (Siegel et al., 1989).

Dynamic modulation of membrane bending is critical to the function of cells, especially in membrane fusion, which is critical to membrane trafficking. The essential step in non-leaky membrane fusion is the rearrangement of the lipid molecules from the two apposed membranes to form a single continuous membrane. During this process, transitory isotropic structures are formed, which resemble the local structure of cubic phases (Rappolt, 2013; Siegel, 1999). Specific membrane curvatures yield membrane domains with specialized roles in membrane folding, protein incorporation and enzymatic activities (Jouhet, 2013; McMahon and Boucrot, 2015; Seddon, 1990; Shearman et al., 2006) (Figure S2). These precise curvatures usually occur through the synthesis of at least one non-lamellar structure-forming component,

which is often the synthesis of large negative curvature lipids (*e.g.,* with phosphatidylethanolamine, phosphatidylserine or phosphoric acid as polar head groups) and large positive-curvature lipids (*e.g.,* with phosphatidylinositol as polar head group) (Chernomordik and Kozlov, 2003). In microorganisms, such as *Escherichia coli* or *Acholeplasma* laidlawii (Rilfors and Lindblom, 2002), that maintain a constant level of non-lamellar structure-forming lipids in the liquid-crystalline phase leads to an increase in the lipid conformational dynamics of the system. Our results suggest a similar role for apolar isoprenoid molecules in archaeal bilayer membranes.

III. Squalane increases water permeability and reduces proton permeability under extreme conditions

Biological membranes act as barriers to solute diffusion and play a central role in energy storage and processing via ion gradients (van Meer et al., 2008). The permeation of nonionic solutes is directly related to membrane fluidity and is affected by different factors, for example, the acyl chain length or the level of unsaturation in the phospholipid hydrocarbon chains (Lande, 1995). If the area between the two membrane leaflets is populated, then apolar organics will also be expected to impact solute permeation. Three molecular models have been proposed for proton leakage across lipid bilayers: the "defect" mechanism (Volkov et al., 1997), the "water wire" mechanism (Nagle and Morowitz, 1978) and the "water cluster" model (Haines, 2001). Despite differences in proton transport mechanisms, all three models suggest that any hydrocarbon in the centre of the lipid bilayer will serve as an inhibitor of proton leakage. Thus, to validate the model proposed for hyperthermophilic archaea, we measured the membrane fluidity, solute and proton permeation across the synthetic archaeal membrane as a function of squalane concentration.

Membrane fluidity was assayed as a function of P and T using laurdan as a reporter probe (Parasassi et al., 1991; Zhang et al., 2006). Laurdan is a fluorescent probe whose emission wavelength is determined by the water content of the lipid bilayer's headgroup region, *i.e.,* is sensitive to the phase state of the membrane (Parasassi et al., 1991). The Laurdan generalized polarization (GP) reports on the fluidity of the membrane (Parasassi et al., 1991). GP values of approximately 0.5 denote ordered gel phases, whereas GP values below zero are typical for fluid-like lipid phases. First, the temperature-dependent GP values measured for membranes in the absence and presence of 1 mol% squalane appeared similar (Figure 3a-c). Up to approximately 45°C, we observed a decrease in the GP, indicating increased conformational disorder in the lipid system upon increasing the temperature. Thereafter, the GP value increased again, pointing to some kind of phase changes. No sharp

phase transitions are observed. This behaviour is characteristic of all archaeal lipid systems studied to date, for which no marked phase transitions have been observed in the 0 to 100°C temperature range (Lindsey et al., 1979). The laurdan fluorescence data are consistent with the coexistence of fluid phases and the effect of temperature on the phases observed by SAXS (Figure 2 right). The higher GP values in the presence of 1 mol% squalane indicate a slightly higher rigidity of the membrane (Figure 3c). Additional Fourier-transform infrared spectroscopy (FT-IR) experiments were performed to yield information on the population of lipid conformers of the membrane. The FT-IR data showed minor changes upon addition of the apolar intercalant (Figure S3 and Figure S4).

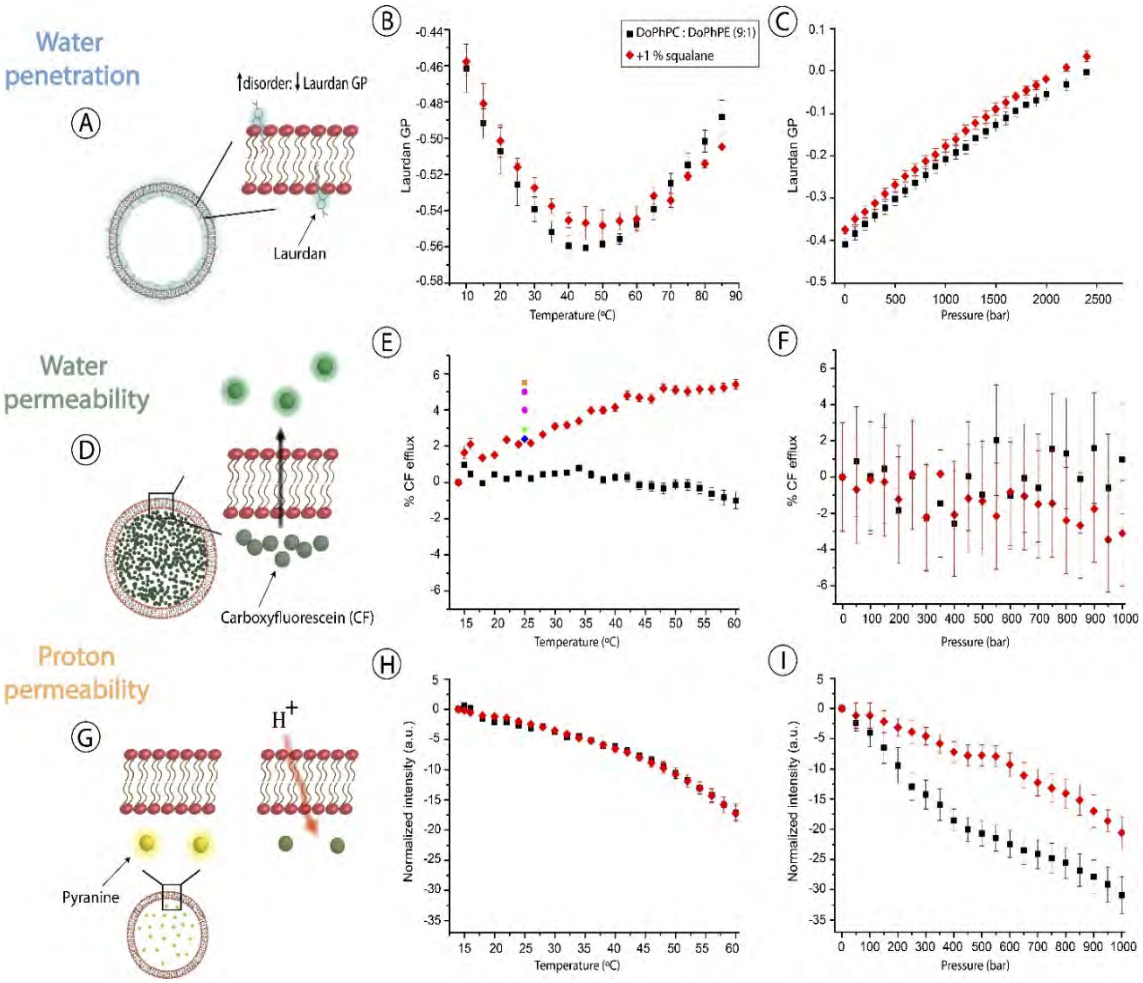

Figure 3. Squalane modulates membrane physico-chemical properties. *Water penetration in the headgroup region of the bilayer measured by Laurdan GP (A-C), water permeability of lipid bilayers measured by carboxyfluorescein (CF) efflux (D-F), and proton permeability of lipid bilayers measured by pyranine fluorescence (G-I) as a function of temperature (middle column) and pressure (right column) for DoPhPC:DoPhPE (9:1) (black spheres) and in the presence of 1 mol% squalane (red triangles). Dots in the temperature-CF efflux data represent an approximation of the %CF efflux for different lipids at 25°C: black square: 1,2-dioleoyl-sn-glycero-3-phosphocholine, red spheres: 1-palmitoyl-2-oleoyl-glycero-3-phosphocholine, green triangle: 1,2-dimyristoyl-sn-glycero-3-phosphocholine and blue diamond: 1,2-diphytanoyl-sn-glycero-3-phosphocholine* (Choquet et al., 1994; El Jastimi et al., 1999; Eriksson et al., 2018; Mathai et al., 2008).

Large-molecule leakage was probed by the carboxyfluorescein (CF) release assay, which is a well-established method that monitors the increase in fluorescence caused by the dilution of the self-quenched CF upon release from leaky liposomes into the surrounding medium (Chen and Knutson, 1988) and thus probes the efflux of molecules from the vesicles. Temperature and hydrostatic pressure (Figure 3d-f) have contrasting impacts on the squalane containing DoPhPC:DoPhPE membranes. The presence of squalane increases the leakage of CF from liposomes upon an increase in temperature, demonstrating an increase in membrane permeability (Figure 3e). Such a tendency has also been reported when other isoprenoid molecules, such as dolichol, were present in the lipid bilayer (Lamson et al., 1994). However, the presence of squalane did not impact CF release as a function of the pressure range covered (Figure 3f). It is noteworthy that the T-induced increase in water permeability allows a level of permeability that is essentially similar to that of classical lipid systems (color dots in Figure 3e), while the intrinsic permeability of the membrane in the absence of squalane is extremely low, as expected for archaeal lipids.

The membrane influx of protons into liposomes was measured by monitoring the emission of pyranine, a pH-sensitive flurophore (Kano and Fendler, 1978) (Figure 3g) that is widely used to study the internal pH of liposomes (Rossignol et al., 1982). Interestingly, no influence of the apolar intercalant on membrane proton leakage was observed upon increasing the temperature (Figure 3h). In contrast, proton permeability into vesicles upon an increase in pressure is strongly decreased when squalane is present (Figure 3i). Such an impact of the intercalant was predicted by different molecular models for the proton leakage of lipid bilayers (Haines, 2001). Increasing pressure increases the packing density of the lipid bilayer, as can also be deduced from lattice parameter values (Figure S1), and the presence of squalane in the centre of the bilayer will further block proton transport. As a consequence, the proton motive force will be enhanced in the membranes containing squalane.

Conclusions

Apolar lipids maintain membrane functionality under combined high temperature and pressure

In the membrane models proposed by Cario (Cario et al., 2015) or Haines (Haines, 2001), the presence of the apolar intercalants within the membrane is expected to affect the stability, but more importantly, the functionality domain of the membrane towards higher temperatures and hydrostatic pressures. Thus, apolar 'lipids' would represent one of the routes by which hyperthermophilic organisms adapt to high-temperature and high-pressure

environments without requiring the synthesis of bipolar, membrane-spanning, monolayer-forming lipids.

The apolar lipids in the archaeal membrane have been localized within the T and P regions 25 and 85 °C and 1 and 1000 bar, respectively, covering the majority of the temperature and pressure conditions encountered in nature. At each condition, squalane remained inserted in the centre of the midplane, parallel to the surface of the membrane, similar to the control conditions at room temperature and ambient pressure (Figure S5). From the intensity of the NSLD data, we can infer that the amount of squalane inserted within the membrane is similar for all temperatures and pressures. The d-spacing of the membrane in the absence of the apolar molecule was essentially insensitive to pressure and temperature (Figure S6 and S7) with a variation in d-spacing between the two most extreme conditions of only 0.2 Å. In contrast, the d-spacing of the membrane containing 1 mol% squalane decreases with increasing pressure from 54.6 to 53.1 Å (Figure S6), indicating that squalane renders the membrane pressure sensitive and significantly more laterally compressible. As expected, the compressibility increases with increasing temperature (Figure S7). Notably, the d-spacing of the membrane containing squalane at 85 °C and 1000 bar is similar to that of the membrane without squalane at room T and ambient P (Figure 4). This finding resembles the "corresponding state principle" that was first formulated by Vihinen (Vihinen, 1987) and Jaenicke (Jaenicke, 2000), stating that the flexibility of a protein adapted to extreme conditions should be the same as the flexibility of a protein under ambient conditions. Here, a similar characteristic is found for membranes functioning under normal conditions but adapted to extreme conditions. Increasing compression of lipid membranes is usually associated with a transition to an ordered phase, an interdigitation of the lipids' hydrophobic chains, and/or to a tilt of the molecules at an angle perpendicular to the surface, which allows for a more compact lipid bilayer (Brooks et al., 2011). In the present case, compression of the membrane does not induce a phase transition to a gel phase or, according to the diffraction data, to an interdigitation of the isoprenoid chains, as evidenced by the calculated dimensions of the hydrophobic domain of the membrane (2*D*c, Figure 1). Therefore, under all P and T conditions, the membrane remains in a fluid-like, liquid-crystalline, and hence functional state.

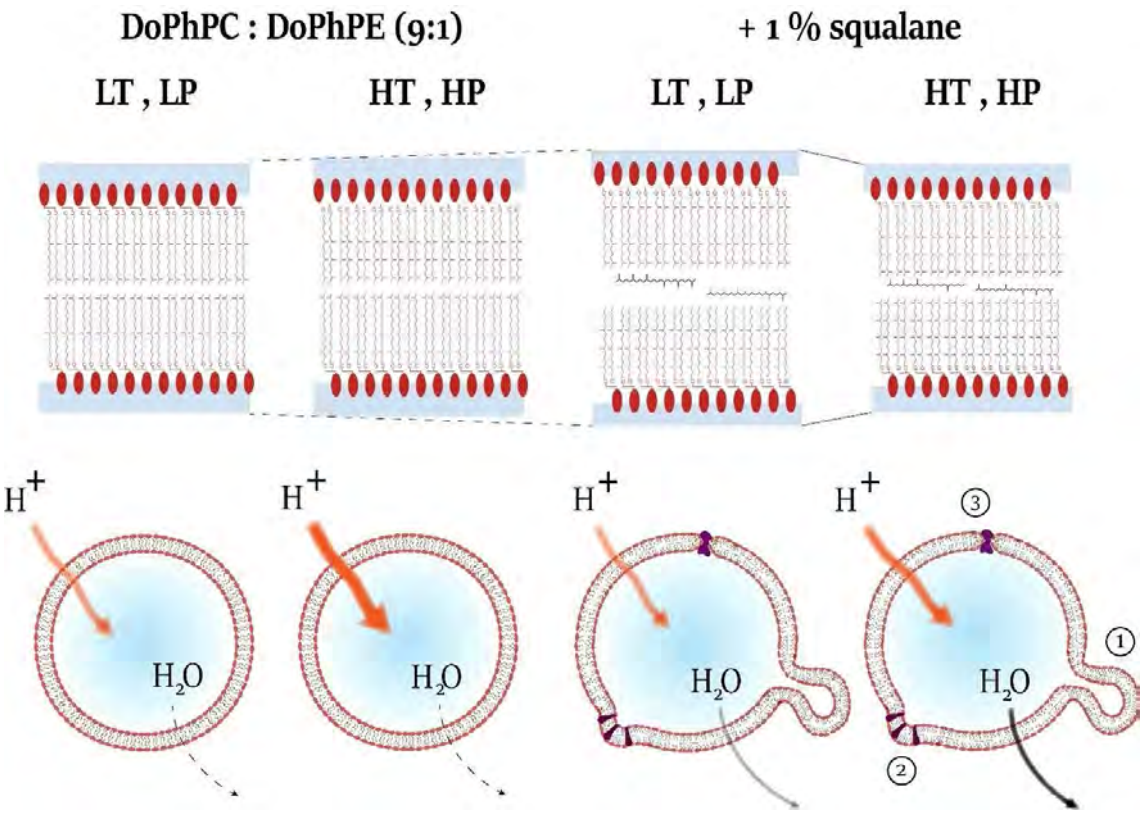

Figure 4. The presence of non-apolar molecules renders the membrane more responsive to pressure, modulates its permeability and facilitates membrane curvature*. Schematic representation of the effect of adding 1 mol% squalane to the DoPhPC:DoPhPE (9:1) membrane at different temperatures and pressures: LT: 25°C, LP: 1 bar, HT: 85°C, HP: 1000 bar. Top: In the absence of squalane, a slight increase in lamellar repeat spacing is observed, which is due to the volume expansion. At LT and LP in the presence of squalane, the lamellar repeat spacing increases due to an increase in the hydrophobic region of the lipid bilayer. The membrane containing 1 mol% squalane is rather compressible, leading to a decrease in the d-spacing. Bottom: In the absence of squalane, the lipid bilayer membrane is slightly impermeable to water efflux but permeable to protons influx. When 1 mol% squalane is added, the lipid vesicles display a higher permeability towards water efflux, similar to that of typical bacterial lipids. However, its proton influx is lower. Furthermore, the presence of squalane induces bending membrane modifications that allow the cell membrane to adopt essential curvatures for different cell functions, such as the formation of vesicles (1), insertion of membrane proteins that need specific curvature (2), and transmembrane proteins anchored in lipid bilayers (3).*

The membrane structure at the highest temperature and pressure suggests a possible role of squalane in modulating membrane fluctuations at the temperatures that hyperthermophilic archaea, such as *T. barophilus,* experience in the hydrothermal vent environment. Our results show a loss of membrane organization at temperatures above 70°C in the absence of squalane (Figure 2 right). In contrast, in the presence of 1 mol% squalane, both lamellar and non-lamellar phases appear stable at all temperatures studied. The compressibility data of the membrane suggest that a second role of squalane may be to keep the membrane impermeable to proton flux, *i.e., to* help sustain the proton motive force of the membrane and reduce water influx across the membrane under high hydrostatic pressures

(Figure 4). Third, our SAXS data strongly associate the presence of squalane with the ability of the archaeal membrane to adapt its membrane curvature (Figure 2 and Figure S2). The clustering of non-lamellar structure-forming lipids is essential in several transient cellular processes, such as membrane fusion and fission. These large negative curvatures are not observed in the absence of squalane, even at the most extreme P and T conditions tested, which strongly indicates that the base amphiphilic archaeal lipids lack the ability to efficiently modulate membrane bending under the physiological conditions of the archaeon (Figure 4). Furthermore, members of the order Thermococcales, including *T. barophilus*, have been shown to produce large quantities of vesicles, often hundreds per cell(Soler et al., 2008). Although it is not yet clear what role these vesicles play in the archaea life cycle, they are proposed to be involved in genetic exchange in hydrothermal vents (Gaudin et al., 2013). Regardless of their function, the production of hundreds of vesicles per cell highlights the ability of the natural membrane to adapt its curvature during the intermediates of the membrane fusion/fission processes (Lindblom and Rilfors, 1989), apolar intercalants embedded in the membrane may be facilitators for approach.

Our results confirm and expand on the hypotheses discussing novel membrane architectures as proposed by Cario and colleagues (Cario et al., 2015). Importantly, we demonstrate that membrane stability and functionality are shifted to higher temperatures under high pressure, which supports the view that apolar lipids may be one of the adaptative routes to high-temperature tolerance in hyperthermophiles.

This is the first time that a molecular model for membrane adaptation to high temperature has been proposed that allows structural and functional stability of the membrane up to at least 100°C. This work has possible important implications in the way we understand membrane adaptation to extreme conditions, especially with regard to the role of bipolar lipids in evolution. It may also help reconsider the apparent contradiction posed by the presence of bipolar lipids in mesophilic environments, such as the open ocean, which did not fit with the proposed temperature adaptation dogma. This study opens new perspectives to expand the model for the cell membranes of bacteria, where apolar intercalants may also be present. More importantly, this novel membrane architecture opens up new perspectives with regard to the stability of early versions of membranes at the origin of life. It will be crucial to test whether apolar molecules can be inserted within the midplane of protolipid bilayers, such as those produced from decanol and decanoic acid (Kapoor et al., 2014), and see whether the stability and functionality domains can be extended to higher or more variable temperature conditions.

A final important prediction of the novel membrane model of Cario and colleagues (Cario et al., 2015) concerns the spatial disposition of the mono- and bipolar lipids in the membrane. Indeed, *T. barophilus* produces between 15% and 50% tetraether lipids, and the ratio increases to 80% of diether lipids in *T. gorgonarius* at the optimal growth temperature of 88°C (Miroshnichenko et al., 1998). Under these conditions, there is a high probability of the existence of membrane domains of diverging lipid compositions. Our results suggest that apolar molecules such as squalane favour phase separation in the membrane (Figure S8) and may promote domain formation. Such distinctive domains must have different physico-chemical properties and therefore different functions related to, for example, fusion, enzymatic activity or membrane protein folding (Cebecauer et al., 2018). Further work will be required to identify the existence of these domains in natural membranes and identify the proteins specific to each type of domain to decipher their role in the cell cycle.

Acknowledgements

We gratefully acknowledge the Institut Laue – Langevin and the Diamond Light Source for the allocation of beam-time, and we thank technicians O. Aguettaz, C. Payre and J. Maurice for their support. We thank the research team Chimie Organique et Bioorganique (UMR 5246, INSA Lyon) and particularly S. Chambert for access to their spectrofluorimeter. This work was supported by the French National Research Agency programmes ANR 2010 BLAN 1725-04 and ANR 17-CE11-0012-01 to PO and JP, the German-French bilateral research cooperation programme “Procope” 2018-2019 to JP and RW, and the Royal Society to PO and NB. MSC was supported by a PhD grant from the French Ministry of Research. We apologize to our colleagues whose relevant work could not be cited due to spatial limitations.

Conflict of interest

The authors declare no conflict of interest.

Materials and methods

Chemicals

The synthetic archaeal lipids 1,2-di-O-phytanyl-*sn*-glycero-3-phosphocholine (DoPhPC) and 1,2-di-O-phytanyl-*sn*-glycero-3-phosphoethanolamine (DoPhPE), were purchased from Avanti Polar Lipids Inc. (Albaster, USA). The apolar isoprenoid used, 2,6,10,15,19,23-hexamethyltetracosane (squalane), was purchased from Sigma-Aldrich (Saint-Louis, USA) in its hydrogenated form and from CDN Isotopes (Pointe-Claire, Canada) in its deuterated form. All other chemicals, including 8-hydroxypyrene-1,3,6-trisulfonic acid trisodium salt (pyranine), 5(6)-carboxyfluorescein (CF) and 6-dodecanoyl-N,N-dimethyl-2-naphthylamine (laurdan), were purchased from Sigma-Aldrich (Saint-Louis, USA).

Neutron diffraction experiments

Contrast variation neutron diffraction is underpinned by the difference in coherent neutron cross sections of ^{1}H and ^{2}H (deuterium, D), which is widely used to highlight parts of a sample. Indeed, D is a much stronger coherent scatterer (scattering length 6.7 fm) compared to H (-3.7 fm) (Bée, 1988). Thus, profiles of the scattering length densities (*i.e.*, the membrane's cross-sectional profile), calculated as the Fourier sum of the structure factors determined by neutron scattering, show increased density at the location of the deuterated molecule.

Neutron diffraction experiments were performed on multiple stacks of oriented membrane bilayers. Bilayers were prepared by spreading 3 mg of DoPhPC:DoPhPE (9:1 molar) in chloroform:methanol (2:1) with or without 1 mol% squalane on a silicon wafer and dried under vacuum. Diffraction patterns were measured on the D16 small-momentum transfer diffractometer(Cristiglio et al., 2015) at the Institut Laue Langevin (Grenoble, France), and we used a cryostat and high-pressure equipment (Lelièvre-Berna et al., 2017; Peters et al., 2018) to precisely control temperature and pressure, respectively. We used an incident wavelength of $\lambda = 4.52$ Å and 2Θ scans with an accessible q-range from 0.06 $Å^{-1}$ to 0.51 $Å^{-1}$. Data obtained at ILL are identified by doi:10.5291/ILL-DATA.8-02-809 and doi:10.5291/ILL-DATA.8-02-818 (Salvador-Castell et al., 2018a, 2018b).

To locate squalane within the membrane system, we made use of the scattering density difference between hydrogen and its isotope deuterium using protonated and deuterated squalane as intercalants in the synthetic membranes (Hauß et al., 2002). This difference makes it possible to determine the position of a deuterated target molecule. The diffraction patterns were measured up to the fourth order of the Bragg reflection of the neutrons scattered by the multistack of lipid bilayers. The integrated intensities of the Bragg

peaks were corrected for absorption and analysed using Gaussian functions (with a maximum error of 5%), which provided a suitable model for describing the shape of the Bragg reflection, and up to four orders of Bragg reflections were taken into account for subsequent analysis.

The sum of neutron scattering lengths per unit volume is known as the neutron scattering length density (NSLD) profile. The NSLD profiles were calculated as discrete sets of Fourier coefficients f_n according to the formula (Katsaras, 1995):

$$\rho_{bilayer}(z) = \frac{2}{D}\sum_{n=1}^{M} f_n \nu_n cos\left(\frac{2n\pi}{D}z\right) \quad \text{(Eq.1)}$$

where D is the lamellar spacing of the bilayers in the z direction (perpendicular to the lipid interface); $z \in \left[\frac{-D}{2}; \frac{D}{2}\right]$. Coefficients f_n can be obtained by $I_n = \frac{|f_n|^2}{Q_z}$, Q_z is the Lorentz correction factor equal to q for oriented bilayers, I_n is the integrated intensity of the n^{th} Bragg peak and v_n corresponds to the phase of the structure factor.

The lamellar d-spacing of the lipid bilayer was determined from the observed 2Θ of the Bragg peak positions according to Bragg's law, $n\lambda = 2d\sin\Theta$, where n is the diffraction order and λ is the selected neutron wavelength. To obtain the phases of the structural factors, each type of squalane sample was measured at four different D_2O-H_2O contrasts (D_2O content: 8%, 20%, 50%, 100%). Therefore, it was possible to use the linear correlation of the structure factor amplitudes and sample D_2O content (Worcester and Franks, 1976) to yield the structure factors for each sample.

The membrane structural parameters were defined at 25°C and 100% relative humidity as follows (Nagle and Tristram-Nagle, 2000): D: lamellar repeat spacing; $2D_C$: thickness of hydrocarbon core, $D_C = V_C/A$; D_B: Gibbs-Luzzati bilayer thickness, $D_B = 2V_L/A$; D_w: Gibbs-Luzzati water thickness, $D_w = D - D_B$; n_w: number of water molecules/lipid, $n_w = AD_w/2V_w$ (V_w: water molecular volume,~ 30 Å^3).

Small-angle X-ray diffraction

Small-angle X-ray diffraction (SAXS) was carried out on fully hydrated lipid solutions prepared from 5 mg of the DoPhC:DoPhPE (9:1 molar) mixture in 20 µL of water with or without 1 mol% of squalane placed inside a pressure chamber (Brooks et al., 2010). The pressure- and temperature-dependent experiments were carried out at six different temperatures (10°C to 85°C, in 15°C steps) and from 1 to 1000 bar (in 50 bar steps). Experiments were performed at beamline I22 of the Diamond Light Source (Didcot, United Kingdom) (Smith et al., 2019) with an energy of 17 keV. The momentum transfer was defined as $q = 4\pi \sin(\Theta)/\lambda$, where 2Θ is the scattering angle. The lattice parameters are given by $a = 2n\pi/q$ and $a = 2(2n\pi/q)/\sqrt{3}$ for a lamellar and a hexagonal phase, respectively, where n= order of reflection. The type of phase

can be distinguished by the characteristics of the SAXS peak ratios for the lamellar phase: 1, 2, 3, 4, the cubic Pn3m phase: √2, √3, 2, √6 and the hexagonal phase: 1, √3, 2, √7.

LUVs preparation

Lipid unilamellar vesicles (LUVs) from DoPhPC: DoPhPE (9:1 molar) were prepared by dissolving the lipids with the appropriate amount of squalane in chloroform/methanol (2:1 v/v) to obtain 1 mol% squalane, vortexing the solution and drying it under a stream of nitrogen gas. The dried solution was left to dry overnight under vacuum. The lipid film was rehydrated with buffers specific to each technique, followed by vortexing and 5 cycles of freezing/thawing. LUVs were formed by pressure extrusion (Hope et al., 1985) passing the solution 11 times at 60°C through a 100 nm polycarbonate membrane using a Mini Extruder® (Avanti Polar Lipids, Inc., USA). After extrusion, the solution was cooled down, and the excess dye was removed by chromatography of the LUVs over Sephadex G-50 M columns. LUVs were used immediately after the chromatography.

Laurdan generalized polarization

Laurdan is a fluorescent probe whose emission wavelength is determined by water penetration into the lipid headgroup region, *i.e.,* is sensitive to the phase state of the membrane. Laurdan was excited at 350 nm, and its emission was measured between 420 and 510 nm. Temperature-dependent measurements were performed using a quartz cuvette with a volume of 100 µL in the temperature range 10 to 85 ± 0.1 °C. The spectral changes of laurdan are quantified by the generalized polarization function, GP, defined as (Parasassi et al., 1990):

$$GP = \frac{I_{440} - I_{490}}{I_{440} + I_{490}}$$

where I_{440} and I_{490} are the emission intensities at 440 and 490 nm, which are characteristic of fluid (liquid-crystalline) and ordered (gel) lipid phase states, respectively. Hence, the GP value reports on the fluidity of the membrane. Laurdan GP measurements were performed on LUVs, which were prepared from a lipid mixture containing 0.2 mol% of the fluorescent probe laurdan. The final lipid concentration in the LUV suspension was adjusted to 1 mM. Temperature-dependent fluorescence spectroscopic measurements were performed on a K2 multi-frequency phase and modulation fluorimeter (ISS, Inc., USA).

5-(6)-Carboxyfluorescein (CF) efflux

LUVs were prepared in a buffer (HEPES 10 mM, 100 mM KCl, 1 mM EDTA pH: 7.8) containing 40 mM CF. At this concentration, CF is self-quenched and the release from the liposomes will increase its fluorescence intensity. The final lipid concentration in the LUV suspension was adjusted to 5 mg/mL, and the fluorescence was monitored at 518 nm (excitation at 492 nm) as a function of temperature (10°C to 60°C) and pressure (1 bar to 1000 bar). At the end of each measurement, a 100% reference point was determined by adding 0.1% Triton X100 to disrupt the liposomes, facilitating complete release of the remaining trapped fluorescent dye. The results are presented as the ratio (Weinstein et al., 1981):

$$\%CFefflux = \frac{F_t - F_0}{F_{max} - F_0} * 100$$

where F_t, F_0 and F_{max} are the fluorescence intensities at time t, time zero, and after total solubilization by Triton X100.

Pyranine fluorescence

The membrane influx of protons into liposomes was measured by monitoring the emission of pyranine, a sensitive pH sensor. LUVs were prepared from a 5 mM HEPES buffer (pH = 7.5) containing 5 mM pyranine, and the final lipid concentration was adjusted to 5 mg/mL. Measurements were performed as a function of temperature (10°C to 60°C) and pressure (1 to 1000 bar) in the presence of 0.1 M HCl as a proton source. All results are normalized to a blank experiment performed under the same conditions in the absence of an external proton source to take care of a possible impact of P and T on the photophysics of the reporter dye.

Supplementary figures

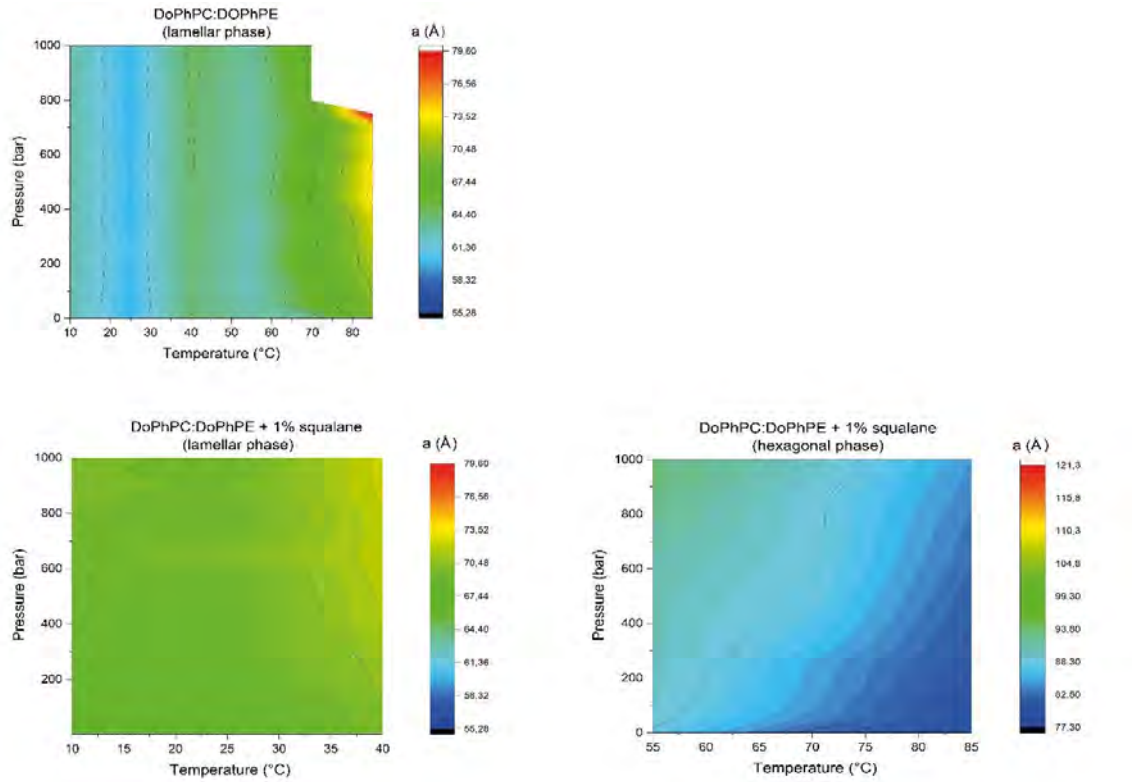

Figure S1. Lattice parameters of lipid phases are modulated by temperature and pressure. *Two-dimensional pressure-temperature colour maps of lattice parameters (d-spacing) for lamellar phases of DohPC:DoPhPE (9:1) (top left) and with 1 mol% squalane (bottom left) and for hexagonal phases of DoPhPC:DoPhPE (9:1) + 1 mol% squalane (right). In the absence of squalane, the membrane is highly unstructured at extreme conditions (70°C – 85°C), and it was not possible to determine its d-spacing in the most extreme conditions (85°C and 700 bar). However, in the presence of squalane, the membrane is highly structured under extreme conditions and presents non-lamellar phases, such as the hexagonal phase.*

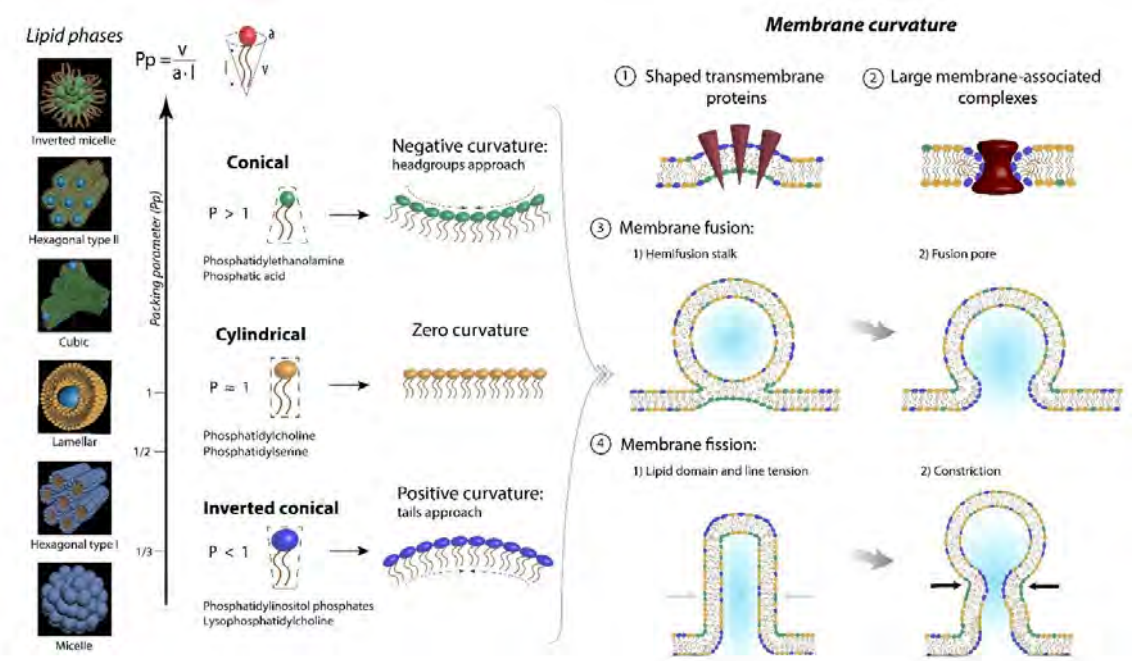

Figure S2. Sketch of different lipid phases that can be detected by SAXS and their significance for cell membranes. *Membrane curvature and relationship with lipid phases detected by SAXS. Left, different lipid phases detected by SAXS and ordered by their packing parameter (Pp=v/a*l, where v is the molecular volume, l is the molecular length, and a is the molecular area at the hydrocarbon-water interface). Molecules with high packing parameter (i.e., small head groups) have a conical geometry and tend to bend to negative curvatures (green), contrary to molecules with little P, which have an inverted conical geometry and bend to positive curvatures (blue). Right, clusters of conical or inverted conical lipids indicate the different curvatures of the membrane: negative (green) and positive curvatures (blue). 1-2: Different proteins anchor to membrane that require characteristic curvatures to be functional. 3: process of membrane fusion, figures represent the two main steps where non-zero curvatures are needed. 4: process of membrane fission, this process also needs characteristic membrane curvatures.*

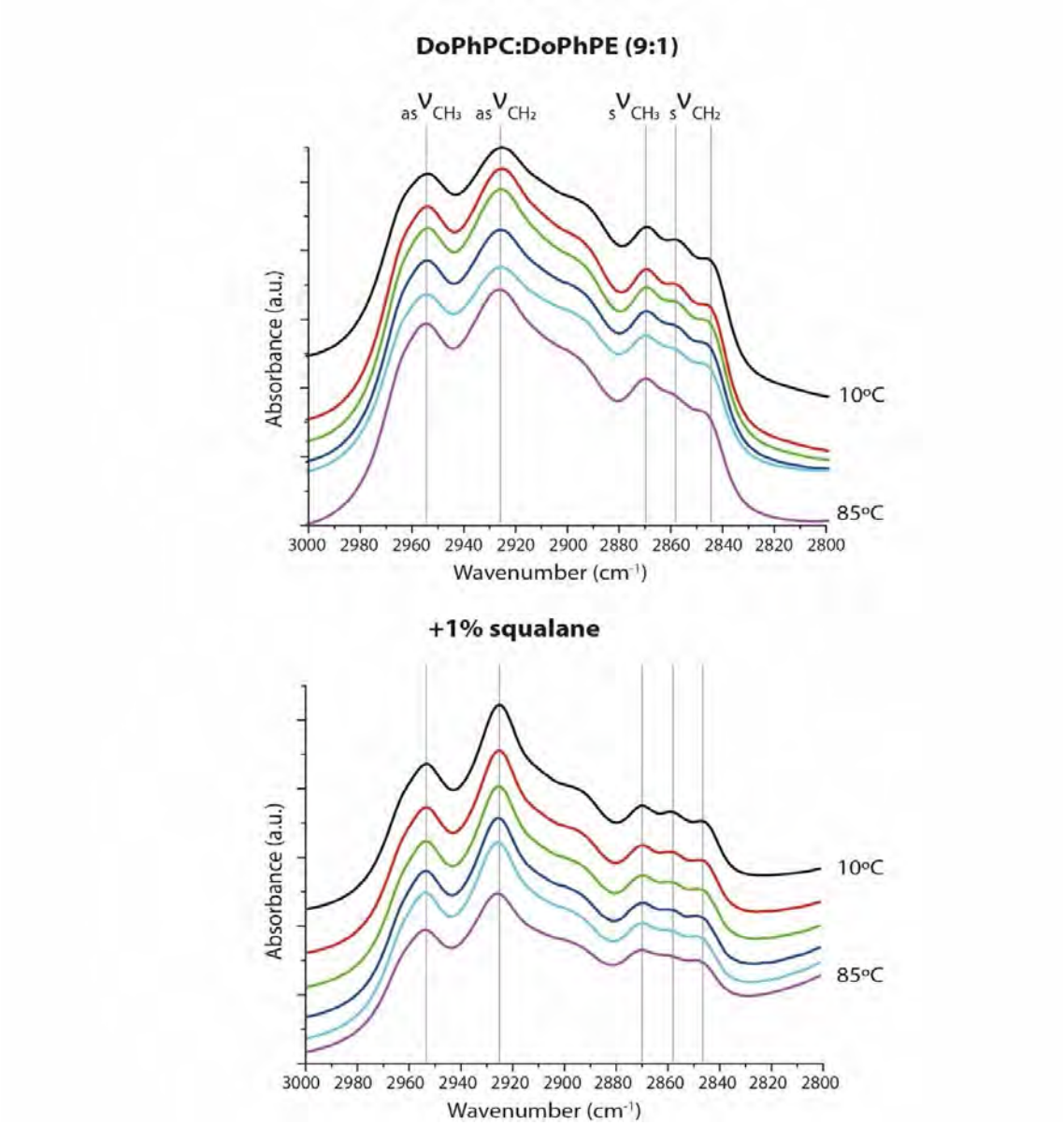

Figure S3. Intramolecular and intermolecular vibrations are slightly sensitive to temperature and the presence of squalane. *Infrared spectra of DoPhPC:DoPhPE (9:1) (above) and DoPhPC:DoPhPE (9:1) with 1 mol% squalane (below) at ambient pressure and different temperatures (black: 10°C, red: 25°C, green: 40°C, blue: 55°C, cyan: 70°C, magenta: 85°C). Asymmetric CH_3 stretching corresponds to approximately 2955 cm-1, asymmetric CH_2 stretching to approximately 2925 cm^{-1}, symmetric CH_2 stretching to approximately 2870 cm^{-1}, and symmetric CH_2 stretching to the double peak at approximately 2845 cm^{-1} and 2855 cm^{-1}.*

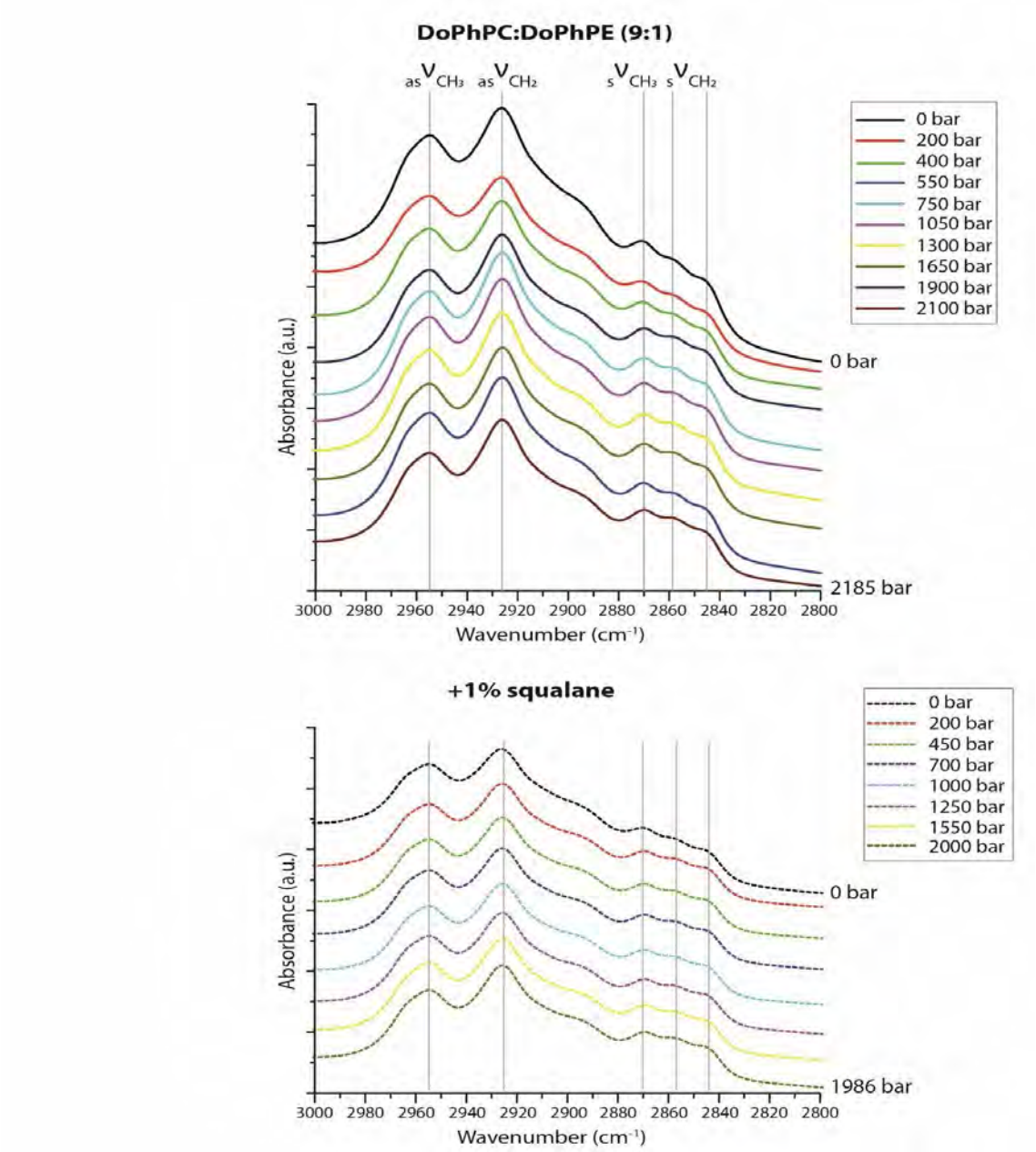

Figure S4. Lipid molecular vibrations are slightly sensitive to pressure and the presence of squalane. *Infrared spectra of DoPhPC:DoPhPE (9:1) (above) and DoPhPC:DoPhPE (9:1) with 1 mol% squalane (below) at 25°C and different applied pressures (black solid line: 0 bar, red solid line: 200 bar, green solid line: 400 bar, blue solid line: 550 bar, cyan solid line: 750 bar, magenta solid line: 1000 bar, yellow solid line: 1330 bar, ochre solid line: 1650 bar, dark blue solid line: 1900 bar, brown solid line: 2100 bar, black dashed line: 0 bar, red dashed line: 200 bar, green dashed line: 450 bar, blue dashed line: 700 bar, cyan dashed line: 1000 bar, magenta dashed line: 1250 bar, yellow dashed line: 1550 bar, ochre dashed line: 2000 bar). Asymmetric CH_3 stretching corresponds to approximately 2955 cm^{-1}, asymmetric CH_2 stretching to approximately 2925 cm^{-1}, symmetric CH_2 stretching to approximately 2870 cm^{-1} and symmetric CH_2 stretching to the double peak at approximately 2845 cm^{-1} and 2855 cm^{-1}.*

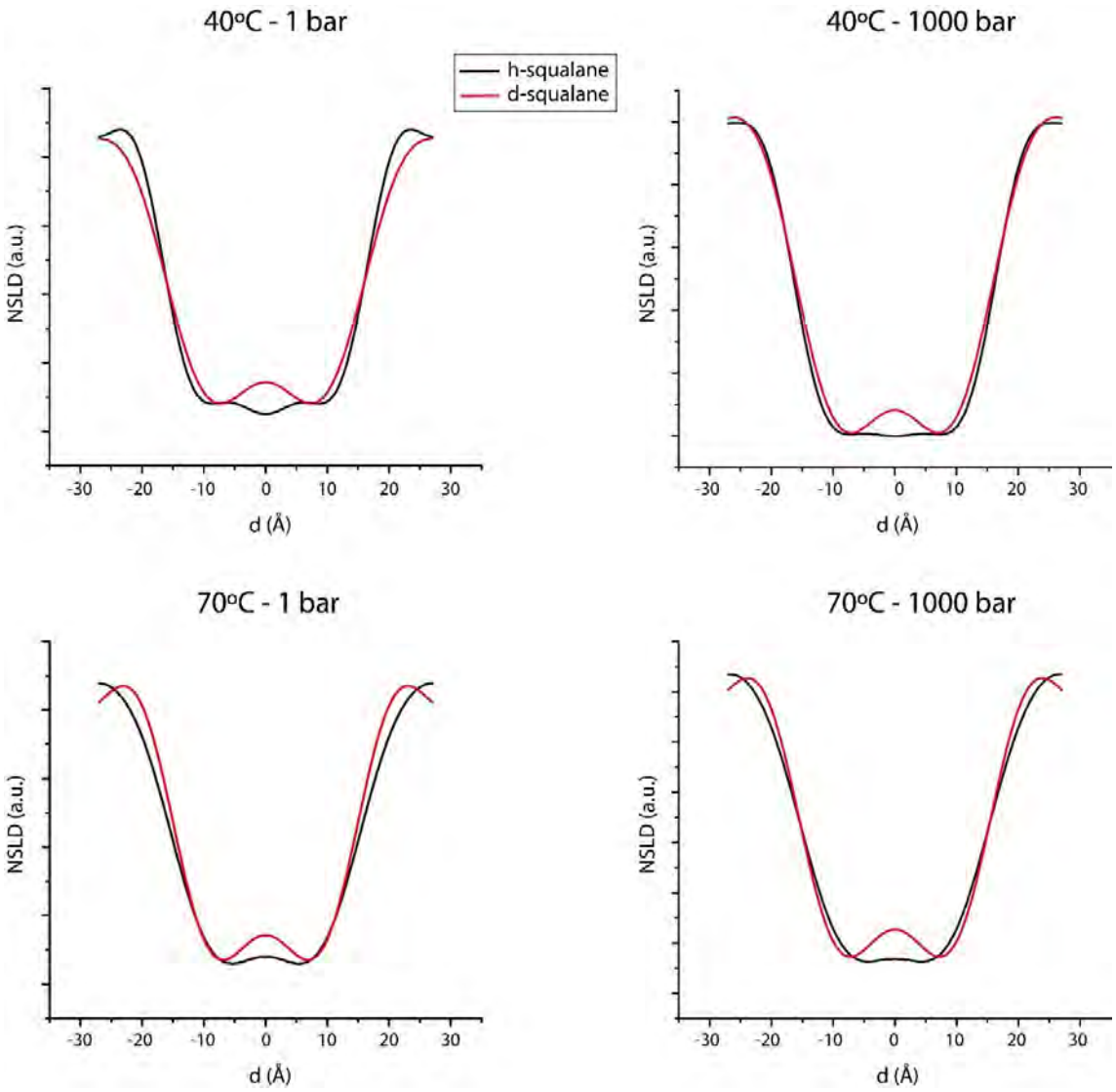

Figure S5. Squalane is placed in the midplane of the bilayer, perpendicular to the lipids, at high temperatures and high hydrostatic pressures. *Neutron scattering length densities of DoPhPC:DoPhPE (9:1) with 1 mol% hydrogenated squalane (black) and 1 mol% deuterated squalane (red) at 40°C, 70°C and 1 bar and 1000 bar. These NSLDs confirm that squalane is positioned at the midplane of the bilayer, even at high temperature and high pressure.*

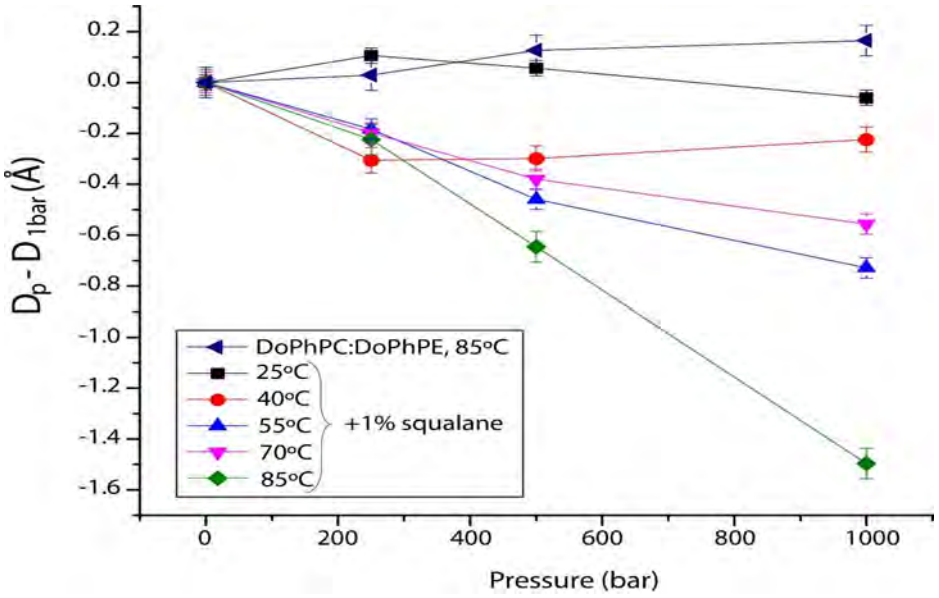

Figure S6. In the presence of squalane, especially at high temperatures, the lipid bilayer is highly compressible. *Variation in the lamellar lattice parameters (Dp: d-spacing at different pressures (1 bar, 250 bar, 500 bar, 1000 bar), D1bar: d-spacing at 1 bar) obtained by multistacking bilayers from neutron diffraction, measured at different pressures for DoPhPC:DoPhPE at 85°C (blue leftward-pointing triangles) and for DoPhPC:DoPhPE (9:1) +1 mol% squalane at 25°C (black squares), 40°C (red spheres), 55°C (blue upward-pointing triangles), 70°C (magenta downward-pointing triangles), and 85°C (green diamonds).*

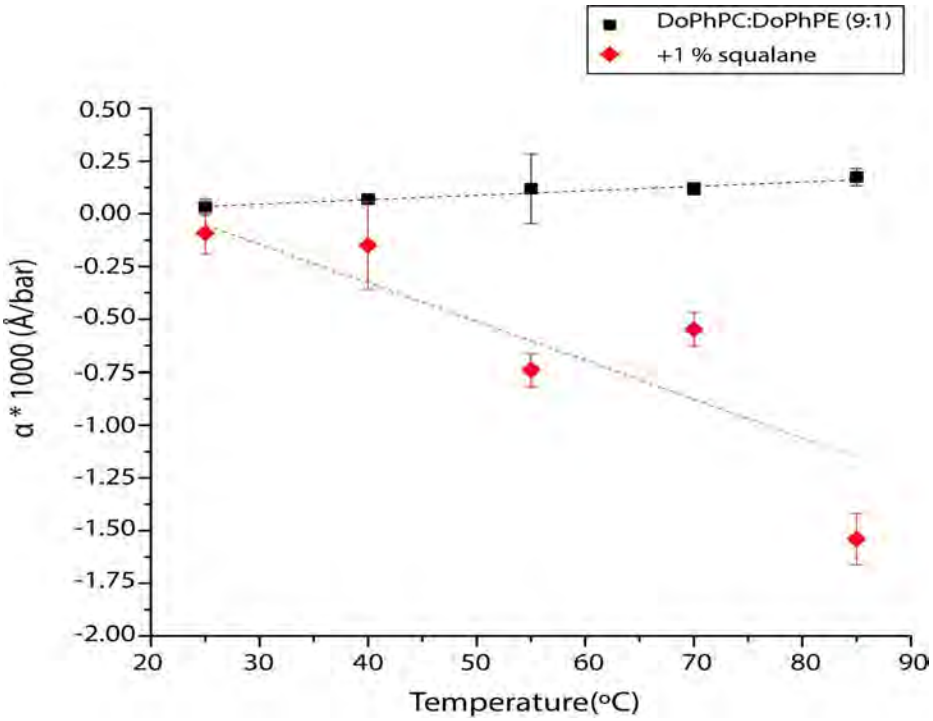

Figure S7. The compressibility of the lipid bilayer in the presence of squalane tends to increase in proportion to temperature. *The task is representation of the slope (α) of the pressure dependence of the d-spacing for different temperatures (Figure S6). The value is multiplied by 1000 to facilitate better visualization. Data are shown for DoPhPC:DoPhPE (9:1) in the absence (black squares) and presence 1 mol% squalane (red triangles). In contrast to the neat lipid mixture, in the presence of squalane, pressure decreases the bilayer thickness, and this effect is more pronounced at high temperatures. Dashed lines are linear fits to guide the eyes.*

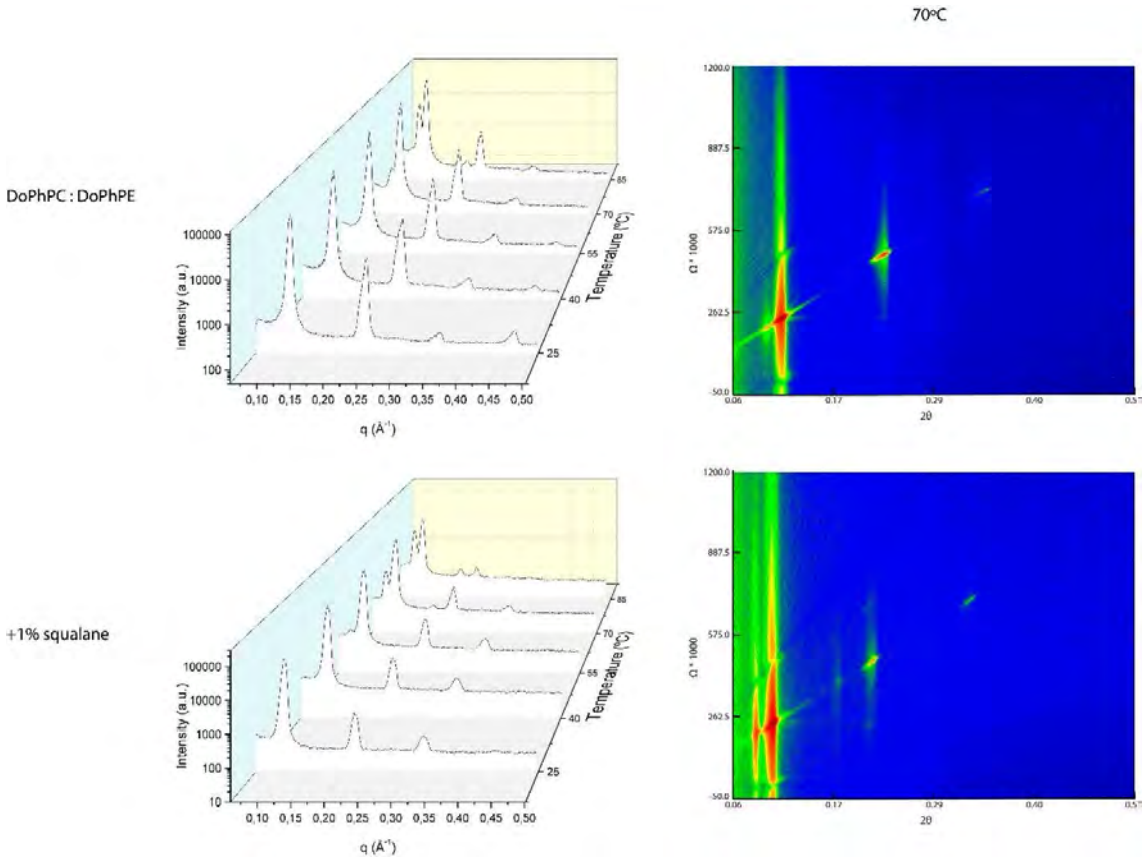

Figure S8. Squalane facilitates the formation of new lipid phases. *Left side, intensities obtained by the neutron diffraction of DoPhPC:DoPhPE (9:1) in the absence and presence of 1 mol% squalane at different temperatures (25°C, 40°C, 55°C, 70°C and 85°C). The corresponding 2D diffraction patterns at 70°C show the coexistence of two lamellar phases in different proportions, which confirms that squalane promotes the emergence of new phases while increasing membrane stability under extreme conditions (e.g., 70°C).*

Chapter 4. Physicochemical impact of apolar polyisoprenoids on a model archaeal membrane

Cell membranes contain diverse concentrations of membrane regulators. For instance, cholesterol represent 23% of membrane lipids of red blood cells, but only 3% of mitochondrial membrane lipids. As one would expect, the quantity of these molecules highly influences the physicochemical properties of the membrane. As an illustration, 15 mol% of cholesterol decreases by 2°C and 3 kcal/mol the lipid main phase transition while at 50 mol%, its transition is completely abolished (McMullen et al., 1993). Sterols, such as cholesterol or hopanoids, their bacterial surrogates, have been detected in none of the Archaea. Thus, it is unclear what molecules play the role of the membrane regulators in such domain. The study of the membrane homeoviscous adaptation in *T. barophilus* demonstrates that apolar isoprenoids play this role in Archaea. Although the quantity of apolar polyisoprenoids' in cells have not been examined in detail yet, their presence has been detected at concentrations ranging from 0.4% to 11% of total content of lipids (Banciu et al., 2005; Cario et al., 2015; Lattuati et al., 1998). The quantity of non-polar polyisoprenoids varies according to the microorganism and as a function of variations in environmental conditions. Recently, we established a direct correlation between the optimal growth conditions of archaea and the length of their apolar polyisorepnoids (Salvador-Castell et al., 2019b). Thus, non-polar polyisoprenoids were proposed as the most probable cholesterol surrogates in Archaea. Membrane regulators influence membrane parameters in a concentration-dependent manner. Consequently, to

confirm the putative role of apolar polyisoprenoids as membrane regulators in Archaea, it was essential to measure this factor in the membrane ultrastructure presented. The following three research manuscripts present the results of structural studies aiming at the demonstration of the concentration dependent effect of squalane on the physicochemical properties of the archaeal lipid bilayer.

Article III. Induction of non-lamellar phases in archaeal lipids at high temperature and high hydrostatic pressure by apolar polyisoprenoids

Marta Salvador-Castell[1], Nicholas J. Brooks[2], Judith Peters[3,4] & Philippe Oger[1]

[1] Université de Lyon, INSA de Lyon, CNRS, UMR 5240, 69211 Villeurbanne, France.

[2] Imperial College London, South Kensington Campus, London SW7 2AZ, England

[3] Université Grenoble Alpes, LiPhy, CNRS, 38000 Grenoble, France

[4] Institut Laue Langevin, 38000 Grenoble, France

Manuscript is under revision for Biochimica et Biophysica Acta - Biomembranes

Foreword

In the previous chapter, it was demonstrated that as low 1 mol% of apolar polyisoprenoid in an archaeal lipid bilayer could induce the formation of cubic phases (Salvador-Castell (3) et al., n.d.). To determine the concentration dependence of the impact of squalane, I conducted a thorough investigation of the effect of apolar polyisoprenoids on membrane curvature. To this end, I identified the lipid phases at full hydration from the DoPhPC:DoPhPE (9:1) mixture in the presence of different percentages of squalane ranging from 0 to 10 mol%., as a function of HT and HHP. The study was realized by SAXS at the I22 beamline of the DLS.

The results confirm that squalane induces the formation of stable non-lamellar phases. For instance, the presence of 5 mol% squalane causes the emergence of a hexagonal phase, in coexistence with the lamellar phase at temperatures up to 55°C and alone at temperatures above 70°C. In contrast, only the hexagonal phase is present in the lipid system with 10 mol% squalane at all temperatures and high pressures tested. As expected, I confirmed that while HT promotes negative curvatures, HHP has the opposite effect by favouring the lamellar phase. In presence of squalane, the lipid system studied here forms non-lamellar phases, and particularly cubic phases, presenting large lattice parameters, e.g. the lattice parameter of the cubic phase formed in presence of 1 mol% squalane is 332 ± 3 Å. Last, it is especially interesting to observe from the same sample how the hexagonal phase swells much more under HHP when it is in coexistence with a lamellar phase (DoPhPC:DoPhPE + 5 mol% squalane), probably due to a change of squalane localization inside the system. Such result confirms that squalane reduces the lipid chain frustration of the system.

This study demonstrates that the fraction of squalane in the system is fundamental to determine the curvature of the membrane. Consequently, the archaeal cell could easily adapt its cell membrane curvature by modifying the proportion of squalane in the membrane to fit cell requirements, such as favouring highly curved domains during fission. This ability to change cell curvature could be essential to adapt membrane functions under extreme and changing environmental conditions.

Induction of non-lamellar phases in archaeal lipids at high temperature and high hydrostatic pressure by apolar polyisoprenoids

Marta Salvador-Castell[1], Nicholas J. Brooks[2], Judith Peters[3,4] & Philippe Oger[1]

[1] Université de Lyon, INSA de Lyon, CNRS, UMR 5240, 69211 Villeurbanne, France.

[2] Imperial College London, South Kensington Campus, London SW7 2AZ, England

[3] Université Grenoble Alpes, LiPhy, CNRS, 38000 Grenoble, France

[4] Institut Laue Langevin, 38000 Grenoble, France

Manuscript is under revision for Biochimica et Biophysica Acta - Biomembranes

Abstract

It is now well established that cell membranes are much more than a barrier that separate the cytoplasm from the outside world. Regarding membrane's lipids and their self-assembling, the system is highly complex, for example, the cell membrane needs to adopt different curvatures to be functional. This is possible thanks to the presence of non-lamellar-forming lipids, which tend to curve the membrane. Here, we present the effect of squalane, an apolar isoprenoid molecule, on an archaea-like lipid membrane. The presence of this molecule provokes negative membrane curvature and forces lipids to self-assemble under inverted cubic and inverted hexagonal phases. Such non-lamellar phases are highly stable under a broad range of external extreme conditions, e.g. temperatures and high hydrostatic pressures, confirming that such apolar lipids could be included in the architecture of membranes arising from cells living under extreme environments.

Keywords

Phospholipids, non-lamellar phases, squalane, archaea

Introduction

Since Singer and Nicolson (Singer and Nicolson, 1972) first defined the membrane as a mosaic of proteins and lipids in a lamellar fluid liquid-crystalline (L_α) phase, our view of the membrane ultrastructure has become more sophisticated, recognizing the existence of membrane domains of specific lipid composition in natural membranes. Each composition corresponds to a particular phase, which play important roles in cell membrane function and cell physiology as they have very specific physicochemical properties, such as different lateral motions, rotations, fluidity, and phase structuration, and promote the formation of lamellar or non-lamellar phase (Cebecauer et al., 2018; Goñi, 2019).

Lamellar, cubic and inverted hexagonal phases possess different bending fluctuations and intrinsic curvatures4, which are mostly defined by the shape of the lipids present in the membrane. This has been rationalized using the critical geometric packing parameter (P_p) concept, which is defined as $P_p = \frac{v}{a \cdot l}$ where *v* is the molecular volume, *l* is the molecular length and *a* is the molecular area at the lipid-water interface (Israelachvili et al., 1976; Kulkarni, 2019). For P_p<1, molecules are inverted cones and tend to produce positive curvatures, i.e. the hydrocarbon chains are closest to each other. For $P_p \approx 0$, lipids have a cylindrical shape and adopt zero curvature, giving rise to lamellar phases. For P_p>1, lipids present conical shapes and adopt negative curvatures and self-assemble under the so-called inverted phases, such as the cubic (Q) and hexagonal (H_{II}) phases, simply to release their curvature frustration (Figure 1). Although the process is not completely understood, it is thought that the precursor of the cubic phase is the formation and later destabilization of interlamellar attachments, while the hexagonal phase starts with a membrane bump that forms high-tension regions (Figure S1) (Ellens et al., 1989; Rappolt et al., 2003; Seddon and Templer, 1993).

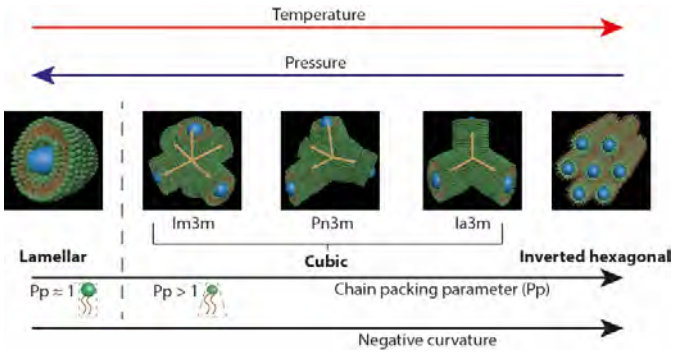

***Figure 9. Schematic representation of different lipid phases as a function of lipid curvature**. The lipid headgroups are represented in green, the hydrocarbon chains in brown and water location in blue. The arrows indicate the direction for the increase of the different parameters: chain packing parameter (P_p), negative intrinsic curvature of the membrane, pressure and temperature.*

Changes between lamellar and non-lamellar former lipid compositions tune the flexibility and curvature of the membrane (Ninham et al., 2017) which is used by cell to tune its membrane functionality by adjusting its membrane lipid compositions to adapt itself and maintain essential functions under different environmental conditions.

Archaeal phospholipids present unique characteristics: a *sn*-glycerol-1-phosphate (G-1-P) backbone, ether linkages, and isoprenoid hydrocarbon chains (De Rosa et al., 1986). The methyl groups along the acyl chains are responsible for the fact that both phospholipid's rotamers are nearly energetically equivalent, thus allowing archaeal lipids to occur in the Lα phase for a broad range of temperature (-120°C to 120°C) (Lindsey et al., 1979; Polak et al., 2014). Isoprenoid chains pack densely, increase membrane viscosity and decrease its water permeability (Shinoda et al., 2004b; Tristram-Nagle et al., 2010). The presence of ether bounds, isoprenoid hydrocarbon chains and transmembrane lipids is thought to be the reason of the incredibly high resistance of archaeal cell membranes to extreme conditions (Chugunov et al., 2014). For example, some Archaea have their optimal growth conditions at low pH, high salinity, high temperature (HT) and/or high hydrostatic pressure (HHP), including a highly stable and selective permeable cell membrane. Intriguingly, liposomes made from archaeal lipids present highly irregular shapes (Gmajner et al., 2011) and indeed, extracellular membrane vesicles are highly produced by Archaea (Gill et al., 2019). All these findings indicate that non-lamellar-forming lipids may play a particular important role in the Archaea domain.

The geometric packing parameter predicts that most archaeal phospholipids will have zero or positive curvatures, which will not favour the formation of the non-lamellar phases indispensable for biological activity. This is for example the case for the membrane lipids of *Thermococcus barophilus* which have phosphatidyl inositol polar headgroup and derivatives of this polar headgroup. Recently, Cario and colleagues (Cario et al., 2015) proposed a novel archaeal membrane architecture for the hyperthermophile and piezophile Archaeon *T. barophilus* in order to explain its ability to thrive at temperatures close to 100°C (Marteinsson et al., 1999). According to this hypothesis, apolar isoprenoid molecules would populate the hydrophobic space between the two bilayer leaflets, thus modifying the membrane properties, decreasing permeability to proton and water and membrane rigidity (Haines, 2001). In addition, the presence of the interleaving molecules within the plane of the membrane is proposed to be implied in modifying the phases transition in the membrane. Indeed, the partitioning of non-polar molecules, such as alkanes, aromatic compounds and isoprenoid chains into the hydrocarbon region, increases the tendency of the lipid layer to adopt a negative interfacial curvature (Lohner et al., 1993; Seddon and Templer, 1995; Tate et al., 1991). Therefore, lipids reduce their hydrocarbon packing stress self-assembling within

inverted non-lamellar phases. For example, the addition of 5% alkane to a mixture of PC/PE-lipids reduces the L_{α}-H_{II} transition by 55°C (Kirk and Gruner, 1985). To date, the effect of apolar lipids on archaeal membranes has not been studied.

Using Small Angle X-ray Scattering (SAXS), we have determined the lipid phases from a mixture of archaeal lipids in presence of different molar percentages (mol%) of the polyisoprenoid squalane at different temperatures and pressures. Here we show that in absence of the apolar intercalant, the archaeal lipids cannot form non-lamellar phases, and that the presence of the apolar molecule imposes highly stable non-lamellar type II Q and H phases.

Results and discussion

I. Archaeal phospholipids self-organize under lamellar phases

Lipid phases in excess of water can be identified by the relative Bragg peak positions in the SAXS patterns (Tyler et al., 2015). Collected data points and phase diagrams are shown in Figure 2. In absence of the apolar molecule, only lamellar phases can be identified in the SAXS spectra (Salvador Castell, unpublished results). At 10°C and ambient pressure, the lattice parameter of the lamellar phase is 62.7 ± 0.6 Å. As expected, the lamellar phase appears sensitive to HT (Figure S2). The lattice parameter increases at least to the highest temperature tested of 85°C. However, starting from 70°C the sample loses its correlation between bilayers and becomes so disordered that only the first diffraction order can be fitted with accuracy. The lattice parameter increases from 62.7 ± 0.6 Å at 10°C to 73.2 ± 1 Å. The lamellar phase appears little sensitive to hydrostatic pressure. Indeed, the lattice parameter varies only within the error bars of the measure. In contrast to other lipid systems in which hydrostatic pressure exert a structuring impact on the bilayers (McCarthy and Brooks, 2016), we see no such effect on DoPhPC:DoPhPE-based membranes. In fact, at the highest combined pressures and temperatures (85°C and >750 bar), no diffraction peaks are visible anymore.

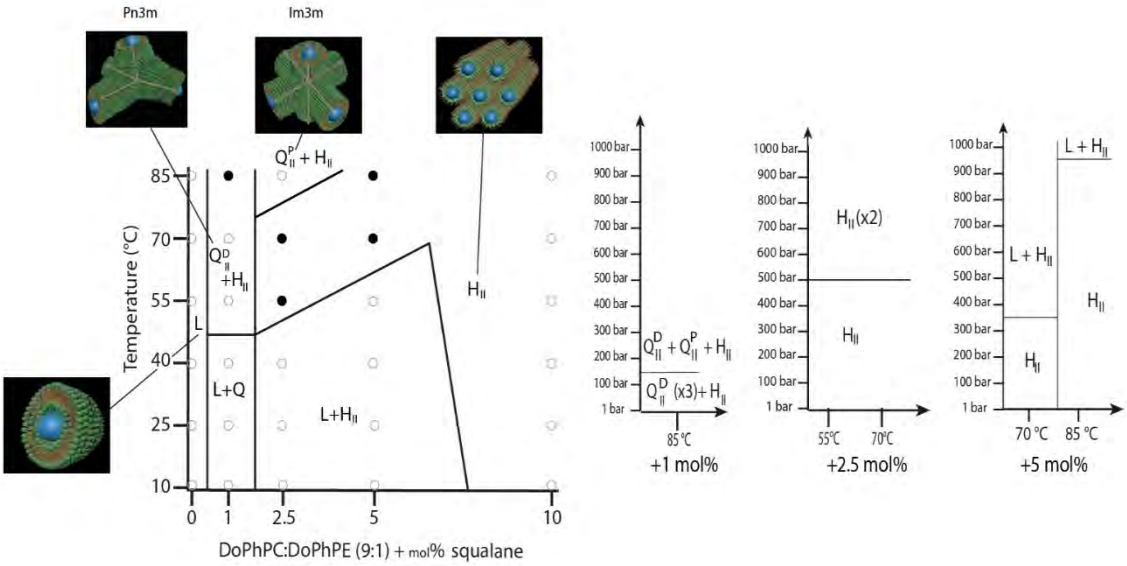

Figure 10. Phase diagrams of the DoPhPC:DoPhPE (9:1) in presence of excess water as a function of the proportion of squalane, temperature (Left panel) and pressure (Right panel) *Left, sketches of each phase (same colour scheme as in figure 1). Full circles indicate conditions under which pressure-induced phase transitions are observed and detailed in the right panel, and open circles those under which no pressure-induced phase transition is observed between 0 and 1000 bar.*

II. Addition of 1 mol% squalane induces the formation of inverted non-lamellar phases

Upon addition of squalane, even at the smallest quantity of 1 mol%, we observed the presence of non-lamellar phases of type II, in co-existence or not with lamellar phases, which suggests that the presence of squalane increases the negative membrane curvature (Salvador Castell, unpublished results). At all temperatures, we observe a cubic phase, in coexistence with a lamellar phase up to 40°C and a hexagonal phase above. In contrast to the lipid system without squalane, the system with 1mol% squalane is both pressure and temperature sensitive. The a_{lam} increases as a function of HHP from 67.6 ± 0.3 Å at ambient pressure to 69.8 ± 0.3 Å at 1000 bar at 10°C for example, but also as a function of temperature where it reaches 69.6 ± 0.5 Å at 40°C and 1 bar (Figure S3). Temperature is known to favour the negative intrinsic curvature of the lipid self-assembly. At temperatures of 55°C and above, a mixture of a Pn3m cubic phase and an inverted hexagonal phase coexist. At 85°C, three different Pn3m phases with very slightly different lattice values coexist, which is indicative that they have most likely different hydration levels (Figure 3). Note the substantial lattice parameters of the cubic phases (a_{Pn3m} = 254 ± 2 Å and a_{Im3m} = 332 ± 3 Å) which reflect the high potential of squalane to reduce chain packing frustration. Values for the lattice parameter for bacterial lipid cubic phases are substantially smaller, such as 105 Å for monoolein (MO) (Kulkarni et al., 2011; Mariani et al., 1988) or 122 Å for 1,2-dioleoyl-sn-glycero-3-phosphoethanolamine (DOPE) (Shyamsunder et al., 1988). However, under certain conditions this lattice parameter can

reach values higher than those measured here, an example is the case of a diphytanoyl PC-cholesterol mixture, in which the Q_{II} phase has a a_{cubic} of 510 Å (Tenchov et al., 2006). At 85°C, we observe the replacement of the Pn3m by the Im3m phase (Figure 3). Thus remarkably, HHP leads to the replacement of a Pn3m cubic phase with a lower a_{cubic} and higher negative curvature to a Im3m's cubic phase with a higher a_{cubic} and lower negative membrane curvature. In accordance with geometric considerations for those coexisting phases (Tenchov et al., 1998; Tenchov and Koynova, 2017), we found that the ratio between their lattice parameters is 1.28. The hexagonal phase has a lattice parameter ranging from 87.9 ± 0.5 Å at 55°C to 80.1 ± 0.5 Å at 85°C under ambient pressure. This a_{hex} is highly sensitive to pressure, ranging from 82.2 ± 0.5 Å at 1 bar to 90.1 ± 0.5 Å at 1000 bar at 70°C for example. This is in accordance with the fact that non-lamellar self-assemblies easily swell at HHP (Brooks, 2014). In addition, such a_{hex} is much higher than the a_{hex} usually obtained for familiar lipids which lie at 52.9 Å at 97°C for MO (Briggs et al., 1996) or 65.8 Å at 70°C for DOPE (Turner and Gruner, 1992), for example. This may be directly related to the ability of squalane to release the chain frustration at H_{II} phases with high a_{hex}.

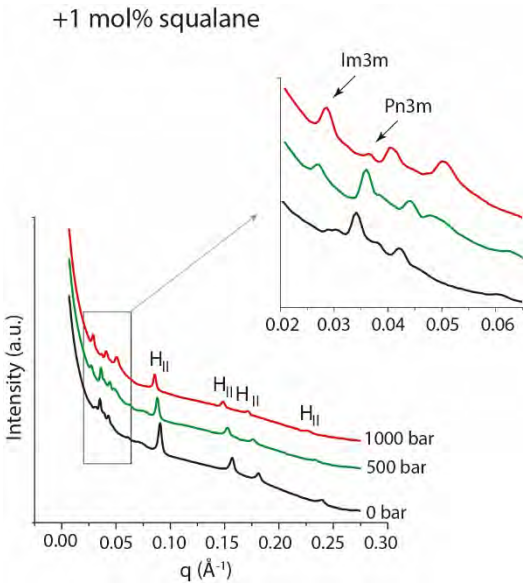

Figure 3. SAXS spectra of the mixture DoPhPC:DoPhPE +1 mol% squalane*. At 85°C and ambient pressure (black), 500 bar (green) and 1000 bar (red). Top inset, zoom into the cubic phase region.*

III. Higher negative curvature in presence of 2.5 mol% of squalane

By further adding squalane, the system presents a coexistence of a lamellar and H_{II} phases at low temperature and no longer a coexistence of lamellar and cubic phases, which is indicative of a further increase of the membrane negative curvature. As for the 1 mol% squalane lipid system, the lamellar phase is present up to 40°C, but in contrast, it seems to be far less sensitive to pressure (Figure S4). At 85°C, the hexagonal phase coexists with two cubic phases, probably Im3m. Remarkably, at 55°C and 70 °C, HHP induces a phase transition to a second hexagonal phase coexisting with the one already presented at low pressures (Figure 4a). We propose that this phase separation could result from the rearrangement of squalane between a squalane rich and a squalane poor phase. As observed before, the hexagonal phase is much more sensitive to temperature and HHP than the lamellar phase. The a_{hex} decreases from 94.6 ± 0.5 Å at 10°C to 77.4 ± 0.5 Å at 85°C at 1 bar and increases from 94.6 ± 0.5 Å to 103.1 ± 0.5 Å at 1 bar to 1000 bar at 10°C (Figure S4b). Last, at 85°C, two pressure-sensitive Im3m phases appear in coexistence with the H_{II} phase (Figure 4b). The a_{cubic} varies from 248 ± 2 Å and 264 ± 2 Å at 1 bar, to 264 ± 2 Å and 279 ± 2 Å, at 1000 bar for the two phases (Figure S4c). The presence of these two Q_{II} phases may be due to different hydration levels as observed at 1 mol% squalane.

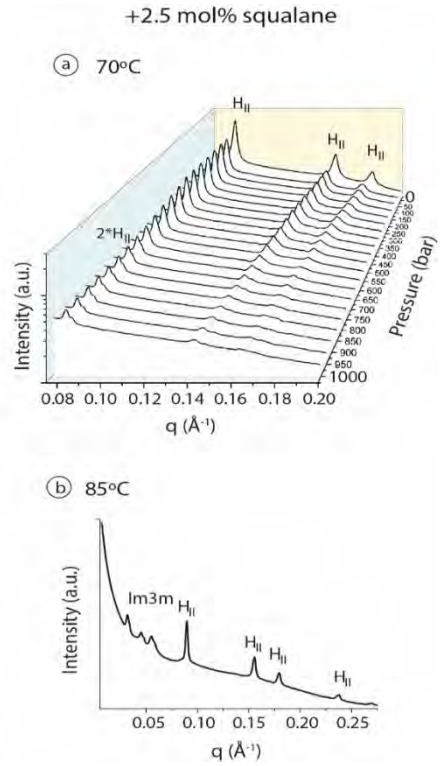

Figure 4. SAXS spectra of the mixture DoPhPC:DoPhPE + 2.5 mol% squalane. a) *At 70°C as a function of applied pressure (from 0 to 1000 bar, 50 bar steps). Two H_{II} coexist above 600 bar.* ***b)*** *At 85°C at ambient pressure, Q_{II} Im3m and the H_{II} phases coexist.*

IV. A competition between lamellar and inverted hexagonal phase appears by adding 5 mol% squalane

In presence of 5 mol% squalane at 1 bar, the system presents a mixture of one lamellar and one inverted hexagonal phase at temperatures up to 55°C (Figure 5a). As expected, temperature increases the membrane's negative curvature and at 70°C and above only the H_{II} is present. In contrast, pressure promotes the lamellar phase, which can be readily observed at 70°C, where the lamellar phase appears above 350 bar. Higher HHP values further increase the structuration of the lamellar phase (Figure 5b). At their highest temperature tested, i.e. 85°C, the lamellar phase appears at 1000 bar. In presence of 5 mol% squalane, the lamellar-to-hexagonal transition is a direct conversion as no cubic phase appears.

Interestingly, HHP swells much more the H_{II} phase than the lamellar one. At 10°C, a_{lam} remains almost constant at 57.8 ± 0.4 Å – 58.0 ± 0.4 Å from 1 bar to 1000 bar but, due to the capability of squalane to reduce chain frustration, the hexagonal phase is able to swell from 111.8 ± 0.5 Å at 1 bar to 121.2 ± 0.5 Å at 1000 bar for the same temperature (Figure 5c and Figure S5).

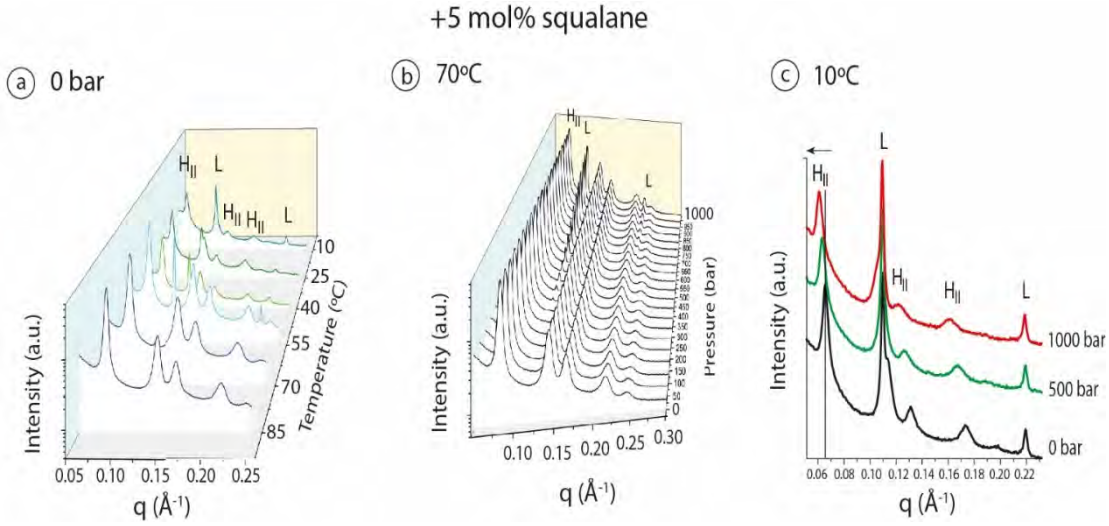

Figure 5. SAXS spectra of the mixture DoPhPC:DoPhPE + 5 mol% squalane. a) *As a function of temperature at ambient pressure (0 bar applied).* ***b)*** *at 70°C as a function of pressure, from 0 to 1000 bar of pressure applied, 50 bar steps. A lamellar phase appears at 350 bar.* ***c)*** *At 10°C as a function of pressure. The L and H_{II} phases coexist at ambient pressure (black), 500 bar (green) and 1000 bar (red).*

The different pressure sensitivities of the L and H_{II} phases are easily observed when plotting Δa, i.e. the difference between the lattice parameter at HHP and at ambient pressure (Figure 6a). The Δa of the lamellar phase is ca. 0.2 Å*kbar^{-1} and not significative. In contrast, the H_{II} phases swell up to 9.5 Å*kbar^{-1} at 10°C and 1.5 Å*kbar^{-1} at 85°C. Familiar Lα phases usually swell up to 2 Å*kbar^{-1} while H_{II} may swell as much as 6 Å*kbar^{-1} (Brooks, 2014). The

swelling of H_{II} decreases with temperature. This unexpected behaviour can be explained by the coexistence of the H_{II} and lamellar phases in the system. Indeed, one can observe the change of slope of Δa at 70°C and 450 bar (Figure 6b), which coincides with the appearance of the lamellar phase in this lipid system: in absence of the lamellar phase, Δa is ~ 1 Å*kbar^{-1}, in presence of the lamellar phase it increases to 5.2 Å*kbar^{-1}. At 85°C, at which no lamellar phase is observed below 1000 bar, the slope of Δa remains close to 1 Å*kbar^{-1}. Such differences may be explained by the partition of two polar headgroups and the apolar molecule squalane between the two phases in coexistence. Indeed, in this lipid mixture we have two lipids with very different curvature. Phospholipids containing PC headgroups present a zero-curvature monolayer and self-assemble in a lamellar phase. DoPhPE easily bends under negative curvatures and therefore induce the formation of inverted non-lamellar phases, such as the H_{II}. Accordingly, when L and H_{II} phases are present, the system may present a "lipid-separation" and DoPhPE may have the tendency to adopt the H_{II} phase with its preferred curvature. When the lamellar phase is present, as at 70°C and pressures above 450 bar, DoPhPE may principally form the H_{II} phase (Figure 6c). This effect was already observed in bacterial-like lipids, which better accommodate in L_β or L_α phases. For example, a decrease in temperature induces domains enriched in saturated phospholipids with small quantities of unsaturated lipids (Baoukina et al., 2012). As DoPhPE has a higher lateral compressibility, H_{II} presents a higher Δa slope when most of DoPhPE is partitioned in the non-lamellar phase and excluded from the L phase. However, the presence of methyls in the hydrocarbon chains could reduce the lateral diffusion of these phospholipids and squalane may aggregate in the chain frustration points and most especially at the interphase points, to fill the voids and release packing tension. The chain-packing frustration increases as the diameter of the hexagonally packed cylindrical inverse micelles increases. When the lamellar phase disappears, the apolar molecule can better distribute along the H_{II} phase and squalane aggregates may disappear (Figure 6c). Therefore, the lattice parameter of the H_{II} phase decreases and consequently its pressure response.

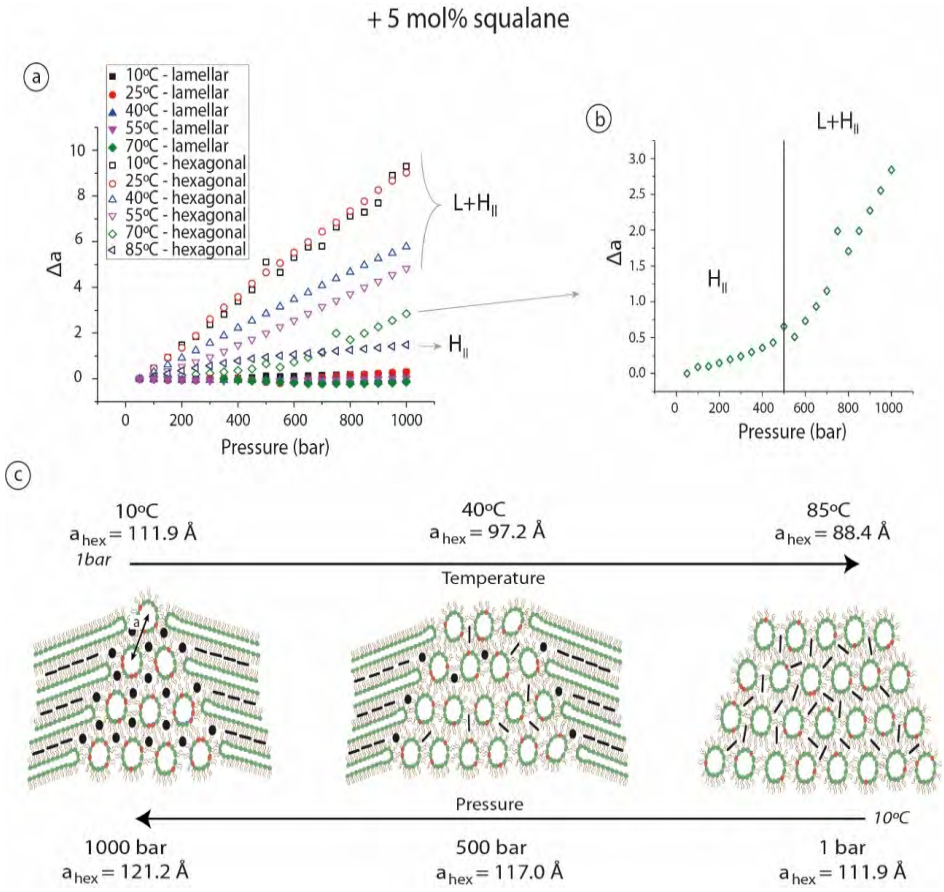

Figure 6. Squalane distribution between lamellar and hexagonal phases. a) *Normalized lattice parameter (Δa) as a function of hydrostatic pressure. The lattice parameter has been normalized to that at ambient pressure for each temperature. L phase (full symbols); H_{II} (empty symbols). Up to 55°C, both, L and H_{II} coexist.* ***b)*** *Detail on Δa as a function of pressure at 70°C.* ***c)*** *Schemes of phase coexistence and lattice parameter evolution as a function of pressure and temperature in the DoPhPC:DoPhPE:5 mol% squalane system. Squalane is represented in black, black spheres represent squalane aggregates, lipid hydrocarbon chains are in brown, lipid headgroups are shown in green (PC) and in red (PE).*

V. Only the inverted hexagonal phase is present when 10 mol% squalane is added

At 10 mol% squalane in the DoPhPC:DoPhPE (9:1) mixture only the H_{II} phase is observed under all temperatures and pressures studied. At ambient pressure, we could detect a slow phase transition between two H_{II} phases. The axially integrated 1-D patterns at 55°C, 70°C and 85°C (Figure 7a) shows the apparition of a H_{II} phase at higher q and the gradual disappearance of the peaks characteristics of the second hexagonal phase. The spectrum at 85°C stills shows shoulders corresponding to the low temperature H_{II} phase. The lattice parameters of H_{II} range from 104.8 ± 0.5 Å at 10°C and 1 bar to 92.8 ± 0.5 Å at 85°C and 1 bar (Figure 7c and Figure S6). As thermal motions increase lipid dynamics, the H_{II} phase is much more pressure sensitive at HT (Figure 7b and 7c). Δa expansion increases from 0.1 Å*kbar^{-1} at 10°C to 3.9 Å*kbar^{-1} at 85°C (Figure 7d). One can notice that the Δa curve as a function of pressure at 40°C presents

2 slopes, consistent with a phase transition between two hexagonal phases. This phase transition also possibly occurs at lower temperature, although very close to 1 bar. Such phase transition is not visible at temperatures above 40°C. These low hexagonal phases differ principally by their ability to swell with pressure, which is congruent with a higher pressure-dependent lateral compressibility of the high temperature hexagonal phase.

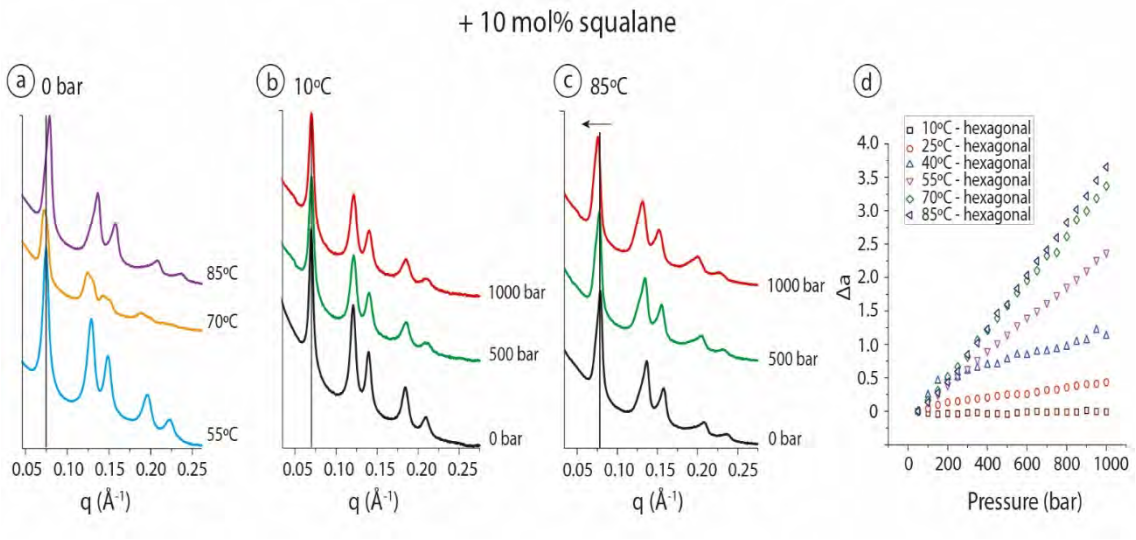

***Figure 7. SAXS spectra of the mixture DoPhPC:DoPhPE + 10 mol% squalane**. **a)** SAXS spectra at ambient pressure for 55°C (blue), 70°C (yellow) and 85°C (magenta). **b-c)** SAXS spectra at 10°C (b) and 85°C (c) of H_{II} phase as a function of pressure. **d)** Normalized lattice parameter of the H_{II} phase as a function of pressure and temperature. Lattice parameter has been normalized to ambient pressure conditions.*

Conclusions

X-ray diffraction experiments clearly show that the addition of squalane drastically changes membrane curvature of a lipid DoPhPC:DoPhPE (9:1) mixture, an effect comparable to that of cholesterol at biological relevant quantities on eukaryote-like lipids (Cheetham et al., 1989; Wang and Quinn, 2002). SAXS data displays the presence of highly stable non-lamellar lipid phases dependent on mol% of squalane, temperature and pressure. The complete understanding of the observed structural transitions will require a deeper study as it will be necessary to consider different kind of interactions, such as lipid-water, lipid-lipid and lipid-squalane. However, the outstanding a_{cubic} values and resistance revealed by the system may be useful for the stabilization or modification of cubosomes and to adjust lipid membrane properties of archaeosomes (Barriga et al., 2019; Benvegnu et al., 2009).

The fact that small quantities of squalane (1 – 10 mol%) are capable to impose negative intrinsic curvatures on the system has biological significance. Our results indicate that archaeal membranes simply require to regulate squalane proportions in the cell membrane to tune its

curvature and flexibility. Accordingly, due to the presence of small amounts of the apolar molecule, archaeal cells would be capable to manage essential cell processes such as fusion and fission (McMahon and Boucrot, 2015). Furthermore, recognizing that squalane is present in archaeal cell membranes and considering the high metastability of all phase transitions in a large range of temperatures and pressures, we can predict that non-lamellar phases and particularly, inverted cubic phases, may be locally present in archaeal membranes.

Conflicts of interest

There are no conflicts to declare.

Acknowledgements

This work was supported by the French National Research Agency programmes ANR 2010 BLAN 1725-04 and ANR 17-CE11-0012-01 to PO and JP and the Royal Society to PO and NB. MSC was supported by a PhD grant from the French Ministry of Research.

Materials and methods

Chemicals

The high purity (>99%) synthetic archaeal lipids 1,2-di-O-phytanyl-*sn*-glycero-3-phosphocholine (DoPhPC) and 1,2-di-O-phytanyl-*sn*-glycero-3-phosphoethanolamine (DoPhPE) were purchased from Avanti Polar Lipids in the lyophilized form and utilized without further purification. 2,6,10,15,19,23-Hexamethyltetracosane (squalane) was bought from Alfa Aesar.

Small angle X-ray scattering

SAXS experiments were performed on beamline I22[24] at the Diamond Light Source (United Kingdom). DoPhPC and DoPhPE were used in a proportion 9:1 molar. Phospholipids with contents of 20% (w/v water) and the adequate quantity of squalane (1%, 2.5%, 5% and 10% molar) were placed inside a pressure chamber[25]. The pressure and temperature dependent experiment was carried out at six different temperatures (10°C, 25°C, 40°C, 55°C, 70°C and 85°C) in pressure jumps of 50 bar from 0 bar to 1000 bar.

The X-ray energy was 17 keV, the momentum transfer is defined as $q= 4\pi*\sin(\Theta)/\lambda$, where 2θ is the scattering angle. The small-angle regime was $0.005 < q < 0.35$ Å-1. The type of phase can be distinguished by the characteristic SAXS peak ratios26: for a lamellar phase they are equidistant, for a hexagonal phase they are: 1, $\sqrt{3}$, 2, $\sqrt{7}$…, for a cubic phase Pn3m they are: $\sqrt{2}$, $\sqrt{3}$, 2, $\sqrt{6}$, $\sqrt{8}$, 3… and for a cubic phase Im3m they are: $\sqrt{2}$,2,$\sqrt{6}$, $\sqrt{8}$, 3... The lattice parameter a is defined as $a_{lam}= 2\pi/q_n$ and $a_{hex}= (2\pi/q_n)*2/3$ for a lamellar and a hexagonal phase, respectively. To determine the lattice parameter for the cubic phase, the experimentally obtained peak position s, where $s= 2*\sin(\Theta)/\lambda = q/2\pi$, is plotted vs $(h^2 + k^2 + l^2)^{1/2}$, where h,k,l are the Miller indices by which the peaks are indexed. The plot should intercept through the origin and be linear with a slope of $1/a_{cubic}$.

Supplementary figures

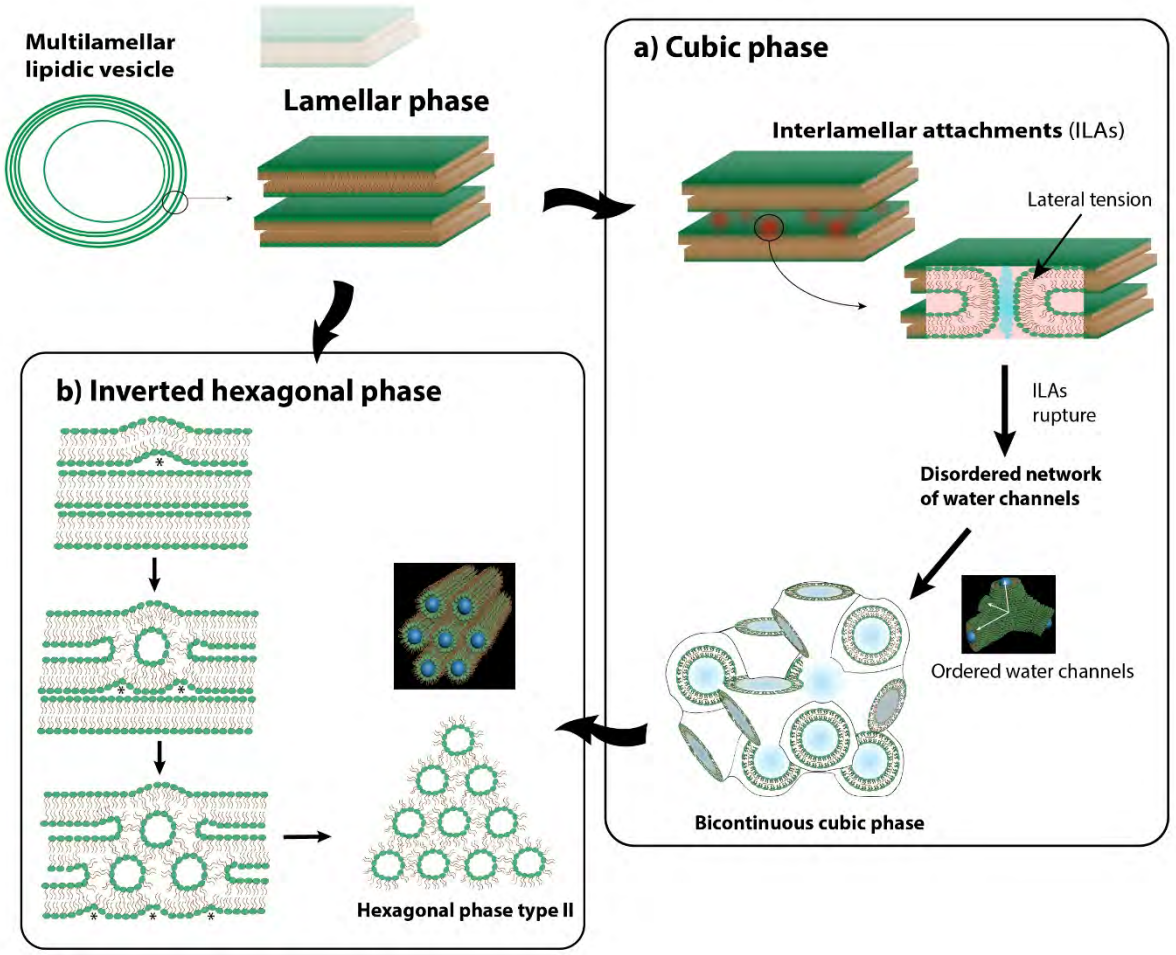

Figure S1. *Schematic representation of the mechanism suggested for the formation of non-lamellar phases. On the one side, the cubic phase is formed after the rupture due to lateral tension of interlamellar attachments (ILAs). On the other side, the inverted hexagonal phase is formed from a cubic phase or from a lamellar phase. In the second case, it begins with a membrane curvature that causes a line tension (*) and to release, lipids self-organize under a cylinder which causes more line tensions and so on. Lipid headgroups and hydrophobic chains are represented in green and brow, respectively.*

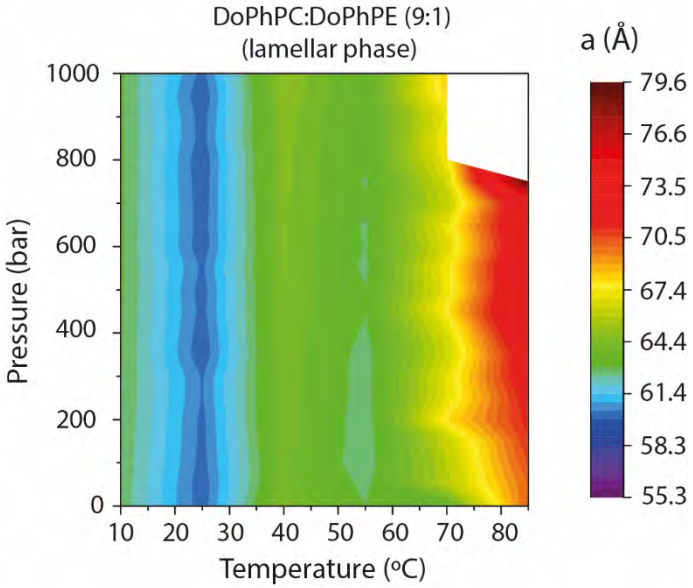

Figure S2. *P,T colour map of lattice parameters for the lamellar phase of DoPhPC:DoPhPE (9:1).*

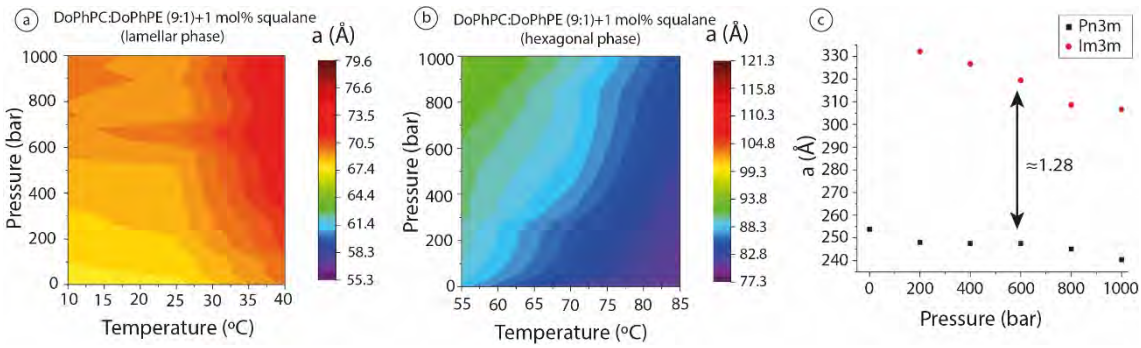

Figure S3. a) *P,T colour map of lattice parameters for the lamellar phase of DoPhPC:DoPhPE (9:1) + 1 mol% squalane.* ***b)*** *P,T colour map of lattice parameters for the inverted hexagonal phase of DoPhPC:DoPhPE (9:1) +1mol%.* ***c)*** *lattice parameters obtained for the cubic phases Pn3m (black) and Im3m (red) found at 85°C for the DoPhPC:DoPhPE (9:1) +1mol% mixture.*

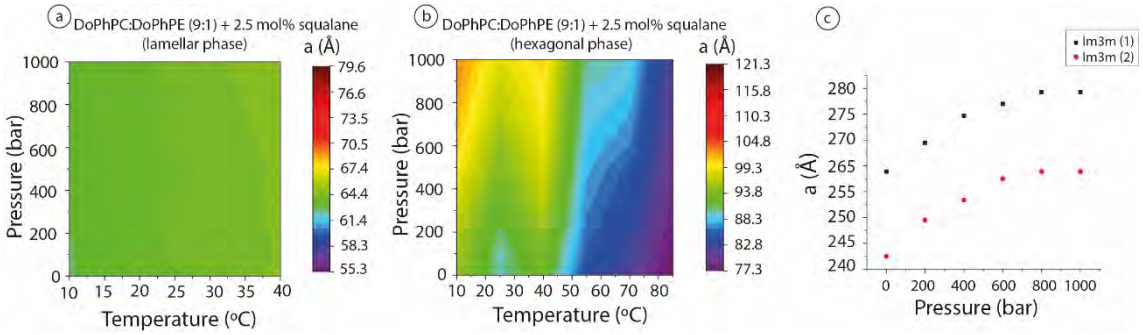

Figure S4. ***a)*** *P,T colour map of lattice parameters for the lamellar phase of DoPhPC:DoPhPE (9:1) + 2.5 mol% squalane.* ***b)*** *P,T colour map of lattice parameters for the inverted hexagonal phase of DoPhPC:DoPhPE (9:1) +2.5 mol%.* ***c)*** *lattice parameters obtained for the cubic phases Im3m (red) found at 85°C for the DoPhPC:DoPhPE (9:1) +2.5 mol% mixture.*

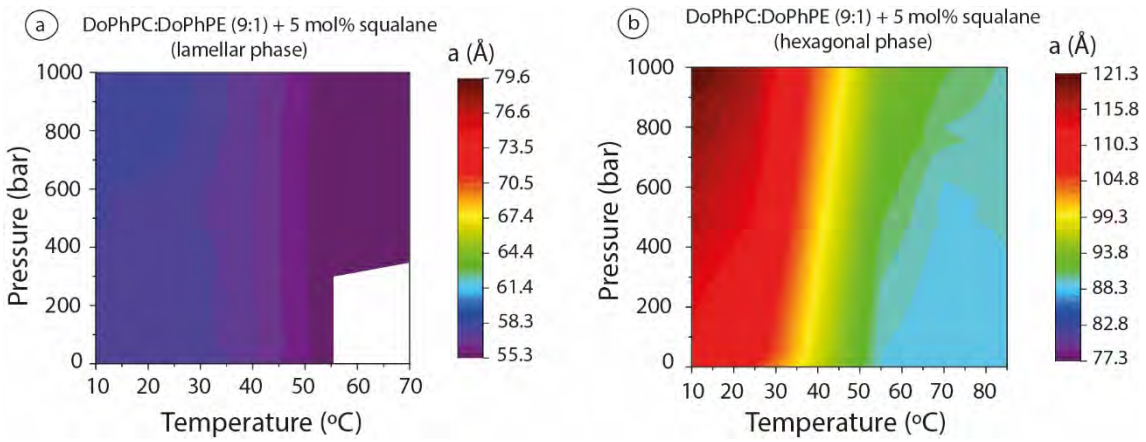

***Figure S5**. **a)** P,T colour map of lattice parameters for the lamellar phase of DoPhPC:DoPhPE (9:1) + 5 mol% squalane. **b)** P,T colour map of lattice parameters for the inverted hexagonal phase of DoPhPC:DoPhPE (9:1) +5 mol%.*

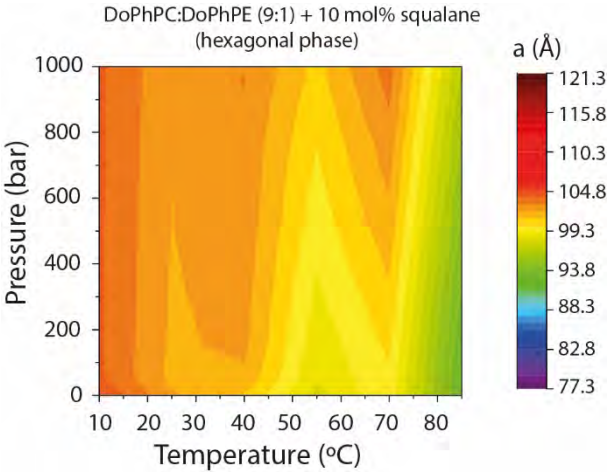

***Figure S6**. P,T colour map of lattice parameters for the inverted hexagonal phase of DoPhPC:DoPhPE (9:1) +10 mol%.*

Article IV. Coexistence of two lipid phases in an archaeal model membrane

Marta Salvador-Castell [1], Bruno Demé [2], Judith Peters [2,3] & Philippe Oger [1]

[1] INSA Lyon, Université de Lyon, CNRS, UMR 5240, F-69621 Villeurbanne, France.

[2] Institut Laue Langevin, F-38000 Grenoble, France.

[3] Université Grenoble Alpes, LiPhy, F-38044 Grenoble, France.

Manuscript in preparation for Biochimica et Biophysica Acta - Biomembranes

Foreword

The lateral arrangement is an essential property of an optimally functional cell membrane. Hence, the purpose of this work was to study the phase separation observed by adding 1 mol% of squalane in the system as a function of squalane concentration in the membrane (Salvador-Castell (3) et al., n.d.). Therefore, I studied the lipid bilayer organisation up to 85 °C of a model archaeal membrane (DoPhPC:DoPhPE) in presence of apolar polyisoprenoid, concentration ranging from 0 to 10 mol. I have determined the position of squalane position for each membrane composition and characterized the different lipid phases by defining their structural parameters. For this, we have used the neutron diffractometer D16 from Institut Laue Langevin.

Using the neutron H/D exchange technique, I stablished that the polyisoprenoid squalane is placed in the midplane of the lipid bilayer, i.e. perpendicular to phytanoyl chains, regardless of its concentration or temperature. However, such localization cannot be extrapolated to all other apolar molecules and, for example, triacontane, a linear hydrocarbon of identical molecular formula than squalane (C30H62), was excluded from the midplane region. The data displayed a clear squalane concentration- and temperature-dependent phase separation. This second phase presents a larger lamellar repeat distance than the original phase. Last, the coexistence of both phases occurs in a highly laterally ordered manner as can be observed by the diffraction patterns obtained from the q_x plan. There is a lateral distance of about 470 ± 20 Å from one phase and its repetition.

The diffraction data suggests that the new membrane architecture presented in this thesis would confer the ability to laterally organize the archaeal cell membrane, opening for the first time the door to the presence of membrane domains in archaeal cells thanks to the presence of apolar polyisoprenoids.

Coexistence of two lipid phases in an archaeal model membrane

Marta Salvador-Castell [1], Bruno Demé [2], Judith Peters [2,3] & Philippe Oger [1]

[1] INSA Lyon, Université de Lyon, CNRS, UMR 5240, F-69621 Villeurbanne, France.

[2] Institut Laue Langevin, F-38000 Grenoble, France.

[3] Université Grenoble Alpes, LiPhy, F-38044 Grenoble, France.

Manuscript in preparation for Biochimica et Biophysica Acta - Biomembranes

Abstract

Cell membranes need to sustain changing and, sometimes, extreme environmental conditions. Microorganisms from the Archaea domain present the most rigid and resistant cell membrane thanks to their particular lipids. Moreover, it has been established that most of Archaea synthesize the methyl-branched molecule squalane, or its unsaturated homologue squalene, which may be part of their cell membrane structure. Using neutron diffraction, we have determined the localization of squalane in an archaeal model membrane and its effect on membrane lateral organization as function of temperature (from 298 K to 358 K). The presence of squalane in the lipid bilayer midplane facilitates lipid phase coexistence. Consequently, such apolar molecule may be useful for archaeal cell membranes to define their lateral organization.

Keywords

Squalane, archaeal model membrane, neutron diffraction, phase coexistence

Introduction

A cell membrane is a dynamic structure composed of proteins and lipids. They are mainly phospholipids which vary in hydrophobic chain length, level of saturation, branching and type of polar head group and hence, display variable properties. Despite this great diversity, a functional cell needs to maintain its membrane under a certain phase that presents specific physicochemical parameters, such as rigidity and permeability. To achieve this, all cells have the capability to control their membranes' lipid composition as function of environmental characteristics, which is named homeoviscous adaptation (Sinensky, 1974). Controlling the composition allows the cell to influence the parameters of its cell membrane and even to provoke the coexistence of two functional lipid bilayer phases (Bagatolli et al., 2010; Cebecauer et al., 2018; Heberle and Feigenson, 2011; Ingólfsson et al., 2014; Schmid, 2017). If lipid phases present not only differences in their bilayer thickness, but also in their physicochemical parameters, such as lipids' dynamics or stiffness, we talk of membrane domains that may present specialized functions, as it is the case of "lipid rafts" in Eukaryotes (George and Wu, 2012; Goñi, 2019; Marquardt et al., 2015; Shaw, 2006). Furthermore, since not all lipids induce the same lipid bilayer curvature, the cell's capacity to control the curvature of specific regions of the cell membrane is highly important, allowing perform essential cellular functions, such as fission or fusion (Frolov et al., 2011; Jarsch et al., 2016; McMahon and Boucrot, 2015). Although coexisting phases in cell membranes may arise in all three domains of life (Kaiser et al., 2009; Strahl and Errington, 2017), i.e. Archaea, Bacteria and Eukarya, their kind of lipids differs.

Archaeal lipids contain unique characteristics relying on a *sn*-glycerol – 1 – phosphate backbone, an enantiomer of the usual bacterial and eukaryal *sn*-glycerol – 3 – phosphate backbone. Besides, and more important from the physical point of view, lipids from Archaea contain ether linkages instead of the familial ester ones and their hydrophobic core is based on isoprenoid units which confer them a methyl-branched structure, very different from the straight acyl chains of bacterial and eukaryal lipids (De Rosa et al., 1986; Gambacorta et al., 1993) (Figure 1).

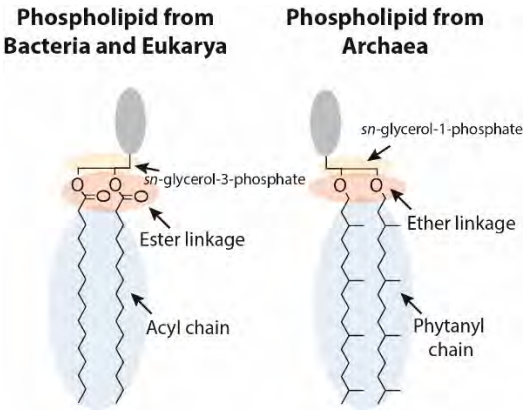

Figure 11. Skeletal representation of phospholipids from Bacteria and Eukarya (left) and from Archaea (right). The arrows indicate the main differences between them.

Lipid phases have been largely studied by many techniques (Ashrafzadeh and Parmryd, 2015; Tyler et al., 2015), as for example, fluorescent methods (Baumgart et al., 2007; McCarthy et al., 2015), atomic force microscopy (Connell and Smith, 2006), molecular dynamic simulations (Laradji and Sunil Kumar, 2005), spin-labelling approaches, such as nuclear magnetic resonance (Schroeter et al., 2017) or electron paramagnetic resonance (Aloi et al., 2017), and scattering procedures, such as neutron reflectivity (de Ghellinck et al., 2015) or neutron diffraction (Ding et al., 2005; Marquardt et al., 2015). Neutron scattering and particularly, neutron diffraction strengths are based on their non-destructive and highly penetrating nature and to their capability to distinguish hydrogen isotopes, i.e. hydrogen (H) and deuterium (D), by their different neutron cross sections (Bée, 1988; Lakey, 2009). Therefore, the studies based on H-D contrast are numerous (Dante et al., 2002; Harroun et al., 2008; Hauß et al., 2005, 2002; Kessner et al., 2008; Luchini et al., 2018; Mojumdar et al., 2013). All these techniques have provided a lot of information about eukaryal-like lipids: from their rigidity or permeability to the coexistence of domains and their lateral organization. Nevertheless, information about archaeal-like lipids remain elusive.

It is known that the extraordinary hydrophobic core of archaeal lipids provides to these cells a more rigid and less permeable cell membrane (Shinoda et al., 2004b), which could partially explain the facility of such microorganisms to live under extreme conditions, such as high temperatures above 358 K and high hydrostatic pressures above 40 MPa. Moreover, apolar molecules like squalane have been presented as putative membrane regulators capable to modify physicochemical properties of archaeal cell membranes (Salvador-Castell et al., 2019b).

Recently, we have demonstrated that low concentrations of squalane, i.e. 1 mol%, reside on the midplane of the lipid bilayer, parallel to the membrane plane, and it is capable to change the physicochemical properties of the archaeal model membrane (Salvador-Castell

(3) et al., n.d.). However, squalane proportions in cells vary between species, but also due to the homeoviscous adaptation (Cario et al., 2015; Clejan et al., 1986). For example, the hyperthermophile and piezophile archaeon *Thermococcus barophilus* contains 1-2 % of squalane (Cario et al., 2015), while bacteria from the strain Bacillus have up to 10-11 % (Clejan et al., 1986). Accordingly, it is important to examine the localization of the apolar molecule inside the lipid bilayer as a function of concentration and its impact on lateral organization at similar native conditions of temperature.

By neutron diffraction, we have now studied a multistack of ordered archaeal-like lipid bilayers on a substrate. The lipids used to model an archaeal membrane were 1,2-di-O-phytanyl-*sn*-glycero-3-phosphocholine (DoPhPC) and 1,2-di-O-phytanyl-*sn*-glycero-3-phosphoethanolamine (DoPhPE) in a ratio of nine to one molar and the addition of different fractions of squalane hydrogenated and squalane deuterated: 1 mol%, 2.5 mol%, 5 mol% and 10 mol%. In the present study, we have determined the localization of squalane, the structural parameters of each system and its lamellar organization from 298 K to 358 K, the native temperature of many Archaea, as a function of the fraction of squalane.

Results and discussion

I. Location of squalane in an archaeal model membrane

The multilayer nature of the sample causes the emergence of Bragg peaks from which it is easy to directly obtain the membrane repeat distance (d), which includes the thickness of the lipid bilayer and its surrounding water layer. Furthermore, the analysis of Bragg peaks allows to obtain the neutron scattering length density (NSLD) profile which depends on the type and number of atomic nuclei in the membrane depth from the surface normal. For convenience, 0 Å represents the midplane of the lipid bilayer. It is important to take into consideration that the quality of NSLD profile depends on the number and intensities of diffraction orders. Here our samples diffracted up to four Bragg peaks (Figure S1). Samples with deuterated squalane present a more intense third order Bragg peak than the samples with hydrogenated squalane (Figure S1). As D isotope has a higher coherent cross section than H (5.6 barn vs 1.8 barn, respectively) (Bée, 1988), the presence of deuterated squalane in the lipid bilayer changes Bragg peaks intensities and hence modifies the NSLD profile.

The NSLD profile of lipid bilayers presents two characteristic maxima attributable to the glycerol backbone of lipids and a minimum intensity that corresponds to the methyl terminals of the lipid chains. The difference of H-D neutron cross sections in neutron diffraction allow us to situate squalane in the midplane of the lipid bilayer (Figure 2). The NSLD

of a sample with h-squalane and another with d-squalane overlaps except for the region from -10 Å to 10 Å, which corresponds to the bilayer midplane. In this bilayer depth, samples with d-squalane present an increase on intensity due to the higher neutron cross section of D. The same difference is observed for all the studied H-D pairs. We could determine, that squalane up to 10 mol% is sitting in the bilayer midplane, parallel to the membrane surface.

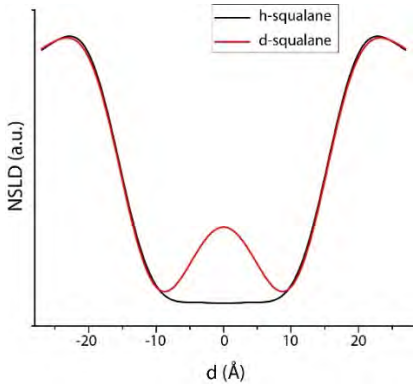

Figure 12. Neutron scattering length density profile of DoPhPC : DoPhPE (9:1) + 5% hydrogenated (black) and deuterated squalane (red). The contrast was 50 %D_2O.

From NSLD profiles, it is also possible to extract the structural parameters of a lipid bilayer (Nagle and Tristram-Nagle, 2000): the lipid bilayer thickness (d_B), the thickness of the bilayer hydrocarbon core ($2d_c$) and the thickness of the water layers between lipid bilayers (d_w) (Table 1). Previously, it was observed that the presence of just 1 mol% squalane was capable to increase the hydrophobic core thickness of the lipid bilayer by populating its midplane (32.2 ± 0.2 Å and 35.0 ± 0.2, respectively) (Salvador-Castell (3) et al., n.d.). In this study, we confirm that such tendency is maintained up to 10 mol% of squalane added into the system (Table 1).

Table 3. Structural parameters of the lipid bilayer in absence (DoPhPC: DoPhPE (9:1)) and in presence of different percentages of squalane measured at full hydration of 8 %D_2O and 298 K. The values from the first two columns were extracted from (Salvador-Castell (3) et al., n.d.).

	DoPhPC :DoPhPE (9 : 1)	**+ 1 mol% squalane**	**+ 2.5 mol% squalane**	**+ 5 mol% squalane**	**+ 10 mol% squalane**
d	51.0 ± 0.1	52.8 ± 0.1	53.7 ± 0.1	56.6 ± 0.1	54.5 ± 0.2
d_B	38.4 ± 0.1	41.8 ± 0.1	43.0 ± 0.1	46.8 ± 0.1	44.1 ± 0.3
$2d_c$	32.2 ± 0.2	35.0 ± 0.2	36.3 ± 0.2	39.2 ± 0.2	36.9 ± 0.5
d_w	12.6 ± 0.1	11.1 ± 0.1	10.7 ± 0.1	9.8 ± 0.1	10.5 ± 0.2

We can observe that the bilayer thickness increases by adding squalane in the lipid bilayer (e.g. from 51.0 ± 0.1 Å in absence to 56.6 ± 0.1 Å in presence of 5 mol% squalane) due to the increase of the hydrophobic core thickness (e.g. from 32.2 ± 0.2 Å in absence to 39.2 ± 0.2 Å in presence of 5 mol% squalane) (Table 1). However, such tendency is no longer observed

when 10 mol% squalane is added. We think that the change of trend resulted from our lipid system reaching saturation between 5 mol% and 10 mol% squalane. This is in concordance with the observation that the maximum percentage of squalene inserted in a 1,2-dioleoyl-*sn*-glycero-3-phosphoethanolamine bilayer is of about 5 % (Turner and Gruner, 1992). The presence of squalane in the midplane has a great impact on the bilayer physicochemistry. For example, it slightly increases water permeability and decreases proton permeability of the membrane (Salvador-Castell (6) et al., n.d.), which could be beneficial for microorganisms living under extreme pH contrasts.

Although here we demonstrate the localization of squalane into the midplane of an archaeal-type lipid bilayer, such position cannot be extrapolated for all the apolar molecules. For example, triacontane, a non-branched apolar molecule with the same molecular formula as squalane, is excluded from the bilayer midplane of DoPhPC:DoPhPE (Figure S2). Accordingly, it seems that the methyl-branched structure is essential to allow the insertion of a long apolar molecule in the bilayer midplane of an archaeal-like bilayer. The isoprenoid structure of squalane probably confers higher rigidity to the molecule compared to triacontane, which may be too flexible to be easily inserted in the lipid bilayer. In the same vein, McIntosh et al. have suggested that triacontane can probably not be inserted perpendicular to acyl chains and only smaller non-branched apolar molecules, such as hexane and octane, are located into the bilayer midplane (McIntosh et al., 1980).

II. Effect of temperature on lateral organization of an archaeal model membrane in presence of squalane

Temperature scan from 298 K to 358 K revealed the appearance of a new lipid phase at high temperatures (Ph_{HT}). Such new phase is diffracted at lower q values and therefore has a higher d-spacing in comparison onto the phase already present at low temperatures (Ph_{LT}) (Table 2 and 3). For instance, at 358 K and in absence of squalane, Ph_{HT}, which is found exclusively at high temperatures, and Ph_{LT} which is also present at lower temperatures, have a lamellar repeat distance of 62.2 ± 0.4 Å and 54.4 ± 0.4 Å, respectively. Such phase separation appeared at 343 K and it constitutes a steady coexistence of two lamellar phases. Probably, high temperatures provoke undulations on the lipid bilayers due to thermal energy, thereby diminishing the line tension between phases frontiers (Baumgart et al., 2003). The reduced line tension would allow the steady coexistence of two phases that otherwise might be a mixture due to line tensions' constraints.

Table 4. Lamellar d-spacing of the lipid bilayer Ph_{LT} in absence (DoPhPC: DoPhPE (9:1)) and in presence of different percentages of squalane measured under different temperatures at 100 % D_2O. The standard deviation is ± 0.4 Å. ;

Ph_{LT}	**298 K**	**313 K**	**328 K**	**343 K**	**358 K**
DoPhPC:DoPhPE (9:1)	52.6 Å	53.0 Å	53.1 Å	53.0 Å	54.4 Å
+ 1 mol% squalane	55.3 Å	55.4 Å	55.2 Å	54.5 Å	55.1 Å
+ 2.5 mol% squalane	52.8 Å	53.0 Å	52.8 Å	52.8 Å	53.2 Å
+ 5 mol% squalane	54.2 Å	54.2 Å	54.2 Å	54.3 Å	N.P.
+ 10 mol% squalane	53.7 ± 0.4 Å	54.6 ± 0.4 Å	54.9 ± 0.4 Å	55.8 ± 0.4 Å	N.P.

Table 5. Lamellar d-spacing of the lipid bilayer Ph_{HT} in absence (DoPhPC: DoPhPE (9:1)) and in presence of different percentages of squalane measured under different temperatures at 100 % D_2O. N.P.: non-present; N.D.: non-determined. The standard deviation is ± 0.5 Å.

Ph_{HT}	**298 K**		**313 K**		**328 K**		**343 K**		**358 K**	
DoPhPC:DoPhPE (9:1)	N.P.		N.P.		N.P.		64.0 Å		62.9 Å	
+ 1 mol% squalane	N.P.		N.P.		N.P.		80.3 Å		73.5 Å	
+ 2.5 mol% squalane	74.1 Å		73.0 Å		72.5 Å		67.5 Å		65.3 Å	
+ 5 mol% squalane	80.4 Å	70.6 Å	77.9 Å	71.7 Å	76.9 Å	71.3 Å	73.6 Å	69.7 Å	73.6 Å	74.1 Å
+ 10 mol% squalane	51.2 Å		52.2 Å		60.9 Å		63.0 Å		66.5 Å	

The appearance of Ph_{HT} is also induced by the presence of the apolar molecule in the system. For example, for the sample containing 2.5 mol% or 5 mol%, Ph_{HT} appears already at 298 K (Figure 3). The appearance of the new phase at lower temperatures when adding squalane means that such apolar molecule destabilize Ph_{LT} and favoured Ph_{HT}. The specific localization of squalane in the midplane of the lipid bilayer may reduce the line tension between both phases, as it already does by packing frustration (Lohner et al., 1993), allowing their coexistence even at low temperatures.

Ph_{HT} is broader than Ph_{LT}, which indicate a reduced capability to organize under lipid bilayers' multistacks. Indeed, for 5 mol% squalane, the Bragg peaks from Ph_{HT} can be fitted by two gaussians (Figure S3). This is a hint for inhomogeneities in the phase and two different

membrane repeat distance. Two lamellar phases that coexist form a continuous columnar arrangement across hundreds of lipid bilayers (Tayebi et al., 2012). The presence of stacked domains caused that the thickness and the diameter of the phase slightly to increase with the number of stacked bilayers, and this can explain the broad peaks that presents Ph_{HT} (Figure 3).

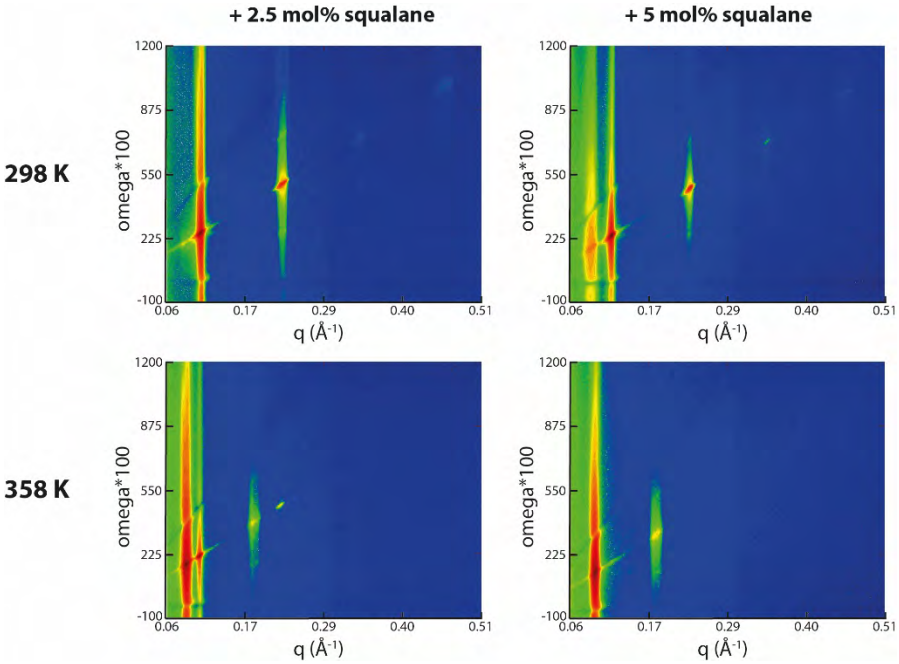

Figure 13. 2D neutron diffractograms of DoPhPC:DoPhPE (9:1) bilayer containing 2.5 mol% (left) and 5 mol% (right) squalane at 298 K (above) and 358 K (bottom). The samples were hydrated with 100 %D_2O. We can clearly see how a new phase is induced by high temperature and high percentages of squalane until it is the only present for the sample with highest content of squalane at 358 K.

The presence of squalane in the lipid bilayer causes very peculiar diffraction patterns as observed in Figure 4a. Such diffraction is present for different samples: 2.5 mol% squalane, 5 mol% and 10 mol% squalane and different temperatures: 328 K, 343 K and back to 298 K. Nevertheless, in all cases, the coexistence of the two phases Ph_{LT} and Ph_{HT} is necessary. The diffraction pattern reveals diverse Bragg peaks presenting up to two diffraction orders out of the q_z plane. These diffraction signals are in the q_x plane and indicate a highly repeated structure through q_x. From the two Bragg peaks arising at q_x, it is possible to extract the repeat spacing in the x-plane (d_x) (Figure 4b), which depends on the quantity of squalane and on the temperature (Table 4). For instance, the sample containing 10 mol% showed a phase separation of 470 ± 20 Å. The organization in the q_x plane is highly stable since the lateral organization was still present 48 h after the temperature scan. Moreover, it seems that the diffraction arises from the first order of Ph_{LT} at an angle θ ~ 10°. We suggest that the angle θ is due to the tilting of Ph_{LT}, since it has already been observed that domains may tilt by an angle depending on their elastic properties and size(Ursell et al., 2009).

Lipid organization on q_x axis has been commonly observed in ripple phases, a lipid phase that appears between the gel and the fluid lipid phases and it is highly characterized by undulations of the lipid bilayer(Katsaras et al., 2000; Lenz and Schmid, 2007; Sengupta et al., 2003; Sun et al., 1996). Nevertheless, this type of organization presents a constant d-spacing and not a coexistence of two phases, as illustrated here.

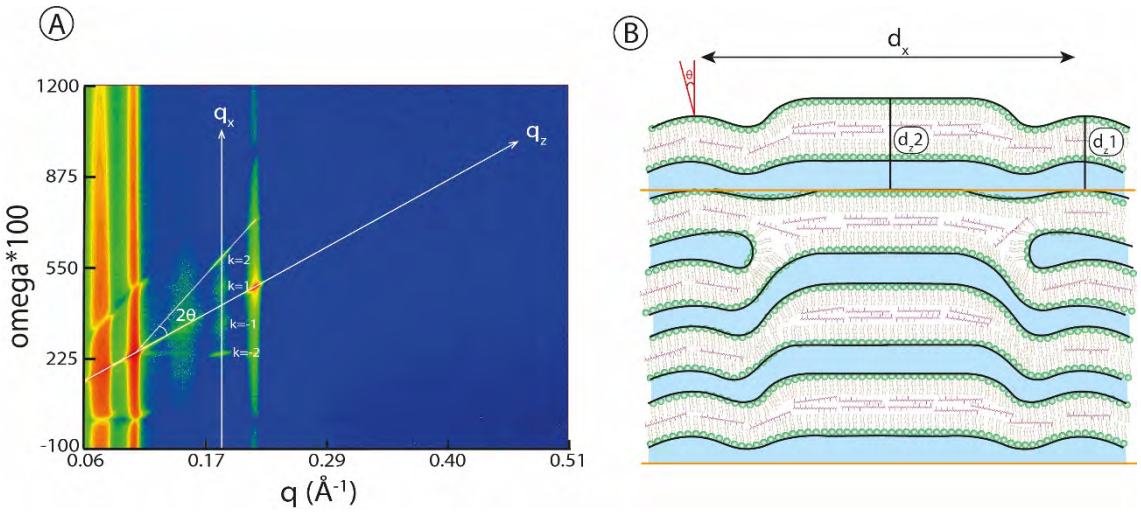

Figure 14. ***A)*** *2D neutron diffractogram patterns of DoPhPC:DoPhPE (9:1) + 10 mol% squalane at 328K. It shows diffraction peaks on two different planes.* ***B)*** *Schematic representation of the 2D diffraction patterns from A. There is a coexistence of two lipid phases on the q_z plane (d_z1 and d_z2), one of them tilted by an angle ϑ and separated by a d_x distance. Lipid headgroups are represented in green, lipid phytanyl chains in brown and squalane molecules in magenta, water regions are represented in blue. The two lines in orange defines an organization that would be repeated along d_z.*

Table 6. Distance of the repeated structure along the qz axis in absence (DoPhPC: DoPhPE (9:1)) and in presence of different percentages of squalane measured under different temperatures at 100 % D_2O. N.P.: non-present. The standard error is ± 20 Å.

d_x	298 K	313 K	328 K	343 K	358 K
DoPhPC:DoPhPE (9:1)	N.P.	N.P.	N.P.	N.P.	N.P.
+ 1 mol% squalane	N.P.	N.P.	N.P.	N.P.	N.P.
+ 2.5 mol% squalane	N.P.	N.P.	250 Å	475 Å	N.P.
+ 5 mol% squalane	N.P.	520 Å	520 Å	N.P.	N.P.
+ 10 mol% squalane	N.P.	N.P.	470 Å	470 Å	N.P.

We propose that the new phase Ph_{HT} is due to the presence of compounds of different curvature. On the one hand, there is the difference in headgroup between DoPhPC and DoPhPE. DoPhPE comprise a small headgroup (-NH_3) which confers a conical shape to this phospholipid which thus tends to adopt a negative curvature, i.e. lipid headgroups approach among each other (Israelachvili et al., 1976; Jarsch et al., 2016; McMahon and Boucrot, 2015). Moreover, such lipid negative curvatures are promoted by high temperatures (Klacsová et al.,

2016). Once the system reaches a critical temperature, the curvatures from both lipids are so different that they segregate inducing the phase separation. All this could explain the small phase separation observed at 343 K for the sample composed by DoPhPC : DoPhPE (9:1). Furthermore, it has recently been presented that squalane possesses a tremendous capability to modulate membrane bending and induce negative curvature to it (Salvador-Castell (4) et al., n.d.). This may explain why phase separation appears at lower temperatures under the presence of squalane: it increases the negative curvature of the membrane and consequently, induces the difference in curvature. Hence, squalane has the capability to laterally organize in a stable manner the lipid membrane. Lateral organization provided by collective aggregation of lipids is essential for cell membranes. The presence of lipid domains of divergent compositions induces the possibility to accommodate proteins with different lipid affinity or requirement, and thus creates the necessary environment for functional heterogeneities in the membrane (Lenne and Nicolas, 2009). Hence, our study demonstrates the ability of apolar polyisoprenoids to induce functional compartmentalization in Archaea. causes functional heterogeneities on lipid bilayers (Risselada, 2017).

Conclusions

The use of neutron diffraction and H-D contrast demonstrated that the methyl-branched apolar molecule squalane is placed in the midplane of the lipid bilayer, parallel to its membrane surface at concentrations from 1 mol% to 10 mol%. This indicates that the novel membrane architecture presented initially for Thermococcales (Cario et al., 2015) would be indeed spread among Archaea domain, including microorganisms containing high quantities of apolar polyisoprenoids.

Furthermore, we have shown that squalane promotes lipid phase separation and a specific and unique lateral organization. Such essential characteristic is polyisoprenoid concentration-dependent. Consequently, Archaea would be able to easily control the lateral heterogeneity of the cell membrane by just modulating the quantity of apolar polyisoprenoids. This indicates that indeed, these apolar molecules could be part of the membrane homeoviscous adaptation in Archaea. Hence, the quantity of apolar lipids could govern the formation of membrane domains with specialized functions, depending on environmental conditions and cell necessities.

As demonstrated here, non-polar polyisoprenoids reside in the midplane of the membrane, which would ease the control of their effects on the cell membrane, such as the lateral organization. Both the location invariance depending on squalane quantity and its

capability to induce lateral organization confirms the potential role of squalane as archaeal membrane regulator.

Acknowledgments

The authors thank the Institut Laue Langevin for the allocation of beamtime (DOI: 10.5291/ILL-DATA.8-02-809). This work was supported by the French National Research Agency programmes ANR 2010 BLAN 1725-04 and ANR 17-CE11-0012-01 to PO and JP. MSC was supported by a PhD grant from the French Ministry of Research.

Materials and methods

Chemicals

1,2-di-O-phytanyl-*sn*-glycero-3-phosphocholine (DoPhPC) and 1,2-di-O-phytanyl-*sn*-glycero-3-phosphoethanolamine (DoPhPE) are both synthetic ether glycerophospholipids, bought from Avanti Polar Lipids (Alabaster, USA) in the lyophilized form and utilized without further purification. Purity guaranteed was > 99%. 2,6,10,15,19,23-Hexamethyltetracosane (squalane) and triacontane were bought from Sigma – Aldrich Co (Montana, USA).

Sample preparation

3 mg of DoPhPC:DoPhPE (9:1 molar) and the correspondent quantity of the apolar molecule in chloroform: methanol (2:1) were spread on a silicon wafer by the "rock and roll" method and dried overnight under high vacuum (Tristram-Nagle, 2007). Thereafter, the sample was hermetically enclosed inside an aluminium sample holder which contained 100 µl of the corresponding D_2O percentage. Finally, the sample holder was left at 50°C for 48h to allow full hydration of lipid bilayers.

Neutron diffraction

Neutron diffraction experiments were performed on the D16 small momentum transfer diffractometer (Cristiglio et al., 2015) at the Institut Laue Langevin (France) using the incident wavelength $\lambda = 4.52$ Å by a 2Θ scan. The accessible q-range was from 0.06 $Å^{-1}$ to 0.51 $Å^{-1}$. The sample holder was placed in a cryostat to precisely control its temperature. The diffraction patterns detected up to fourth order of the Bragg diffraction of the neutrons scattered by the multistack of lipid bilayers. The data is available at DOI:10.5291/ILL-DATA.8-02-809 (Salvador-Castell et al., 2018a).

Data treatment was performed by LAMP (Richard et al., 1996) and OriginPro (OriginPro, Version 2016. OriginLab Corporation, Northampton, MA, USA.). To consider the efficiency of the detector, a calibration file was loaded before any treatment. The calibration file consists in a measurement of H_2O scattering. The background, obtained by measuring an empty sample holder two times as long as the samples, was subtracted from sample diffractograms. The integrated intensities of the Bragg peaks were corrected according to the absorption and analysed by a Gaussian function, which can be used in this case as a suitable model for describing the shape of the reflection. The angle θ of a Bragg peak is related to the scattering vector q by Eq. (1):

$$q = \frac{4\pi\, sin(\theta)}{\lambda}, \quad (1)$$

where λ is the wavelength. The lamellar d-spacing d, representing the thickness of the lipid bilayer together with its water layer, was calculated from the q difference between the two first Bragg orders according to Eq. (2):

$$d = \frac{2\pi}{q_2 - q_1} \quad (2)$$

The sum of neutron scattering lengths per unit volume is known as neutron scattering length density (NSLD) profile (Bée, 1988; Marquardt et al., 2015). The NSLD can be calculated as a discrete set of Fourier coefficients f_n according to the Eq. (3) (Katsaras, 1995):

$$\rho_{bilayer}(z) = \frac{2}{d}\sum_{n=1}^{M} f_n\, v_n\, cos(\frac{2n\pi}{d} z) \quad (3)$$

where coefficients f_n can be found due to the formula $I_n = \frac{|f_n|^2}{Q_z}$, here, Q_z^{-1} is a Lorentz factor which corresponds to the q position of the Bragg peak for oriented bilayers and I_n is the integrated intensity of the *n*-th Bragg peak; d is the lamellar spacing of the bilayers in the z direction perpendicular to the lipid bilayer; $z \in \left[-\frac{d}{2}; \frac{d}{2}\right]$. In order to determine the phases of the structure factors, it is possible to use the linear correlation of the structure factor amplitudes and sample D_2O content (Worcester and Franks, 1976). Therefore, each type of squalane sample was measured at three different D_2O/H_2O contrasts: 8 %D_2O, 50 %D_2O and 100 %D_2O.

Supplementary figures

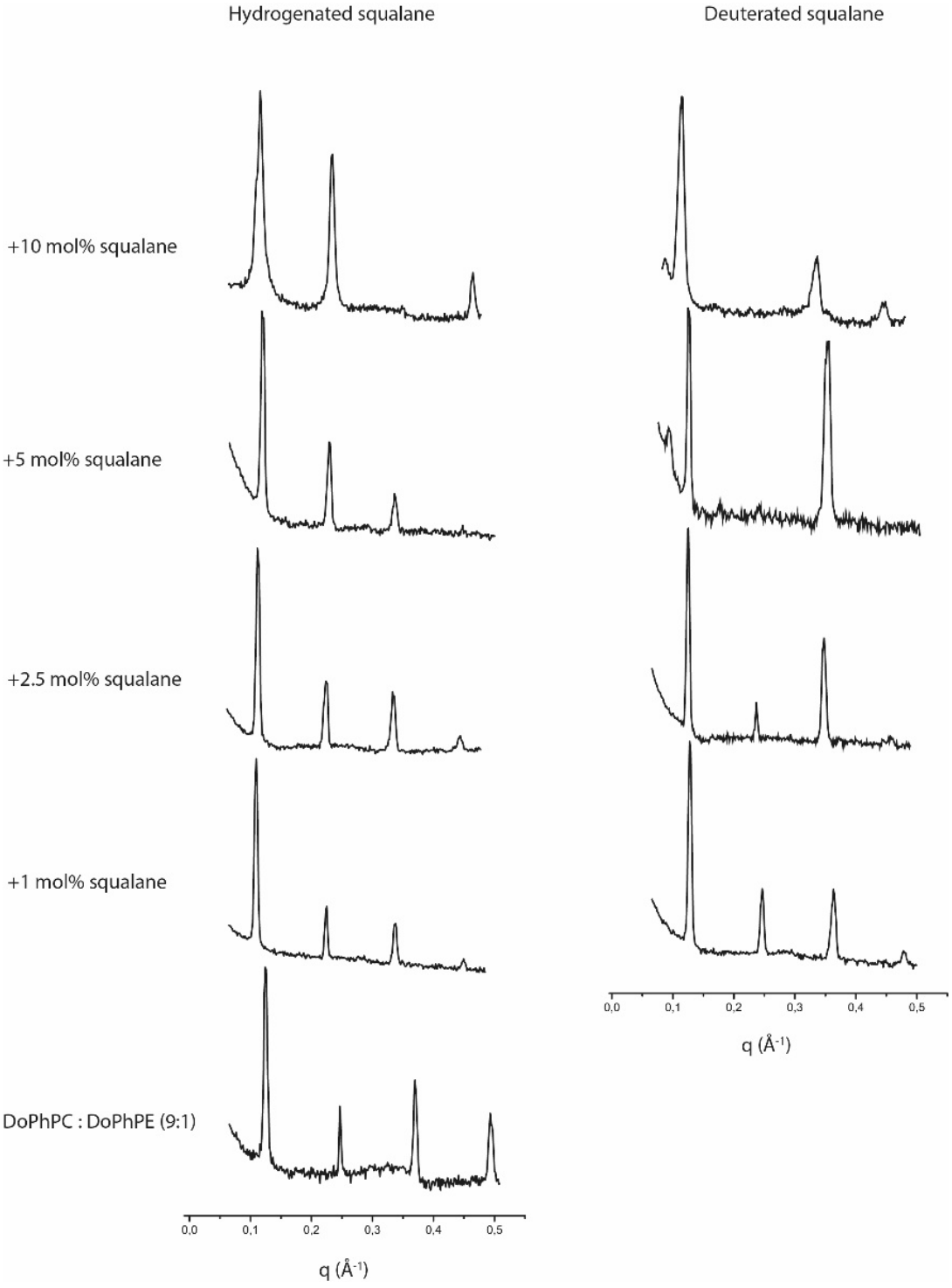

Figure S1. Intensity (a.u.) vs q plot of DoPhPC:DoPhPE (9:1) in absence and in presence of hydrogenated (left) and deuterated squalane under 8 %D_2O of contrast and 298 K.

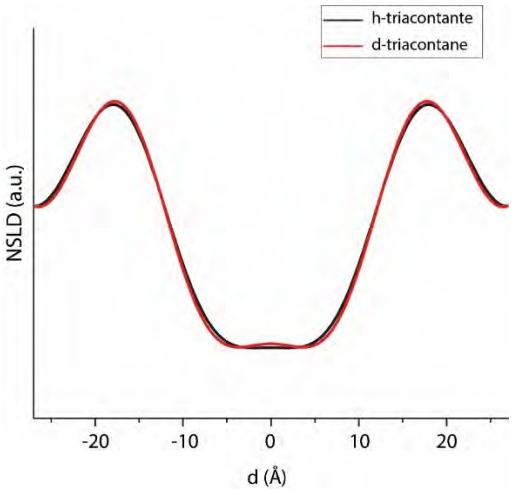

Figure S2. Neutron scattering length density profile of DoPhPC:DoPhPE (9:1) and 5 mol% hydrogenated (black) and deuterated (red) triacontane at 298 K, complete humidity at 8 %D_2O.

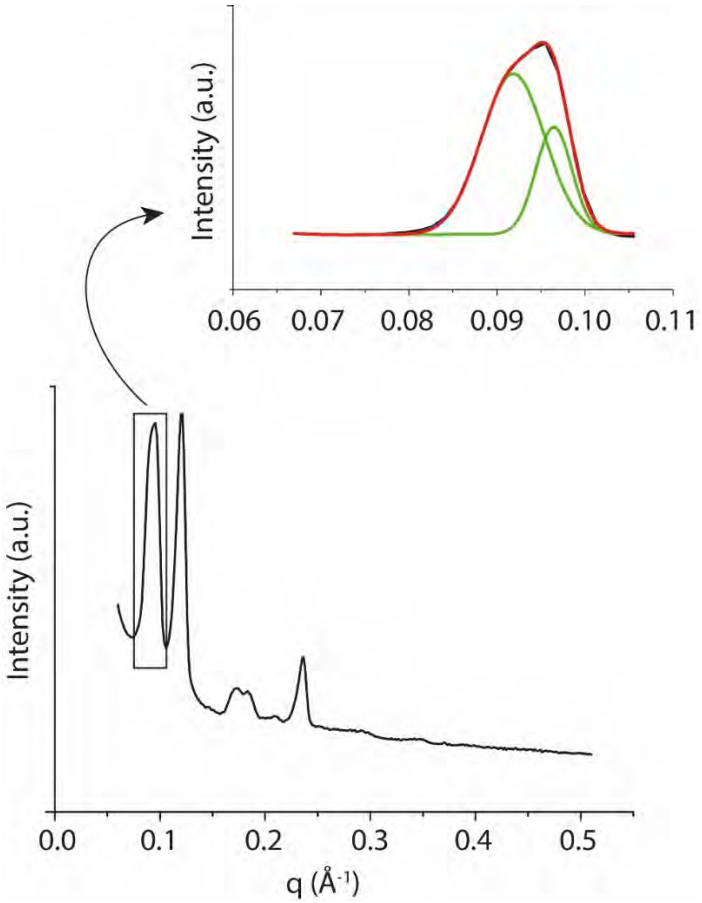

Figure S3. Intensity vs q plot of neutron diffraction from DoPhPC:DoPhPE (9:1) with 5 mol% squalane at 328 K. The region from the first Bragg peak is zoom in and it is fitted (red curve) with two Gaussians (green curves).

Article V. Non-polar molecule as regulator of archaeal lipid bilayer properties

Marta Salvador-Castell [1], Nicholas J. Brooks [2], Roland Winter [3], Judith Peters [4,5] &

Philippe Oger[1]

[1] INSA Lyon, Université de Lyon, CNRS, UMR 5240, F-69621 Villeurbanne, France.

[2] Imperial College London, South Kensington Campus, London SW7 2AZ, England.

[3] Technnische Universität Dortmund, 44227 Dortmund, Germany.

[4] Université Grenoble Alpes, LiPhy, F-38044 Grenoble, France.

[5] Institut Laue Langevin, F-38000 Grenoble, France.

Manuscript in preparation for Soft matter

Foreword

In this chapter, I have demonstrated that the apolar lipid squalane is able to modify the curvature and promote a lipid phase coexistence in a concentration-dependent manner. Nevertheless, to confirm the putative role of apolar polyisoprenoids as membrane regulators, it remained necessary to determine the impact of squalane on other physicochemical parameters of the archaeal model membrane (DoPhPC:DoPhPE). Noticeably, the hypothesis implies that the presence of squalane in the midplane of the membrane should modify its permeability and fluidity. Therefore, this article presents the results of a study of the effect of squalane on the permeability and fluidity of the archaeal lipid bilayer under extreme conditions. For this purpose, I followed different fluorescent approaches: CF efflux, Pyranine intensity and Laurdan GP.

The results presented here show that the presence of squalane in the archaeal lipid bilayer impacts water permeability leading to an increase of water permeability at HT, quantified by CF efflux, and proton permeability leading to a decrease of protons permeability at HHP, as seen by monitoring Pyranine fluorescence intensity. Last, only the sample with the highest percentage of squalane, i.e. 10 mol%, exhibits a significantly different behaviour which was attributed to a slightly higher membrane fluidity.

All these results finish to demonstrate the anticipated membrane properties of the membrane model proposed by Cario et al. (2015), noticeably with regards to improved stability at HHP and HT, and improved physicochemical parameters. The fact that squalane,

even at low concentrations, alters membrane permeability can be of particular interest for the cell. For example, the decrease of proton permeability would allow the cell to easily maintain proton gradients, and hence increase the energetic efficiency of the respiratory chains and the synthesis of ATP. On the other side, the increased water permeability could be useful for archaeal cells as an adaptation tool, in response to osmotic stress. Interestingly, the modulation of membrane parameters by the regulation of the proportion of intra-membrane squalane appears energetically favourable in comparison to *de novo* phospholipid synthesis, which fits the extreme lifestyle of Archaea.

Non-polar molecule as regulator of archaeal lipid bilayer properties

Marta Salvador-Castell [1], Nicholas J. Brooks [2], Roland Winter [3], Judith Peters [4,5] &

Philippe Oger[1]

[1] INSA Lyon, Université de Lyon, CNRS, UMR 5240, F-69621 Villeurbanne, France.

[2] Imperial College London, South Kensington Campus, London SW7 2AZ, England.

[3] Technnische Universität Dortmund, 44227 Dortmund, Germany.

[4] Université Grenoble Alpes, LiPhy, F-38044 Grenoble, France.

[5] Institut Laue Langevin, F-38000 Grenoble, France.

Manuscript in preparation for Soft matter

Abstract

The modification of archaeal lipid bilayer properties by the apolar molecule squalane may support cell membrane adaptation to specific environmental conditions of temperature and hydrostatic pressure. This work reports squalane effects on permeability and fluidity of model membranes composed by archaeal lipids. We have measured Carboxyfluorescein efflux, proton permeability using Pyranine fluorescence intensity and Laurdan generalized polarization from liposomes under high temperature and high hydrostatic pressure conditions. Even low concentrations of squalane (1 mol%) are capable to enhance solute permeation by increasing membrane fluidity, but at the same time, decreasing proton permeability of the lipid bilayer. Such effects favour indeed viability under extreme conditions and demonstrate that apolar polyisoprenoids are membrane regulators in Archaea.

Keywords

Polyisoprenoids, squalane, archaea, cell membrane, permeability, fluorescence

Introduction

Archaeal membranes are composed by phospholipids with unique structures to keep plasma barriers functional under their habitual living extreme conditions. The structure of archaeal lipids is based on phospholipids with condensed isoprenoid hydrocarbon chains via ether bonds to a *sn*-2,3-glycerol phosphate backbone (Langworthy et al., 1982) (Figure 1). Furthermore, archaea may contain lipids with two polar heads, which can form a lipid monolayer (De Rosa et al., 1983; Langworthy et al., 1982) and are much more rigid and tightly packed (Chong, 2010; Gliozzi et al., 2002; Komatsu and Chong, 1998), instead of the conventional lipid bilayer. The exceptional features of archaeal lipids have promoted research on such membranes. Interestingly, new molecules, such as squalene, have been associated to membranes of archaeon adapted to live under high temperature and high hydrostatic pressure conditions (*ca*. 400 bar) (Cario et al., 2015; Salvador-Castell et al., 2019b). Squalene and its completely saturated form squalane are apolar molecules composed by six isoprenoids units (Figure 1) which are placed in the bilayer midplane, perpendicular to lipids (Hauß et al., 2002; Salvador-Castell (3) et al., n.d.).

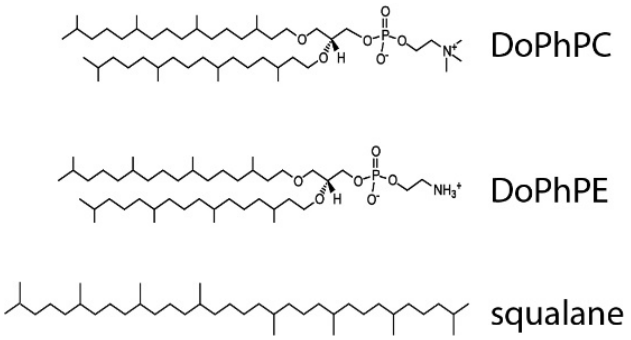

Figure 15. Skeletal formula of the archaeal lipids 1,2-di-O-phytanyl-sn-glycero-3-phosphocholine (DoPhPC), 1,2-di-O-phytanyl-sn-glycero-3-phosphoethanolamine (DoPhPE) and 2,6,10,15,19,23-Hexamethyltetracosane (squalane).

The presence of ether bonds and bipolar lipids confer unusual high stability to the archaeal membranes and makes them highly impermeable to solutes and protons (Balleza et al., 2014; Guler et al., 2009; Matsuki et al., 2007; Shinoda et al., 2004a, 2004b; Tristram-Nagle et al., 2010). Solute permeability through lipid bilayers is based on the Overton's solubility diffusion model (cited in Al-Awqati, 1999) in which it was stated that the membrane permeability depends on its lipid solubility (Figure 2a). Accordingly, charged and bigger molecules present faster translocation than neutral and smaller ones (Hannesschlaeger et al., 2019; Shinoda, 2016). Nevertheless, two main factors concern this one-slab model: first, the low correlation between water permeability and the lipid hydrophobic core thickness and second, although branched and linear acyl chains have a similar water solubility, water molecules have a lower local diffusion in membranes with isoprenoid ramified chains (Nagle

et al., 2008; Tristram-Nagle et al., 2010). Consequently, a three-slab model was presented by Nagle *et al.* including the concept of area *per* lipid ratio in the permeability estimation. Therefore, it considers the lipid head groups as the initial permeation barriers and present the hydrocarbon core thickness as a secondary contribution (Mathai et al., 2008; Nagle et al., 2008) (Figure 2b). Finally, a pore model presented by Nagle and Scott that assumes that molecules traverse lipid bilayers through transient defects needs also to be considered (Nagle and Scott, 1978) (Figure 2c). Such mechanism is important on the borders between different lipid phases since increased area variances generate a line tension and thus facilitate the creation of the necessary membrane defects. Accordingly, a maximum water permeability is present when two lipid phases coexist (Blok et al., 1975).

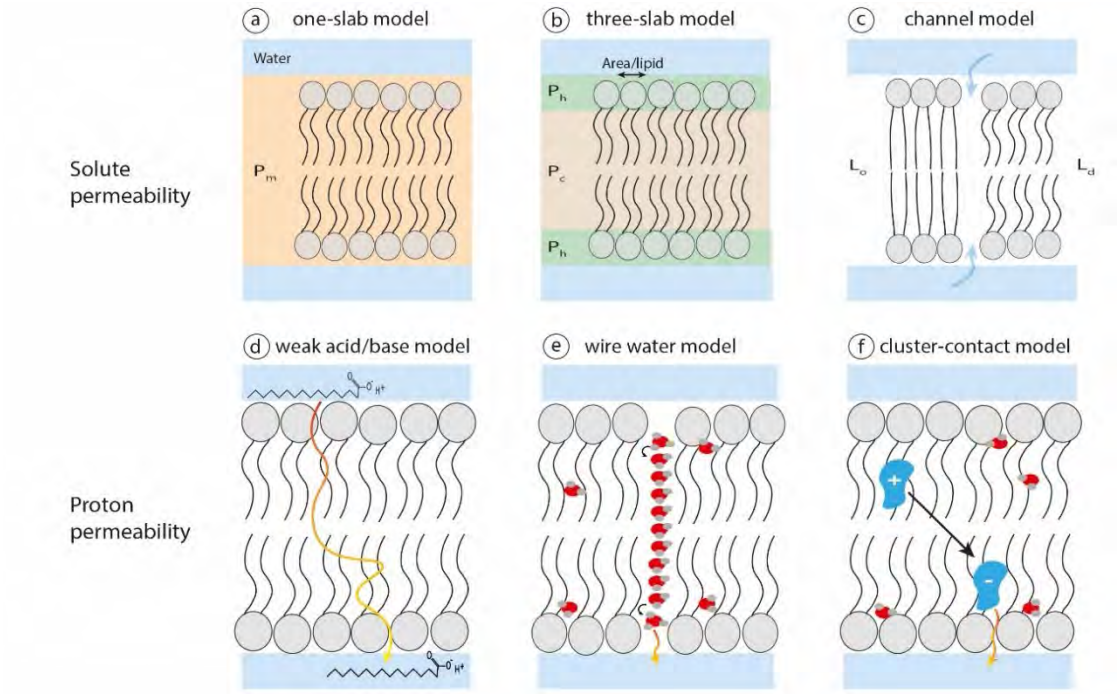

Figure 2. Above: Three models to explain lipid bilayer permeability to solutes. a) The one-slab model represents the membrane as one homogenous oil layer with permeability, P_m. b) The three-slab model differentiates two headgroup slabs that bind a central hydrocarbon slab. P_h is the permeability in each headgroup slab and P_c is the permeability in the hydrocarbon slab. c) The channel model suggests that line tensions on the border of different lipid phases (liquid crystalline ordered, L_o, or liquid crystalline disordered, L_d) form a pore. Below: Different models to describe the proton permeability of a lipid bilayer. d) The weak acid/base model is based on artefacts, such as non-esterified fatty acids, that can diffuse through the bilayer carrying a proton. e) The wire water model is based on the capability of a water molecule network to diffuse protons by the "proton jump" mechanism. Oxygens and hydrogens from water molecules are represented by red and grey spheres, respectively. f) The cluster-contact model considers that water clusters in the hydrophobic region are attracted due to their different charges allowing the diffusion of protons. The size of molecules is not at scale.

Nevertheless, all models presented to explain solute permeability fail when referring to the large proton permeation, which correlates weakly with fluidity, but exponentially and inversely proportional to the membrane thickness (Lande, 1995; Paula et al., 1996), suggesting different mechanisms for protons or other solutes permeability. For detailed reviews see

Decoursey, 2003; Hannesschlaeger et al., 2019; Nichols and Abercrombie, 2010. Interestingly, proton permeability is independent from pH-values but only the pH difference between both bilayer sides seems important. A first hypothesis to explain proton membrane permeation suggests that weakly acidic contaminants, such as non-esterified fatty acids, become protonated and diffuse together with a proton to the other side of the bilayer where they release it (Gutknecht, 1984) (Figure 2d). Another explanation is the presence of water wires extended in the hydrophobic region of the membrane, which provide a pathway for proton transport by Grotthuss' conductance (Nagle and Morowitz, 1978; Nichols and Deamer, 1980) (Figure 2e). Consequently, proton permeability should increase when water permeation is increased but this correlation does not exist. For instance, the liquid ordered phase achieved in presence of cholesterol decreases water permeability but increases proton permeation (Gensure et al., 2006). Last, the cluster-contact model suggests that the transfer of protons could be done through contact of a water cluster with another molecular cluster of opposite charge (Haines, 2001) (Figure 2f).

Fluorescence spectroscopy is a powerful tool to study membrane physicochemical properties of lipid membranes, such as permeability or hydration. For this purpose, it is necessary to introduce a fluorescent probe responding to its environment into the membrane or inside liposomes (Klymchenko and Kreder, 2014; Kyrychenko, 2015; Sezgin et al., 2014). Among such environment sensitive probes, there are dyes with concentration dependent intensities, such as Carboxyfluorescein (CF) (Chen and Knutson, 1988) or Calcein (Oku et al., 1982). Others are pH sensitive, *e.g*. Pyranine (Kano and Fendler, 1978) and coumarin derivatives (Hua et al., 2016), and others present a shift of fluorescent emission depending on water surrounding and thus report on lipid packing, such as Laurdan (Parasassi et al., 1990) or Prodan (Macgregor and Weber, 1981).

Here, we will complete previous fluorescent published results (Salvador-Castell (3) et al., n.d.) on physicochemical properties of an archaeal-like lipid bilayer composed by 1,2-di-O-phytanyl-*sn*-glycero-3-phosphocholine (DoPhPC) and 1,2-di-O-phytanyl-*sn*-glycero-3-phosphoethanolamine (DoPhPE), in presence of the apolar molecule squalane (Figure 1) under high temperatures and high hydrostatic pressures. Both parameters, pressure and temperature, highly affect cell membrane properties. In short, thermal fluctuations increase disorder in phospholipid membranes and induce a phase transition to a higher disordered lipid phase (Laggner and Kriechbaum, 1991). In contrary, high pressure increases order in the membrane and decreases hydrocarbon chains' fluidity (Brooks et al., 2011; Winter and Jeworrek, 2009). Firstly, we present permeability studies to water and protons taking advantage of CF self-quenching and Pyranine sensitivity to protons, respectively. Secondly, we analysed membrane hydration as function of temperature by polarization of Laurdan.

Results and Discussion

I. CF permeability

CF encapsulated into liposomes at high concentrations is almost completely self-quenched and thus presents a nearly zero fluorescent intensity (Chen and Knutson, 1988). Consequently, a CF efflux from vesicles results in an increase of fluorescent intensity (Figure 3a).

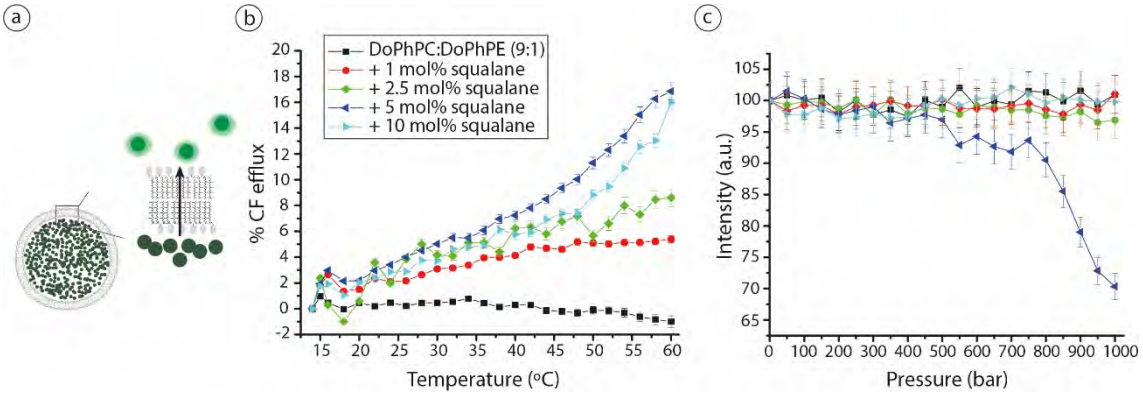

Figure 3. a) Schematic representation of the CF efflux technique, inside liposomes. CF is self-quenched but the fluorescence intensity emerges once it is released from liposomes due to a concentration decrease. The size of probes is not at scale. b) % CF efflux as a function of temperature and c) CF normalized intensity versus high hydrostatic pressure applied on liposomes composed of DoPhPC:DoPhPE (9:1) in absence (black squares) or in presence of different squalane percentages: 1 mol% (red spheres), 2.5 mol% (green diamonds), 5 mol% (blue left triangles) and 10 mol% (cyan left triangles).

Contrary to the presence of cholesterol (Bhattacharya and Haldar, 2000; Mathai et al., 2008), squalane facilitates the CF efflux from liposomes, such squalane dependent effect is more pronounced at high temperatures (Figure 3b). Liposomes composed by DoPhPC:DoPhPE (9:1) consists in a highly stable bilayer and impermeable to solutes. By just adding 1mol% squalane to the lipid mixture, the CF efflux increases significantly, such effect is more pronounced by increasing squalane proportion (2.5 mol%, 5 mol% and 10 mol%). The increase of CF efflux is an indication that squalane fluidizes the hydrocarbon region of the lipid bilayer. Surprisingly, the highest CF efflux is present for the sample containing 5 mol% squalane and not the one with the highest quantity of squalane, *i.e.* 10 mol%. Such tendency was checked several times and it might be explained by the presence of numerous membrane regions. Squalane rich and non-rich domains could cause the presence of domain boundaries present at 5 mol%, which might result in higher CF efflux via the channel mechanism (Figure 2c). Alternatively, the sample with 10 mol% may mostly contain squalane rich regions and boundaries with squalane poor regions would not be representative.

Conversely, no CF efflux was detected from liposomes against high hydrostatic pressure (Figure 3c). Interestingly, the sample with 5 mol% is still the one with a peculiar behaviour: its fluorescent intensity decreases at pressures above 500 bar. Such phenomenon

may be explained by the fact that, probably due to lipid – probe interactions, CF never presents a complete self-quenching in liposomes (Chen and Knutson, 1988). In the same vein, the dye sulforhodamine is 99.9% self-quenched in solution but just by 90% in liposomes (Bae and Yoon, 2013). Moreover, as suspected for the results of CF permeability against temperature, the lipid membrane with this squalane percentage may present diverse domains. Moreover, an increase in pressure induce domain segregation (Hamada et al., 2011), causing a higher membrane tension and, once a critical domain size is reached, forming a bud to release this tension (Jülicher and Lipowsky, 1993; Lipowsky, 1992). Nevertheless, such phenomenon occurs without forming pores in the bilayer and thus without CF release. Therefore, the budding causes the separation of smaller vesicles that might change probe's intensity and could explain its decrease. Budding of lipid vesicles are characteristic on phase-separated membranes and on multicomponent membranes. Indeed, it was observed that budding may be caused by high hydrostatic pressure (Nicolini et al., 2006), osmotic pressure (Dobereiner et al., 1993; Hamada et al., 2007) or in the presence of enzymes (Staneva et al., 2004) or detergents (Staneva et al., 2005). Furthermore, budding sites should be regions of high curvature, which is in accordance with previous SAXS results on the same system (Salvador-Castell (4) et al., n.d.).

II. Proton permeability

Pyranine is a suitable fluorescence dye to determine pH in the interior of phospholipid vesicles (Figure 4a). After adding HCl at the outside of vesicles, proton permeability of lipid membranes is initiated and determined over temperature and pressure scans via Pyranine intensity.

Our results show no difference of proton permeability from archaeal-like lipid vesicles in absence or in presence of squalane against temperature. However, the sample at 5 mol% squalane behaves differently again and it presents a smaller proton permeability. Last, a slight increase is discernible on proton permeability for all samples above 45°C (Figure 4b).

Interestingly, squalane prevents lipid bilayer proton permeability against pressure (Figure 4c). Though between 1 mol% to 5 mol% squalane, the decrease on proton permeability is not directly proportional to squalane concentration, its tendency is always the same. Last, at concentrations of 10 mol%, squalane can completely block proton transit.

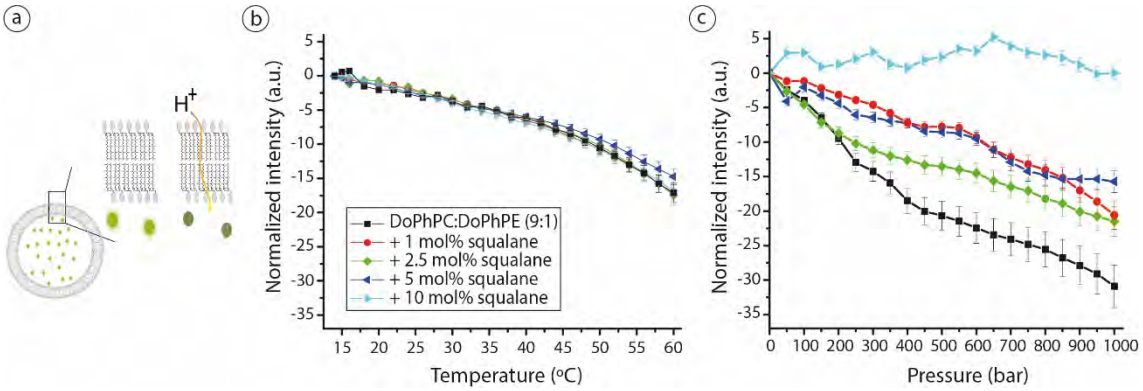

Figure 4. a) Schematic representation of the Pyranine technique to measure pH inside vesicles. Initially, Pyranine is encapsulated in the liposomes and the entrance of protons will cause a decrease on Pyranine fluorescent intensity. The size of probes is not at scale. b) Pyranine normalized intensity inside vesicles as a function of temperature and c) hydrostatic pressure applied on liposomes of DoPhPC:DoPhPE (9:1) in absence (black squares) or in presence of diverse squalane percentages: 1 mol% (red spheres), 2.5 mol% (green diamonds), 5 mol% (blue left triangles) and 10 mol% (cyan left triangles).

High hydrostatic pressure perturbs lipid molecular packing by modifying line tension and bending rigidity of liposomes (Nicolini et al., 2006; Purushothaman et al., 2015). Moreover, this environmental parameter separates lipid domains and can induce small domains or merging of highly ordered domains (McCarthy et al., 2015). All such membrane disturbances could explain the high proton permeation of liposomes in absence of squalane when hydrostatic pressure is applied. The decrease of proton permeability by adding squalane is related to the proton mechanism through a lipid bilayer and the position of squalane: protons need a traversal to pass the highly hydrophobic region of the lipid bilayer (Figure 2d-f), but the presence of the apolar molecule in the bilayer midplane could separate lipid leaflets and therefore stop the protons' pathway. Moreover, such phenomenon is in concordance with a higher hydrocarbon core thickness (Paula et al., 1996; Salvador-Castell (5) et al., n.d.). Until reaching 10 mol% squalane concentration, when domains would be certainly negligible and the overall presence of squalane in the bilayer midplane may prevent protons to pass between layers. Accordingly, the presence of squalane and similar molecules would be a great advantage for piezophiles since they could modulate proton membrane permeation just by modifying apolar polyisoprenoid molecule levels.

III. Lipid bilayer fluidity

Laurdan is a fluorescent probe sensitive to its water environment, *i.e*. polarity, and hence on lipid packing and phases (Bagatolli, 2012). When the probe is placed at a low polar or high polar environment, it presents a blue or green emission, respectively. The value of its GP suggests such polarity, on the one side, Laurdan GP about 0.6-0.8 indicates that the phospholipid bilayer is under a gel phase and on the other side, values about (-0.4)-(-0.2)

illustrate a more fluid state for usual lipids, the liquid crystalline phase (Parasassi et al., 1991, 1990) (Figure 5a).

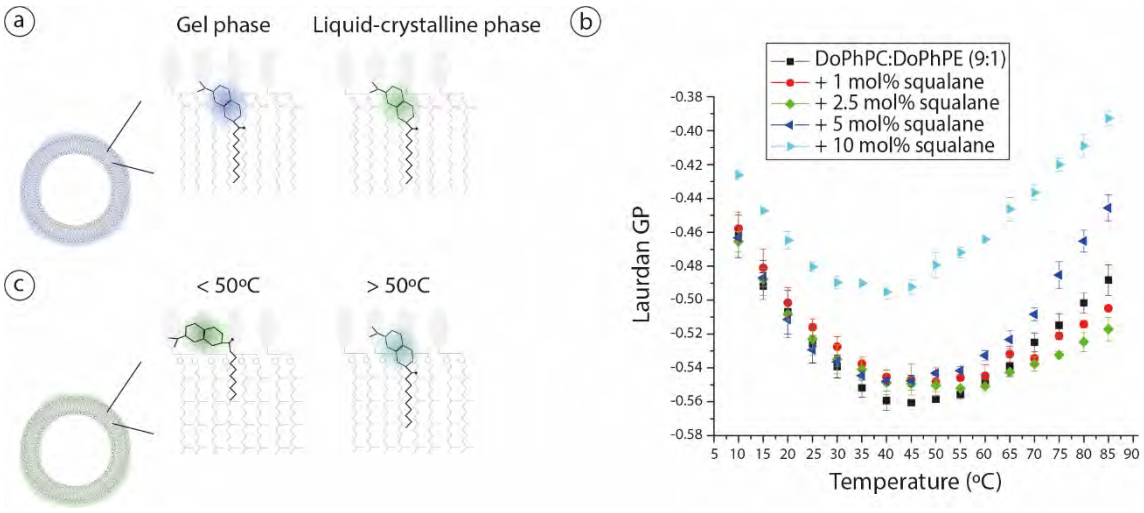

Figure 5. a) Schematic representation of Laurdan position in a lipid bilayer composed by conventional diester phospholipids. While lipids are highly ordered in a gel phase, Laurdan emits in the blue region. A phase transition to a more disordered phase, the liquid-crystalline phase, induces an emission shift to green values. b) Laurdan GP values from liposomes of DoPhPC:DoPhPE (9:1) in absence (black squares) or in presence of different squalane percentages: 1 mol% (red spheres), 2.5 mol% (green diamonds), 5 mol% (blue left triangles) and 10 mol% (cyan left triangles). c) Schematic representation of Laurdan emplacement suggested for bilayers composed of archaeal-like diether lipids: Up to 50°C, the fluorescent dye may adopt a L-shape form which would be consistent with the low Laurdan GP values. However, above 50°C, there is a probe relocation to a deeper position that gives a change on dye emission and an increase on Laurdan GP values.

In the lipid systems studied here, GP values are below -0.40 at all temperatures (Figure 5b) and all samples, *i.e.* in absence and in presence of squalane. Moreover, they present a similar behaviour: up to 40°C, GP decreases when increasing temperature, then, between 40°C and 50°C, they reach a plateau and lastly, above 50°C, GP increases proportionally to temperature (Figure 5b). Such negative values are indicative of a liquid crystalline phase in membranes of familiar diester lipids. However, these extremely low values are not in agreement with the low water permeation and the slow motions attributed to archaeal diether lipids (Shinoda et al., 2004a). Moreover, the Laurdan GP increased above 50ºC is contradictory to the fact that temperature increases molecular motions, disorder and consequently water permeation and thus, GP should present lower values at higher temperatures (Parasassi et al., 1994; Periasamy et al., 2009).

The probe position in the lipid bilayer could explain the unusual Laurdan GP values. It was shown that, due to the highly rigid and tight membrane, Laurdan adopts an “L-shape” when anchored in tetraether monolayers (Bagatolli et al., 2000): Laurdan’s chromophore group, *i.e.* naphthalene rings, resides in the head group region perpendicular to lipids and only its hydrocarbon tail penetrates parallel to lipids in the hydrophobic region. Accordingly, contrary to the probe disposition when anchored on usual diester lipids, where the

chromophore group is at 10 Å from the bilayer midplane (Antollini and Barrantes, 1998), the naphthalene rings are highly exposed to water molecules in tetraether monolayers, which could explain the low GP values. A similar effect could explain the unusual negative GP values presented here, although in this case the membrane is a bilayer composed by diether phytanoyl lipids. We thus suggest that the phytanoyl chains prevent the anchorage of the chromophore group inside the bilayer and thus it is highly exposed to water molecules in a similar way that on the "L-shape" disposition (Figure 5c).

The blue-shift emission observed at high temperatures could be explained by a probe relocation maybe due to a slow phase transition between fluid phases. An increase in temperature causes higher disorder in lipid bilayers, especially in their hydrocarbon chains, and it could lead to a higher insert of naphthalene rings into lipid bilayers at temperatures above 50°C. Similarly, Prodan, a closely related probe to Laurdan, is placed in a more hydrophobic environment at high pressures (Chong, 1988). Therefore, the effect of environmental changes on probe location needs to be considered. Interestingly, the sample with highest squalane proportion is the one that presents an overall higher GP values and in which the GP increase begins at lower temperatures. Considering all previous interpretations, it would denote that the sample containing 10 mol% squalane presents a global higher fluidity since Laurdan is capable to be inserted more deeply in the lipid bilayer and thus it presents higher GP values. Such fluidizing effect of squalene has recently been observed on asolectin liposomes (Costa et al., 2018).

Conclusions

The presence of squalane or similar molecules in archaeal membranes suggests that these apolar molecules may play a role in cell membrane adaptation to extreme conditions (Salvador-Castell (3) et al., n.d.). Here, we have used archaeal-like phospholipids to study the effect of squalane on permeation and hydration of archaeal bilayers at high temperatures and high hydrostatic pressures. Laurdan GP demonstrates that such apolar molecule is capable of increasing membrane fluidity and, although without disturbing it excessively, it induces solute permeability through lipid bilayer even at the lowest concentration studied, *i.e.* 1 mol %. However, probably due to its position in the midplane of the bilayer and an increase on bilayer thickness, squalane reduces proton bilayer permeability at high pressures, which could be essential for piezophile microorganisms. Interestingly, we obtained one more evidence that protons follow a different permeation pathway than other solutes through lipid bilayers, although this time in bilayers composed by archaeal-like lipids.

Accordingly, it is noteworthy that squalane and, by extrapolation, other apolar polyisoprenoids as lycopene are capable to modulate in a concentration manner the physicochemical properties of the archaeal bilayer. Since archaeal lipids are highly impermeable to solutes even at extreme conditions, the incorporation of apolar lipids would be an easy way to modify this essential characteristic. This would allow Archaea to reach membrane parameter values as non-extremophiles cells at their optimal environmental conditions, which would accomplish the "corresponding state principle" (Vihinen, 1987), and to modify its solute permeability depending on cell needs. Last, the decrease of proton permeability facilitates the proton membrane gradient at extreme conditions and therefore basic functions, such as ATP production. All these indicate that apolar polyisoprenoids may indeed play a role as membrane regulator, a comparable function as sterols or hopanoids in eukaryal and bacterial cells, respectively.

Acknowledgements

This work was supported by the French National Research Agency programmes ANR 2010 BLAN 1725-04 and ANR 17-CE11-0012-01 to PO and JP and the German-French bilateral research cooperation programme "Procope" 2018-2019 to JP and RW. MSC was supported by a PhD grant from the French Ministry of Research. We thank the research team Chimie Organique et Bioorganique (UMR 5246, INSA Lyon) and particularly S. Chambert for access to their spectrofluorimeter.

Materials and methods

Materials

1,2-di-O-phytanyl-*sn*-glycero-3-phosphocholine (DoPhPC) and 1,2-di-O-phytanyl-*sn*-glycero-3-phosphoethanolamine (DoPhPE) were bought from Avanti Polar Lipids. Purity guaranteed was > 99%. 2,6,10,15,19,23-Hexamethyltetracosane (squalane), 5(6)-Carboxyfluorescein (CF), 8-Hydroxypyrene-1,3,6-trisulfonic acid trisodium salt (Pyranine) and 6-Dodecanoyl-N,N-dimethyl-2-naphthylamine (Laurdan) were bought from Sigma – Aldrich Co.

Liposome formation

DoPhPC and DoPhPE in a proportion 9: 1 were dissolved in a chloroform: methanol (2: 1) solution. Squalane was dissolved in chloroform and added at different proportions to obtain 1 mol%, 2.5 mol%, 5 mol% and 10 mol%, respectively. Such solutions were vortexed, dried under a steam of nitrogen gas and left overnight under high vacuum to complete evaporation. Then, the lipid film was rehydrated with a given buffer, followed by vortexing, sonication for five minutes and five cycles of freezing/thawing. To form large unilamellar vesicles (LUVs), the solution was passed through a 100 nm polycarbonate filter by pressure extrusion 11 times at 55°C using a Mini Extruder ® from Avanti Polar Lipids. Consecutively, it was cooled down and the free dye was removed by chromatography over a prepacked P-10 desalting column from GE Healthcare. Liposomes were kept in ice and used immediately.

CF efflux

When CF is trapped inside liposomes at high concentrations, *i.e.* > 1 mM, it is mostly self-quenched, thus non-fluorescent (Chen and Knutson, 1988). Its leakage through the lipid bilayer will diminish its concentration and hence, its fluorescent intensity will increase. The buffer used was HEPES 10 mM, KCl 100 mM, EDTA 1 mM and CF 40 mM at pH 7.8. The final DoPhPC:DoPhPE concentration was 6 mM. Regarding the temperature measurements, the fluorimeter Jasco Spectrofluorometer FP – 8500 was connected to a water circuit. For pressure measurements, we used a special fluorimeter equipped with a home-made chamber to create high hydrostatic pressures. The fluorescent excitation was placed at 492 nm and emission maximum was read at 518 nm. The permeability of CF was investigated in a temperature range from 10°C to 60°C and in a pressure range applied from 0 bar to 1000 bar. At the end of the temperature measurement, all trapped fluorescent dye was released by adding 0.1% Triton X100. Finally, CF efflux was calculated as (Parasassi et al., 1990):

$$\%\ CF\ efflux = \frac{F_t - F_0}{F_{max} - F_o} \quad \text{(Eq. 1)}$$

where F_t, F_0 and F_{max} are the fluorescence intensities at time t, time zero, and after total solubilisation by Triton X100.

Pyranine fluorescence

Pyranine is a pH-sensitive dye, this means that a pH variation causes a shift on its emission spectrum (Kano and Fendler, 1978). It has been largely used to detect pH changes inside liposomes (Berglund et al., 1999; Elferink et al., 1994; Johnson, 1998; Rossignol et al., 1982). In this fluorescent experience, HEPES 5 mM at pH 7.5 together with Pyranine 5 mM was used to rehydrate the lipid film. The final lipid concentration was 6 mM and LUVs were used immediately after size exclusion chromatography. pH permeability of lipid bilayer was investigated in temperature range from 10°C to 60°C and in a pressure range applied from 0 bar to 1000 bar. The first pH permeability measurement, called blank, was realized just by increasing the temperature or the pressure. Then, the measurement was repeated but this time adding 10 µl of HCl 0.1 M giving an initial pH 3 outside the liposomes. To separate the effect of temperature and pressure from proton permeability, we subtracted the blank to the second measurement. The fluorimeters used were the same as described in the CF efflux section. The excitation wavelength was 470 nm and emission was read between 500 nm and 520 nm with its maximum at 510 nm.

Laurdan Generalized Polarization

Laurdan is an environment sensitive fluorophore widely used to quantify the lipid packing. The polycyclic aromatic compound naphthalene possesses a dipole moment that causes reorientation of water molecules which results in a red-shift of the probe emission (Sanchez et al., 2007). Accordingly, after excitation at 350 nm, the emission spectrum of Laurdan in phospholipid membranes present two local maxima, one at about 440 nm for ordered lipid (gel) phases and the other around 490 nm for the more disordered lipid phases (liquid-crystalline). 0.2 mol% of Laurdan was added to the lipids dissolved in chloroform/methanol. The lipid film was resuspended in HEPES 5 mM at pH 7.5 with a final concentration of 1 mM. To precisely quantify the polarity change, we used the general polarization (GP) term (Parasassi et al., 1991, 1990):

$$GP = \frac{I_{440} - I_{490}}{I_{440} + I_{490}} \quad \text{(Eq. 2)}$$

where I_{440} and I_{490} are the emission intensities at 440 and 490 nm, respectively. GP values can range from +1 to -1, *i.e.* -1 being the highest lipid membrane fluidity.

The temperature-dependent measurements were performed on a K2 multifrequency phase and modulation fluorimeter (ISS Inc.). We used a quartz cuvette with a volume of 100 µL in a temperature range of 5-90 °C. Temperature control was achieved using a circulating water bath with an accuracy of ± 0.1 °C.

Chapter 5. Conclusions and perspectives

The studies presented permit to answer some of the questions about how cell membranes can adapt to extreme conditions. Indeed, apolar polyisoprenoids, such as squalane, can be inserted in the archaeal cell membrane and, most importantly, such molecules provide additional capabilities to the lipid bilayer. Squalane is placed in the midplane of the archaeal lipid bilayer, oriented perpendicular to phospholipids' hydrophobic chains. The presence of non-polar polyisoprenoids has various physicochemical implications that ease the lipid bilayer to remain structured and functional under extreme conditions, to be adapted to changing environments and provides new putative functions to the membrane.

First, the specific position of squalane in the lipid bilayer decreases the packing frustration of the lipid chains and, consequently, allows the model membrane to adopt highly curved structures, such as the non-lamellar phases revealed by SAXS. Moreover, these non-lamellar structures are more stable at HT and HHP than the lamellar phase. This may point to modifications on bilayer bending rigidity caused by the presence of squalane. Together with the steady lipid phase coexistence uncovered by neutron diffraction, it indicates that the presence of squalane can allow the cell to maintain different, probably specialized, membrane domains. Especially curved membrane domains are necessary for the cell for several functions. As an illustration, they are essential for cell fusion, fission and for intercellular communication by nanotubes and nanopods, all common processes in Archaea. Furthermore, the presence of membrane domains is necessary to control protein-membrane interactions and anchorage since not all domains interact equally with proteins. The notable capability of squalane to

induce lipid self-assembly under non-lamellar phases opens up to the interesting question whether cubic phases are present *per se* in native archaeal cell membranes, maybe to accommodate proteins, or locally formed at infoldings of the plasma membrane.

Secondly, by fluorescent methods, I have demonstrated that apolar polyisoprenoids molecules influence considerably the permeability of archaeal model membranes. Accordingly, squalane increases water lipid bilayer permeability, probably by increasing membrane fluidity, but in opposite, it decreases proton permeability. Although an increase in water permeability could be treated as a disadvantage, the embedding of polyisoprenoids may be of utility for adapting cell membrane permeability to changing conditions. Intriguingly, the sample containing 5 mol% squalane presents exceptional behaviours that would require a deeper study to confirm the hypothesis proposed. By the CF efflux essay, this sample shows a water permeability higher than the sample containing 10 mol% squalane, due perhaps to the presence of more lipid phase boundaries. This would cause the increase of water permeability by the formation of channels between phases. Furthermore, its CF fluorescence intensity, which is supposed to be self-quenched, decreases at HHP. This may be caused by the presence of numerous lipid phases that are even more segregated due to the increase of pressure; more domains mean an increase in membrane line tensions, which may be finally released by the membrane budding and the final bud fission. This would lead to the formation of smaller vesicles. Consequently, CF may be trapped in smaller vesicles with smaller volumes and therefore, it may be more concentrated, and its self-quenching would increase. The fact that it occurs only at the sample containing 5 mol% squalane indicates that this lipid bilayer should be the one with most important phase boundaries and that at 10 mol% of squalane, it may be a more homogeneous system.

Last, both detected effects of squalane, i.e. modification of membrane curvature and permeability, are heavily squalane-concentration dependent. This implies that cells may be able to change membrane domains' sizes and shapes and control their membrane flexibility, fluidity and permeability adjusting the quantity of apolar polyisoprenoid in the cell membrane. Such capability would be of significant utility for all kinds of cells, but particularly to extremophiles as they could easily adapt their membrane properties to extremely variable environmental conditions.

Therefore, the new membrane ultrastructure based on apolar polyisoprenoids as membrane regulators confers the lipid membrane two essential characteristics common in all functional cell membranes: dynamism and heterogeneity. The membrane is dynamic thanks to the presence of different membrane curvatures and even non-lamellar phases and presents

lateral heterogeneity as a result of lipid phases coexistence. All this happens by shifting the bilayer stability domain under combined HT and HHP.

The conclusion of this work has a prominent biological impact. It analyses and discusses a new membrane ultrastructure in which non-polar polyisoprenoids play a leading role. Such apolar molecules have been scarcely studied and there is still little information about their distribution through the Archaea domain. It would be necessary to perform an extensive, exhaustive search for these apolar polyisoprenoids in the whole domain Archaea to define the phylogenetic distribution of these molecules, their quantity and type, i.e. number of terpene units and level of unsaturation, and if a relation exists between polyisoprenoid types, or their presence and environmental conditions. For instance, the second part of the introduction section chapter (Salvador-Castell et al., 2019) shows that, the number of terpene units may be correlated with the optimal growth temperature of the cells, it is directly correlated with the optimal growth salinity and that alkaliphile archaea, which contain low levels of bipolar lipids, present high fractions of non-polar polyisoprenoids (Salvador-Castell et al., 2019). Moreover, the role of apolar polyisoprenoids in the homeoviscous cell membrane adaptation of *T. barophilus* suggests that this effect could be found on other archaea; however, it needs to be confirmed.

I have determined squalane position in a reconstructed archaeal lipid bilayer. However, since many archaea, such as *T. barophilus*, also contain bipolar lipids, it would be interesting to study the apolar polyisoprenoid position with both kind of lipids, i.e. monopolar and bipolar. All archaea have quinones in their membranes, even those that only produce bipolar lipids. These quinones are anchored in the membrane by a polyisoprenoids tail resembling squalane. Hence, even in a packed monolayer, there is space to accommodate non-polar polyisoprenoids. However, the presence of the polar headgroup of quinone may help in its stabilisation in the membrane. Because of the absence of its polar headgroup in squalane, localization of apolar polyisoprenoids in archaeal monolayers needs to be confirmed experimentally.

There are plenty of compelling membrane parameters that could be impacted by the presence of apolar polyisoprenoid molecules. Neutron diffraction and SAXS studies demonstrated that polyisoprenoids modify the membrane structure but information on dynamics, another essential parameter of cell membrane, is still missing. For instance, apolar molecules may modify the lateral diffusion of lipids or their local mobility. These parameters are of high relevance since molecules are not just anchored in the cell membrane, but their diffusion determines, partially, their properties. Neutron scattering techniques, such as elastic incoherent neutron scattering or quasielastic neutron scattering, would provide information

about such impact in the picosecond range. Furthermore, the C-H bond dynamics could be studied by nuclear magnetic resonance under a nanosecond time scale. Considering the results presented in this thesis, I expect that apolar polyisoprenoids would slightly increase local movements of lipids, which could explain the increase on water permeability, but at the same time, I think that apolar lipids could reduce molecular dynamics of the hydrophobic terminal methyls. This would reinforce the decrease of proton permeability that is already caused physically by squalane localization in the bilayer midplane. Dynamics in lipid membranes is a collective property that determines, for example, membrane undulations and the energy required to change membrane curvature, i.e. the bending energy.

As demonstrated by SAXS, polyisoprenoids induce the formation of highly negatively curved membranes, i.e. cubic and inverted hexagonal phases. Hence, membrane bending rigidity should be significantly reduced in presence of such apolar lipids. This can be verified within the ns range by Neutron Spin Echo (NSE), a technique that yields information about vibrations and arrangements of molecules. In NSE, the sample, in this case lipid bilayers, is placed between two homogenous magnetic field paths that rule the spin polarization of neutrons. The presence of the sample will change neutron speed and thus, the spin polarization at the end of the second magnetic field path. All such studies on membrane parameters could be done under extreme conditions, like HT, HHP or extreme pH, to determine the impact of environmental properties. Lastly, squalane may probably influence protein functionality, as acyl chain composition does. It would be thus interesting a project based on the properties of voltage-gated or mechanosensitive ion channels in absence and in presence of polyisoprenoids.

During my experiments, I found difficulties to synthesize GUVs of a reasonable size (> 5 μm) by electroformation from archaeal synthetic lipids in presence of squalane. GUVs from usual eukaryal lipids are already more unstable than smaller unilamellar vesicles, such as SUVs and LUVs. The combination of the capability of squalane to induce highly curved membranes could explain that such vesicles are not easy to synthesize by the usual electroformation protocol. Although I could not dedicate too much time to it, I think that it would be necessary to refine the technique. Consequently, as GUVs are easily observable under optical microscopy, it would be feasible to use other relevant techniques. For example, it would be possible to study bending rigidity on a larger timescale than by NSE. This would allow to have a complete picture of membrane bending rigidity since the parameters at macroscopic and nanoscopic scales could differ. Another compelling application would be to observe artificial exocytosis mechanism after microelectroinjection and incorporation of fluorescent dyes. This could directly confirm that squalane facilitates membrane functions that requires remarkably curved regions, such as fusion and fission.

Thanks to a collaboration with a laboratory of chemical synthesis, we have obtained archaeal lipids with different headgroups. These lipids will allow the determination of the effect of lipid headgroups on archaeal membrane bilayers but also on the impact of polyisoprenoids. To go further, it would be appealing to synthesize fluorescent-label archaeal lipids, if possible, with selective partitioning on different lipid phases. This would enable a large number of novel fluorescent experiments on archaeal model membranes. For example, the observation of phase separation and fusion phenomena in unilamellar vesicles by confocal microscopy and the study of lipid dynamics by Fluorescence Recovery After Photobleaching (FRAP), Fluorescence Resonance Energy Transfer (FRET) or Fluorescence Correlation Spectroscopy (FCS). FRAP is based on the fluorescent intensity after photobleaching and it is possible to extract information about the mobile fraction, which corresponds to how much intensity is recovered after bleaching, and the diffusion time. FRET is extensively used to monitor lipid mixing and membrane fusion and it is based on the energy transfer between two fluorescent molecules. FCS gives information about molecular diffusion, e.g. average transit time and apparent diffusion coefficient, by following the fluctuations of fluorescence intensity for a single spot. Therefore, such results would be complementary of neutron scattering experiments and would contribute to understand the effect of apolar molecules on membrane dynamics. Another experiment could be to fuse GUVs with archaeal cells. GUVs should be fluorescent tagged to check the correct fusion of GUVs and cells. Consequently, it would be possible to study the effect of polyisoprenoids on almost native cell membranes. Another possibility is to compare portions of natural membranes from a polyisoprenoid-containing microorganism and another that does not contain it by isolating giant plasma membrane vesicles, for example.

Based on the experimental results, I suggested that archaeal lipid bilayers are organized in membrane domains thanks to apolar polyisoprenoids. Nevertheless, other complementary experiences can be done for a better characterization of such phase coexistence on model membranes. For example, it would be interesting to estimate the size and number of domains and thus evaluate the lipid lateral heterogeneity. Therefore, these results could be extrapolated to determine the organization of native archaeal cell membranes. To do this, it would be possible to use Atomic Force Microscopy, a technique that can measure the roughness of a lipid bilayer deposited on a substrate.

Another important and useful characteristic would be lipid partitioning to understand polyisoprenoid-lipid interactions. For example, sphingomyelin and phosphatidylserine have a higher cholesterol partition coefficient than phosphatidylethanolamine. Thus, partition coefficients from lipids with polyisoprenoids may also differ. Contrary to cholesterol, I expect that phospholipids with small head groups, such as phosphatidylethanolamine, would present

higher affinity to polyisoprenoids since they reduce the packing frustration of its curvature. To study this, it would be feasible, for instance, to simply mix squalane at high concentrations (ca. 20 mol%) with archaeal large unilamellar liposomes of different compositions. Consequently, not all squalane would be introduced and after separation by size chromatography, it would be possible to analyse its composition by Thin-Layer Chromatography/Mass Spectroscopy and detect the quantity of squalane inserted in each sample. If squalane can be inserted at a higher rate for a determined lipid mixture, it would indicate that squalane partitioning exist. If lipid partitioning exists and if it has been possible to synthesize fluorescent tags or deuterated archaeal-like lipids, it would open the door to many other experiments, as for example, fluorescent or neutron scattering techniques but this time distinguishing lipid phases. Thus, physicochemical properties of each phase, such as dynamics or fluidity, could arise. This is especially important because if, as expected, physicochemical parameters differ, we could really define them as membrane domains, with probably specific functions, and not a mere phase separation.

Another essential question that launches this project is if domains would be detectable on native archaeal membranes that contain the apolar molecules. To answer it, first of all, I would check if the presence of squalane increases detergent resistance to domains, as for “lipid rafts” on eukaryotes. If so, it would be possible to extract domains from native membranes by differentiating detergent-resistant membrane fractions. Such partitioning and differential detergent resistance may explain the difficulties encountered with the purification of archaeal lipids from certain species. Another option, dependent on polyisoprenoid partitioning and the availability of fluorescent-labelled archaeal-like lipids, would be to directly observe them by fluorescence after introducing the dyes in the cell membrane.

This work has been done to find out the effect of apolar molecules inserted in an archaeal model membrane. However, the same membrane ultrastructure may be useful to explain the stability of the membranes of the first cells, e.g. the protomembranes. Membranes from protocells should be composed of simple molecules, like single-chain amphiphiles, which are synthesized by abiotic reactions as the Fisher—Tropsch-type. It has been proposed that life originated at hydrothermal vents, meaning under HT and HHP. Nevertheless, it is still an open question how protocells could have a stable and selective permeable membrane under these extreme conditions. According to the results presented in this work, the presence of simple non-apolar molecules could increase protomembrane stability and therefore allow the first cell compartmentalization. For example, as it occurs in the archaeal model presented here, the localization of apolar molecules in the midplane of protomembranes could lead to a diminution of protomembrane proton permeability and shift its stability domain to extreme environmental conditions.

Finally, the exceptional properties that squalane confers to the lipid bilayer could have biotechnological applications using archaeal lipids and probably also eukaryal lipids. It is known that squalane is also placed in the midplane of an eukaryal model membrane; nevertheless, it would be crucial to go further and determine its physicochemical impact on eukaryal lipid bilayers. Consequently, the physicochemical changes that apolar molecules would provide to lipid membranes could be used to modify liposomes currently employed for drug delivery. Furthermore, ultrasonic drug delivery could be highly impacted by the presence of polyisoprenoid molecules. This technique is based on the disruption of the drug carrier by ultrasounds that causes the liposome resizing into smaller vesicles, thus inducing the drug releasing.

Similarly, it would be interesting to exploit the large and stable cubic phases induced by the presence of squalane for cubosomes' or hexosomes' synthesis. Cubosomes and hexosomes are drug nanocarriers with lipids under a non-lamellar phase stabilized by a polymer outer corona. Therefore, polyisoprenoid molecules could be useful to modulate the size of the periodic membrane or the pores inside these structures, for example.

In conclusion, though much remains to be done, in this work I introduced the foundations of the physicochemical characteristics of a new membrane ultrastructure, with apolar polyisoprenoids as the main characters. The novel characteristics that apolar lipids provide to lipid bilayers may be useful for diverse biotechnological applications but specially, it entails a new vision of archaeal cell membranes. Such novel ultrastructure may probably be spread amongst the Archaea domain since non-polar polyisoprenoids have been found in almost all analysed archaea. Apolar lipids confer to the archaeal cell membrane the capacity to change its curvature, to organize in different lipid phases and to be structured under extreme conditions, such as HT and HHP. This thesis demonstrates the importance of apolar lipids on archaeal membrane functions and adaptive capabilities to extreme conditions and opens the discussion about the heterogeneity of archaeal cell membranes without the need of bipolar phospholipids. The presence of apolar polyisoprenoids causes a lipid phase coexistence that indicates the eventual domains formation in cell membrane, which could present differentiate functions. Moreover, the model presented here demonstrates that archaeal cell membranes are not so "static and lethargic" as was thought before and, that to the contrary, they respond flexibly to environmental conditions and to cell necessities thanks to polyisoprenoids.

Résumé

Il y a à peu près 4 milliards d'années, la vie apparaissait sur Terre. La théorie la plus acceptée propose que la vie soit apparue dans l'environnement marin, et plus spécifiquement, près des sources hydrothermales des fonds océaniques, et, ultérieurement, se soit adaptée aux environnements de surface. Aujourd'hui, les fonds marins et les sources hydrothermales sont des environnements présentant une grande variété biologique d'êtres vivants. Ce sont des organismes dits extrêmophiles, car leurs conditions optimales de croissance sont considérées extrêmes par rapport aux conditions optimales de croissance des humains. Au niveau des sources de l'océan profond, les températures des fluides hydrothermaux peuvent atteindre 400°C et les pressions hydrostatiques jusqu'à 110 MPa, c.-à-d. 1100 fois la pression en surface. Les organismes qui vivent près de ces sources hydrothermales sont donc piézophiles et (hyper)thermophiles, puisque leur croissance est optimale sous hautes pressions hydrostatiques (HPH) et hautes températures (HT) respectivement. Comme exemples d'hyperthermophiles et piézophiles, on peut nommer *Methanocaldococcus jannaschii* (T_{opt}= 85°C et P_{opt}= 75 MPa) (Kaneshiro and Clark, 1995), *Methanopyrus kandleri* (T_{opt}=105°C et P_{opt}= 20 MPa) (Takai et al., 2008) ou *Thermococcus barophilus* (T_{opt}= 85°C et P_{opt}= 40 MPa) (Marteinsson et al., 1999).

Tous les organismes possèdent un génome/protéome adapté à leurs conditions de croissance optimale. Les extrêmophiles ne sont pas une exception. Ce qui définit le caractère fonctionnel d'un système biologique est ce que l'on appelle le principe de correspondance (Jaenicke, 2000; Vihinen, 1987), qui dit que les valeurs physiologiques que peuvent prendre un paramètre particulier sont comprises dans une gamme très restreinte, quelques soient les conditions environnementales et les mécanismes adaptatifs sous-jacents . D'un point de vue pratique cela se traduit par le fait que la flexibilité d'une protéine ou la fluidité d'une membrane fonctionnelle seront les mêmes dans une cellule d'Escherichia *coli* et *T. barophilus*

dans leurs conditions de vie optimales, c'est-à-dire pression ambiante et 37°C pour *E. coli* et 400 bar et 85°C pour *T. barophilus*. Toutes variations en dehors de ces valeurs conduisent à une déstabilisation des fonctions et/ou de la structure des biomolécules. Ainsi, on note que le protéome des piézophiles présente une dynamique propre (Martinez et al., 2016; Ohmae et al., 2012). Par exemple, en condition de pression et température ambiantes, conditions suboptimales pour *T. barophilus*, le protéome présente une flexibilité très importante en comparaison des protéomes des organismes mésophiles. Une augmentation de la pression hydrostatique et de la température provoque une transition de phase du protéome pour des valeurs proches des minima physiologiques de cette espèce, ce qui indique le passage à une conformation fonctionnelle du protéome (Peters et al., 2014; Salvador-Castell et al., 2019a). En dehors de ces conditions optimales, les organismes sont stressés et contrecarrent les effets délétères des conditions environnementales par divers mécanismes, comme la synthèse d'osmolytes pour stabiliser les protéines (Cario et al., 2016; Gao et al., 2017; Salvador-Castell et al., 2019a) ou l'adaptation de leur composition protéique et lipidique (Vannier, 2016; Cario 2015). Parmi les composants cellulaires, la membrane plasmique est un des plus sensibles aux variations des conditions environnementales, alors que pour être fonctionnelle, ses paramètres physico-chimiques (dynamique, organisation latérale ou perméabilité) doivent demeurer dans une gamme très restreinte de valeurs. Pour maintenir leur membrane dans le domaine fonctionnel, les organismes en modifient la composition en lipides, ce que l'on appelle l'adaptation homéovisqueuse (Synensky 1974).

Ce travail de doctorat concerne l'étude des adaptations moléculaires d'un groupe de microorganismes polyextrêmophiles, les Thermococcales, et plus spécifiquement sur l'adaptation de la membrane de l'espèce *T. barophilus*, qui est piézophile et hyperthermophile (Marteinsson 1999). *T. barophilus* est une Archée, modèle de référence établi pour l'adaptation à la HPH. Les archées sont des procaryotes unicellulaires formant un des trois domaines de la vie (Woese and Fox, 1977). Bien que souvent confondues avec bactéries, parce qu'elles ont une morphologie similaire, des ARN ribosomiques et une organisation génomique similaire aux bactéries, les archées possèdent des caractéristiques partagées avec les eucaryotes (protéines ribosomiques, transcription et régulation), mais aussi des caractéristiques uniques comme leurs lipides membranaires. La structure des phospholipides d'archées est basée sur deux chaines phytanes connectés grâce à des liaisons type éther à une partie polaire par de stéréochimie inverse par rapport au bactéries/eucaryotes, le *sn*-glycerol-1-phosphate (De Rosa et al., 1986) (Figure 1). Les chaines isoprènes des lipides d'archées forment une couche plus compacte, rigide et imperméable que celle formée par les phospholipides bactériens ou eucaryotes. Par ailleurs, les archées synthétisent des lipides

bipolaires, transmembranaires qui forment des monocouches encore plus rigide et résistante aux stress environnementaux que la bicouche lipidique habituelle (Chang, 1994).

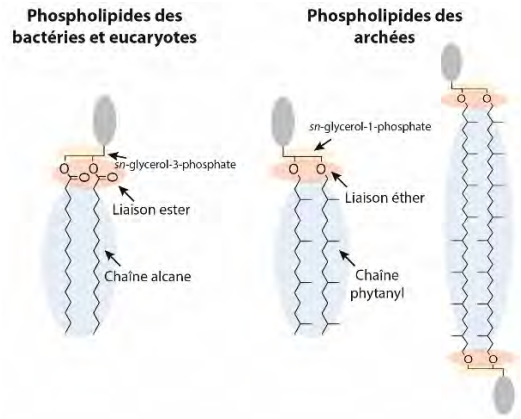

Figure 16. Comparaison des phospholipides habituels chez les Bactérie et Eucaryote (à gauche) et chez les Archaea (à droite). La sphère en gris représente la tête polaire des phospholipides.

Comme ils ont été initialement observés chez les archées hyperthermophiles, ces lipides bipolaires ont été rapidement identifiés comme la voie de l'adaptation membranaire des archées à la HT. Néanmoins, cette affirmation a été mise en doute pour une grande variété des archées hyperthermophiles, notamment celles qui sont capables de synthétiser uniquement des lipides monopolaires. C'est le cas par exemple pour *Methanopyrus kandleri* ou *Aeropyrum pernix* dont les membranes ne contiennent que lipides monopolaires (Hafenbradl et al., 1996) ou le groupe des Thermococcales, dont les membranes contiennent une majorité de lipides monopolaires (Cario et al., 2015). Ainsi, la composition des membranes de ces organismes suppose qu'il existe d'autres routes d'adaptation à la HT chez les Archées. Pendant l'étude de la réponse homéovisqueuse en fonction de la température et de la pression chez *T. barophilus*, Cario *et al.* ont observé que cette réponse impliquait une variation du rapport entre lipides monopolaires et bipolaires, comme attendu en raison de la différence de comportement des membranes en mono- ou en bi-couche. Mais, la réponse homéovisqueuse semble aussi impliquer la variation du nombre d'insaturations de molécules apolaires de type polyisoprène, ce qui implique que ces molécules apolaires pourraient être lipides structuraux de la membrane de *T. barophilus.* Ces molécules ont une structure proche chaines phytanes des lipides membranaires, mais sont issus d'une voie de synthèse totalement différente.

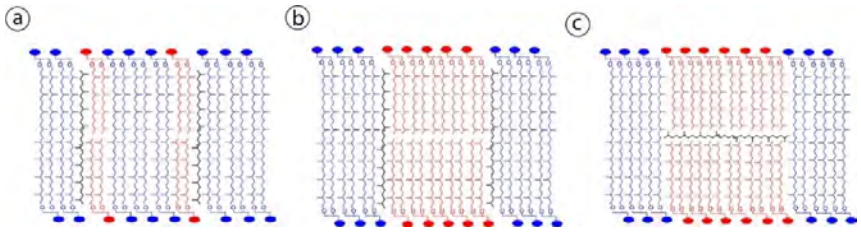

Figure 2. Modèles membranaires en présence de polyisoprènes apolaires présentés par (Cario et al., 2015) *a) les lipides apolaires se placent parallèles aux phospholipides. B) pareil que dans le cas A, mais les polyisoprènes différentient domaines membranaires. C) les lipides apolaires se situent au milieu de la bicouche lipidique et les domaines de bicouche et monocouche lipidique est bien différentié.*

L'objectif de ce travail de doctorat est de valider cette nouvelle architecture membranaire et de caractériser l'impact des polyisoprènes apolaires sur les propriétés physico-chimiques et mécaniques de la membrane. En conséquence, je cherche à évaluer si les polyisoprènes apolaires, qui sont largement distribués tout au long du domaine Archaea (Salvador-Castell et al., 2019b), sont effectivement des régulateurs membranaires. Autrement dit, s'ils sont capables de modifier les propriétés physicochimiques de la membrane pour une meilleure adaptation aux conditionnes extrêmes.

En premier lieu, pour valider le nouveau modèle d'architecture membranaire, il a été nécessaire d'établir et de caractériser les propriétés physico-chimiques d'une bicouche lipidique avec lipides de type archée, qui servira comme modèle de membrane d'archée tout au long de ce travail de thèse. Nous avons choisi de travailler avec deux lipides d'archées synthétiques disponibles commercialement, le 1,2-O-diphytanoyl-sn-glycero-3-phosphocholine (DoPhPC) et le 1,2-O-diphytanoyl-sn-glycero-3-phosphoethanolamine (DoPhPE) en proportion molaire 9 : 1. Comme modèle de polyisoprène apolaire, nous avons utilisé le squalane.

Dans un premier temps, j'ai cherché à localiser les polyisoprènes non-polaires dans la membrane reconstruite avec nos lipides synthétiques. En utilisant le contraste neutronique entre le deutérium et l'hydrogène, j'ai démontré par diffraction que le squalane se place au milieu de la bicouche lipidique perpendiculairement aux chaines lipidiques, quelques soient les conditions en pression hydrostatique et température. Cette méthode de contraste entre H et D est basée sur la différence de diffraction entre ces deux isotopes de l'hydrogène : ^{1}H et ^{2}H (deutérium). Ainsi, la différence du profile de densité de deux bicouches lipidiques égales contenant squalane hydrogéné ou deutéré, montre la position du squalane (Figure 3).

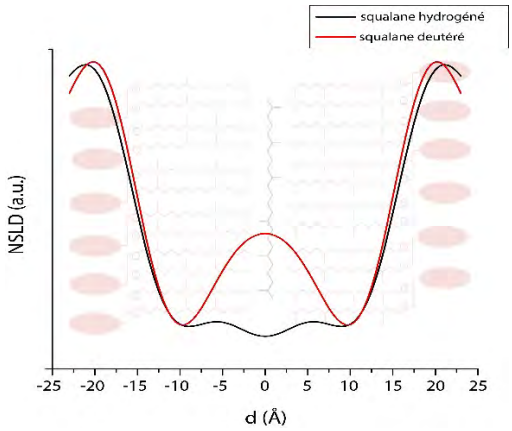

Figure 3. Profile de densité neutronique de DoPhPC: DoPhPE (9:1) en présence de squalane hydrogéné (noir) et deutéré (rouge). d représente l'épaisseur de la bicouche lipidique, étant d = 0 Å son centre.

À partir des profils de densité, j'ai déterminé les paramètres de la bicouche en absence et en présence du lipide apolaire. Je montre une augmentation de l'épaisseur de la région hydrophobe de la bicouche lipidique. Cette augmentation est dépendante de la quantité de squalane. Par exemple, l'épaisseur de la bicouche en absence de squalane est de 32.2 ± 0.2 Å et de 39.2 ± 0.2 Å en présence de 5 mol%.

Une fois démontrée la localisation des polyisoprènes apolaires au milieu de la bicouche, j'ai fait une caractérisation exhaustive des effets de leur présence dans la bicouche sur les paramètres de la membrane, et par conséquent, démontré si ces lipides apolaires peuvent jouer le rôle de régulateurs membranaires. Dans ce but, j'ai étudié différents paramètres physicochimiques du modèle membranaire : courbure membranaire, organisation latérale, perméabilité et fluidité.

La courbure membranaire a été mesurée par diffusion des rayonnements X aux petits angles (SAXS, Small Angle X-ray Scattering). Cette technique détermine l'autoassemblage de phospholipides en solution. Les différents types de phases lipidiques apportent des informations sur la courbure membranaire. Par exemple, la phase lamellaire indique une courbure nulle de la membrane, tandis qu'une phase cubique ou hexagonale inverse indiquent que les lipides adoptent une courbure négative. Mes résultats montrent qu'en ajoutant du squalane à la bicouche de lipides d'archées, la membrane adopte une structuration latérale plus grande et une courbure plus négative puisque les lipides s'autoassemblent en phases cubiques et hexagonales inverses (Figure 4). Les régions de courbures différentes de zéro sont essentielles pour diverses fonctions cellulaires, telles que l'ancrage de certaines protéines membranaires, la fusion ou la fission des membranes. De manière intéressante, en absence

de squalane nous n'observons aucune formation de ces phases cubiques et hexagonales. Ainsi, la présence de polyisoprènes apolaires dans la membrane lui apporte de nouvelles fonctionnalités.

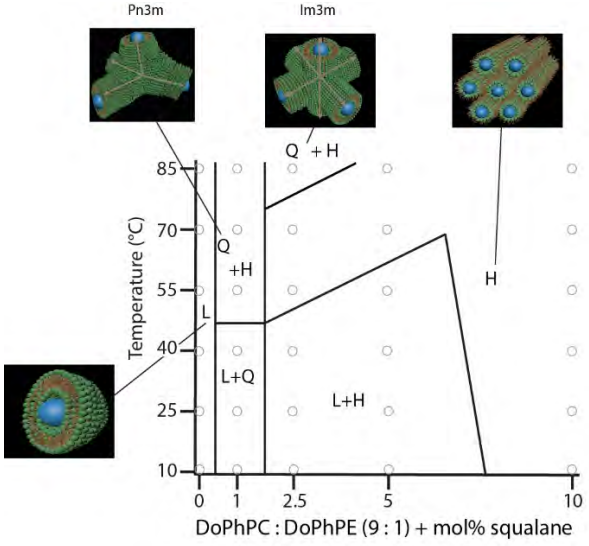

Figure 4. Diagramme de phases de DoPhPC : DoPhPE (9 : 1) avec différents pourcentages de squalane. Les phases représentées sont L : lamellaire, Q : cubique et H : hexagonale. Les cercles gris représentent les conditionnes mesurées. Les têtes polaires sont représentées en vert et les chaines hydrophobes en marron, l'eau est représentée par les sphères bleues.

En outre, par diffraction neutronique, nous avons observé une coexistence de phases induites par la présence du polyisoprène et la HT. Cette nouvelle phase est une phase lamellaire présentant un paramètre de maille, c.-à-d. une épaisseur de la bicouche lipidique et des couches d'eau qui l'entourent, plus grande que la phase originale : 74.1 ± 0.5 Å contre 52.8 ± 0.5 Å pour en présence ou absence de 2.5 mol% squalane à 25°C respectivement. Par ailleurs, la coexistence des deux phases présente un grand ordre puisque les diffractogrammes montrent une répétition dans le plan de la membrane d'environ 470 ± 20 Å (Figure 5). L'organisation latérale qu'apportent les lipides apolaires est fondamentale pour la membrane cellulaire puisqu'elle ne doit pas être complètement homogène et permet de former des domaines ordonnés différentiellement, possédant donc des propriétés physiques différentes, capables de porter des fonctions biologiques spécialisées. Il s'agit de la première mise en évidence que des domaines membranaires pourraient exister dans la membrane des archées, et qu'elle pourrait donc être compartimentalisée comme l'est la membrane des eucaryotes ou des bactéries.

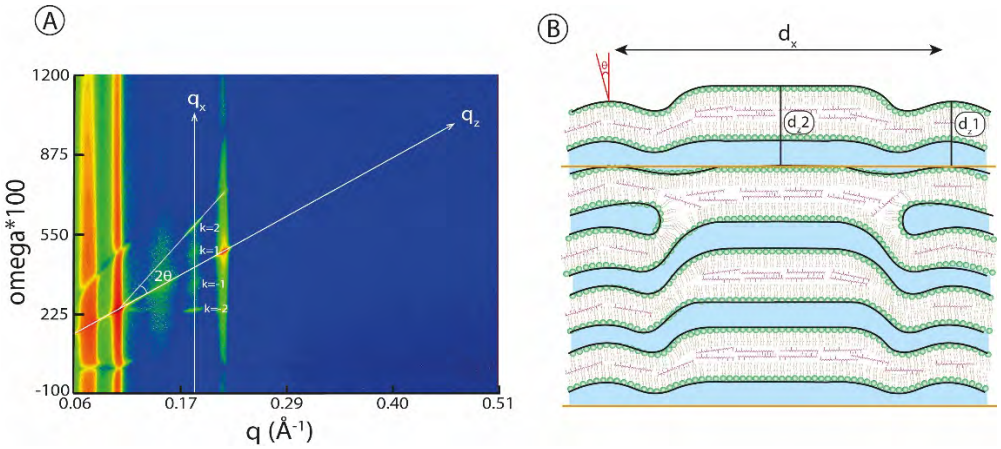

Figure 5. A) signal obtenu par diffraction neutronique à partir de DoPhPC : DoPhPE (9 : 1) en présence de 10 mol% squalane où ils sont facilement détectables les pics de Bragg dans les deux directions : la normale, q_z et le plan, q_x. B) représentation graphique du diffractogramme d'A. Les têtes polaires des lipides sont en vert, les chaines hydrophobes en marron, le squalane en magenta et l'eau en bleu.

Finalement, en utilisant d'approches de fluorescence, j'ai déterminé la perméabilité membranaire à l'eau et aux protons et la fluidité membranaire en absence et présence de squalane. La présence des lipides apolaires augmente la perméabilité à l'eau à HT mais diminue la perméabilité de la membrane aux protons à HPH, tandis que la fluidité membranaire est significativement affectée uniquement en présence de la plus haute concentration de squalane utilisée : 10 mol%. D'un côté, l'induction de perméabilité à l'eau du squalane pourrait servir pour contrôler et adapter cette propriété de la membrane en fonction des conditions environnementales, car la bicouche lipidique des archées est très imperméable à l'eau. D'un autre côté, la baisse de la perméabilité aux protons serait très utile à la cellule pour maintenir le gradient de protons qui essentiel pour synthétiser de l'ATP et contrôler le fonctionnement des protéines transmembranaires.

L'ensemble des résultats de cette thèse valident une nouvelle architecture membranaire où les polyisoprènes apolaires, placés au milieu de la bicouche lipidique, sont capables de jouer le rôle de régulateurs membranaires. Ces lipides apolaires apportent deux caractéristiques basiques, mais essentielles pour n'importe quelle membrane cellulaire fonctionnelle : dynamisme et hétérogénéité. La proportion en lipide apolaire permet de moduler la courbure membranaire, ce qui apporte le dynamisme nécessaire pour l'adaptation homéovisqueuse, et la coexistence de phases, c'est-à-dire l'hétérogénéité nécessaire (Figure 6) pour fonctionnaliser la membrane. Tout cela se fait en augmentant la stabilité membranaire en pression hydrostatique et en température qui permet à une bicouche d'être stable et biologiquement fonctionnelle y compris à des températures proches de 100°C. Mon travail met donc en évidence une nouvelle route adaptative aux milieux extrêmes qui n'implique pas la synthèse de lipides dipolaires. Ce nouveau modèle membranaire pourrait être applicable

aux premières cellules et expliquer comment celles-ci ont pu créer des protomembranes stables dans les conditions extrêmes des systèmes hydrothermaux profonds.

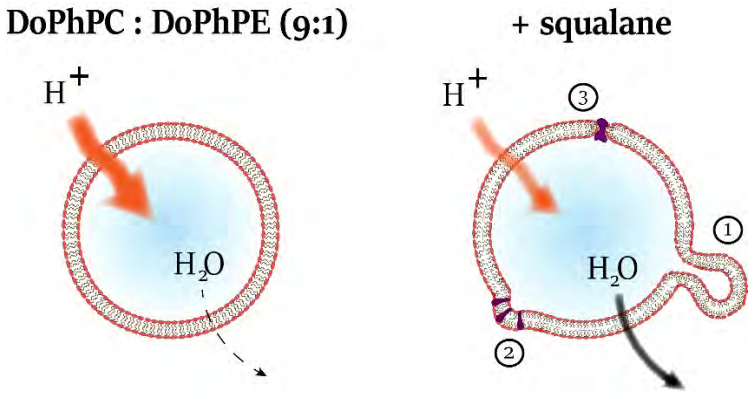

Figure 6. Représentation graphique de l'effet du squalane à HT et HPH. La présence de ce polyisoprène diminue la perméabilité membranaire aux protons et augmente celle à l'eau. En outre, le squalane induit la formation de domaines membranaires lesquelles pourraient être utiles pour la fission (1), ancrage de protéines (2) et positionner protéines transmembranaires (3).

References

Abe, F., 2007. Exploration of the effects of high hydrostatic pressure on microbial growth, physiology and survival: perspectives from piezophysiology. *Bioscience, Biotechnology, and Biochemistry* **71**, 2347–2357. https://doi.org/10.1271/bbb.70015

Abe, F., Kato, C., Horikoshi, K., 1999. Pressure-regulated metabolism in microorganisms. *Trends in Microbiology* **7**, 447–453. https://doi.org/10.1016/S0966-842X(99)01608-X

Adkins, I., Hradilova, N., Palata, O., Sadilkova, L., Palova-Jelinkova, L., Spisek, R., 2018. High hydrostatic pressure in cancer immunotherapy and biomedicine. *Biotechnology Advances* **36**, 577–582. https://doi.org/10.1016/j.biotechadv.2018.01.015

Ahammer, L., Grutsch, S., Kamenik, A.S., Liedl, K.R., Tollinger, M., 2017. Structure of the major apple allergen Mal d 1. *Journal of Agricultural and Food Chemistry* **65**, 1606–1612. https://doi.org/10.1021/acs.jafc.6b05752

Al-Awqati, Q., 1999. One hundred years of membrane permeability: Does overton still rule? *Nature Cell Biology* **1**, E201–E202. https://doi.org/10.1038/70230

Al-Ayoubi, S.R., Schummel, P.H., Golub, M., Peters, J., Winter, R., 2017. Influence of cosolvents, self-crowding, temperature and pressure on the sub-nanosecond dynamics and folding stability of lysozyme. *Physical Chemistry Chemical Physics* **19**, 14230–14237. https://doi.org/10.1039/c7cp00705a

Alain, K., Marteinsson, V.T., Miroshnichenko, M.L., Bonch-Osmolovskaya, E.A., Prieur, D., Birrien, J.-L., 2002. *Marinitoga piezophila* sp. nov., a rod-shaped, thermo-piezophilic bacterium isolated under high hydrostatic pressure from a deep-sea hydrothermal vent. *International Journal of Systematic and Evolutionary Microbiology* **52**, 1331–1339. https://doi.org/10.1099/ijs.0.02068-0

Aloi, E., Oranges, M., Guzzi, R., Bartucci, R., 2017. Low-temperature dynamics of chain-labeled lipids in ester- and ether-linked phosphatidylcholine membranes. *The Journal of Physical Chemistry B* **121**, 9239–9246. https://doi.org/10.1021/acs.jpcb.7b07386

Ananta, E., Knorr, D., 2004. Evidence on the role of protein biosynthesis in the induction of heat tolerance of *Lactobacillus rhamnosus* GG by pressure pre-treatment. *International Journal of Food Microbiology* **96**, 307–313. https://doi.org/10.1016/j.ijfoodmicro.2004.04.012

Andersson, M., Jackman, J., Wilson, D., Jarvoll, P., Alfredsson, V., Okeyo, G., Duran, R., 2011. Vesicle

and bilayer formation of diphytanoylphosphatidylcholine (DPhPC) and diphytanoylphosphatidylethanolamine (DPhPE) mixtures and their bilayers' electrical stability. *Colloids and Surfaces B: Biointerfaces* **82**, 550–561. https://doi.org/10.1016/j.colsurfb.2010.10.017

Angelova, M.I., Bitbol, A.-F., Seigneuret, M., Staneva, G., Kodama, A., Sakuma, Y., Kawakatsu, T., Imai, M., Puff, N., 2018. pH sensing by lipids in membranes: the fundamentals of pH-driven migration, polarization and deformations of lipid bilayer assemblies. *Biochimica et Biophysica Acta (BBA) - Biomembranes* **1860**, 2042–2063. https://doi.org/10.1016/j.bbamem.2018.02.026

Antollini, S.S., Barrantes, F.J., 1998. Disclosure of discrete sites for phospholipid and sterols at the protein - lipid interface in native acetylcholine receptor-rich membrane. *Biochemistry* **37**, 16653–16662. https://doi.org/10.1021/bi9808215

Arp, A.J., Childress, J.J., 1983. Sulfide binding by the blood of the hydrothermal vent tube worm *Riftia pachyptila*. *Science* **219**, 295–297. https://doi.org/10.1126/science.219.4582.295

Ashrafzadeh, P., Parmryd, I., 2015. Methods applicable to membrane nanodomain studies? *Essays In Biochemistry* **57**, 57–68. https://doi.org/10.1042/bse0570057

Baba, T., Toshima, Y., Minamikawa, H., Hato, M., Suzuki, K., Kamo, N., 1999. Formation and characterization of planar lipid bilayer membranes from synthetic phytanyl-chained glycolipids. *Biochimica et Biophysica Acta - Biomembranes* **1421**, 91–102. https://doi.org/10.1016/S0005-2736(99)00114-5

Bae, W., Yoon, T.-Y., 2013. Properties of self-quenching fluorescence dye for vesicle-vesicle content mixing system. *Biophysical Journal* **104**, 88a. https://doi.org/10.1016/j.bpj.2012.11.527

Bagatolli, L., 2012. Laurdan fluorescence properties in membranes: a journey form the fluorometer to the microscope, in: Mély, Y., Guportail, G. (Eds.), Fluorescent Methods to Study Biological Membranes. Springer-Verlag Berlin Heidelberg, pp. 3–35. https://doi.org/10.1007/4243_2012_42

Bagatolli, L., Gratton, E., Khan, T.K., Chong, P.L., 2000. Two-photon fluorescence microscopy studies of bipolar tetraether giant liposomes from thermoacidophilic archaebacteria *Sulfolobus acidocaldarius. Biophys J* **79**, 416–425. https://doi.org/10.1016/S0006-3495(00)76303-X

Bagatolli, L.A., Ipsen, J.H., Simonsen, A.C., Mouritsen, O.G., 2010. An outlook on organization of lipids in membranes: Searching for a realistic connection with the organization of biological membranes. *Progress in Lipid Research* **49**, 378–389. https://doi.org/10.1016/j.plipres.2010.05.001

Balasubramaniam, V.M. (Bala), Martínez-Monteagudo, S.I., Gupta, R., 2015. Principles and application of high pressure–based technologies in the food industry. *Annual Review of Food Science and Technology* **6**, 435–462. https://doi.org/10.1146/annurev-food-022814-015539

Balleza, D., Garcia-Arribas, A.B., Sot, J., Ruiz-Mirazo, K., Goñi, F.M., 2014. Ether- *versus* ester-linked phospholipid bilayers containing either linear or branched apolar chains. *Biophysical Journal* **107**, 1364–1374. https://doi.org/10.1016/j.bpj.2014.07.036

Balny, C., Masson, P., Heremans, K., 2002. High pressure effects on biological macromolecules: from structural changes to alteration of cellular processes. *Biochimica et Biophysica Acta (BBA) - Protein Structure and Molecular Enzymology* **1595**, 3–10. https://doi.org/10.1016/S0167-4838(01)00331-4

Banciu, H., Sorokin, D.Y., Rijpstra, W.I.C., Sinninghe Damsté, J.S., Galinski, E.A., Takaichi, S., Muyzer, G., Kuenen, J.G., 2005. Fatty acid, compatible solute and pigment composition of obligately

chemolithoautotrophic alkaliphilic sulfur-oxidizing bacteria from soda lakes. *FEMS Microbiology Letters* **243**, 181–187. https://doi.org/10.1016/j.femsle.2004.12.004

Baoukina, S., Mendez-Villuendas, E., Bennett, W.F.D., Tieleman, D.P., 2012. Computer simulations of the phase separation in model membranes. *Faraday Discussions* **161**, 63–75. https://doi.org/10.1039/c2fd20117h

Barriga, H.M.G., Holme, M.N., Stevens, M.M., 2019. Cubosomes: the next generation of smart lipid nanoparticles? *Angewandte Chemie - International Edition* **58**, 2958–2978. https://doi.org/10.1002/anie.201804067

Bartlett, D.H., 2002. Pressure effects on in vivo microbial processes. *Biochimica et Biophysica Acta 1595* **1595**, 367–381. https://doi.org/10.1002/smj

Bartlett, D.H., 1999. Microbial adaptations to the psychrosphere/piezosphere. *Journal of molecular microbiology and biotechnology* **1**, 93–100.

Bartlett, D.H., Kato, C., Horikoshi, K., 1995. High pressure influences on gene and protein expression. *Research in Microbiology* **146**, 697–706. https://doi.org/10.1016/0923-2508(96)81066-7

Baumgart, T., Hunt, G., Farkas, E.R., Webb, W.W., Feigenson, G.W., 2007. Fluorescence probe partitioning between Lo/Ld phases in lipid membranes. *Biochimica et Biophysica Acta - Biomembranes* **1768**, 2182–2194. https://doi.org/10.1016/j.bbamem.2007.05.012

Bée, M., 1988. Quasielastic neutron scattering: principles and applications in solid state chemistry, biology and materials science. Adam Hilger, Philadelphia, PA.

Benvegnu, T., Lemiègre, L., Cammas-marion, S., 2009. New generation of liposomes called archaeosomes based on natural or synthetic archaeal lipids as innovative formulations for drug delivery. *Recent Patents on Drug Delivery & Formulation* **33**, 206–220. https://doi.org/10.2174/187221109789105630

Berglund, A.H., Nilsson, R., Liljenberg, C., 1999. Permeability of large unilamellar digalactosyldiacylglycerol vesicles for protons and glucose - Influence of α-tocopherol, β-carotene, zeaxanthin and cholesterol. *Plant Physiology and Biochemistry* **37**, 179–186. https://doi.org/10.1016/S0981-9428(99)80032-1

Bhattacharya, S., Haldar, S., 2000. Interactions between cholesterol and lipids in bilayer membranes. Role of lipid headgroup and hydrocarbon chain-backbone linkage. *Biochimica et Biophysica Acta - Biomembranes* **1467**, 39–53. https://doi.org/10.1016/S0005-2736(00)00196-6

Bidle, K.A., Bartlett, D.H., 1999. RecD function is required for high-pressure growth of a deep-sea bacterium. *Journal of Bacteriology* **181**, 2330–2337.

Birrien, J.L., Zeng, X., Jebbar, M., Cambon-Bonavita, M.A., Quérellou, J., Oger, P., Bienvenu, N., Xiao, X., Prieur, D., 2011. *Pyrococcus yayanosii* sp. nov., an obligate piezophilic hyperthermophilic archaeon isolated from a deep-sea hydrothermal vent. *International Journal of Systematic and Evolutionary Microbiology* **61**, 2827–2831. https://doi.org/10.1099/ijs.0.024653-0

Biscoito, M., Segonzac, M., Almeida, A.J., Desbruyères, D., Geistdoerfer, P., Turnipseed, M., Van Dover, C., 2002. Fishes from the hydrothermal vents and cold seeps - An update. *CBM - Cahiers de Biologie Marine* **43**, 359–362.

Black, E.P., Setlow, P., Hocking, A.D., Stewart, C.M., Kelly, A.L., Hoover, D.G., 2007. Response of spores to high-pressure processing. *Comprehensive Reviews in Food Science and Food Safety* **6**, 103–119. https://doi.org/10.1111/j.1541-4337.2007.00021.x

Blicher, A., Wodzinska, K., Fidorra, M., Winterhalter, M., Heimburg, T., 2009. The temperature

dependence of lipid membrane permeability, its quantized nature, and the influence of anesthetics. *Biophysical Journal* **96**, 4581–4591. https://doi.org/10.1016/j.bpj.2009.01.062

Bliznyuk, A., Golan, H., Grossman, Y., 2018. Marine mammals' NMDA receptor structure: possible adaptation to high pressure environment. *Frontiers in Physiology* **9**, 1–12. https://doi.org/10.3389/fphys.2018.01633

Blok, M.C., Van Der Neut-Kok, E.C.M., Van Deenen, L.L.M., De Gier, J., 1975. The effect of chain length and lipid phase transitions on the selective permeability properties of liposomes. *BBA - Biomembranes* **406**, 187–196. https://doi.org/10.1016/0005-2736(75)90003-6

Boehr, D.D., McElheny, D., Dyson, H.J., Wright, P.E., 2010. Millisecond timescale fluctuations in dihydrofolate reductase are exquisitely sensitive to the bound ligands. *Proceedings of the National Academy of Sciences* **107**, 1373–1378. https://doi.org/10.1073/pnas.0914163107

Bothun, G.D., Knutson, B.L., Berberich, J.A., Strobel, H.J., Nokes, S.E., 2004. Metabolic selectivity and growth of *Clostridium thermocellum* in continuous culture under elevated hydrostatic pressure. *Applied Microbiology and Biotechnology* **65**, 149–157. https://doi.org/10.1007/s00253-004-1554-1

Briggs, J., Chung, H., Caffrey, M., Phase, T.T., 1996. The temperature-composition phase diagram and mesophase structure characterization of the monoolein / water system. *J. Phys. II France* **6**, 723–751. https://doi.org/10.1051/jp2:1996208

Bright, M., Lallier, F.H., 2010. The biology of vestimentiferan tubeworms. *Oceanography and Marine Biology: An Annual Review* **48**, 213–266.

Brooks, N.J., 2014. Pressure effects on lipids and bio-membrane assemblies. *IUCrJ* **1**, 470–477. https://doi.org/10.1107/S2052252514019551

Brooks, N.J., Ces, O., Templer, R.H., Seddon, J.M., 2011. Pressure effects on lipid membrane structure and dynamics. *Chemistry and Physics of Lipids* **164**, 89–98. https://doi.org/10.1016/j.chemphyslip.2010.12.002

Brooks, N.J., Gauthe, B.L.L.E., Terrill, N.J., Rogers, S.E., Templer, R.H., Ces, O., Seddon, J.M., 2010. Automated high pressure cell for pressure jump x-ray diffraction. *Review of Scientific Instruments* **81**, 1–10. https://doi.org/10.1063/1.3449332

Brouillet, M., Gautier, H., Miègeville, A.F., Bouler, J.M., Merle, C., Caillon, J., 2009. Inactivation of *Staphylococcus aureus* in calcium phosphate biomaterials via isostatic compression. *Journal of Biomedical Materials Research - Part B Applied Biomaterials* **91**, 348–353. https://doi.org/10.1002/jbm.b.31408

Brown, A., Thatje, S., 2018. NMDA receptor regulation is involved in the limitation of physiological tolerance to both low temperature and high hydrostatic pressure. *Frontiers in Marine Science* **5**, 1–4. https://doi.org/10.3389/fmars.2018.00093

Brown, D.A., London, E., 1998. Functions of lipid rafts in biological membranes. *Annual Review of Cell and Developmental Biology* **14**, 111–136. https://doi.org/10.1146/annurev.cellbio.14.1.111

Bull, M.K., Zerdin, K., Howe, E., Goicoechea, D., Paramanandhan, P., Stockman, R., Sellahewa, J., Szabo, E.A., Johnson, R.L., Stewart, C.M., 2004. The effect of high pressure processing on the microbial, physical and chemical properties of Valencia and Navel orange juice. *Innovative Food Science and Emerging Technologies* **5**, 135–149. https://doi.org/10.1016/j.ifset.2003.11.005

Butz, P., Koller, W.D., Tauscher, B., Wolf, S., 1994. Ultra-high pressure processing of onions: chemical and sensory changes. *LWT - Food Science and Technology* **27**, 463–467.

https://doi.org/10.1006/fstl.1994.1093

Callac, N., Oger, P., Lesongeur, F., Rattray, J.E., Vannier, P., Michoud, G., Beauverger, M., Gayet, N., Rouxel, O., Jebbar, M., Godfroy, A., 2016. *Pyrococcus kukulkanii* sp. nov., a hyperthermophilic, piezophilic archaeon isolated from a deep-sea hydrothermal vent. *International Journal of Systematic and Evolutionary Microbiology* **66**, 3142–3149. https://doi.org/10.1099/ijsem.0.001160

Campanaro, S., Vezzi, A., Vitulo, N., Lauro, F.M., D'Angelo, M., Simonato, F., Cestaro, A., Malacrida, G., Bertoloni, G., Valle, G., Bartlett, D.H., 2005. Laterally transferred elements and high pressure adaptation in *Photobacterium profundum* strains. *BMC Genomics* **6**, 1–15. https://doi.org/10.1186/1471-2164-6-122

Cario, A., Grossi, V., Schaeffer, P., Oger, P.M., 2015. Membrane homeoviscous adaptation in the piezo-hyperthermophilic archaeon *Thermococcus barophilus*. *Frontiers in Microbiology* **6**, 1–12. https://doi.org/10.3389/fmicb.2015.01152

Cario, A., Jebbar, M., Thiel, A., Kervarec, N., Oger, P.M., 2016. Molecular chaperone accumulation as a function of stress evidences adaptation to high hydrostatic pressure in the piezophilic archaeon *Thermococcus barophilus*. *Scientific Reports* **6**, 1–8. https://doi.org/10.1038/srep29483

Castellini, M.A., Castellini, J.M., Rivera, P.M., 2001. Adaptations to pressure in the RBC metabolism of diving mammals. *Comparative Biochemistry and Physiology - A Molecular and Integrative Physiology* **129**, 751–757. https://doi.org/10.1109/CEIDP.2008.4772920

Cebecauer, M., Amaro, M., Jurkiewicz, P., Sarmento, M.J., Šachl, R., Cwiklik, L., Hof, M., 2018. Membrane lipid nanodomains. *Chemical Reviews* **118**, 11259–11297. https://doi.org/10.1021/acs.chemrev.8b00322

Chang, E.L., 1994. Unusual thermal stability of liposomes made from bipolar tetraether lipids. *Biochemical and Biophysical Research Communications*. https://doi.org/10.1006/bbrc.1994.1983

Cheetham, J.J., Wachtel, E., Bach, D., Epand, R.M., 1989. Role of the stereochemistry of the hydroxyl group of cholesterol and the formation of monbilayer structures in phosphatidylethanolamines. *Biochemistry* **28**, 8928–8934. https://doi.org/10.1021/bi00448a036

Chen, R.F., Knutson, J.R., 1988. Mechanism of fluorescence concentration quenching of carboxyfluorescein in liposomes: energy transfer to nonfluorescent dimers. *Analytical Biochemistry* **172**, 61–77. https://doi.org/10.1016/0003-2697(88)90412-5

Chernomordik, L. V., Kozlov, M.M., 2003. Protein-lipid interplay in fusion and fission of biological membranes. *Annual Review of Biochemistry* **72**, 175–207. https://doi.org/10.1146/annurev.biochem.72.121801.161504

Cheung, C.Y., Green, D.J., Litt, G.J., Laugharn, J.A., 1998. High-pressure-mediated dissociation of immune complexes demonstrated in model systems. *Clinical Chemistry* **44**, 299–303.

Chicón, R., Belloque, J., Alonso, E., Mart N-Lvarez, P.J., Pez-Fandi, A.R.L., 2008. Hydrolysis under high hydrostatic pressure as a means to reduce the binding of β-Lactoglobulin to immunoglobulin E from human sera. *Journal of Food Protection* **71**, 1453–1459. https://doi.org/10.4315/0362-028X-71.7.1453

Chong, P.L.G., 2010. Archaebacterial bipolar tetraether lipids: physico-chemical and membrane properties. *Chemistry and Physics of Lipids* **163**, 253–265. https://doi.org/10.1016/j.chemphyslip.2009.12.006

Chong, P.L.G., 1988. Effects of hydrostatic pressure on the location of Prodan in lipid bilayers and cellular membranes. *Biochemistry* **27**, 399–404. https://doi.org/10.1021/bi00401a060

Choquet, C.G., Patel, G.B., Sprott, G.D., Beveridge, T.J., 1994. Stability of pressure-extrudes liposomes made from archaeobacterial ether lipids. *Applied Microbiology and Biotechnology* **42**, 375–384. https://doi.org/10.1007/s002530050266

Chugunov, A.O., Volynsky, P.E., Krylov, N.A., Boldyrev, I.A., Efremov, R.G., 2014. Liquid but durable: molecular dynamics simulations explain the unique properties of archaeal-like membranes. *Scientific reports* **4**, 7462. https://doi.org/10.1038/srep07462

Chura-Chambi, R.M., Cordeiro, Y., Malavasi, N. V., Lemke, L.S., Rodrigues, D., Morganti, L., 2013. An analysis of the factors that affect the dissociation of inclusion bodies and the refolding of endostatin under high pressure. *Process Biochemistry* **48**, 250–259. https://doi.org/10.1016/j.procbio.2012.12.017

Clejan, S., Krulwich, T.A., Mondrus, K.R., Seto-Young, D., 1986. Membrane lipid composition of obligately and facultatively alkalophilic strains of *Bacillus* spp. *Journal of Bacteriology* **168**, 334–340. https://doi.org/10.1128/jb.168.1.334-340.1986

Collins, M.D., Hummer, G., Quillin, M.L., Matthews, B.W., Gruner, S.M., 2005. Cooperative water filling of a nonpolar protein cavity observed by high-pressure crystallography and simulation. *Proceedings of the National Academy of Sciences* **102**, 16668–16671. https://doi.org/10.1073/pnas.0508224102

Collins, M.D., Kim, C.U., Gruner, S.M., 2011. High-pressure protein crystallography and NMR to explore protein conformations. *Annual Review of Biophysics* **40**, 81–98. https://doi.org/10.1146/annurev-biophys-042910-155304

Connell, S.D., Smith, D.A., 2006. The atomic force microscope as a tool for studying phase separation in lipid membranes (review). *Molecular Membrane Biology* **23**, 17–28. https://doi.org/10.1080/09687860500501158

Costa, M.A., Mangione, M.R., Santonocito, R., Passantino, R., Giacomazza, D., Librizzi, F., Moran, O., Carrotta, R., 2018. Biophysical characterization of asolectin-squalene liposomes. *Colloids and Surfaces B: Biointerfaces* **170**, 479–487. https://doi.org/10.1016/j.colsurfb.2018.06.032

Cristiglio, V., Giroud, B., Didier, L., Demé, B., 2015. D16 is back to business: more neutrons, more space, more fun. *Neutron News* **26**, 22–24. https://doi.org/10.1080/10448632.2015.1057051

Dalmaso, G.Z.L., Ferreira, D., Vermelho, A.B., 2015. Marine extremophiles a source of hydrolases for biotechnological applications. *Marine Drugs* **13**, 1925–1965. https://doi.org/10.3390/md13041925

Dalmasso, C., Oger, P., Selva, G., Courtine, D., L'Haridon, S., Garlaschelli, A., Roussel, E., Miyazaki, J., Reveillaud, J., Jebbar, M., Takai, K., Maignien, L., Alain, K., 2016. *Thermococcus piezophilus* sp. nov., a novel hyperthermophilic and piezophilic archaeon with a broad pressure range for growth, isolated from a deepest hydrothermal vent at the Mid-Cayman Rise. *Systematic and Applied Microbiology* **39**, 440–444. https://doi.org/10.1016/j.syapm.2016.08.003

Daniel, I., Oger, P., Winter, R., 2006. Origins of life and biochemistry under high-pressure conditions. *Chemical Society Reviews* **35**, 858–875. https://doi.org/10.1039/b517766a

Dante, S., Hauss, T., Dencher, N.A., 2002. β-Amyloid 25 to 35 is intercalated in anionic and zwitterionic lipid membranes to different extents **83**, 2610–2616.

de Ghellinck, A., Shen, C., Fragneto, G., Klösgen, B., 2015. Probing the position of resveratrol in lipid

bilayers: a neutron reflectivity study. *Colloids and Surfaces B: Biointerfaces* **134**, 65–72. https://doi.org/10.1016/j.colsurfb.2015.06.028

De Rosa, M., Gambacorta, A., Gliozzi, A., 1986. Structure, biosynthesis, and physicochemical properties of archaebacterial lipids. *Microbiological reviews* **50**, 70–80.

De Rosa, M., Gambacorta, A., Nicolaus, B., 1983. A new type of cell membrane, in thermophilic archaebacteria, based on bipolar ether lipids. *Journal of Membrane Science* **16**, 287–294. https://doi.org/10.1016/S0376-7388(00)81316-2

Decoursey, T.E., 2003. Voltage-gated proton channels and other proton transfer pathways. *Physiological Reviews* **83**, 475–579. https://doi.org/10.1152/physrev.00028.2002

Demazeau, G., Rivalain, N., 2011. High hydrostatic pressure and biology: a brief history. *Applied Microbiology and Biotechnology* **89**, 1305–1314. https://doi.org/10.1007/s00253-010-3070-9

Ding, L., Weiss, T.M., Fragneto, G., Liu, W., Yang, L., Huang, H.W., 2005. Distorted hexagonal phase studied by neutron diffraction: lipid components demixed in a bent monolayer. *Langmuir* **21**, 203–210. https://doi.org/10.1021/la047876u

Ding, W., Palaiokostas, M., Shahane, G., Wang, W., Orsi, M., 2017. Effects of high pressure on phospholipid bilayers. *Journal of Physical Chemistry B* **121**, 9597–9606. https://doi.org/10.1021/acs.jpcb.7b07119

Dobereiner, H., Käs, J., Noppl, D., Sprenger, I., Sackmann, E., 1993. Budding and fission of vesicles. *Biophysical Journal* **65**, 1396–1403. https://doi.org/10.1016/S0006-3495(93)81203-7

Dover, C.L. Van, German, C.R., Speer, K.G., Parson, L.M., Vrijenhoek, R.C., 2002. Evolution and biogeography of deep-sea vent and seep invertebrates. *Science* **295**, 1253–1257. https://doi.org/10.1126/science.1067361

Dowhan, W., 1997. Molecular basis for membrane phospholipid diversity: Why are there so many lipids? *Annual Review of Biochemistry* **66**, 199–232. https://doi.org/10.1146/annurev.biochem.66.1.199

Dumard, C.H., Barroso, S.P.C., Santos, A.C. V., Alves, N.S., Couceiro, J.N.S.S., Gomes, A.M.O., Santos, P.S., Silva, J.L., Oliveira, A.C., 2017. Stability of different influenza subtypes: How can high hydrostatic pressure be a useful tool for vaccine development? *Biophysical Chemistry* **231**, 116–124. https://doi.org/10.1016/j.bpc.2017.04.002

Dumorné, K., Córdova, D.C., Astorga-Eló, M., Renganathan, P., 2017. Extremozymes: a potential source for industrial applications. *Journal of Microbiology and Biotechnology* **27**, 649–659. https://doi.org/10.4014/jmb.1611.11006

Dutra Albuquerque, E., Gonçalves Torres, F.A., Ribeiro Fernandes, A.A., Fernandes, P.M.B., 2016. Combined effects of high hydrostatic pressure and specific fungal cellulase improve coconut husk hydrolysis. *Process Biochemistry* **51**, 1767–1775. https://doi.org/10.1016/j.procbio.2016.07.010

Eisenmenger, M.J., Reyes-De-Corcuera, J.I., 2009. High pressure enhancement of enzymes: a review. *Enzyme and Microbial Technology* **45**, 331–347. https://doi.org/10.1016/j.enzmictec.2009.08.001

El Jastimi, R., Edwards, K., Lafleur, M., 1999. Characterization of permeability and morphological perturbations induced by nisin on phosphatidylcholine membranes. *Biophysical Journal* **77**, 842–852. https://doi.org/10.1016/S0006-3495(99)76936-5

Elferink, M.G.L., de Wit, J.G., Driessen, A.J.M., Konings, W.N., 1994. Stability and proton-permeability

of liposomes composed of archaeal tetraether lipids. *Biochimica et Biophysica Acta (BBA) - Biomembranes* **1193**, 247–254. https://doi.org/10.1016/0005-2736(94)90160-0

Ellens, H., Siegel, D.P., Alford, D., Yeagle, P.L., Boni, L., Lis, L.J., Quinn, P.J., Bentz, J., 1989. Membrane fusion and inverted phases. *Biochemistry* **28**, 3692–3703. https://doi.org/10.1021/bi00435a011

Engelman, D.M., 2005. Membranes are more mosaic than fluid. *Nature* **438**, 578–580. https://doi.org/10.1038/nature04394

Eriksson, E.K., Agmo Hernández, V., Edwards, K., 2018. Effect of ubiquinone-10 on the stability of biomimetic membranes of relevance for the inner mitochondrial membrane. *Biochimica et Biophysica Acta (BBA) - Biomembranes* **1860**, 1205–1215. https://doi.org/10.1016/j.bbamem.2018.02.015

Ernst, R., Ejsing, C.S., Antonny, B., 2016. Homeoviscous adaptation and the regulation of membrane lipids. *Journal of Molecular Biology* **428**, 4776–4791. https://doi.org/10.1016/j.jmb.2016.08.013

Estevez-Burugorri, L., Degraeve, P., Espeillac, S., Lemay, P., 2000. High-pressure induced recovery of β-galactosidases from immunoadsorbents: stability of antigens and antibodies. Comparison with usual elution procedures. *Biotechnology Letters* **22**, 1319–1329. https://doi.org/10.1023/A:1005659215110

Evert-Arriagada, K., Hernández-Herrero, M.M., Juan, B., Guamis, B., Trujillo, A.J., 2012. Effect of high pressure on fresh cheese shelf-life. *Journal of Food Engineering* **110**, 248–253. https://doi.org/10.1016/j.jfoodeng.2011.05.011

Fang, J., Zhang, L., Bazylinski, D.A., 2010. Deep-sea piezosphere and piezophiles : geomicrobiology and biogeochemistry. *Trends in Microbiology* **18**, 413–422. https://doi.org/10.1016/j.tim.2010.06.006

Farkas, D.F., Hoover, D.G., 2000. High pressure processing. *Journal of Food Science,* **65**, 47–64.

Feller, G., 2013. Psychrophilic enzymes: from folding to function and biotechnology. *Scientifica* **2013**, 1–28. https://doi.org/10.1155/2013/512840

Ferreira, E., Mendes, Y.S., Silva, J.L., Galler, R., Oliveira, A.C., Freire, M.S., Gaspar, L.P., 2009. Effects of hydrostatic pressure on the stability and thermostability of poliovirus: a new method for vaccine preservation. *Vaccine* **27**, 5332–5337. https://doi.org/10.1016/j.vaccine.2009.06.099

Frey, B., Franz, S., Sheriff, A., Korn, A., Bluemelhuber, G., Gaipl, U.S., Voll, R.E., Meyer-Pittroff, R., Herrmann, M., 2004. Hydrostatic pressure induced death of mammalian cells engages pathways related to apoptosis or necrosis. *Cellular and molecular biology* **50**, 459–467. https://doi.org/10.1170/T534

Frolov, V.A., Shnyrova, A. V., Zimmerberg, J., 2011. Lipid polymorphisms and membrane shape. *Cold Spring Harbor Perspectives in Biology* **3**. https://doi.org/10.1101/cshperspect.a004747

Gambacorta, A., Trincone, A., Nicolaus, B., Lama, L., De Rosa, M., 1993. Unique features of lipids of Archaea. *Systematic and Applied Microbiology* **16**, 518–527. https://doi.org/10.1016/S0723-2020(11)80321-8

Gan, B.S., Krump, E., Shrode, L.D., Grinstein, S., 1998. Loading pyranine via purinergic receptors or hypotonic stress for measurement of cytosolic pH by imaging. *American Journal of Physiology-Cell Physiology* **275**, C1158–C1166. https://doi.org/10.1152/ajpcell.1998.275.4.C1158

Gao, M., Berghaus, M., Möbitz, S., Schuabb, V., Erwin, N., Herzog, M., Julius, K., Sternemann, C., Winter, R., 2018. On the origin of microtubules' high-pressure sensitivity. *Biophysical Journal* **114**, 1080–1090. https://doi.org/10.1016/j.bpj.2018.01.021

Gao, M., Held, C., Patra, S., Arns, L., Sadowski, G., Winter, R., 2017. Crowders and cosolvents—Major contributors to the cellular milieu and efficient means to counteract environmental stresses. *ChemPhysChem* **18**, 2951–2972. https://doi.org/10.1002/cphc.201700762

Garcia, A.E., Paschek, D., 2008. Simulation of the pressure and temperature folding/unfolding equilibrium of a small RNA hairpin. *Journal of the American Chemical Society* **130**, 815–817. https://doi.org/10.1021/ja074191i

Gaudin, M., Gauliard, E., Schouten, S., Houel-Renault, L., Lenormand, P., Marguet, E., Forterre, P., 2013. Hyperthermophilic archaea produce membrane vesicles that can transfer DNA. *Environmental Microbiology Reports* **5**, 109–116. https://doi.org/10.1111/j.1758-2229.2012.00348.x

Gauger, D.R., Binder, H., Vogel, A., Selle, C., Pohle, W., 2002. Comparative FTIR-spectroscopic studies of the hydration of diphytanoylphosphatidylcholine and -ethanolamine, in: Journal of Molecular Structure. pp. 211–220. https://doi.org/10.1016/S0022-2860(02)00254-5

Gensure, R.H., Zeidel, M.L., Hill, W.G., 2006. Lipid raft components cholesterol and sphingomyelin increase H + /OH − permeability of phosphatidylcholine membranes . *Biochemical Journal* **398**, 485–495. https://doi.org/10.1042/bj20051620

George, K.S., Wu, S., 2012. Lipid raft: a floating island of death or survival. *Toxicology and Applied Pharmacology* **259**, 311–319. https://doi.org/10.1016/j.taap.2012.01.007

Giel-Pietraszuk, M., Barciszewski, J., 2005. A nature of conformational changes of yeast tRNAPhe: high hydrostatic pressure effects. *International Journal of Biological Macromolecules* **37**, 109–114. https://doi.org/10.1016/j.ijbiomac.2005.09.003

Gill, S., Catchpole, R., Forterre, P., 2019. Extracellular membrane vesicles in the three domains of life and beyond. *FEMS Microbiology Reviews* **43**, 273–303. https://doi.org/10.1093/femsre/fuy042

Girard, E., Marchal, S., Perez, J., Finet, S., Kahn, R., Fourme, R., Marassio, G., Dhaussy, A.C., Prangé, T., Giffard, M., Dulin, F., Bonneté, F., Lange, R., Abraini, J.H., Mezouar, M., Colloc'h, N., 2010. Structure-function perturbation and dissociation of tetrameric urate oxidase by high hydrostatic pressure. *Biophysical Journal* **98**, 2356–2364. https://doi.org/10.1016/j.bpj.2010.01.058

Gliozzi, A., Relini, A., Chong, P.L.G., 2002. Structure and permeability properties of biomimetic membranes of bolaform archaeal tetraether lipids. *Journal of Membrane Science* **206**, 131–147. https://doi.org/10.1016/S0376-7388(01)00771-2

Gmajner, D., Grabnar, P.A., Žnidarič, M.T., Štrus, J., Šentjurc, M., Ulrih, N.P., 2011. Structural characterization of liposomes made of diether archaeal lipids and dipalmitoyl-L-α-phosphatidylcholine. *Biophysical Chemistry* **158**, 150–156. https://doi.org/10.1016/j.bpc.2011.06.014

Golub, M., Lehofer, B., Martinez, N., Ollivier, J., Kohlbrecher, J., Prassl, R., Peters, J., 2017. High hydrostatic pressure specifically affects molecular dynamics and shape of low-density lipoprotein particles. *Scientific Reports* **7**, 46034. https://doi.org/10.1038/srep46034

Golub, M., Martinez, N., Peters, J., Michoud, G., Ollivier, J., Jebbar, M., Oger, P., 2018. The Effect of Crowding on Protein Stability, Rigidity, and High Pressure Sensitivity in Whole Cells. *Langmuir* **34**, 10419–10425. https://doi.org/10.1021/acs.langmuir.8b01240

Goñi, F.M., 2019. "Rafts": a nickname for putative transient nanodomains. *Chemistry and Physics of Lipids* **218**, 34–39. https://doi.org/10.1016/j.chemphyslip.2018.11.006

Goñi, F.M., 2014. The basic structure and dynamics of cell membranes: an update of the Singer-

Nicolson model. *Biochimica et Biophysica Acta - Biomembranes* **1838**, 1467–1476. https://doi.org/10.1016/j.bbamem.2014.01.006

Gonthier, J., Barrett, M.A., Aguettaz, O., Baudoin, S., Bourgeat-Lami, E., Demé, B., Grimm, N., Hauß, T., Kiefer, K., Lelièvre-Berna, E., Perkins, A., Wallacher, D., 2019. BerILL: the ultimate humidity chamber for neutron scattering. *Journal of Neutron Research* **21**, 65–76. https://doi.org/10.3233/JNR-190109

Grassle, F.J., 1985. Hydrothermal vent animals: distribution and biology. *Science* **229**, 713–717. https://doi.org/10.1126/science.229.4715.713

Gruner, S., Cullis, P.R., Hope, M.J., Tilcock, C.P.S., 1985. Lipid polymorphism: the molecular basis of nonbilayer phases. *Annual Review of Biophysics and Biomolecular Structure* **14**, 211–238. https://doi.org/10.1146/annurev.biophys.14.1.211

Gu, R., Feng, Y., Guo, S., Zhao, S., Lu, X., Fu, J., Sun, X., Sun, Y., 2017. Improved cryotolerance and developmental competence of human oocytes matured in vitro by transient hydrostatic pressure treatment prior to vitrification. *Cryobiology* **75**, 144–150. https://doi.org/10.1016/j.cryobiol.2016.12.009

Guimarães, L.L., Toledo, M.S., Ferreira, F.A.S., Straus, A.H., Takahashi, H.K., 2014. Structural diversity and biological significance of glycosphingolipids in pathogenic and opportunistic fungi. *Frontiers in Cellular and Infection Microbiology* **4**, 1–8. https://doi.org/10.3389/fcimb.2014.00138

Guler, S.D., Ghosh, D.D., Pan, J., Mathai, J.C., Zeidel, M.L., Nagle, J.F., Tristram-Nagle, S., 2009. Effects of ether vs. ester linkage on lipid bilayer structure and water permeability. *Chemistry and Physics of Lipids* **160**, 33–44. https://doi.org/10.1016/j.chemphyslip.2009.04.003

Gutknecht, J., 1984. Proton/hydroxide conductance through lipid bilayer membranes. *The Journal of Membrane Biology* **82**, 105–112. https://doi.org/10.1007/BF01870737

Hafenbradl, D., Keller, M., Stetter, K.O., 1996. Lipid analysis of Methanopyrus kandleri. *FEMS Microbiology Letters* **136**, 199–202. https://doi.org/10.1016/0378-1097(96)84201-7

Haines, T.H., 2001. Do sterols reduce proton and sodium leaks through lipid bilayers? *Progress in Lipid Research* **40**, 299–324. https://doi.org/10.1016/S0163-7827(01)00009-1

Hajam, I.A., Dar, P.A., Won, G., Lee, J.H., 2017. Bacterial ghosts as adjuvants: mechanisms and potential. *Veterinary Research* **48**, 1–13. https://doi.org/10.1186/s13567-017-0442-5

Hamada, T., Kishimoto, Y., Nagasaki, T., Takagi, M., 2011. Lateral phase separation in tense membranes. *Soft Matter* **7**, 9061–9068. https://doi.org/10.1039/c1sm05948c

Hamada, T., Miura, Y., Ishii, K.I., Araki, S., Yoshikawa, K., Vestergaard, M., Takagi, M., 2007. Dynamic processes in endocytic transformation of a raft-exhibiting giant liposome. *Journal of Physical Chemistry B* **111**, 10853–10857. https://doi.org/10.1021/jp075412

Hannesschlaeger, C., Horner, A., Pohl, P., 2019. Intrinsic membrane permeability to small molecules. *Chemical Reviews* **119**, 5922–5953. https://doi.org/10.1021/acs.chemrev.8b00560

Harroun, T.A., Katsaras, J., Wassall, S.R., 2008. Cholesterol is found to reside in the center of a polyunsaturated lipid membrane. *Biochemistry* **47**, 7090–7096. https://doi.org/10.1021/bi800123b

Harroun, T.A., Wignall, G.D., Katsaras, J., 2006. Neutron scattering for biology, in: Fitter, J., Gutberlet, T., Katsaras, J. (Eds.), Neutron Scattering in Biology. Techniques and Applications. Springer. https://doi.org/10.1007/3-540-29111-3

Hauß, T., Dante, S., Dencher, N.A., Haines, T.H., 2002. Squalane is in the midplane of the lipid bilayer : implications for its function as a proton permeability barrier. *Biochimica Et Biophysica Acta* **1556**, 149–154. https://doi.org/doi.org/10.1016/S0005-2728(02)00346-8

Hauß, T., Dante, S., Haines, T.H., Dencher, N.A., 2005. Localization of coenzyme Q10 in the center of a deuterated lipid membrane by neutron diffraction. *Biochimica et Biophysica Acta - Bioenergetics* **1710**, 57–62. https://doi.org/10.1016/j.bbabio.2005.08.007

Hazael, R., Meersman, F., Ono, F., McMillan, P., 2016. Pressure as a limiting factor for life. *Life* **6**, 34. https://doi.org/10.3390/life6030034

Heberle, F.A., Feigenson, G.W., 2011. Phase separation in lipid membranes. *Cold Spring Harbor Perspectives in Biology* **3**, a004630. https://doi.org/10.1101/cshperspect.a004630

Helfrich, W., 1973. Elastic properties of lipid bilayers: theory and possible experiments. *Zeitschrift für Naturforschung C* **28**, 693–703. https://doi.org/10.1515/znc-1973-11-1209

Heremans, K., 2004. Biology under extreme conditions. *High Pressure Research* **24**, 57–66. https://doi.org/10.1080/08957950310001635828

Hikida, Y., Kimoto, M., Hirao, I., Yokoyama, S., 2017. Crystal structure of deep vent DNA polymerase. *Biochemical and Biophysical Research Communications* **483**, 52–57. https://doi.org/10.1016/j.bbrc.2017.01.007

Hill, C., Cotter, P.D., Sleator, R.D., Gahan, C.G.M., 2002. Bacterial stress response in Listeria monocytogenes: jumping the hurdles imposed by minimal processing. *International Dairy Journal* **12**, 273–283. https://doi.org/10.1016/S0958-6946(01)00125-X

Hope, A.B., Aschberger, P.A., 1970. Effects of temperature on membrane permeability to ions. *Australian Journal of Biological Sciences* **23**, 1047–1060. https://doi.org/10.1071/BI9701047

Hope, M.J., Bally, M.B., Webb, G., Cullis, P.R., 1985. Production of large unilamellar vesicles by a rapid extrusion procedure. Characterization of size distribution, trapped volume and ability to maintain a membrane potential. *BBA - Biomembranes* **812**, 55–65. https://doi.org/10.1016/0005-2736(85)90521-8

Houska, M., Heroldova, M., Vavrova, H., Kucera, P., Setinova, I., Havranova, M., Honzova, S., Strohalm, J., Kminkova, M., Proskova, A., Novotna, P., 2009. Is high-pressure treatment able to modify the allergenicity of the main apple juice allergen, Mal d1? *High Pressure Research* **29**, 14–22. https://doi.org/10.1080/08957950802454068

Howe, A., 2008. Deep-sea hydrothermal vent fauna: evolution, dispersal, succession and biogeography. *Macalester Reviews in Biogeography* **1**.

Hradilova, N., Sadilkova, L., Palata, O., Mysikova, D., Mrazkova, H., Lischke, R., Spisek, R., Adkins, I., 2017. Generation of dendritic cell-based vaccine using high hydrostatic pressure for non-small cell lung cancer immunotherapy. *PLoS ONE* **12**, 1–18. https://doi.org/10.1371/journal.pone.0171539

Hsieh, C.-H., Sue, S.-C., Lyu, P.-C., Wu, W., 1997. Membrane packing geometry of diphytanoylphosphatidylcholine is highly sensitive to hydration: phospholipid polymorphism induced by molecular rearrangement in the headgroup region **73**, 870–877. https://doi.org/10.1016/S0006-3495(97)78120-7

Hua, C.J., Zhang, K., Xin, M., Ying, T., Gao, J.R., Jia, J.H., Li, Y.J., 2016. High quantum yield and pH sensitive fluorescence dyes based on coumarin derivatives: fluorescence characteristics and theoretical study. *RSC Advances* **6**, 49221–49227. https://doi.org/10.1039/c6ra05996a

Huang, H.-W., Lung, H.-M., Yang, B.B., Wang, C.-Y., 2014. Responses of microorganisms to high hydrostatic pressure processing. *Food Control* **40**, 250–259. https://doi.org/10.1016/J.FOODCONT.2013.12.007

Huang, H.W., Wu, S.J., Lu, J.K., Shyu, Y.T., Wang, C.Y., 2017. Current status and future trends of high-pressure processing in food industry. *Food Control* **72**, 1–8. https://doi.org/10.1016/j.foodcont.2016.07.019

Huang, Q., Rodgers, J.M., Hemley, R.J., Ichiye, T., 2017. Extreme biophysics: enzymes under pressure. *Journal of Computational Chemistry* **38**, 1174–1182. https://doi.org/10.1002/jcc.24737

Hung, W.C., F.Y., C., Huang, H.W., 2000. Order-disorder transition in bilayers of diphytanolyl phosphatidylcholine. *Biochimica et Biophysica Acta* **1467**, 198–206. https://doi.org/10.1016/s0005-2736(00)00221-2

Husslein, T., Newns, D.M., Pattnaik, P.C., Zhong, Q., Moore, P.B., Klein, M.L., 1998. Constant pressure and temperature molecular-dynamics simulation of the hydrated diphytanolphosphatidylcholine lipid bilayer. *Journal of Chemical Physics* **109**, 2826–2832. https://doi.org/10.1063/1.476835

Hyde, S., Andersson, S., Larsson, K., Blum, Z., Landh, T., Lidin, S., Ninham, B., 1997. The language of shape: The role of curvature in condensed matter, 1st ed. Elsevier Science S.A., Amsterdam.

Ichiye, T., 2018. Enzymes from piezophiles. *Seminars in Cell and Developmental Biology* **84**, 138–146. https://doi.org/10.1016/j.semcdb.2018.01.004

Ingólfsson, H.I., Melo, M.N., Van Eerden, F.J., Arnarez, C., Lopez, C.A., Wassenaar, T.A., Periole, X., De Vries, A.H., Tieleman, D.P., Marrink, S.J., 2014. Lipid organization of the plasma membrane. *Journal of the American Chemical Society* **136**, 14554–14559. https://doi.org/10.1021/ja507832e

Israelachvili, J.N., Mitchell, D.J., Ninham, B.W., 1976. Theory of self-assembly of hydrocarbon amphiphiles into micelles and bilayers. *Journal of the Chemical Society, Faraday Transactions 2* **72**, 1525. https://doi.org/10.1039/f29767201525

Jacobsen, A.C., Jensen, S.M., Fricker, G., Brandl, M., Treusch, A.H., 2017. Archaeal lipids in oral delivery of therapeutic peptides. *European Journal of Pharmaceutical Sciences* **108**, 101–110. https://doi.org/10.1016/j.ejps.2016.12.036

Jacquemet, A., Barbeau, J., Lemiègre, L., Benvegnu, T., 2009. Archaeal tetraether bipolar lipids: structures, functions and applications. *Biochimie* **91**, 711–717. https://doi.org/10.1016/j.biochi.2009.01.006

Jaenicke, R., 2000. Stability and stabilization of globular proteins in solution. *Journal of Biotechnology* **79**, 193–203. https://doi.org/10.1016/S0168-1656(00)00236-4

Janakiram, N.B., Mohammed, A., Rao, C. V., 2015. Sea cucumbers metabolites as potent anti-cancer agents. *Marine Drugs* **13**, 2909–2923. https://doi.org/10.3390/md13052909

Jarsch, I.K., Daste, F., Gallop, J.L., 2016. Membrane curvature in cell biology: an integration of molecular mechanisms. *Journal of Cell Biology* **214**, 375–387. https://doi.org/10.1083/jcb.201604003

Jebbar, M., Franzetti, B., Girard, E., Oger, P., 2015. Microbial diversity and adaptation to high hydrostatic pressure in deep-sea hydrothermal vents prokaryotes. *Extremophiles* **19**, 721–740. https://doi.org/10.1007/s00792-015-0760-3

Johnson, I., 1998. Fluorescent probes for living cells. *Histochemical Journal* **30**, 123–140.

https://doi.org/10.1023/A:1003287101868

Jorgensen, B.B., D'Hondt, S., 2006. A starving majority deep beneath the seafloor. *Science* **314**, 932–934. https://doi.org/10.1126/science.1133796

Jouhet, J., 2013. Importance of the hexagonal lipid phase in biological membrane organization. *Frontiers in Plant Science* **4**, 1–5. https://doi.org/10.3389/fpls.2013.00494

Jülicher, F., Lipowsky, R., 1993. Domain-induced budding of vesicles. *Physical Review Letters* **70**, 2964–2967. https://doi.org/10.1103/PhysRevLett.70.2964

Kaiser, H.J., Lingwood, D., Levental, I., Sampaio, J.L., Kalvodova, L., Rajendran, L., Simons, K., 2009. Order of lipid phases in model and plasma membranes. *Proceedings of the National Academy of Sciences* **106**, 16645. https://doi.org/10.1073/pnas.0908987106

Kallmeyer, J., Pockalny, R., Adhikari, R.R., Smith, D.C., D'Hondt, S., 2012. Global distribution of microbial abundance and biomass in subseafloor sediment. *Proceedings of the National Academy of Sciences* **109**, 16213–16216. https://doi.org/10.1073/pnas.1203849109

Kaneshiro, S.M., Clark, D.S., 1995. Pressure effects on the composition and thermal-behavior of lipids from the deep-sea thermophile Methanococcus-Jannaschii. *Journal of Bacteriology* **177**, 3668–3672. https://doi.org/10.1128/jb.177.13.3668-3672.1995

Kano, K., Fendler, J.H., 1978. Pyranine as a sensitive pH probe for liposome interiors and surfaces. pH gradients across phospholipid vesicles. *BBA - Biomembranes* **509**, 289–299. https://doi.org/10.1016/0005-2736(78)90048-2

Kapoor, S., Berghaus, M., Suladze, S., Prumbaum, D., Grobelny, S., Degen, P., Raunser, S., Winter, R., 2014. Prebiotic cell membranes that survive extreme environmental pressure conditions - suport.info. *Angewandte Chemie - International Edition* **53**, 8397–8401. https://doi.org/10.1002/anie.201404254

Kapoor, S., Triola, G., Vetter, I.R., Waldmann, H., Winter, R., 2012. Revealing conformational substates of lipidated N-ras protein by pressure modulation. *Biophysical Journal* **102**, 1468. https://doi.org/10.1016/j.bpj.2012.02.038

Kara, S., Babii, O., Tkachenko, A.N., Ulrich, A.S., Afonin, S., Komarov, I. V., 2017. Diphytanoyl lipids as model systems for studying membrane-active peptides. *Biochimica et Biophysica Acta - Biomembranes* **1859**, 1828–1837. https://doi.org/10.1016/j.bbamem.2017.06.003

Katsaras, J., 1995. X-ray diffraction studies of oriented lipid bilayers. *Biochemistry and Cell Biology* **73**, 209–218. https://doi.org/10.1139/o95-025

Katsaras, J., Tristram-Nagle, S., Liu, Y., Headrick, R.L., Fontes, E., Mason, P.C., Nagle, J.F., 2000. Clarification of the ripple phase of lecithin bilayers using fully hydrated, aligned samples. *Physical Review E* **61**, 5668–5677. https://doi.org/10.1103/PhysRevE.61.5668

Kaur, B.P., Kaushik, N., Rao, P.S., Mishra, H.N., 2015. Chilled storage of high pressure processed black tiger shrimp (Penaeus monodon). *Journal of Aquatic Food Product Technology* **24**, 283–299. https://doi.org/10.1080/10498850.2013.772271

Kawamoto, J., Sato, T., Nakasone, K., Kato, C., Mihara, H., Esaki, N., Kurihara, T., 2011. Favourable effects of eicosapentaenoic acid on the late step of the cell division in a piezophilic bacterium, Shewanella violacea DSS12, at high-hydrostatic pressures. *Environmental Microbiology* **13**, 2293–2298. https://doi.org/10.1111/j.1462-2920.2011.02487.x

Kelly, R.H., Yancey, P.H., 1999. High contents of trimethylamine oxide correlating with depth in deep-sea teleost fishes, skates, and decapod crustaceans. *Biological Bulletin* **196**, 18–25.

https://doi.org/10.2307/1543162

Kessner, D., Kiselev, M.A., Hauß, T., Dante, S., Wartewig, S., Neubert, R.H.H., 2008. Localisation of partially deuterated cholesterol in quaternary SC lipid model membranes: a neutron diffraction study. *European Biophysics Journal* **37**, 1051–1057. https://doi.org/10.1007/s00249-008-0265-4

Kim, M.Y., Lee, S.H., Jang, G.Y., Park, H.J., Li, M., Kim, S., Lee, Y.R., Noh, Y.H., Lee, J., Jeong, H.S., 2015. Effects of high hydrostatic pressure treatment on the enhancement of functional components of germinated rough rice (Oryza sativa L.). *Food Chemistry* **166**, 86–92. https://doi.org/10.1016/j.foodchem.2014.05.150

Kirk, G.L., Gruner, S.M., 1985. Lyotropic effects of alkanes and headgroup composition on the L_α -H_{II} lipid liquid crystal phase transition : hydrocarbon packing versus intrinsic curvature. *Journal de Physique* **46**, 761–769. https://doi.org/10.1051/jphys:01985004605076100

Kitahara, R., Sareth, S., Yamada, H., Ohmae, E., Gekko, K., Akasaka, K., 2000. High pressure NMR reveals active-site hinge motion of folate-bound Escherichia coli dihydrofolate reductase. *Biochemistry* **39**, 12789–12795. https://doi.org/10.1021/bi0009993

Klacsová, M., Bóta, A., Balgavý, P., 2016. DOPC-DOPE composition dependent L_α-H_{II} thermotropic phase transition: SAXD study. *Chemistry and Physics of Lipids* **198**, 46–50. https://doi.org/10.1016/j.chemphyslip.2016.05.004

Klymchenko, A.S., Kreder, R., 2014. Fluorescent probes for lipid rafts: from model membranes to living cells. *Chemistry and Biology* **21**, 97–113. https://doi.org/10.1016/j.chembiol.2013.11.009

Koga, Y., 2012. Thermal adaptation of the archaeal and bacterial lipid membranes. *Archaea* **2012**, 1–6. https://doi.org/10.1155/2012/789652

Komatsu, H., Chong, P.L.G., 1998. Low permeability of liposomal membranes composed of bipolar tetraether lipids from thermoacidophilic archaebacterium Sulfolobus acidocaldarius. *Biochemistry* **37**, 107–115. https://doi.org/10.1021/bi972163e

Kučerka, N., Nieh, M.P., Katsaras, J., 2011. Fluid phase lipid areas and bilayer thicknesses of commonly used phosphatidylcholines as a function of temperature. *Biochimica et Biophysica Acta - Biomembranes* **1808**, 2761–2771. https://doi.org/10.1016/j.bbamem.2011.07.022

Kulkarni, C. V., 2019. Calculating the 'chain splay' of amphiphilic molecules: Towards quantifying the molecular shapes. *Chemistry and Physics of Lipids* **218**, 16–21. https://doi.org/10.1016/j.chemphyslip.2018.11.004

Kulkarni, C. V., Wachter, W., Iglesias-Salto, G., Engelskirchen, S., Ahualli, S., 2011. Monoolein: A magic lipid? *Phys. Chem. Chem. Phys.* **13**, 3004–3021. https://doi.org/10.1039/C0CP01539C

Kurosaka, G., Abe, F., 2018. The YPR153W gene is essential for the pressure tolerance of tryptophan permease Tat2 in the yeast Saccharomyces cerevisiae. *High Pressure Research* **38**, 90–98. https://doi.org/10.1080/08957959.2017.1413367

Kusube, M., Kyaw, T.S., Tanikawa, K., Chastain, R.A., Hardy, K.M., Cameron, J., Bartlett, D.H., 2017. Colwellia marinimaniae sp. nov., a hyperpiezophilic species isolated from an amphipod within the challenger deep, Mariana Trench. *International Journal of Systematic and Evolutionary Microbiology* **67**, 824–831. https://doi.org/10.1099/ijsem.0.001671

Kyrychenko, A., 2015. Using fluorescence for studies of biological membranes: a review. *Methods and Applications in Fluorescence* **3**, 42003. https://doi.org/10.1088/2050-6120/3/4/042003

Laggner, P., Kriechbaum, M., 1991. Phospholipid phase transitions: kinetics and structural mechanisms. *Chemistry and Physics of Lipids* **57**, 121–145. https://doi.org/10.1016/0009-

3084(91)90072-J

Lakey, J.H., 2009. Neutrons for biologists: A beginner's guide, or why you should consider using neutrons. *Journal of the Royal Society, Interface / the Royal Society* **6 Suppl 5**, S567-73. https://doi.org/10.1098/rsif.2009.0156.focus

Lakowicz, J.R., 2006. Principles of fluorescence spectroscopy, 3rd ed. ed. Springer-Verlag.

Lamson, M.J., Herbette, L.G., Peters, K.R., Carson, J.H., Morgan, F., Chester, D.C., Kramer, P.A., 1994. Effects of hexagonal phase induction by dolichol on phospholipid membrane permeability and morphology. *International Journal of Pharmaceutics* **105**, 259–272. https://doi.org/10.1016/0378-5173(94)90111-2

Lande, M.B., 1995. The relationship between membrane fluidity and permeabilities to water, solutes, ammonia, and protons. *The Journal of General Physiology* **106**, 67–84. https://doi.org/10.1085/jgp.106.1.67

Langworthy, T.A., Tornabene, T.G., Holzer, G., 1982. Lipids of Archaebacteria. *Zentralblatt für Bakteriologie Mikrobiologie und Hygiene: I. Abt. Originale C* **3**, 228–244. https://doi.org/10.1016/S0721-9571(82)80036-7

Laradji, M., Sunil Kumar, P.B., 2005. Domain growth, budding, and fission in phase-separating self-assembled fluid bilayers. *The Journal of Chemical Physics* **123**, 224902. https://doi.org/10.1063/1.2102894

Larsson, K., 1989. Cubic lipid-water phases: structures and biomembrane aspects. *Journal of Physical Chemistry* **93**, 7304–7314. https://doi.org/10.1021/j100358a010

Lattuati, A., Guezennec, J., Metzger, P., Largeau, C., 1998. Lipids of Thermococcus hydrothermalis, an archaea isolated from a deep- sea hydrothermal vent. *Lipids* **33**, 319–326. https://doi.org/10.1007/s11745-998-0211-0

Lauro, F.M., Chastain, R.A., Blankenship, L.E., Yayanos, A.A., Bartlett, D.H., 2007. The unique 16S rRNA genes of piezophiles reflect both phylogeny and adaptation. *Applied and Environmental Microbiology* **73**, 838–845. https://doi.org/10.1128/AEM.01726-06

Le Chatelier, H.L., 1884. Sur un enoncé général des lois des équilibres chimiques. *Comptes-rendus de l'Académie des sciences* **99**, 786–789.

Lehofer, B., Golub, M., Kornmueller, K., Kriechbaum, M., Martinez, N., Nagy, G., Kohlbrecher, J., Amenitsch, H., Peters, J., Prassl, R., 2018. High hydrostatic pressure jnduces a lipid phase transition and molecular rearrangements in low-density lipoprotein nanoparticles. *Particle and Particle Systems Characterization* **35**. https://doi.org/10.1002/ppsc.201800149

Lelièvre-Berna, E., Demé, B., Gonthier, J., Gonzales, J.P., Maurice, J., Memphis, Y., Payre, C., Oger, P., Peters, J., Vial, S., 2017. 700 MPa sample stick for studying liquid samples or solid-gas reactions down to 1.8 K and up to 550 K. *Journal of Neutron Research* **19**, 77–84. https://doi.org/10.3233/JNR-170044

Lemay, P., 2002. The use of high pressure for separation and production of bioactive molecules. *Biochimica et Biophysica Acta - Protein Structure and Molecular Enzymology* **1595**, 357–366. https://doi.org/10.1016/S0167-4838(01)00356-9

Lenne, P.F., Nicolas, A., 2009. Physics puzzles on membrane domains posed by cell biology. *Soft Matter* **5**, 2841–2848. https://doi.org/10.1039/b822956b

Lenz, O., Schmid, F., 2007. Structure of symmetric and asymmetric "ripple" phases in lipid bilayers. *Physical Review Letters* **98**. https://doi.org/10.1103/PhysRevLett.98.058104

Li, L., Kato, C., Nogi, Y., Horikoshi, K., 1998. Distribution of the pressure-regulated operons in deep-sea bacteria. *FEMS Microbiology Letters* **159**, 159–166. https://doi.org/10.1016/S0378-1097(97)00560-0

Li, Y., Yang, W., Chung, S.Y., Chen, H., Ye, M., Teixeira, A.A., Gregory, J.F., Welt, B.A., Shriver, S., 2013. Effect of pulsed ultraviolet light and high hydrostatic pressure on the antigenicity of almond protein extracts. *Food and Bioprocess Technology* **6**, 431–440. https://doi.org/10.1007/s11947-011-0666-8

Librizzi, F., Carrotta, R., Peters, J., Cupane, A., 2018. The effects of pressure on the energy landscape of proteins. *Scientific Reports* **8**, 2037. https://doi.org/10.1038/s41598-018-20417-x

Lindblom, G., Rilfors, L., 1992. Nonlamellar phases formed by membrane lipids. *Advances in Colloid and Interface Science* **41**, 101–125. https://doi.org/10.1016/0001-8686(92)80009-M

Lindblom, G., Rilfors, L., 1989. Cubic phases and isotropic structures formed by membrane lipids — possible biological relevance. *Biochimica et Biophysica Acta (BBA) - Reviews on Biomembranes* **988**, 221–256. https://doi.org/10.1016/0304-4157(89)90020-8

Lindquist, S., Craig, E.A., 1988. The heat-shock proteins. *Annual review of genetics* **22**, 631–677. https://doi.org/0.1146/annurev.ge.22.120188.003215

Lindsey, H., Petersen, N.O., Chan, S.I., 1979. Physicochemical characterization of 1,2-diphytanoyl-*sn*-glycero-3-phosphocholine in model membrane systems. *Biochimica et biophysica acta* **555**, 147–67. https://doi.org/10.1016/0005-2736(79)90079-8

Lipowsky, R., 1992. Budding of membranes induced by intramembrane domains. *Journal de Physique II* **2**, 1825–1840. https://doi.org/10.1051/jp2:1992238

Llères, D., Swift, S., Lamond, A.I., 2007. Detecting protein-protein interactions in vivo with FRET using multiphoton fluorescence lifetime imaging microscopy (FLIM), in: Current Protocols in Cytometry. John Wiley & Sons, Inc., Hoboken, NJ, USA, pp. 1–19. https://doi.org/10.1002/0471142956.cy1210s42

Lohner, K., Degovics, G., Laggner, P., Gnamusch, E., Paltauf, F., 1993. Squalene promotes the formation of nonbilayer stuctures in phospholipid model membranes. *Biochimica Et Biophysica Acta* **1152**, 69–77. https://doi.org/doi.org/10.1016/0005-2736(93)90232-O

Luchini, A., Delhom, R., Demé, B., Laux, V., Moulin, M., Haertlein, M., Pichler, H., Strohmeier, G.A., Wacklin, H., Fragneto, G., 2018. The impact of deuteration on natural and synthetic lipids: a neutron diffraction study. *Colloids and Surfaces B: Biointerfaces* **168**, 126–133. https://doi.org/10.1016/j.colsurfb.2018.02.009

Ludwig, H., 2003. Effects of high pressure on Bacteria and Funghi, in: Advances in High Pressure Bioscience and Biotechnology II (Ed.), Winter, R. Springer, pp. 259–265.

Lund, P., Tramonti, A., De Biase, D., 2014. Coping with low pH: molecular strategies in neutralophilic bacteria. *FEMS Microbiology Reviews* **38**, 1091–1125. https://doi.org/10.1111/1574-6976.12076

Luong, T.Q., Kapoor, S., Winter, R., 2015. Pressure - A gateway to fundamental insights into protein solvation, dynamics, and function. *ChemPhysChem* **16**, 3555–3571. https://doi.org/10.1002/cphc.201500669

Lyatskaya, Y., Liu, Y., Tristram-Nagle, S., Katsaras, J., Nagle, J.F., 2000. Method for obtaining structure and interactions from oriented lipid bilayers. *Physical Review E* **63**, 011907. https://doi.org/10.1103/PhysRevE.63.011907

Macdonald, A.G., Martinac, B., 2005. Effect of high hydrostatic pressure on the bacterial mechanosensitive channel MscS. *European Biophysics Journal* **34**, 434–441. https://doi.org/10.1007/s00249-005-0478-8

Macgregor, R.B., Weber, G., 1981. Fluorophores in polar media: spectral effects of the Langevin distribution of electrostatic interactions. *Annals of the New York Academy of Sciences* **366**, 140–154. https://doi.org/10.1111/j.1749-6632.1981.tb20751.x

Mañas, P., Mackey, B.M., 2004. Morphological and physiological changes induced by high hydrostatic pressure in exponential- and stationary-phase cells of *Escherichia coli*: relationship with cell death. *Applied and Environmental Microbiology* **70**, 1545–1554. https://doi.org/10.1128/AEM.70.3.1545-1554.2004

Marguet, E., Gaudin, M., Gauliard, E., Fourquaux, I., le Blond du Plouy, S., Matsui, I., Forterre, P., 2013. Membrane vesicles, nanopods and/or nanotubes produced by hyperthermophilic archaea of the genus Thermococcus . *Biochemical Society Transactions* **41**, 436–442. https://doi.org/10.1042/bst20120293

Mariani, P., Luzzati, V., Delacroix, H., 1988. Cubic phases of lipid-containing systems. Structure analysis and biological implications. *Journal of Molecular Biology* **204**, 165–189. https://doi.org/10.1016/0022-2836(88)90607-9

Marion, J., Trovaslet, M., Martinez, N., Masson, P., Schweins, R., Nachon, F., Trapp, M., Peters, J., 2015. Pressure-induced molten globule state of human acetylcholinesterase: structural and dynamical changes monitored by neutron scattering. *Physical Chemistry Chemical Physics* **17**, 3157–3163. https://doi.org/10.1039/c4cp02992e

Marquardt, D., Heberle, F.A., Greathouse, D. V., Koeppe, R.E., Standaert, R.F., Van Oosten, B.J., Harroun, T.A., Kinnun, J.J., Williams, J.A., Wassall, S.R., Katsaras, J., 2016. Lipid bilayer thickness determines cholesterols location in model membranes. *Soft Matter* **12**, 9417–9428. https://doi.org/10.1039/c6sm01777k

Marquardt, D., Heberle, F.A., Nickels, J.D., Pabst, G., Katsaras, J., 2015. On scattered waves and lipid domains: detecting membrane rafts with X-rays and neutrons. *Soft Matter* **11**, 9055–9072. https://doi.org/10.1039/C5SM01807B

Marteinsson, V.T., Birrien, J.-L., Reysenbach, A., Vernet, M., Marie, D., Gambacorta, A., Messner, P., Sleytr, U.B., Prieur, D., 1999. *Thermococcus barophilus* sp. nov., a new barophilic and hyperthermophilic archaeon isolated under high hydrostatic pressure from a deep-sea hydrothermal vent. *International Journal of Systematic Bacteriology* **49**, 351–359. https://doi.org/doi.org/10.1099/00207713-49-2-351

Martinez, N., Michoud, G., Cario, A., Ollivier, J., Franzetti, B., Jebbar, M., Oger, P., Peters, J., 2016. High protein flexibility and reduced hydration water dynamics are key pressure adaptive strategies in prokaryotes. *Scientific Reports* **6**, 1–11. https://doi.org/10.1038/srep32816

Mathai, J.C., Tristram-Nagle, S., Nagle, J.F., Zeidel, M.L., 2008. Structural determinants of water permeability through the lipid membrane. *The Journal of General Physiology* **131**, 69–76. https://doi.org/10.1085/jgp.200709848

Matsuki, H., Miyazaki, E., Sakano, F., Tamai, N., Kaneshina, S., 2007. Thermotropic and barotropic phase transitions in bilayer membranes of ether-linked phospholipids with varying alkyl chain lengths. *Biochimica et Biophysica Acta - Biomembranes* **1768**, 479–489. https://doi.org/10.1016/j.bbamem.2006.10.005

Matsuura, Y., Takehira, M., Joti, Y., Ogasahara, K., Tanaka, T., Ono, N., Kunishima, N., Yutani, K., 2015.

Thermodynamics of protein denaturation at temperatures over 100°C: CutA1 mutant proteins substituted with hydrophobic and charged residues. *Scientific Reports* **5**, 1–9. https://doi.org/10.1038/srep15545

McCarthy, N.L.C., Brooks, N.J., 2016. Using high pressure to modulate lateral structuring in model lipid membranes, in: Advances in Biomembranes and Lipid Self-Assembly. Elsevier Inc., pp. 75–89. https://doi.org/10.1016/bs.abl.2016.04.004

McCarthy, N.L.C., Ces, O., Law, R. V., Seddon, J.M., Brooks, N.J., 2015. Separation of liquid domains in model membranes induced with high hydrostatic pressure. *Chemical Communications* **51**, 8675–8678. https://doi.org/10.1039/c5cc02134k

McIntosh, T.J., Simon, S.A., MacDonald, R.C., 1980. The organization of *n*-alkanes in lipid bilayers. *Biochimica et Biophysica Acta (BBA) - Biomembranes* **597**, 445–463. https://doi.org/10.1016/0005-2736(80)90219-9

McMahon, H.T., Boucrot, E., 2015. Membrane curvature at a glance. *Journal of Cell Science* **128**, 1065–1070. https://doi.org/10.1242/jcs.114454

McMullen, T.P.W., Lewis, R.N.A.H., McElhaney, R.N., 1993. Differential scanning calorimetric study of the effect of cholesterol on the thermotropic phase behavior of a homologous series of linear saturated phosphatidylcholines. *Biochemistry* **32**, 516–522. https://doi.org/10.1021/bi00053a016

Meersman, F., Daniel, I., Bartlett, D.H., Winter, R., Hazael, R., McMillan, P.F., 2013. High-pressure biochemistry and biophsics. *Reviews in Mineralogy and Geochemistry* **75**, 607–648. https://doi.org/10.2138/rmg.2013.75.19

Mentré, P., Hoa, G.H.B., 2001. Effects of high hydrostatic pressures on living cells: a consequence of the properties of macromolecules and macromolecule-associated water. *International Review of Cytology* **201**, 1–84. https://doi.org/10.1016/S0074-7696(01)01001-4

Michiels, C., Bartlett, D.H., Aertsen, A., 2008. High-pressure microbiology, Animal Genetics. ASM Press.

Milianta, P.J., Muzzio, M., Denver, J., Cawley, G., Lee, S., 2015. Water permeability across symmetric and asymmetric droplet interface bilayers: interaction of cholesterol sulfate with DPhPC. *Langmuir* **31**, 12187–12196. https://doi.org/10.1021/acs.langmuir.5b02748

Miroshnichenko, M.L., Gongadze, G.M., Rainey, F.A., Kostyukova, A.S., Lysenko, A.M., Chernyh, N.A., BonchOsmolovskaya, E.A., 1998. *Thermococcus gorgonarius* sp. nov. and *Thermococcus pacificus* sp. nov.: heterotrophic extremely thermophilic archaea from New Zealand submarine hot vents. *Int. J. System. Bacteriol.* **48**, 23–29. https://doi.org/10.1099/00207713-48-1-23

Mojumdar, E.H., Groen, D., Gooris, G.S., Barlow, D.J., Lawrence, M.J., Deme, B., Bouwstra, J.A., 2013. Localization of cholesterol and fatty acid in a model lipid membrane: a neutron diffraction approach. *Biophysical Journal* **105**, 911–918. https://doi.org/10.1016/j.bpj.2013.07.003

Mota, M.J., Lopes, R.P., Delgadillo, I., Saraiva, J.A., 2015. Probiotic yogurt production under high pressure and the possible use of pressure as an on/off switch to stop/start fermentation. *Process Biochemistry* **50**, 906–911. https://doi.org/10.1016/j.procbio.2015.03.016

Mota, M.J., Lopes, R.P., Delgadillo, I., Saraiva, J.A., 2013. Microorganisms under high pressure - Adaptation, growth and biotechnological potential. *Biotechnology Advances* **31**, 1426–1434. https://doi.org/10.1016/j.biotechadv.2013.06.007

Nagle, J.F., 1976. Theory of lipid monolayer and bilayer phase transitions: effect of headgroup

interactions. *The Journal of Membrane Biology* **27**, 233–250. https://doi.org/10.1007/BF01869138

Nagle, J.F., Mathai, J.C., Zeidel, M.L., Tristram-Nagle, S., 2008. Theory of passive permeability through lipid bilayers. *The Journal of General Physiology* **131**, 77–85. https://doi.org/10.1085/jgp.200709849

Nagle, J.F., Morowitz, H.J., 1978. Molecular mechanisms for proton transport in membranes. *Proceedings of the National Academy of Sciences* **75**, 298–302. https://doi.org/10.1073/pnas.75.1.298

Nagle, J.F., Scott, H.L., 1978. Lateral compressibility of lipid mono- and bilayers. Theory of membrane permeability. *BBA - Biomembranes* **513**, 236–243. https://doi.org/10.1016/0005-2736(78)90176-1

Nagle, J.F., Tristram-Nagle, S., 2000. Structure of lipid bilayers. *Biochimica et Biophysica Acta - Reviews on Biomembranes* **1469**, 159–195. https://doi.org/10.1016/S0304-4157(00)00016-2

Neumann, D., Lichtenberger, O., Günther, D., Tschiersch, K., Nover, L., 1994. Heat-shock proteins induce heavy-metal tolerance in higher plants. *Planta* **194**, 360–367. https://doi.org/10.1007/BF00197536

Nichols, J.W., Abercrombie, R.F., 2010. A view of hydrogen/hydroxide flux across lipid membranes. *Journal of Membrane Biology* **237**, 21–30. https://doi.org/10.1007/s00232-010-9303-0

Nichols, J.W., Deamer, D.W., 1980. Net proton-hydroxyl permeability of large unilamellar liposomes measured by an acid-base titration technique. *Proceedings of the National Academy of Sciences* **77**, 2038–2042. https://doi.org/10.1073/pnas.77.4.2038

Nicolaus, B., Kambourova, M., Oner, E.T., 2010. Exopolysaccharides from extremophiles: from fundamentals to biotechnology. *Environmental Technology* **31**, 1145–1158. https://doi.org/10.1080/09593330903552094

Nicolini, C., Celli, A., Gratton, E., Winter, R., 2006. Pressure tuning of the morphology of heterogeneous lipid vesicles: a two-photon-excitation fluorescence microscopy study. *Biophysical Journal* **91**, 2936–2942. https://doi.org/10.1529/biophysj.106.088716

Niemeyer, B., Jansen, J., 2007. An innovative approach for sorptive separation of amphiphilic biomolecules applying high hydrostatic pressure. *Journal of Supercritical Fluids* **39**, 354–361. https://doi.org/10.1016/j.supflu.2006.03.015

Ninham, B.W., Larsson, K., Lo Nostro, P., 2017. Two sides of the coin. Part 1. Lipid and surfactant self-assembly revisited. *Colloids and Surfaces B: Biointerfaces* **152**, 326–338. https://doi.org/10.1016/j.colsurfb.2017.01.022

Nogi, Y., Kato, C., 1999. Taxonomic studies of extremely barophilic bacteria isolated from the Mariana Trench and description of *Moritella yayanosii* sp. nov., a new barophilic bacterial isolate. *Extremophiles* **3**, 71–77. https://doi.org/10.1007/s007920050101

Oger, P., Cario, A., 2014. La vie sous pression des microorganismes piézophiles. *Biologie Aujourd'hui* **208**, 193–206. https://doi.org/10.1051/jbio/2014023

Oger, P., Deme, B., Peters, J., Salvador Castell, M., 2016. Investigating the ultrastructure of an archaeal membrane containing apolar structural lipids. Institut Laue-Langevin (ILL). https://doi.org/10.5291/ILL-DATA.8-02-762

Oger, P.M., Cario, A., 2013. Adaptation of the membrane in Archaea. *Biophysical chemistry* **183**, 42–56. https://doi.org/10.1016/j.bpc.2013.06.020

Oger, P.M., Jebbar, M., 2010. The many ways of coping with pressure. *Research in Microbiology* **161**, 799–809. https://doi.org/10.1016/j.resmic.2010.09.017

Ohmae, E., Murakami, C., Tate, S.I., Gekko, K., Hata, K., Akasaka, K., Kato, C., 2012. Pressure dependence of activity and stability of dihydrofolate reductases of the deep-sea bacterium *Moritella profunda* and *Escherichia coli*. *Biochimica et Biophysica Acta - Proteins and Proteomics* **1824**, 511–519. https://doi.org/10.1016/j.bbapap.2012.01.001

Oku, N., Kendall, D.A., MacDonald, R.C., 1982. A simple procedure for the determination of the trapped volume of liposomes. *BBA - Biomembranes* **691**, 332–340. https://doi.org/10.1016/0005-2736(82)90422-9

Oliveira, A.C., Gaspar, L.P., Da Poian, A.T., Silva, J.L., 1994. Arc repressor will not denature under pressure in the absence of water. *Journal of Molecular Biology*. https://doi.org/10.1006/jmbi.1994.1433

Oliveira, A.C., Ishimaru, D., Gonçalves, R.B., Smith, T.J., Mason, P., Sá-Carvalho, D., Silva, J.L., 1999. Low temperature and pressure stability of picornaviruses: implications for virus uncoating. *Biophysical Journal* **76**, 1270–1279. https://doi.org/10.1016/S0006-3495(99)77290-5

Orcutt, B.N., LaRowe, D.E., Biddle, J.F., Colwell, F.S., Glazer, B.T., Reese, B.K., Kirkpatrick, J.B., Lapham, L.L., Mills, H.J., Sylvan, J.B., Wankel, S.D., Wheat, C.G., 2013. Microbial activity in the marine deep biosphere: progress and prospects. *Frontiers in Microbiology* **4**, 1–15. https://doi.org/10.3389/fmicb.2013.00189

Orcutt, B.N., Sylvan, J.B., Knab, N.J., Edwards, K.J., 2011. Microbial ecology of the dark ocean above, at, and below the seafloor. *Microbiology and Molecular Biology Reviews* **75**, 361–422. https://doi.org/10.1128/MMBR.00039-10

OriginPro, Version 2016. OriginLab Corporation, Northampton, MA, USA., n.d.

Ourisson, G., Rohmer, M., Poralla, K., 1987. Prokaryotic hopanoids and other polyterpenoid sterol surrogates. *Ann. Rev. Microbiol.* **41**, 301–333. https://doi.org/10.1146/annurev.mi.41.100187.001505

Pagán, R., Mackey, B., 2000. Relationship between membrane damage and cell death in pressure-treated Escherichia coli cells: Differences between exponential- and stationary-phase cells and variation among strains. *Applied and Environmental Microbiology* **66**, 2829–2834. https://doi.org/10.1128/AEM.66.7.2829-2834.2000

Panick, G., Malessa, R., Winter, R., Rapp, G., Frye, K.J., Royer, C.A., 1998. Structural characterization of the pressure-denatured state and unfolding/refolding kinetics of staphylococcal nuclease by synchrotron small-angle X-ray scattering and Fourier-transform infrared spectroscopy. *Journal of Molecular Biology* **275**, 389–402. https://doi.org/10.1006/jmbi.1997.1454

Parasassi, T., De Stasio, G., d'Ubaldo, A., Gratton, E., 1990. Phase fluctuation in phospholipid membranes revealed by Laurdan fluorescence. *Biophysical Journal* **57**, 1179–1186. https://doi.org/10.1016/S0006-3495(90)82637-0

Parasassi, T., De Stasio, G., Ravagnan, G., Rusch, R.M., Gratton, E., 1991. Quantitation of lipid phases in phospholipid vesicles by the generalized polarization of Laurdan fluorescence. *Biophysical journal* **60**, 179–89. https://doi.org/10.1016/S0006-3495(91)82041-0

Parasassi, T., Di Stefano, M., Loiero, M., Ravagnan, G., Gratton, E., 1994. Influence of cholesterol on phospholipid bilayers phase domains as detected by Laurdan fluorescence. *Biophysical journal* **66**, 120–32. https://doi.org/10.1016/S0006-3495(94)80763-5

Parasassi, T., Krasnowska, E.K., Bagatolli, L., Gratton, E., 1998. Laurdan and prodan as polarity-sensitive fluorescent membrane probes. *Journal of Fluorescence* **8**, 365–373. https://doi.org/10.1023/A:1020528716621

Patterson, M.F., 2005. Microbiology of pressure-treated foods. *Journal of Applied Microbiology* **98**, 1400–1409. https://doi.org/10.1111/j.1365-2672.2005.02564.x

Paula, S., Volkov, A.G., Van Hoek, A.N., Haines, T.H., Deamer, D.W., 1996. Permeation of protons, potassium ions, and small polar molecules through phospholipid bilayers as a function of membrane thickness. *Biophysical Journal* **70**, 339–348. https://doi.org/10.1016/S0006-3495(96)79575-9

Peñas, E., Gomez, R., Frias, J., Baeza, M.L., Vidal-Valverde, C., 2011. High hydrostatic pressure effects on immunoreactivity and nutritional quality of soybean products. *Food Chemistry* **125**, 423–429. https://doi.org/10.1016/j.foodchem.2010.09.023

Periasamy, N., Teichert, H., Weise, K., Vogel, R.F., Winter, R., 2009. Effects of temperature and pressure on the lateral organization of model membranes with functionally reconstituted multidrug transporter LmrA. *Biochimica et Biophysica Acta - Biomembranes* **1788**, 390–401. https://doi.org/10.1016/j.bbamem.2008.09.017

Peters, J., Golub, M., Demé, B., Gonthier, J., Maurice, J., Payre, C., Sadykov, R., Lelièvre-Berna, E., 2018. New pressure cells for membrane layers and systems in solutions up to 100°C. *Journal of Neutron Research* **20**, 1–10. https://doi.org/10.3233/JNR-180055

Peters, J., Martinez, N., Michoud, G., Cario, A., Franzetti, B., Oger, P., Jebbar, M., 2014. Deep sea microbes probed by incoherent neutron scattering under high hydrostatic pressure. *Zeitschrift fur Physikalische Chemie* **228**, 1121–1133. https://doi.org/10.1515/zpch-2014-0547

Picard, A., Daniel, I., Montagnac, G., Oger, P., 2007. *In situ* monitoring by quantitative Raman spectroscopy of alcoholic fermentation by *Saccharomyces cerevisiae* under high pressure. *Extremophiles* **11**, 445–452. https://doi.org/10.1007/s00792-006-0054-x

Pohle, W., Selle, C., Fritzsche, H., Binder, H., 1998. Fourier transform infrared spectroscopy as a probe for the study of the hydration of lipid self-assemblies. I. Methodology and general phenomena. *Biospectroscopy* **4**, 267–280. https://doi.org/10.1002/(SICI)1520-6343(1998)4:4<267::AID-BSPY5>3.0.CO;2-#

Polak, A., Tarek, M., Tomšič, M., Valant, J., Poklar Ulrih, N., Jamnik, A., Kramar, P., Miklavčič, D., 2014. Structural properties of archaeal lipid bilayers: small-angle X-ray scattering and molecular dynamics simulation study. *Langmuir* **30**, 8308–8315. https://doi.org/10.1021/la5014208

Polydera, A.C., Stoforos, N.G., Taoukis, P.S., 2003. Comparative shelf life study and vitamin C loss kinetics in pasteurised and high pressure processed reconstituted orange juice. *Journal of Food Engineering* **60**, 21–29. https://doi.org/10.1016/S0260-8774(03)00006-2

Potekhin, S.A., Senin, A.A., Abdurakhmanov, N.N., Tiktopulo, E.I., 2009. High pressure stabilization of collagen structure. *Biochimica et Biophysica Acta - Proteins and Proteomics* **1794**, 1151–1158. https://doi.org/10.1016/j.bbapap.2009.04.005

Powalksa, E., Jannosch, S., Kinne-Saffran, E., Kinne, R.K.H., Fontes, C.F.L., Mignaco, J.A., Winter, R., 2007. Fluorescence spectroscopic studies of pressure and temperature effects on Na + , K + -ATPase reconstituted into phospholipid bilayers and model raft mixture. *Biochemistry* **46**, 1672–1683. https://doi.org/10.1021/bi062235e

Pribenszky, C., Du, Y., Molnár, M., Harnos, A., Vajta, G., 2008. Increased stress tolerance of matured pig oocytes after high hydrostatic pressure treatment. *Animal Reproduction Science* **106**, 200–

207. https://doi.org/10.1016/j.anireprosci.2008.01.016

Pribenszky, C., Molnár, M., Cseh, S., Solti, L., 2005. Improving post-thaw survival of cryopreserved mouse blastocysts by hydrostatic pressure challenge. *Animal Reproduction Science* **87**, 143–150. https://doi.org/10.1016/j.anireprosci.2004.09.007

Purushothaman, S., Cicuta, P., Ces, O., Brooks, N.J., 2015. Influence of high pressure on the bending rigidity of model membranes. *Journal of Physical Chemistry B* **119**, 9805–9810. https://doi.org/10.1021/acs.jpcb.5b05272

Quinn, P.J., 1988. Effects of temperature on cell membranes. *Symposia of the Society for Experimental Biology* **42**, 237–258.

Rand, R.P., Parsegian, V.A., 1989. Hydration forces between phospholipid bilayers. *BBA - Reviews on Biomembranes* **988**, 351–376. https://doi.org/10.1016/0304-4157(89)90010-5

Rappolt, M., 2013. Formation of curved membranes and membrane fusion processes studied by synchrotron X-ray-scattering techniques, 1st ed, Advances in Planar Lipid Bilayers and Liposomes. Copyright © 2013 Elsevier Inc. All rights reserved. https://doi.org/10.1016/B978-0-12-411516-3.00002-4

Rappolt, M., Hickel, A., Bringezu, F., Lohner, K., 2003. Mechanism of the lamellar/inverse hexagonal phase transition xamined by high resolution X-ray diffraction. *Biophysical Journal* **84**, 3111–3122. https://doi.org/10.1016/S0006-3495(03)70036-8

Rayan, G., Macgregor, R.B., 2009. Pressure-induced helix-coil transition of DNA copolymers is linked to water activity. *Biophysical Chemistry* **144**, 62–66. https://doi.org/10.1016/j.bpc.2009.06.007

Rayan, G., Macgregor, R.B., 2005. Comparison of the heat- and pressure-induced helix-coil transition of two DNA copolymers. *Journal of Physical Chemistry B* **109**, 15558–15565. https://doi.org/10.1021/jp050899c

Redwood, W.R., Pfeiffer, F.R., Weisbach, J.A., Thompson, T.E., 1971. Physical properties of bilayer membranes formed from a synthetic saturated phospholipid in n-decane. *BBA - Biomembranes* **233**, 1–6. https://doi.org/10.1016/0005-2736(71)90351-8

Reed, C.J., Lewis, H., Trejo, E., Winston, V., Evilia, C., 2013. Protein adaptations in archaeal extremophiles. *Archaea* **2013**. https://doi.org/10.1155/2013/373275

Richard, D., Ferrand, M., Kearley, G.J., 1996. Analysis and visualisation of neutron-scattering data. *Journal of Neutron Research* **4**, 33–39. https://doi.org/10.1080/10238169608200065

Rilfors, L., Lindblom, G., 2002. Regulation of lipid composition in biological membranes—biophysical studies of lipids and lipid synthesizing enzymes. *Colloids and Surfaces B: Biointerfaces* **26**, 112–124. https://doi.org/10.1016/S0927-7765(01)00310-1

Risselada, H.J., 2017. Membrane fusion stalks and lipid rafts: a love-hate relationship. *Biophysical Journal* **112**, 2475–2478. https://doi.org/10.1016/j.bpj.2017.04.031

Ritz, M., Freulet, M., Orange, N., Federighi, M., 2000. Effects of high hydrostatic pressure on membrane proteins of Salmonella typhimurium. *International Journal of Food Microbiology* **55**, 115–119. https://doi.org/10.1016/S0168-1605(00)00165-3

Roche, J., Caro, J.A., Norberto, D.R., Barthe, P., Roumestand, C., Schlessman, J.L., Garcia, A.E., Garcia-Moreno E., B., Royer, C.A., 2012. Cavities determine the pressure unfolding of proteins. *Proceedings of the National Academy of Sciences* **109**, 6945–6950. https://doi.org/10.1073/pnas.1200915109

Roche, J., Ying, J., Maltsev, A.S., Bax, A., 2013. Impact of hydrostatic pressure on an intrinsically disordered protein: a high-pressure NMR study of α-synuclein. *Chembiochem.* **14**. https://doi.org/10.1016/j.dcn.2011.01.002.The

Rosenbaum, E., Gabel, F., Durá, M.A., Finet, S., Cléry-Barraud, C., Masson, P., Franzetti, B., 2012. Effects of hydrostatic pressure on the quaternary structure and enzymatic activity of a large peptidase complex from *Pyrococcus horikoshii*. *Archives of Biochemistry and Biophysics* **517**, 104–110. https://doi.org/10.1016/j.abb.2011.07.017

Rossignol, M., Thomas, P., Grignon, C., 1982. Proton permeability of liposomes from natural phospholipid mixtures. *Biochimica et Biophysica Acta (BBA) - Biomembranes* **684**, 195–199. https://doi.org/10.1016/0005-2736(82)90005-0

Sako, Y., Nomura, N., Uchida, A., Ishida, Y., Morii, H., Koga, Y., Hoaki, T., Maruyama, T., 1996. Aeropyrum pernix gen. nov., sp. nov., a novel aerobic hyperthermophilic archaeon growing at temperatures up to 100 °C. *International Journal of Systematic Bacteriology* **46**, 1070–1077. https://doi.org/10.1099/00207713-46-4-1070

Salvador-Castell (1), M., Oger, P., Peters, J., 2020. High-pressure adaptation of extremophiles and biotechnological applications, in: Salwan, R. (Ed.), Physiological and Biotechnological Aspects of Extremophiles. Elsevier.

Salvador-Castell (2), M., Demé, B., Peters, J., Oger, P., n.d. Structural characterization of an archaeal-like lipid bilayer as function of hydration and temperature. *Unpublished results*.

Salvador-Castell (3), M., Golub, M., Erwin, N., Demé, B., Brooks, N., Winter, R., Peters, J., Oger, P., n.d. Apolar lipids, the archaeal toolbox to membrane adaptation to extreme conditions. *Submitted*.

Salvador-Castell (4), M., Brooks, N.J., Peters, J., Oger, P., n.d. Induction of non-lamellar phases in archaeal lipids at high temperature and high hydrostatic pressure by apolar polyisoprenoids. *Submitted*.

Salvador-Castell (5), M., Demé, B., Peters, J., Oger, P., n.d. Coexistence of two lipid phases on an archaeal model membrane. *Unpublished results*.

Salvador-Castell (6), M., Brooks, N., Winter, R., Peters, J., Oger, P., n.d. Non-polar molecule as regulator of archaeal lipid bilayer properties. *Unpublished results*.

Salvador-Castell, M., Deme, B., Peters, J., Oger, P., 2018a. Constructing a comprehensive model of the archaeal membrane ILL 8-02-809. *Insitut Laue Langevin (ILL)*. https://doi.org/10.5291/ILL-DATA.8-02-809

Salvador-Castell, M., Deme, B., Peters, J., Oger, P., 2018b. Constructing a comprehensive model of the archaeal membrane. *Insitut Laue Langevin (ILL)* 818. https://doi.org/10.5291/ILL-DATA.8-02-818

Salvador-Castell, M., Golub, M., Martinez, N., Ollivier, J., Peters, J., Oger, P., 2019a. First study of osmolytes impact in whole cells of high temperature-adapted microorganisms. *Soft Matter* **accepted**.

Salvador-Castell, M., Tourte, M., Oger, P.M., 2019b. In search for the membrane regulators of Archaea. *International Journal of Molecular Sciences* **20**, 4434. https://doi.org/10.3390/ijms20184434

Sanchez, S.A., Tricerri, M.A., Gunther, G., Gratton, E., 2007. Laurdan generalized polarization: from cuvette to microscope. *Modern Research and Educational Topics in Microscopy* **2**, 1007–1014.

Santoro, M.G., 2000. Heat shock factors and the control of the stress response. *Biochemical Pharmacology* **59**, 55–63. https://doi.org/10.1016/S0006-2952(99)00299-3

Saragusty, J., Arav, A., 2011. Current progress in oocyte and embryo cryopreservation by slow freezing and vitrification. *Reproduction* **141**, 1–19. https://doi.org/10.1530/REP-10-0236

Sazonova, S., Galoburda, R., Gramatina, I., 2017. Application of high-pressure processing for safety and shelf-life quality of meat- a review. *11th Baltic Conference on Food Science and Technology "FOODBALT 2017"* 17–22.

Schmid, F., 2017. Physical mechanisms of micro- and nanodomain formation in multicomponent lipid membranes. *Biochimica et Biophysica Acta - Biomembranes* **1859**, 509–528. https://doi.org/10.1016/j.bbamem.2016.10.021

Schnablegger, H., Singh, Y., 2013. The SAXS guide: Getting acquainted with the principles. *Anton Paar* 124.

Schrenk, M.O., Huber, J.A., Edwards, K.J., 2010. Microbial provinces in the subseafloor. *Annual review of marine science* **2**, 279–304. https://doi.org/10.1146/annurev-marine-120308-081000

Schroeder, G., Bates, S.S., La Barre, S., 2018. Bioactive marine molecules and derivatives with biopharmaceutical potential. *Blue Biotechnology* 611–641. https://doi.org/10.1002/9783527801718.ch19

Schroeter, A., Stahlberg, S., Školová, B., Sonnenberger, S., Eichner, A., Huster, D., Vávrová, K., Hauß, T., Dobner, B., Neubert, R.H.H., Vogel, A., 2017. Phase separation in ceramide[NP] containing lipid model membranes: neutron diffraction and solid-state NMR. *Soft Matter* **13**, 2107–2119. https://doi.org/10.1039/C6SM02356H

Schuabb, C., Berghaus, M., Rosin, C., Winter, R., 2015. Exploring the free energy and conformational landscape of tRNA at high temperature and pressure. *ChemPhysChem* **16**, 138–146. https://doi.org/10.1002/cphc.201402676

Sears, V.F., 1992. Neutron scattering lengths and cross sections. *Neutron News* **3**, 26–37. https://doi.org/10.1080/10448639208218770

Seddon, J.M., 1990. Structure of the inverted hexangonal (H_{II}) phase, and non-lamellar phase-transitions of lipids. *Biochimica et biophysica acta* **1031**, 1–69. https://doi.org/10.1016/0304-4157(90)90002-T

Seddon, J.M., Templer, R.H., 1995. Polymorphism of lipid-water systems, in: Lipowsky, R., Sackmann, E. (Eds.), Handbook of Biological Physicsf. Elsevier Science B.V., pp. 97–160. https://doi.org/10.1016/S1383-8121(06)80020-5

Seddon, J.M., Templer, R.H., 1993. Cubic phases of self-assembled amphiphilic aggregates. *Philosophical Transactions of the Royal Society A* **344**, 339–356. https://doi.org/doi.org/10.1098/rsta.1993.0096

Sengupta, K., Raghunathan, V.A., Katsaras, J., 2003. Structure of the ripple phase of phospholipid multibilayers. *Physical Review E - Statistical Physics, Plasmas, Fluids, and Related Interdisciplinary Topics* **68**, 12. https://doi.org/10.1103/PhysRevE.68.031710

Sezgin, E., Levental, I., Mayor, S., Eggeling, C., 2017. The mystery of membrane organization: Composition, regulation and physiological relevance of lipid rafts. *Nat Rev Mol Cell Biol* **18**, 361–374. https://doi.org/10.1038/nmeth.2839.A

Sezgin, E., Sadowski, T., Simons, K., 2014. Measuring lipid packing of model and cellular membranes with environment sensitive probes. *Langmuir* **30**, 8160–8166.

https://doi.org/10.1021/la501226v

Shaw, A.S., 2006. Lipid rafts: Now you see them, now you don't. *Nature Immunology* **7**, 1139–1142. https://doi.org/10.1038/ni1405

Shearman, G.C., Ces, O., Templer, R.H., Seddon, J.M., 2006. Inverse lyotropic phases of lipids and membrane curvature. *Journal of Physics: Condensed Matter* **18**, S1105–S1124. https://doi.org/10.1088/0953-8984/18/28/S01

Shinoda, W., 2016. Permeability across lipid membranes. *Biochimica et Biophysica Acta - Biomembranes* **1858**, 2254–2265. https://doi.org/10.1016/j.bbamem.2016.03.032

Shinoda, W., Mikami, M., Baba, T., Hato, M., 2004a. Dynamics of a highly branched lipid bilayer: a molecular dynamics study. *Chemical Physics Letters* **390**, 35–40. https://doi.org/10.1016/j.cplett.2004.03.145

Shinoda, W., Mikami, M., Baba, T., Hato, M., 2004b. Molecular dynamics study on the effects of chain branching on the physical properties of lipid bilayers: 2. Permeability. *Journal of Physical Chemistry B* **108**, 9346–9356. https://doi.org/10.1021/jp035998+

Shinoda, W., Mikami, M., Baba, T., Hato, M., 2003. Molecular dynamics study on the effect of chain branching on the physical properties of lipid bilayers: structural stability. *The Journal of Physical Chemistry B* **107**, 14030–14035. https://doi.org/10.1021/jp035493j

Shinoda, W., Shinoda, K., Baba, T., Mikami, M., 2005. Molecular dynamics study of bipolar tetraether lipid membranes. *Biophysical Journal* **89**, 3195–3202. https://doi.org/10.1529/biophysj.105.060962

Shyamsunder, E., Gruner, S.M., Tate, M.W., Turner, D.C., So, P.T.C., Tilcock, C.P.S., 1988. Observation of inverted cubic phase in hydrated dioleoylphosphatidylethanolamine membranes. *Biochemistry* **27**, 2332–2336. https://doi.org/10.1021/bi00407a014

Siegel, D.P., 1999. The modified stalk mechanism of lamellar/inverted phase transitions and its implications for membrane fusion. *Biophysical Journal* **76**, 291–313. https://doi.org/10.1016/S0006-3495(99)77197-3

Siegel, D.P., Banschbach, J., Yeagle, P.L., 1989. Stabilization of H_{II} phases by low levels of diglycerides and alkanes: an NMR, calorimetric, and x-ray diffraction study. *Biochemistry* **28**, 5010–5019. https://doi.org/10.1021/bi00438a016

Siliakus, M.F., van der Oost, J., Kengen, S.W.M., 2017. Adaptations of archaeal and bacterial membranes to variations in temperature, pH and pressure. *Extremophiles* **21**, 651–670. https://doi.org/10.1007/s00792-017-0939-x

Silva, J.L., Foguel, D., Poian, A.T. Da, Prevelige, P.E., 1996. The use of hydrostatic pressure as a tool to study viruses and other macromolecular assemblages. *Current Opinion in Structural Biology* **6**, 166–175. https://doi.org/10.1002/aic.690140505

Silva, J.L., Luan, P., Glaser, M., Voss, E.W., Weber, G., 1992. Effects of hydrostatic pressure on a membrane-enveloped virus: high immunogenicity of the pressure-inactivated virus. *Journal of Virology* **66**, 2111–2117.

Silva, J.L., Oliveira, A.C., Gomes, A.M.O., Lima, L.M.T.R., Mohana-Borges, R., Pacheco, A.B.F., Foguel, D., 2002. Pressure induces folding intermediates that are crucial for protein-DNA recognition and virus assembly. *Biochimica et Biophysica Acta - Protein Structure and Molecular Enzymology* **1595**, 250–265. https://doi.org/10.1016/S0167-4838(01)00348-X

Silva, J.L., Oliveira, A.C., Vieira, T.C.R.G., de Oliveira, G.A.P., Suarez, M.C., Foguel, D., 2014. High-

pressure chemical biology and biotechnology. *Chemical Reviews* **114**, 7239–7267. https://doi.org/10.1021/cr400204z

Simonato, F., Campanaro, S., Lauro, F.M., Vezzi, A., D'Angelo, M., Vitulo, N., Valle, G., Bartlett, D.H., 2006. Piezophilic adaptation: a genomic point of view. *Journal of Biotechnology* **126**, 11–25. https://doi.org/10.1016/j.jbiotec.2006.03.038

Sinensky, M., 1974. Homeoviscous adaptation-A homeostatic process that regulates the viscosity of membrane lipids in Escherichia coli. *Proceedings of the National Academy of Sciences* **71**, 522–525. https://doi.org/10.1073/pnas.71.2.522

Singer, S.J.J., Nicolson, G.L.L., 1972. The fluid mosaic model of the structure of cell membranes. *Science* **175**, 720–731. https://doi.org/10.1126/science.175.4023.720

Smeller, L., 2002. Pressure–temperature phase diagrams of biomolecules. *Biochimica et Biophysica Acta (BBA) - Protein Structure and Molecular Enzymology* **1595**, 11–29. https://doi.org/10.1016/S0167-4838(01)00332-6

Smith, A.J., Davidson, L.S., Emmins, J.H., Bardsley, J.C.H., Holloway, P., Malfois, M., Marshall, A.R., Pizzey, C.L., Rogers, S.E., Shebanova, O., Snow, T., Williams, E.P., Terrill, N.J., 2019. I22: SAXS/WAXS beamline at Diamond Light Source -- an overview of 10 years operation. *Preprint* **arXiv:1903**.

Smith, P.H., Hungate, R.E., 1958. Isolation and characterization of *Methanobacterium ruminantium* n. sp. *Journal of bacteriology* **75**, 713–8.

Soler, N., Marguet, E., Verbavatz, J.M., Forterre, P., 2008. Virus-like vesicles and extracellular DNA produced by hyperthermophilic archaea of the order Thermococcales. *Research in Microbiology* **159**, 390–399. https://doi.org/10.1016/j.resmic.2008.04.015

Somero, G.N., 1995. Proteins and temperature. *Annual Review of Physiology* **57**, 43–68. https://doi.org/10.1146/annurev.ph.57.030195.000355

Sonavane, S., Chakrabarti, P., 2008. Cavities and atomic packing in protein structures and interfaces. *PLoS Computational Biology* **4**. https://doi.org/10.1371/journal.pcbi.1000188

Sprott, G.D., Agnew, B.J., Patel, G.B., 1997. Structural features of ether lipids in the archaeobacterial thermophiles *Pyrococcus furiosus* , *Methanopyrus kandleri* , *Methanothermus fervidus* , and *Sulfolobus acidocaldarius*. *Canadian Journal of Microbiology* **43**, 467–476. https://doi.org/10.1055/s-2003-39679

Staneva, G., Angelova, M.I., Koumanov, K., 2004. Phospholipase A2 promotes raft budding and fission from giant liposomes. *Chemistry and Physics of Lipids* **129**, 53–62. https://doi.org/10.1016/j.chemphyslip.2003.11.005

Staneva, G., Seigneuret, M., Koumanov, K., Trugnan, G., Angelova, M.I., 2005. Detergents induce raft-like domains budding and fission from giant unilamellar heterogeneous vesicles: A direct microscopy observation. *Chemistry and Physics of Lipids* **136**, 55–66. https://doi.org/10.1016/j.chemphyslip.2005.03.007

Stewart, L.C., Kates, M., Ekiel, I.H., Smith, I.C.P., 1990. Molecular order and dynamics of diphytanylglycerol phospholipids: a 2H and 31P-NMR study. *Chemistry and Physics of Lipids* **54**, 115–129. https://doi.org/10.1016/0009-3084(90)90066-Z

Strahl, H., Errington, J., 2017. Bacterial membranes: structure, domains, and function. *Annual Review of Microbiology* **71**, 519–538. https://doi.org/10.1146/annurev-micro-102215-095630

Sun, W.J., Tristram-Nagle, S., Suter, R.M., Nagle, J.F., 1996. Structure of the ripple phase in lecithin

bilayers. *Proceedings of the National Academy of Sciences of the United States of America* **93**, 7008–7012. https://doi.org/10.1073/pnas.93.14.7008

T. Baumgart, S. Hess, W. Webb, 2003. Imaging coexisting fluid domains in biomembrane models coupling curvature and line tension. *Nature* **425**, 821–824. https://doi.org/doi.org/10.1038/nature02013

Tabrizi, C.A., Walcher, P., Mayr, U.B., Stiedl, T., Binder, M., McGrath, J., Lubitz, W., 2004. Bacterial ghosts - Biological particles as delivery systems for antigens, nucleic acids and drugs. *Current Opinion in Biotechnology* **15**, 530–537. https://doi.org/10.1016/j.copbio.2004.10.004

Takahashi, S., Sugimoto, N., 2015. Pressure-dependent formation of i-motif and G-quadruplex DNA structures. *Physical Chemistry Chemical Physics* **17**, 31004–31010. https://doi.org/10.1039/c5cp04727g

Takahashi, S., Sugimoto, N., 2013. Effect of pressure on thermal stability of G-Quadruplex DNA and double-stranded DNA structures. *Molecules* **18**, 13297–13319. https://doi.org/10.3390/molecules181113297

Takai, K., Nakamura, K., Toki, T., Tsunogai, U., Miyazaki, M., Miyazaki, J., Hirayama, H., Nakagawa, S., Nunoura, T., Horikoshi, K., 2008. Cell proliferation at 122 °C and isotopically heavy CH_4 production by a hyperthermophilic methanogen under high-pressure cultivation. *Proceedings of the National Academy of Sciences* **105**, 10949–10954. https://doi.org/10.1073/pnas.0712334105

Tate, M.W., Eikenberry, E.F., Turner, D.C., Shyamsunder, E., Gruner, S.M., 1991. Nonbilayer phases of membrane lipids. *Chemistry and Physics of Lipids* **57**, 147–164. https://doi.org/10.1016/0009-3084(91)90073-K

Tayebi, L., Ma, Y., Vashaee, D., Chen, G., Sinha, S.K., Parikh, A.N., 2012. Long-range interlayer alignment of intralayer domains in stacked lipid bilayers. *Nature Materials* **11**, 1074–1080. https://doi.org/10.1038/nmat3451

Taylor, A.C., 1962. Responses of cells to pH changes in the medium. *The Journal of Cell Biology* **15**, 201–209. https://doi.org/10.1083/jcb.15.2.201

Tenchov, B., Koynova, R., 2017. Cubic phases in phosphatidylethanolamine dispersions: formation, stability and phase transitions. *Chemistry and Physics of Lipids* **208**, 65–74. https://doi.org/10.1016/j.chemphyslip.2017.09.005

Tenchov, B., Koynova, R., Rapp, G., 1998. Accelerated formation of cubic phases in phosphatidylethanolamine dispersions. *Biophysical Journal* **75**, 853–866. https://doi.org/10.1016/S0006-3495(98)77574-5

Tenchov, B.G., MacDonald, R.C., Siegel, D.P., 2006. Cubic phases in phosphatidylcholine-cholesterol mixtures: cholesterol as membrane "fusogen." *Biophysical Journal* **91**, 2508–2516. https://doi.org/10.1529/biophysj.106.083766

Tornabene, T.G., 1979. Diphytanyl and dibiphytanyl glycerol ether lipids of methanogenic archaebacteria. *Science* **203**, 51–53. https://doi.org/10.1126/science.758677

Tornabene, T.G., Langworthy, T. a, Holzer, G., Oró, J., 1979. Squalenes, phytanes and other isoprenoids as major neutral lipids of methanogenic and thermoacidophilic "archaebacteria". *Journal of molecular evolution* **13**, 73–83. https://doi.org/10.1007/BF01732755

Tortorella, E., Tedesco, P., Palma Esposito, F., January, G.G., Fani, R., Jaspars, M., de Pascale, D., 2018. Antibiotics from deep-sea microorganisms: current discoveries and perspectives. *Marine drugs*

16, 1–16. https://doi.org/10.3390/md16100355

Trapp, M., Gutberlet, T., Juranyi, F., Unruh, T., Deḿ, B., Tehei, M., Peters, J., 2010a. Hydration dependent studies of highly aligned multilayer lipid membranes by neutron scattering. *Journal of Chemical Physics* **133**, 1–7. https://doi.org/10.1063/1.3495973

Trapp, M., Juranyi, F., Tehei, M., Van Eijck, L., Demé, B., Gutberlet, T., Peters, J., 2010b. Elastic scattering studies of aligned DMPC multilayers on different hydrations. *Spectroscopy* **24**, 461–466. https://doi.org/10.3233/SPE-2010-0481

Trapp, M., Marion, J., Tehei, M., Demé, B., Gutberlet, T., Peters, J., 2013. High hydrostatic pressure effects investigated by neutron scattering on lipid multilamellar vesicles. *Physical Chemistry Chemical Physics* **15**, 20951–20956. https://doi.org/10.1039/c3cp52762j

Tristram-Nagle, S., Kim, D.J., Akhunzada, N., Kuerka, N., Mathai, J.C., Katsaras, J., Zeidel, M., Nagle, J.F., 2010. Structure and water permeability of fully hydrated diphytanoylPC. *Chemistry and Physics of Lipids* **163**, 630–637. https://doi.org/10.1016/j.chemphyslip.2010.04.011

Tristram-Nagle, S.A., 2007. Preparation of oriented, fully hydrated lipid samples for structure determination using X-ray scattering. *Methods in Molecular Biology* **400**, 63–75. https://doi.org/10.1385/1-59745-519-9:63

Turner, D.C., Gruner, S.M., 1992. X-ray diffraction reconstruction of the inverted hexagonal (H_{II}) phase in lipid-water systems. *Biochemistry* **31**, 1340–1355. https://doi.org/10.1021/bi00120a009

Tyler, A.I.I., Law, R. V., Seddon, J.M., 2015. Methods in membrane lipids, 2nd ed, Methods in Molecular Biology, Methods in Molecular Biology. Springer New York, New York, NY. https://doi.org/10.1007/978-1-4939-1752-5

Ulmer, H.M., Herberhold, H., Fahsel, S., Gänzle, M.G., Winter, R., Vogel, R.F., 2002. Effects of pressure-induced membrane phase transitions on inactivation of HorA, an ATP-dependent multidrug resistance transporter, in Lactobacillus plantarum. *Applied and Environmental Microbiology* **68**, 1088–1095. https://doi.org/10.1042/CS20150223

Ursell, T.S., Klug, W.S., Phillips, R., 2009. Morphology and interaction between lipid domains. *Proceedings of the National Academy of Sciences* **106**, 13301–13306. https://doi.org/10.1073/pnas.0903825106

Usui, K., Hiraki, T., Kawamoto, J., Kurihara, T., Nogi, Y., Kato, C., Abe, F., 2012. Eicosapentaenoic acid plays a role in stabilizing dynamic membrane structure in the deep-sea piezophile Shewanella violacea: a study employing high-pressure time-resolved fluorescence anisotropy measurement. *Biochimica et Biophysica Acta - Biomembranes* **1818**, 574–583. https://doi.org/10.1016/j.bbamem.2011.10.010

Valentine, R.C., Valentine, D.L., 2004. Omega-3 fatty acids in cellular membranes: a unified concept. *Progress in Lipid Research* **43**, 383–402. https://doi.org/10.1016/j.plipres.2004.05.004

Valeur, B., Berberan-Santos, M.N., 2012. Molecular fluorescence: principles and applications, 2nd ed. ed. Wiley-VCH, Weinheim, Germany.

Van de Vossenberg, J.L.C.M., Driessen, A.J.M., Konings, W.N., 1998. The essence of being extremophilic: the role of the unique archaeal membrane lipids. *Extremophiles* **2**, 163–170. https://doi.org/10.1007/s007920050056

van Meer, G., Voelker, D.R., Feigenson, G.W., 2008. Membrane lipids: Where they are and how they behave. *Nat Rev Mol Cell Biol* **9**, 112–124. https://doi.org/10.1038/nrm2330.Membrane

Vanga, S.K., Singh, A., Raghavan, V., 2017. Review of conventional and novel food processing methods on food allergens. *Critical Reviews in Food Science and Nutrition* **57**, 2077–2094. https://doi.org/10.1080/10408398.2015.1045965

Vanlint, D., Mebhratu, M.T., Michiels, C.W., Aertsen, A., 2008. Using mild high-pressure shock to generate bacterial ghosts of *Escherichia coli*. *Zeitschrift fur Naturforschung - Section B Journal of Chemical Sciences* **63**, 765–768. https://doi.org/10.1515/znb-2008-0626

Veatch, S.L., Keller, S.L., 2002. Organization in lipid membranes containing cholesterol. *Physical Review Letters* **89**, 1–4. https://doi.org/10.1103/PhysRevLett.89.268101

Vihinen, M., 1987. Relationship of protein flexibility to thermostability. *Protein Engineering* **1**, 477–480. https://doi.org/10.1093/protein/1.6.477

Vogel, R.F., Linke, K., Teichert, H., Ehrmann, M.A., 2008. High pressure modulated transport and signaling functions of membrane proteins in models and *in vivo*. *Journal of Physics: Conference Series* **121**. https://doi.org/10.1088/1742-6596/121/11/112005

Volkov, A.G., Paula, S., Deamer, D.W., 1997. Two mechanisms of permeation of small neutral molecules and hydrated ions across phospholipid bilayers. *Bioelectrochemistry and Bioenergetics* **42**, 153–160. https://doi.org/10.1016/S0302-4598(96)05097-0

Wang, C.Y., Huang, H.W., Hsu, C.P., Yang, B.B., 2016. Recent advances in food processing using high hydrostatic pressure technology. *Critical Reviews in Food Science and Nutrition* **56**, 527–540. https://doi.org/10.1080/10408398.2012.745479

Wang, X., Quinn, P.J., 2002. Cubic phase is induced by cholesterol in the dispersion of 1-palmitoyl-2-oleoyl-phosphatidylethanolamine. *Biochimica et Biophysica Acta - Biomembranes* **1564**, 66–72. https://doi.org/10.1016/S0005-2736(02)00402-9

Weinstein, J.N., Klausner, R.D., Innerarity, T., Ralston, E., Blumenthal, R., 1981. Phase transition release, a new approach to the interaction of proteins with lipid vesicles - Application to lipoproteins. *Biochimica et Biophysica Acta (BBA) - Biomembranes* **647**, 270–284. https://doi.org/10.1016/0005-2736(81)90255-8

Welch, T.J., Farewell, A., Neighardt, F.C., Bartlett, D.H., 1993. Stress response in *Escherichia coli* induced by elevated hydrostatic pressure. *Journal of Bacteriology* **175**, 7170–7177. https://doi.org/10.1128/jb.175.22.7170-7177.1993

White, S.H., Jacobs, R.E., King, G.I., 1987. Partial specific volumes of lipid and water in mixtures of egg lecithin and water. *Biophysical Journal* **52**, 663–665. https://doi.org/10.1016/S0006-3495(87)83259-9

Winter, R., Dzwolak, W., 2005. Exploring the temperature-pressure configurational landscape of biomolecules: from lipid membranes to proteins. *Philosophical transactions. Series A* **363**, 537–563. https://doi.org/10.1098/rsta.2004.1507

Winter, R., Jeworrek, C., 2009. Effect of pressure on membranes. *Physica B: Condensed Matter* **405**, 2820–2826. https://doi.org/10.1016/j.physb.2010.04.005

Woese, C.R., Fox, G.E., 1977. Phylogenetic structure of the prokaryotic domain: the primary kingdoms. *Proceedings of the National Academy of Sciences* **74**, 5088–5090. https://doi.org/10.1073/pnas.74.11.5088

Woese, C.R., Kandler, O., Wheelis, M.L., 1990. Towards a natural system of organisms: proposal for the domains Archaea, Bacteria, and Eucarya. *Proceedings of the National Academy of Sciences* **87**, 4576–4579. https://doi.org/10.1073/pnas.87.12.4576

Woese, C.R., Magrum, L.J., Fox, G.E., 1978. Archaebacteria. *Journal of Molecular Evolution* **11**, 245–252. https://doi.org/10.1007/BF01734485

Worcester, D.L., Franks, N.P., 1976. Structural analysis of hydrated egg lecithin and cholesterol bilayers II.Neutron diffraction. *Journal of Molecular Biology* **100**, 359–378. https://doi.org/doi.org/10.1016/S0022-2836(76)80068-X

Wu, Y., He, K., Ludtke, S.J., Huang, H.W., 1995. X-ray diffraction study of lipid bilayer membranes interacting with amphiphilic helical peptides: diphytanoyl phosphatidylcholine with alamethicin at low concentrations. *Biophysical journal* **68**, 2361–9. https://doi.org/10.1016/S0006-3495(95)80418-2

Wuytack, E.Y., Diels, A.M.J., Michiels, C.W., 2002. Bacterial inactivation by high-pressure homogenisation and high hydrostatic pressure. *International Journal of Food Microbiology* **77**, 205–212. https://doi.org/10.1016/S0168-1605(02)00054-5

Yancey, P., Clark, M., Hand, S., Bowlus, R., Somero, G., 1982. Living with water stress: evolution of osmolyte systems. *Science* **217**, 1214–1222. https://doi.org/10.1126/science.7112124

Yang, L., Huang, H.W., 2002. Observation of a membrane fusion intermediate structure. *Science* **297**, 1877–1879. https://doi.org/10.1126/science.1074354

Yasmann, A., Sukharev, S., 2015. Properties of diphytanoyl phospholipids at the air-water interface. *Langmuir* **31**, 350–357. https://doi.org/10.1021/la503800g

Zhang, Y.-L., Frangos, J.A., Chachisvilis, M., 2006. Laurdan fluorescence senses mechanical strain in the lipid bilayer membrane. *Biochemical and biophysical research communications* **347**, 838–41. https://doi.org/10.1016/j.bbrc.2006.06.152

Zhang, Y., Li, X., Xiao, X., Bartlett, D.H., 2015. Current developments in marine microbiology: high-pressure biotechnology and the genetic engineering of piezophiles. *Current Opinion in Biotechnology* **33**, 157–164. https://doi.org/10.1016/j.copbio.2015.02.013

Zhao, S., Baik, O.D., Choi, Y.J., Kim, S.M., 2014. Pretreatments for the efficient extraction of bioactive compounds from plant-based biomaterials. *Critical Reviews in Food Science and Nutrition* **54**, 1283–1297. https://doi.org/10.1080/10408398.2011.632698

Zhou, H., Wang, C., Ye, J., Tao, R., Chen, H., Li, W., Cao, F., 2016. Improvement of allergenicity and functional properties of proteins from ginkgo seeds by high hydrostatic pressure treatment. *Nongye Gongcheng Xuebao/Transactions of the Chinese Society of Agricultural Engineering* **32**, 292–298. https://doi.org/10.11975/j.issn.1002-6819.2016.08.041